INVESTIGATION OF SUBUNIT INTERACTIONS IN *trp* REPRESSOR UNDER VARYING SOLUTION CONDITIONS USING FLUORESCENCE SPECTROSCOPIC METHODS

By

Kathleen S. Martin

A thesis submitted in partial fulfillment of the requirements for the degree of

Master of Science

(Pharmacy)

at the

University of Wisconsin-Madison

1992

INVESTIGATION OF SUBUNIT INTERACTIONS IN *trp* REPRESSOR UNDER VARYING SOLUTION CONDITIONS USING FLUORESCENCE SPECTROSCOPIC METHODS

Kathleen S. Martin

Under the supervision of Professor Catherine A. Royer

at the

University of Wisconsin-Madison

ABSTRACT

The oligomeric state of the trp repressor (TR) has not been defined in the absence or presence of DNA. We proposed TR oligomerization to be energetically linked to protein-DNA binding. Fluorescence anisotropy has been used, in addition to the fluorescence lifetime of an extrinsic probe, to investigate the size of TR oligomers upon protein dilution in the range of 60 to 0.05 μM (TR concentration as a dimer). pH, salt concentration and corepressor (L-tryptophan) concentration were varied to understand the nature of the forces between TR subunits. The interaction between TR dimers was found to be electrostatic, destabilized by increasing salt concentration and increasing pH (range 6.0

to 8.5). TR multimers were also destabilized to dimers by corepressor. The results suggest an influence of solution conditions on TR-DNA binding through effects on protein subunit and protein-ligand interactions.

Approved 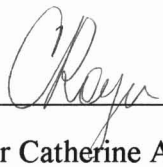

Professor Catherine A. Royer

Date 11-25-92

To

Mom and Dad

Stan

Cynthia, Robert and Daniel

Acknowledgements

I am sincerely grateful for the many friends and colleagues who encouraged me to return to the academic life and to graduate school. I am also extremely appreciative for those who have given me the kind word and outstretched hand when needed as I have progressed toward my goals in the pharmaceutics graduate program.

The excitement for biophysics of my mentor, Catherine A. Royer, has been extremely contagious and I am grateful I have been here to catch it. I appreciate the encouragement and the support, scientific and financial, that I have received. I am anxious to begin working toward new discoveries we will make together.

I would like to give special thanks to Dr. George Zografi and Dr. Kenneth Connors for serving on my committee. Returning to graduate school was not an easy decision. The expectations for a UW-Madison graduate student are high. Knowing that I have the support of Dr. Zografi and Dr. Connors has been, and will continue to be, a great source of encouragement for me.

My sincere gratitude goes out to many others who have provided friendship, help, many discussions and always encouragement. I am very grateful for the time and energy Veronique LeTilly and Olivier Sire have spent in trying to make an analytical chemist into a real biochemist. I might have once thought that to be an impossible task. The many hours of discussion (and debate) on why and how certain things are as they are (and why I should accept it) are greatly appreciated.

I thank Dr. Tom Record for allowing me to participate in his group meetings. Special thanks are due to Paula Schlax, Pete Schlax, and Mark Levandoski. I appreciate the many helpful discussions, hints and general support.

To Bruce, Ben and Mark and many other Hutchinson lab scientists: thanks, thanks, thanks. I have borrowed your equipment, used your space and attempted to copy all knowledge from your brains. And you gave it all!

Thanks also to my many good friends in the Pharmaceutics program who have helped me in so many ways. Special thanks to Sandy Koppenol (when **do** you eat dinner, anyway?), Miriam Franchini (can the gerbils come out to play?), Shyue-Fang Hsu (what did Dr. Wright say you do with a monochrometer?)

and Ray Skwierczynski (for the many discussions on the academic life and pursuit of baseball). To all my friends: Thank you.

I cannot end my acknowledgments without a special thanks to Stan, Cynthia, Robert and Daniel, who are as involved with my projects and work as I am. I appreciate all the weekends you've spent away so I could concentrate on my work. I appreciate your patience when I was home, but busy in my study. Discussions of my protein, experiments and particularly my "emzymes" have done much to help keep laughter a part of the work toward this degree. I love you all and am grateful for your love. Thank you.

TABLE OF CONTENTS

I. INTRODUCTION

The *trp* repressor[1] is an *Escherichia coli* transcriptional regulatory protein. TR represses transcription initiation by binding to at least five DNA operons which are involved in aromatic amino acid biosynthesis. Of these operons, the *trp*R gene encodes a polypeptide chain of 108 amino acids (Figure 1) that dimerizes to form the *trp* aporepressor. In this way, TR regulates its own production. The *trp*EDCBA gene encodes different proteins involved in the synthesis of the amino acid L-tryptophan. The regulation of transcription by TR is modulated by the intracellular concentration of L-tryptophan. When two molecules of L-tryptophan are bound to the trp aporepressor, the aporepressor is converted to the putative active trp repressor. As the cellular concentration of L-tryptophan increases, repression of the transcription occurs by binding of TR to the DNA operons. Binding to *trp*EDCBA represses L-tryptophan production, hence the corepressor concentration is modulated by a negative feedback loop. Binding of the corepressor is essential to enable specific interaction between TR and its DNA operons.

---

[1] *trp* repressor acronyms used: TR = active repressor species (no oligomeric state implied); TR_m = monomer polypeptide chain; TR_d = dimer of 2 intertwined monomer polypeptide chains; ApoR = repressor without L-tryptophan ligands; TR-DNS = dansyl labeled TR.

The three-dimensional structure of the aporepressor, TR_d and a repressor-DNA fragment cocrystal have been described by crystallographic and NMR studies. The TR monomer has a molecular weight of 12,356 (Gunsalus and Yanofsky, 1980), and has a secondary structure which contains six α-helices, designated A-F. TR is unusual in that the monomer as pictured from the dimeric crystal structure is not globular, as has been proposed for many of the oligomeric DNA binding proteins (Schevitz *et al.*, 1985; Marmorstein *et al.*, 1987; Zhang, *et al.*, 1987). In fact, the monomer so pictured would be predicted to be very unstable, with an extremely small buried hydrophobic core and large accessible surface (Janin *et al.*, 1988). In contrast, the TR dimer has a globular appearance and overall structure generally accepted for subunits in multimeric proteins (Figure 2). The subunit interface comprising the dimer hydrophobic core is composed primarily of interlinked and opposing α-helices identified as A, B, C, (residues 18-90, Otwinowski *et al.*, 1988) and F (residues 94-105) from each monomer subunit and is unchanged upon binding of the corepressor (L-tryptophan) to ApoR to form TR (Zhang *et al.*, 1987; Lawson *et al.*, 1988). The *trp* repressor contains, in part, the DNA binding motif known as the "helix-turn-helix" (HTH), which includes the D and E helices and the connecting three amino acid "turn" (residues 68-92) (Kelley and Yanofsky, 1985; Schevitz *et al.*, 1985; Zhang *et al.*, 1987; Otwinowski *et al.*, 1988). There are

two of these putative DNA binding regions per TR dimer, which have been collectively referred to as the "flexible reading heads" of TR, both being necessary for DNA binding. In the aporepressor, the HTH motifs are not positioned to fit precisely to the DNA operon surface. Upon binding of corepressor to two binding sites in the aporepressor, the HTHs are moved away from each other (Figure 3). It has been suggested that this realignment of the flexible reading heads allows interaction with the different DNA operator sites with varying affinities (Zhang *et al.*, 1987; Kumamoto *et al.*, 1987; Klig *et al.*, 1988). The modification of tertiary structure in the TR_d upon binding of L-tryptophan is supported by crystallography (Zhang *et al.*, 1987; Otwinowski *et al.*, 1988) and by use of mono-specific anti-*trp* repressor immunoglobulins (Tsapakos *et al.*, 1985).

The first 15 amino acids on the amino terminus of each polypeptide (Figure 3) have been found to be disordered by both crystallography (Schevitz, *et al.*, 1985; Zhang, *et al.*, 1987; and Otwinowski, *et al.*, 1988) and NMR (Arrowsmith, *et al.*, 1989). Several roles for the amino terminal "arms" have been suggested. Carey (1989) found diminished DNA binding for a chymotryptic TR fragment lacking the first 6 amino acids of the TR polypeptide, suggesting a contribution to DNA binding energy from the arms. Hurlburt and Yanofsky (1992) suggested a role for the

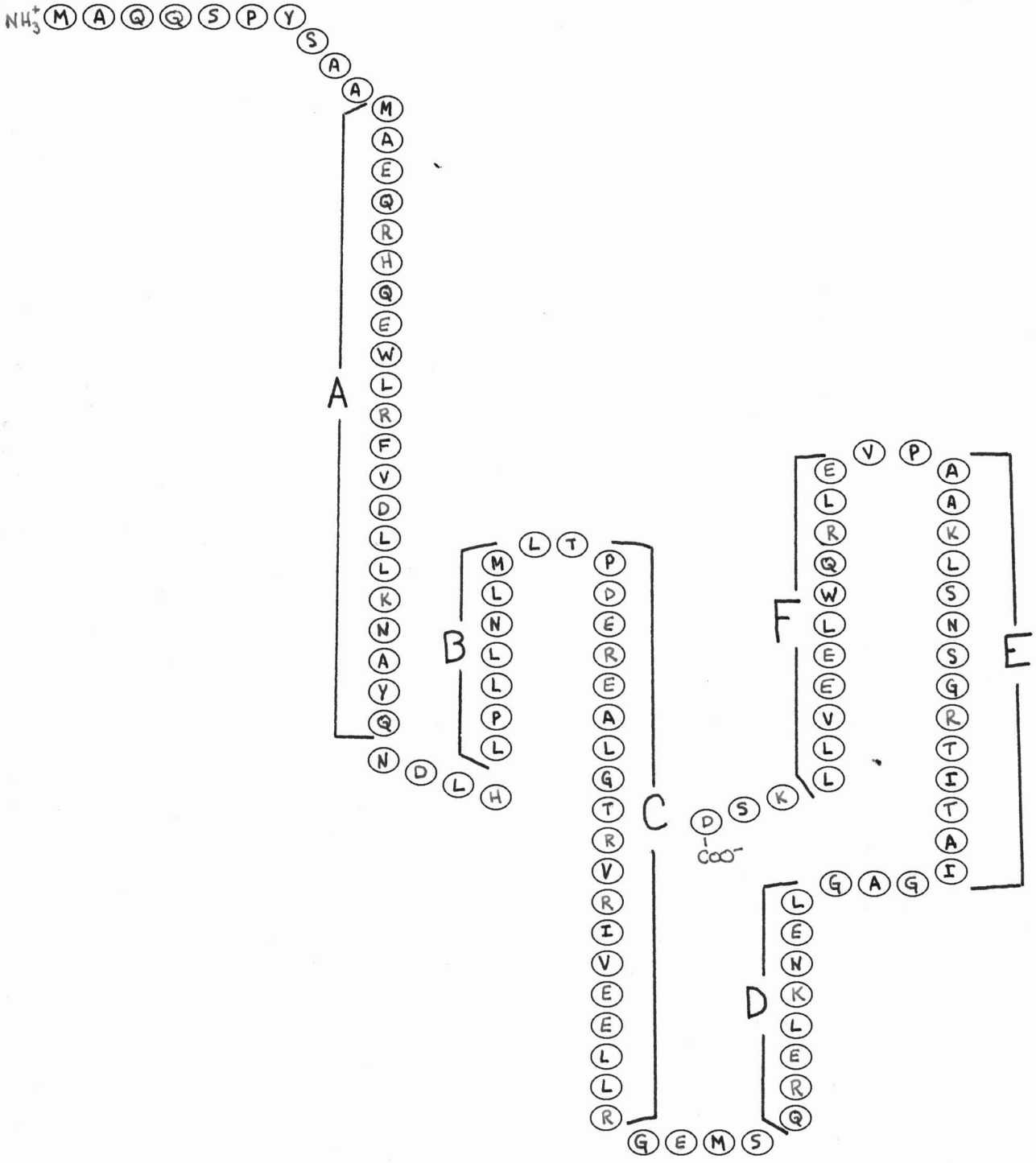

Figure 1. The TR monomer polypeptide chain. The single letter codes denote the amino acids. Red denotes uncharged, polar residues. Black denotes non-polar residues. Blue denotes residues which have a negative charge at pH 6.0. Green denotes residues which have a positive charge at pH 6.0. (Sequence, Gunsalus and Yanofsky, 1980)

Figure 2. Crystallographic structure of the TR dimer drawn from coordinates in the Brookhaven Protein Data Bank (crystal coordinates from Zhang, et al., 1987). Superimposed over the atomic structure is a ribbon diagram indicating the α-helix positions in TR. One polypeptide chain is blue. The other is red, with positively charged (arginine, histidine and lysine) and negatively charged (glutamic acid and asparagine) amino acids highlighted in green and white, respectively.

Note the overall symmetry of the dimer. Residues 8-108 are represented. The first 7 amino acids are omitted because no defined positions have been found. Serine 8, the first amino acid in the red polypeptide chain, is shown top and center on the picture. The first residue of the blue polypeptide chain is in the lower central portion of the dimer. The D and E helices (DNA binding regions) are at the left and right ends of the TR dimer as shown here.

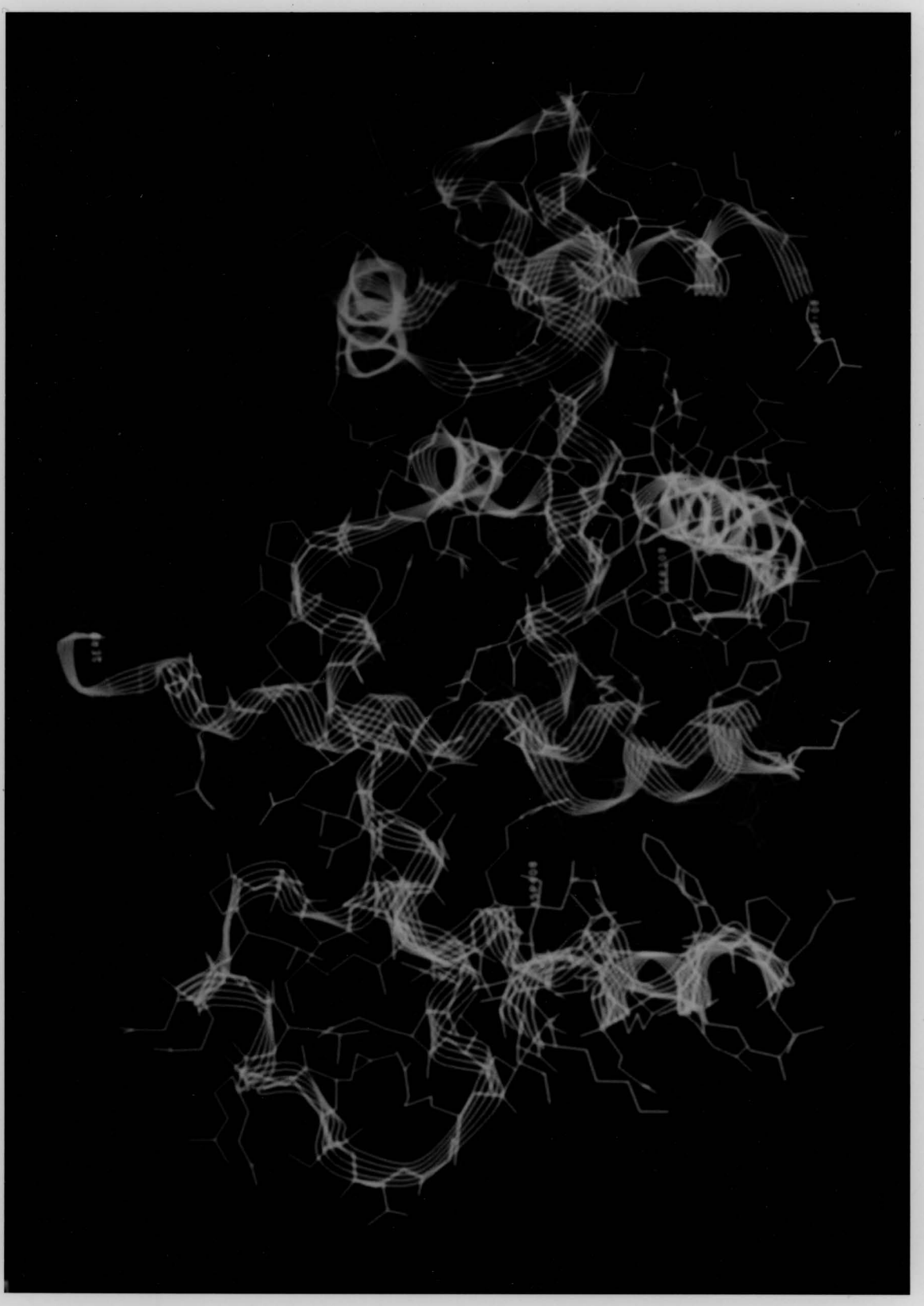

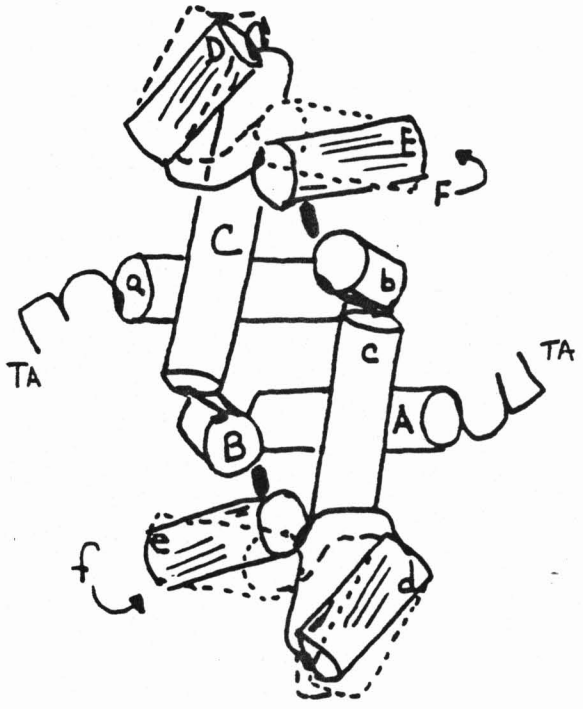

Figure 3. Barrel diagram of the *trp* repressor dimer. Shaded barrels indicate the relative positions of the D and E helices (DNA binding regions) in the aporepressor (absence of corepressor). Barrels drawn with broken lines show the relative positions of the helices in the presence of corepressor, L-tryptophan, for the liganded TR. Black ovals (near the E/e helices) denote the corepressor binding sites. To distinguish between the two polypeptide chains, the barrels are labeled (A-F) for one chain and (a-f) for the other. The amino terminal arms are denoted TA.

arms in folding of the nascent polypeptide chains or facilitation of non-specific DNA association following their investigation in which these codons were removed from the TR coding regions of the DNA prior to transcription. In both cases, the amino terminal arms were implicated in stabilization of structure and this may suggest involvement in TR subunit interactions.

Although the TR has been accepted as a dimer by virtue of crystallographic "evidence", the oligomeric state of the active *trp* repressor has not been unequivocally resolved. The experimental data available have been interpreted in terms of a dimeric TR, yet are contradictory. Zubay and coworkers (1972) determined the molecular weight of TR to be 5.8×10^4, using a Sephadex G-100 column and molecular weight standards, which would suggest tetrameric TR. Electrophoretic data (Joachimiak *et al.*, 1983) suggested a dimeric form for the active repressor. Sedimentation results (Joachimiak *et al.*, 1983) found the aporepressor molecular weight to be approximately that of the active *trp* repressor, but slightly higher than expected for dimeric TR (apparent molecular weight of approximately 26,000 KD). Crystallographic studies of TR have been done on TR_d (Schevitz *et al.*, 1985), ApoR (Zhang *et al.*, 1987), and a TR/DNA fragment co-crystal (Otwinowski *et al.*, 1988), which have provided some insight into contacts between the

biological macromolecules. However the limitations of crystallographic data must be understood as the results are considered. The solutions from which the crystals are grown may not mimic the *E. coli* environment in which the protein is active. The crystallographic data indicate a dimeric protein for ApoR, TR_d and DNA bound *trp* repressor. NMR (Lane *et al.*, 1986; Arrowsmith *et al.*, 1989, 1991a and 1991b; and Hyde *et al.*, 1989 and 1991) has also been utilized to study TR. NMR work was primarily done to obtain structural information on the active repressor in solution. The NMR data were evaluated in light of the crystallography data, possibly creating bias in the interpretation of the results as a TR dimer in solution. Tetrameric TR, in addition to higher order oligomers, was found in the absence and presence of corepressor, L-tryptophan, using fluorescence steady-state and time-resolved anisotropy and size exclusion chromatography (Fernando, 1991 and Fernando and Royer, 1992). Apparent molecular weights for TR in solution corresponding to tetrameric and dimeric TR have been found using molecular sieve chromatography, depending on the solution conditions (Liu, 1991). It is evident from evaluation of these data that the *trp* repressor exists in solution, in the absence of DNA, in at least two forms, dimeric and tetrameric.

Controversy also exists in the accepted oligomeric form of TR which binds to DNA. Haydock and Somerville (1984), using electrophoresis of TR and labeled operator-bearing restriction fragments, investigated the DNA binding of TR. Under the test conditions, they found only one stable complex when operator DNA was saturated with TR, with a repressor to operator ratio of 4:1. From this, it was concluded that the TR preparation was only 20% active. Interestingly, in the same work, they determined using immunological studies that only a minor fraction of the aporepressor was unable to bind L-tryptophan. This suggests that TR was present and active, although the activities of ligand and DNA binding are not necessarily linked. Other DNA binding studies did not report activities, which may be a factor in the reported results. Filter binding (Klig *et al.*, 1987) was done to measure specific binding of TR to DNA, and found 1.34 repressor dimers bound to operator DNA under the experimental conditions. Tandem binding of TR to DNA has been demonstrated (Kumamoto *et al.*, 1987, Bass, *et al.*, 1987; Marmorstein *et al.*, 1991). In a concentration range of 5-500 nM TR_m, protection areas of different sizes were observed in DNase footprinting experiments for three different TR operators. Some of the operator DNA areas protected upon TR binding were considerably larger than dimeric TR was predicted to contact. This suggested the possibility that TR bound to the operators as 1, 2, or 3

dimers. Binding of more than one TR dimer to DNA in a tandem configuration has been determined to be stereochemically feasible (Otwinowski, *et al.*, 1987; Haran, *et al.*, 1992). Carey (1988) developed a gel retardation assay for assessing *trp* repressor-DNA binding. In a pH 6.0 buffer system, at TR_d concentrations of 100 nM and above, two bands with retarded mobility relative to free DNA were observed. This suggested that TR bound to DNA in more than one fixed stoichiometry. Further, the gel results using 415 (operator) bp and 75 (non-operator) bp *E. coli* DNA fragments showed that the operator fragment could bind a number of TR dimers sufficient to coat the DNA. The 75-bp fragment had twice as many TR dimers bound than the number necessary to coat its length (at 250 nM TR_d; Carey, 1988). The gel mobility assay results implicate at least two modes of TR binding to DNA. Liu (1991) found TR bound to DNA with a stoichiometry of 1 or 2 dimers per operator using gel retardation assays, depending upon the length of the target DNA sequence. Therefore, various experimental techniques used to study TR-DNA binding to date suggest that the accepted notion of TR binding solely as a dimer to DNA is incomplete, and that different modes of binding may be involved.

It is evident that the oligomeric state of TR is dependent upon a number of variables, including corepressor

concentration, TR concentration and DNA sequence. A key issue in comparing TR study results is the wide variety of conditions utilized for the different experimental techniques. In many of the procedures, the experimental conditions are set to those in which the study can be carried out (i.e., the assay determines the conditions, not the system under test). Therefore, the observations, while reproducible under the test conditions, may not be relevant to the *in vivo* equilibria involved and may suggest non-physiological TR forms.

The importance of protein-protein interactions in the modulation of transcription is becoming more widely accepted. There are now many examples of protein subunit associations which regulate transcription. As a recent example, *fos* and *jun* are nuclear transforming proteins encoded by proto-oncogenes. The proteins bind to each other, forming stable heterodimers *in vivo*, and can also form homodimeric complexes with highly different affinities. DNA binding of these eukaryotic gene regulatory proteins is modulated by the relative concentrations of the two transforming proteins (Turner and Tjian, 1989; Kouzarides and Ziff, 1989). While there are many examples of molecular biological studies on protein-protein interactions implicated in transcriptional regulation (reviewed by Johnson and McKnight, 1989; specific examples include:

Murre, *et al.*, 1989; Gartenberg, *et al.*, 1990; Blackwood and Eisenman, 1991), the study of the energetics involved in the association processes is only slowly beginning to receive attention (Koblan and Ackers, 1991; Fernando and Royer, 1992).

The overall energetics of the TR system involve coupled equilibria, including, at least, the binding of corepressor (Bennett, *et al.*, 1976; Gunsalus and Yanofsky, 1980; Zurawski, *et al.*, 1981) and the oligomeric state of the protein (Fernando and Royer, 1992). To study the influence of solution conditions on TR subunit interactions it is of great importance that the study be conducted with the system at equilibrium. Fluorescence spectroscopy is a tool which has become well established for the study of biological equilibria (Weber, 1953 and 1992). Fluorescence anisotropy is a solution-based technique, with the time scale of fluorescence overlapping the timescale of physical processes in solution, such as the rotational diffusion of biological macromolecules. Fluorescence is also highly sensitive and therefore well suited for the study of low concentrations of proteins and DNA needed to observe interactions between these biological macromolecules in the equilibrium rather than stoichiometric limit. Solution conditions can be readily modified. Fluorescence anisotropy permits direct

observation of the variation in the size of a macromolecular complex.

Both intrinsic tryptophan fluorescence and fluorescence of an extrinsic, covalently bound probe have been used to investigate subunit equilibria in the TR system (Fernando and Royer, 1992). The fluorescence lifetime of the covalent probe 5-dimethylamino-naphthalene-1-sulfonyl chloride (DNS) is 10-20 ns. Brownian motion or rotational diffusion of proteins of 25-50 KD molecular weight occurs within the timespan of the DNS lifetime (Weber, 1992). The molecular weights of the TR dimer and tetramer are in this range and therefore TR oligomer size can be observed by monitoring the depolarization of anisotropy for DNS covalently bound to TR. An additional advantage of the covalent DNS labeling of TR is that it allows the study of the influence of corepressor (L-tryptophan) binding on the TR subunit equilibria. The absorption and emission maxima for DNS are at higher wavelengths than those for the corepressor, L-tryptophan. Therefore, the L-tryptophan present at high concentration in the buffer does not interfere with the DNS fluorescence signal.

II. OBJECTIVE

Conflicting evidence exists regarding the oligomeric state of the protein both in the absence and presence of DNA. Systematic characterization of the effects of solution conditions on protein-protein interactions in the TR system has not been done. The objective of this work is to characterize the oligomeric state of the *trp* repressor as a function of the protein concentration and solution conditions, including salt concentration, pH and corepressor concentration. The intracellular environment of *E. coli* is subject to variations in ion, TR and corepressor concentrations and all may contribute to modulation of TR-DNA binding. The anisotropy of a covalently bound dansyl label is used as a probe to monitor the correlation time of the protein. Given that TR forms oligomers, dilution/correlation time profiles as a function of corepressor concentration, salt concentration, and pH are used to gain insight into the types of forces dictating the oligomeric state of TR at equilibrium. Characterization of the multiple, coupled equilibria (protein-protein, protein-ligand and protein-DNA) involved in transcriptional regulation is necessary for complete understanding of the physicochemical mechanisms of transcriptional control.

This work establishes the solution conditions under which higher order TR oligomers are observed in the absence of DNA. The implications of this work on the DNA binding of TR are considered in light of the DNA binding work to date. Characterizing the factors which influence protein oligomerization may lead to a greater understanding of the regulation of transcription and provide a basis for its therapeutic modulation.

III. MATERIALS AND METHODS

A. Protein Preparation

1. Protein Purification

An *E. coli* strain, CY15071, which overproduces the *trp* repressor (Paluh and Yanofsky, 1986) was obtained from Dr. Kathleen Matthews, Rice University. Strain CY15071 is a derivative of *E. coli* W3110, which is a *lac*I^q strain. These cells are transformed by expression plasmids which have been constructed to contain a strong, regulated promotor to direct transcription (*tac* promotor), the *trp* repressor coding region, a strong transcription termination region immediately following the cloning sites (rpoC), and a synthetic DNA segment containing the ribosome binding site for the *trp* leader peptide. This genetic engineering was done to allow regulated expression of TR to produce large amounts of the wild-type repressor and can also be used to transcribe mutant repressors. The natural TR expression signals are relatively weak, as is the natural ribosome binding site, which limits the amount of TR which can be produced in the unaltered cell lines, necessitating a way to enhance TR production for studies. Following introduction into *E. coli* cells, the constructed plasmid is replicated to a fixed number, which is denoted the "copy number". The

plasmid in strain CY15071, pJPR2, (Paluh and Yanofsky, 1986) has been estimated to have a copy number of 60. This means ≈ 60 plasmids are present in each *E. coli* cell to produce TR. Transcription in *lac*I^q cells is turned on (induced) by IPTG (isopropylthiogalactoside). The cells are grown in the absence of IPTG until a large colony of cells is present. IPTG is then added a specified time before cell harvest, stimulating TR production.

After cell harvest, the TR purification method of Joachimiak, *et al.*, 1983 with the following modifications was carried out. Cells were suspended in 100 mL of 0.1 M TRIS-HCl, pH 7.5, for each 60 g of cells. The cells were broken by three successive passages through a pressurized extruder. The extract was centrifuged for 30 minutes at 8,000 rpm on a Sorvall R-5B centrifuge with a GS3 rotor at 5° C. Streptomycin sulfate was added to the supernatant while stirring to a final concentration of 1% in order to remove some of the proteins (TR remains in the supernatant). The solution was stirred at 4° C for 60 minutes and then heated to 62° C for 5 minutes. A large amount of precipitate forms during this process. The mixture was cooled on ice to 15° C and then centrifuged (5° C) for 20 minutes at 10,000 rpm. The supernatant was precipitated with 45% ammonium sulfate, stirred for 45 minutes at 4° C, centrifuged for 20 minutes at 10,000 rpm and reprecipitated

with 75% ammonium sulfate. After being stirred at 4° C for 60 minutes, the solution was centrifuged (5° C) for 20 minutes at 10,000 rpm. The pellet was then resuspended in a minimal volume 10 mM potassium phosphate, 0.1 M KCl, and 0.1 mM EDTA, pH 7.6. A 400-mL phosphocellulose column (P11, Whatman, Maidstone, England) was equilibrated with 10 mM potassium phosphate, 0.2 M KCl and 0.1 mM EDTA, pH 7.6, until the elution buffer had the same pH and conductivity as the starting buffer. Following overnight dialysis of the partially purified protein (volume ratio of protein:buffer, 1:400) in 10 mM potassium phosphate, 0.1 M KCl, 0.1 mM EDTA, pH 7.5 (three buffer changes were made during the dialysis), the dissolved pellet was loaded onto the P11 column and a KCl gradient (0.2-0.5 M KCl) was run. Fractions which contained 10 mg or more of protein were retained. The fractions collected from the leading or trailing edges of the protein peak containing 20 mg TR or less were combined, concentrated (Centriprep™ tubes, Amicon, Danvers, MA), and dialyzed twice for 3 hours in 2 liters of 10 mM phosphate buffer, pH 7.6 (volume ratio of protein:buffer ≈ 1:500). Further purification was then carried out on these fractions on a 25-mL Reactive Blue 2-Sepharose CL-6B (Sigma, St. Louis, MO) column with a KCl gradient of 0 to 1 M KCl in 10 mM phosphate, 0.1 mM EDTA, pH 7.6 buffer. The purified repressor was greater than 95% pure as estimated from silver staining of an SDS-polyacrylamide gel. Each fraction

containing TR was stored at -70° C in the elution buffer (10 mM potassium phosphate, pH 7.6, with 0.5 or 1 M KCl). Protein concentrations were determined using a molar absorptivity of 1.45×10^4 cm^{-1} M^{-1} per monomer (Joachimiak *et al.*, 1983).

2. DNS labeling

Aliquots (1 mL) of purified TR were dialyzed against 1 liter of 0.24 M potassium phosphate buffer, pH 8.0 for 3 hours. 25 µL of a 0.02 M solution of dansyl chloride (Molecular Probes, Eugene, Oregon) (Figure 4) was added to the solution of protein and the reaction was allowed to proceed for 15 min. DNS forms a highly stable sulfonamide derivative with amines (Haugland, 1983). To effect separation of free and bound dye fractions, the solution was immediately applied to a Sephadex G-25 superfine column whose total volume was approximately 10 mL. The column was pre-equilibrated with 10 mM phosphate, 0.1 mM EDTA, pH 7.6. The protein was collected in 0.6 mL fractions. The most concentrated fractions were combined and the concentrations of TR_d and labeling ratio (L.R.) were determined. The ratio of probe to protein for the TR-DNS preparations (labeling ratio) was determined by taking absorption measurements at 280 and 340 nm. The A_{280} corresponds to absorption from the protein and from the DNS label and the A_{340} corresponds to absorption

from the label alone. The labeling ratio (L.R.) was calculated using Equation 1:

$$L.R. = (A_{340}/E_{DNS340})/((A_{280} - 1/2\ A_{340})/E_{prot280}) \quad (1)$$

(Jameson, 1978)

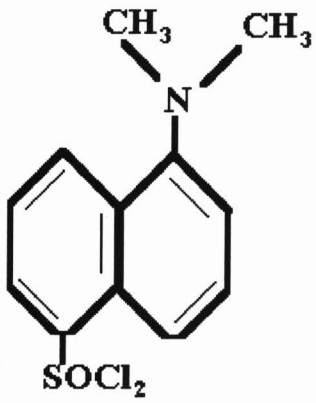

Figure 4. The chemical structure of the extrinsic fluorescence probe dansyl chloride.

3. Chymotryptic Digests

Chymotryptic digests of the labeled repressor were carried out following the method of Carey (1989). The enzyme, α-chymotrypsin, was purchased from Boehringer-Mannheim (Indianapolis, IN). The products of the digest were separated using molecular sieve chromatography on a 250-mL Sephadex G-50 (fine) (Sigma, St. Louis, MO) column. The elution buffer was 10 mM phosphate (Mallinckrodt), 7.6 M urea (ICN Biochemicals, Cleveland OH), pH 7.6. The eluate was collected in 2-mL fractions, which were measured for absorbance (280 nm) (to quantify the protein content) and fluorescence (Excitation wavelength was 340 nm). Emission was collected using a 460 nM cuton filter, Hoya Optics, Freemont CA.) to quantify the amount of the DNS label. Selected fractions were analyzed by SDS-PAGE and silver stain (Rapid-Ag-Stain kit, ICN Biochemicals, Cleveland OH). SDS-PAGE was done under standard conditions for the LKB 2001 Vertical Electrophoresis unit (Pharmacia, Uppsala, Sweden) using discontinuous gels (3% stacking gel and 10-18% resolving gels).

B. Experimental

1. Dilution Study Experimental Design

DNS labeled TR was dialyzed under different solution conditions and the fluorescence anisotropy or lifetime measurements were made to gain information on the oligomeric state of TR. Dialysis was carried out in test buffers composed of 10 mM potassium phosphate (KH_2PO_4/K_2HPO_4, Mallickrodt), 0.1 mM EDTA (Baker Analyzed), with concentrations of KCl (Mallinckrodt) ranging from 0 to 500 mM. After all reagents were fully dissolved, the pH was adjusted to 6.0, 7.6, or 8.5 using standardized 1 N KOH (Fisher Scientific) to the chosen pH, +/- 0.01 pH unit.

The protein samples were dialysed overnight at 4° C (volume ratio of protein:buffer, 1:1000) in the test buffer. Equilibration of the protein with l-tryptophan requires approximately 24 hours (Fernando and Royer, 1992). A dialysis period of 15-21 hours was found to provide reproducible results and was the time period used throughout this work. No interference from free dye was observed in the dialysis buffer. Samples were allowed to equilibrate at room temperature (approximately 20° C) for 1 to 1-1/2 hours prior to the start of the dilution study experiment.

Two different preparations of TR were used, and different fractions from each preparation were also used in these experiments. Stock concentrations of the TR in the various fractions used ranged from 2-4 mg/mL.

a. Steady-state Fluorescence: Anisotropy Experiments

Following DNS labeling, the protein was divided into 2 or 3 aliquots of approximately 550 μL each and transferred to Spectra/Por 1 dialysis tubing (6,000-8,000 molecular weight cut off, 10 mm wide), which had been extensively cleaned to remove fluorescent contaminants. Each aliquot was placed in 1 liter of a freshly prepared test buffer. Following dialysis, fluorescence anisotropy measurements were made on each sample, followed by serial dilution of the protein by approximately 0.1 log unit of TR concentration using dialysis test buffer to generate a plot of anisotropy against concentration. Figure 5 depicts an expected anisotropy/dilution profile. The concentration region in which reversible association takes place (non-horizontal) is clearly distinguishable from regions where this is negligible (horizontal).

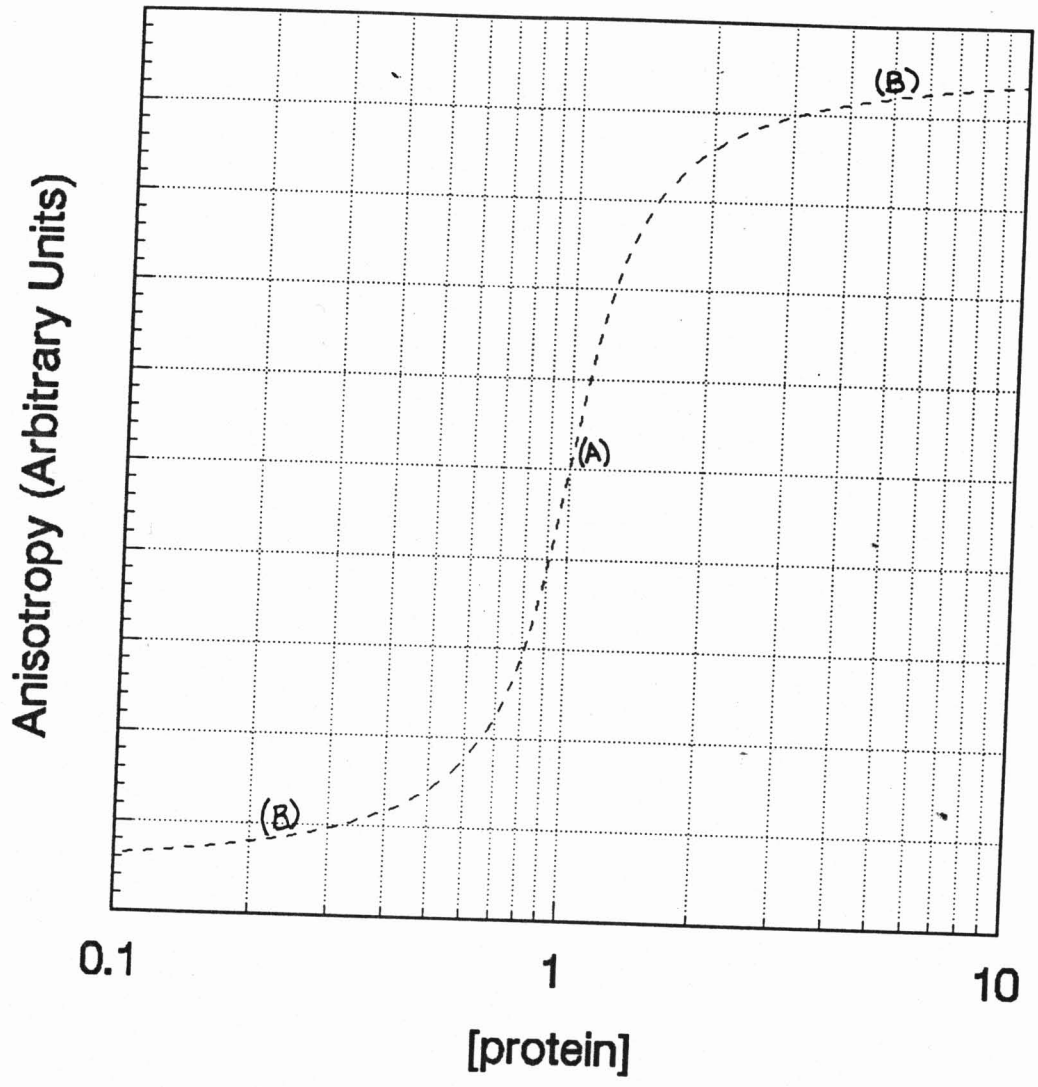

Figure 5. Arbitrary dilution curve with the protein concentration increasing to the right along the x-axis. Reversible association is observed in the non-horizontal region of the curve (A). Plateau regions (B) indicate no equilibria over the concentration ranges where the curve is horizontal.

b. Time-resolved Fluorescence: Lifetime experiments

Following steady-state anisotropy measurements, remaining TR-DNS aliquots were pooled from the most concentrated dilutions and the absorbance was measured to determine the TR concentration. For protein samples which had no tryptophan in the test buffer, the absorbance at 280 nm was measured and the concentration of TR was calculated directly. For protein samples with tryptophan in the test buffer, the absorbance was measured at 340 nm. Using the labeling ratio (Equation 1) that was calculated prior to the experiment, the concentration of TR was obtained. These aliquots were then frozen, along with approximately 10 mL of the test buffer, and stored until a later date, in most cases. These aliquots were used as the high concentration sample in the dilution lifetime measurements. Some of the test samples were stored at -20° C until test (up to 3 months), others were stored at -70° C, and some samples were used immediately following the dilution/anisotropy experiments. The results did not show any bias by any of the storage temperatures or storage duration. This was ascertained by comparison of average lifetimes for samples which were freshly prepared, stored at -20° C, and stored at -70° C. For dilution/lifetime experiments, three concentrations of TR were used. The high concentration sample ranged from 20-50 μg/mL; serial dilutions to

10 μg/mL and then to 1 or 2 μg/mL were taken, diluting with the appropriate test buffer. Following the collection of phase and modulation data using the ISS software (ISS, Urbana, IL), the average lifetimes were obtained for each concentration simultaneously, using Globals Limited software, as will be described in the *Data Analysis* section.

2. Instrumentation

a. Steady-state Fluorescence Anisotropy Measurements

Steady state measurements were performed on an ISS KOALA spectrophotometer in analog acquisition mode using a 300 Watt Xenon arc lamp from ILC Technologies (Sunnyvale, CA). Steady-state polarization measurements on the TR-DNS samples were measured in L format (Figure 6) exciting at 350 nm with 8 nm bandwidth and using a Y460 cuton filter (Hoya Optics, Freemont, CA) in emission. Buffer background was subtracted for all samples.

b. DNS Fluorescence Lifetime Measurements

Lifetime measurements on TR-DNS were performed using the multi-frequency phase/modulation acquisition electronics from ISS, Inc (Urbana, IL) with the KOALA sample compartment. Fluorescence phase shift and modulation data

were measured at modulation frequencies ranging from approximately 3 to 100 MHz. Each phase and modulation value collected is the average of several measurements, each being the average of a large number of phase or modulation readings. The excitation was from externally pulse-picked output (355 nm) of the Coherent Third Harmonic Generator (THG) coupled with the Coherent Antares modelocked doubled Nd-YAG laser. An external Bragg cell (Model N13380 NEOS, Melbourne FL) was driven with the Coherent cavity dumping electronics normally used in conjunction with the 700 series dye lasers. The diffracted beam was collected into an optical fiber model 77598 (Oriel Corp, Stratford CT) and focused into the KOALA sample compartment with a 5 cm quartz lens. The cavity dumper was run in either divide by 10 or divide by 20 modes with base frequencies either near 2 or 4 MHz. Emission was monitored through a Y460 cuton filter from Hoya Optics and compared to p-bis[2-(5-phenyloxazolyl)] benzene (POPOP) (Eastman Kodak, Syracuse NY), which has a lifetime of 1.32 ns in ethanol (Gratton et al., 1984b).

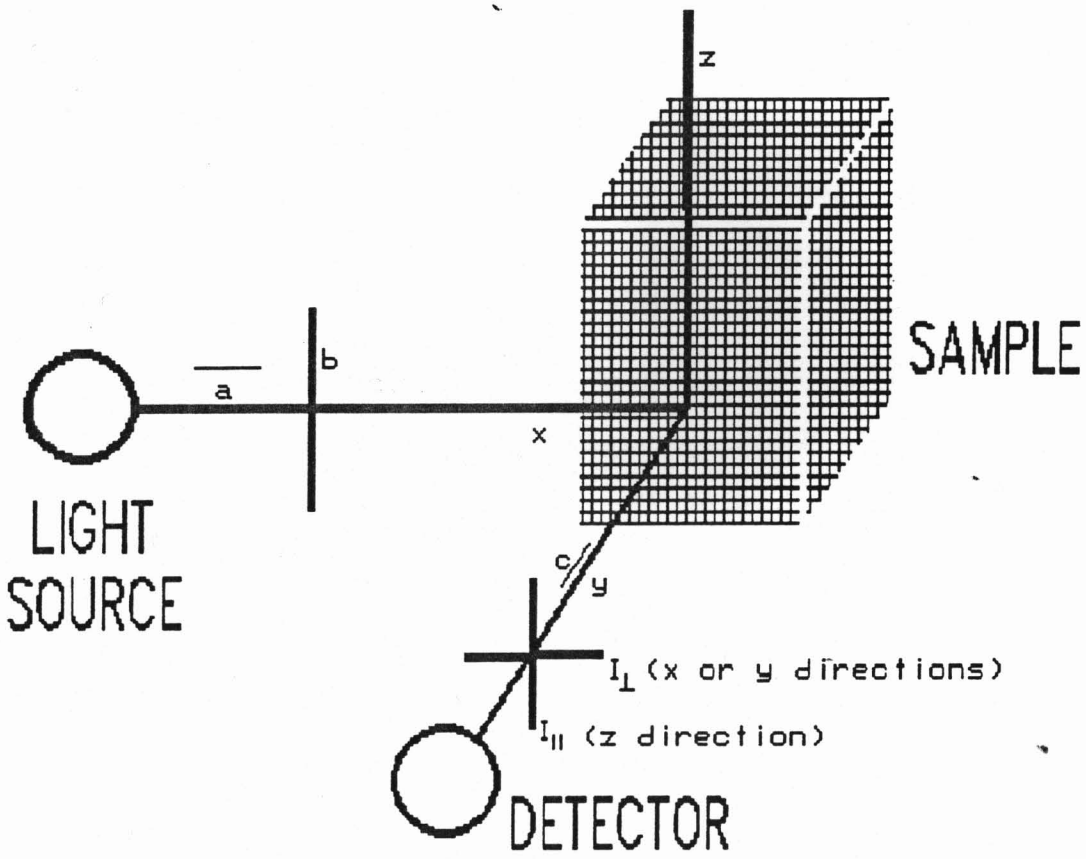

Figure 6. Schematic illustration of fluorescence anisotropy experimental set up. (a) indicates the excitation light propagation direction (x-axis). (b) indicates the polarization of the excitation light (z-axis). (c) Detector is placed at 90^{o} angle to incident light to collect emitted light (y-axis). $I_{||}$ and $I_{\perp}$ are defined as shown in the diagram.

3. Data Analysis

Two fluorescence parameters are needed for calculation of an average correlation time for the macromolecule under study: the steady-state anisotropy and the lifetime of the fluorophore. Where a population of lifetimes contributes to the measured lifetime, as is the case in this work, the calculated lifetime is an average lifetime, $<\tau>$, and the calculated correlation time, $<\tau_c>$ is an average of all the species in the solution under test. The average correlation time is obtained from the Perrin equation (See Theoretical Background), using the measured anisotropy and DNS lifetime values.

The lifetime data are obtained from multi-frequency phase and modulation data, which were collected by the instrumentation described. Harmonic fluorescence spectroscopic methods have been detailed in the literature (Weber, 1981; Jameson and Gratton, 1983; Gratton, *et al.*, 1984a and b). Analysis is done to fit the measured phase and modulation data to resolve the lifetime components and fractional intensity contributions using Globals Unlimited (Urbana, IL) software. The phase delay and modulation ratio of the fluorescence are determined relative to the reference standard POPOP. Well established statistical methods based

on analysis of the chi-square are used (Beechem, *et al.*, 1989).

The Marquardt algorithm was used for the data fitting. The quality of the fit was judged by the value of the chi-square parameter and examination of the residuals at each frequency. With the global analysis software, multiple data sets for the magic angle[2] lifetime experiments at differing tryptophan concentrations, potassium chloride concentrations and pH were analyzed simultaneously in the frequency domain according to appropriate physical models to obtain a consistent set of intensity decay parameters.

For the purposes of calculating the average correlation time, the fractional contribution of each lifetime component was used to calculate the average fluorescence lifetime of the DNS as a function of TR_d concentration. Changes in the average correlation time are of interest because the changes represent the rotational diffusion of the TR-DNS and are therefore indicative of changing size of macromolecular complexes. Average lifetimes (computed using the fitted fractional contributions and lifetime components) were

---

[2]The "magic angle" conditions are a defined orientation of polarizers chosen to avoid spectral artifacts caused by the enhancement of the transmission efficiency for vertically polarized light at short wavelengths, which can result in spectral shifts due to the wavelength, not the sample. Magic angle conditions include a vertical excitation polarizer, and an emission polarizer oriented at 54.7^{o} from the vertical. Since $\cos^2(54.7^{o}) = 0.333$ and $\sin^2(54.7^{o}) = 0.667$, these polarizer settings result in $I_{\parallel}$ being enhanced two times over $I_{\perp}$. This results in a signal proportional to the total fluorescence intensity, I_T.

plotted as a function of TR concentration and a linear regression line was generated. The average DNS lifetime at each concentration for which an anisotropy measurement was taken was extrapolated or interpolated from the linear regression lines for each test system studied. Average correlation times $<\tau_c>$ of the TR-DNS as a function of TR_d concentration were calculated using the Perrin equation (Theoretical Background). The average correlation time was then plotted versus protein concentration.

IV. THEORETICAL BACKGROUND

A. Fluorescence Anisotropy

The anisotropy of fluorescence is defined as the ratio of the net polarized component of the fluorescence emission intensity to the total fluorescence emission intensity:

$$A = (I_{||} - I_{\perp}) / (I_{||} + 2I_{\perp}) \qquad (2)$$

Figure 6 illustrates the instrumental set up schematically and also shows the definitions of $I_{||}$ and $I_{\perp}$. The lifetime of a fluorophore is the time period between absorption of light by the fluorophore and subsequent emission of the light (at a different wavelength than the incident light). If a fluorophore is excited by incident light and no movement occurs prior to emission, the resultant anisotropy is determined solely by the angle between the emission and absorption fluorophore dipoles (Figure 7). This is the limiting anisotropy, A_0, which is the maximum anisotropy value which can occur for a fluorophore. In solution, a fluorophore is subject to rotational diffusion, or Brownian motion, which results in reorientation of the fluorophore during the fluorophore lifetime. The resultant measured anisotropy, (A), is decreased from the fluorophore's limiting value.

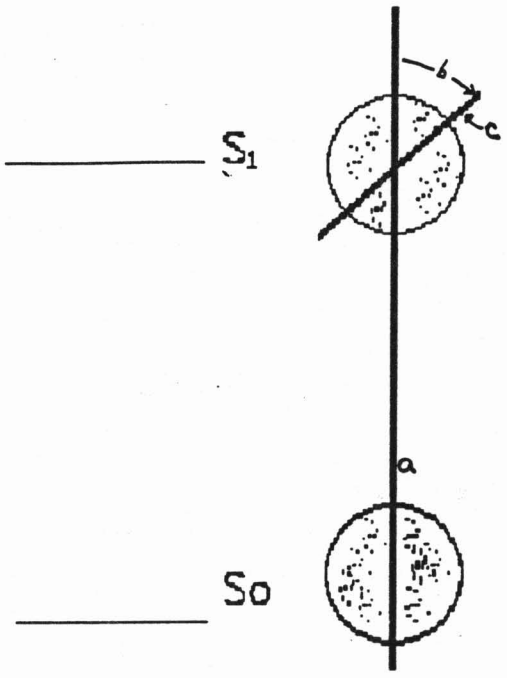

Figure 7. Diagram illustrating the origin of A_0. The long vertical line (a) represents the probe dipole in the ground (S_0) electronic state. It is drawn for both the ground and excited (S_1) states to show the angular displacement (b) between the ground state dipole and the excited state dipole (c). Without any rotation of the probe, there is a loss of fluorescence anisotropy upon excitation, which is the result of the dipole change for the particular probe used

Two parameters affect the observed anisotropy of a fluorophore covalently bound to a macromolecule: the macromolecular rotational diffusion and the intrinsic fluorophore motions. Due to the relative amplitude of the two motions, the depolarization of the anisotropy is mainly determined by the macromolecular reorientation (Figure 8). Because the environment of the probe may change upon oligomer dissociation, changes in anisotropy may also have contributions from changes in probe mobility.

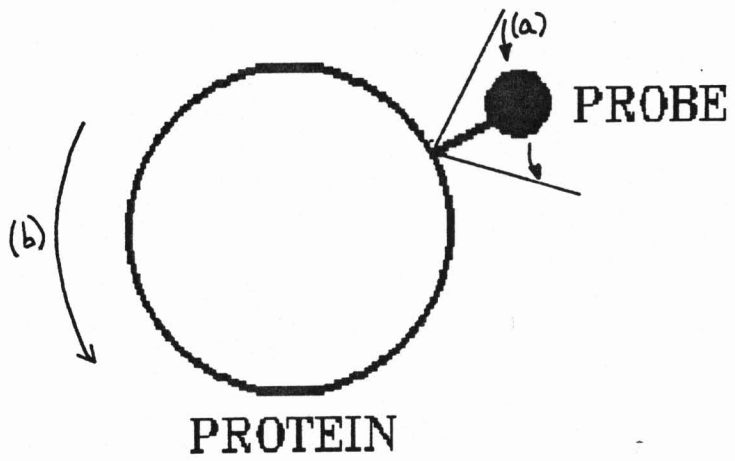

Figure 8. Diagram illustrating (a) the local motion of the probe and (b) the global Brownian rotation of the complex. The complex moves very slowly relative to the small probe, although the probe's motion is restricted by the covalent bond to the protein.

The observed steady-state anisotropy is also dependent upon the lifetime (τ) of the fluorophore as illustrated by an equation first derived by Perrin to describe the depolarization of the fluorescence of organic molecules represented as rigid particles allowed unrestricted motion[3]:

$$\frac{A_0}{A} - 1 = \frac{\tau}{\tau_c} \qquad (3)$$

where A is the measured anisotropy of the macromolecule, A_0 is the limiting anisotropy for the fluorophore (or the anisotropy due to emission without reorientation), τ is the lifetime of the fluorophore and τ_c is the correlation time (or tumbling time) for the macromolecule. The Perrin equation quantifies the effects of rotational diffusion on anisotropy and shows that a change in the fluorescence lifetime of the fluorophore will alter the anisotropy value. The length of time in which the anisotropy is monitored is the lifetime of the DNS. The only motions observable in the fluorescence lifetime of the DNS are the global motions of the macromolecule and the local probe motions. If the DNS lifetime becomes shorter, there is less time between absorption and emission for rotation of the macromolecule.

---

[3]This is one form of the Perrin equation. Others can be found in several sources, including: Perrin, 1926; Weber, 1953; Lakowicz, 1983; Fernando, 1991.

The observed anisotropy value is then artificially higher than if the lifetime had remained unchanged. The opposite result is obtained if the probe lifetime increases under the test conditions. In this way, changes in DNS lifetime which occur with oligomer dissociation can change the dilution curve profile. Therefore, lifetime changes, induced, for example, by subunit dissociation, can influence the shape of an anisotropy dilution profile.

Brownian motion or rotation in solution is directly influenced by the size of the macromolecule. Larger complexes will rotate more slowly in solution than smaller complexes (Figure 9). The correlation time is therefore directly related to complex size.

The primary advantage of the fluorescence anisotropy method over other methods of the rotational diffusion properties of proteins is that it allows investigation of systems at equilibrium. The ease and accuracy of anisotropy determinations in a variety of ionic environments, concentration and temperature ranges augment the utility of the technique. In a fluorescence anisotropy experiment, only the complexes with specific dipole orientations are excited by the incident polarized light, not the entire population. As a result, the population remains randomly oriented at all times. The process of diffusion is

therefore maintained by the mixing of two types of molecules rather than the existence of an orientation gradient of the population (Weber, 1966). If the size of the macromolecule under test does not change with a change in concentration, there is no equilibrium involved in the concentration range considered and no change in the correlation time is observed. Any protein concentration dependent anisotropy change or change in any other fluorescence parameter (lifetime, color, normalized intensity) is necessarily the result of a shift in protein subunit equilibria. This is the result of changes in the environment of the amino acids at the subunit boundary upon dissociation as well as the conformational rearrangements which can occur following the separation of the subunits. In an aqueous environment, the change in the interface environment from bound (solvent excluded) to unbound (solvated) is extensive.

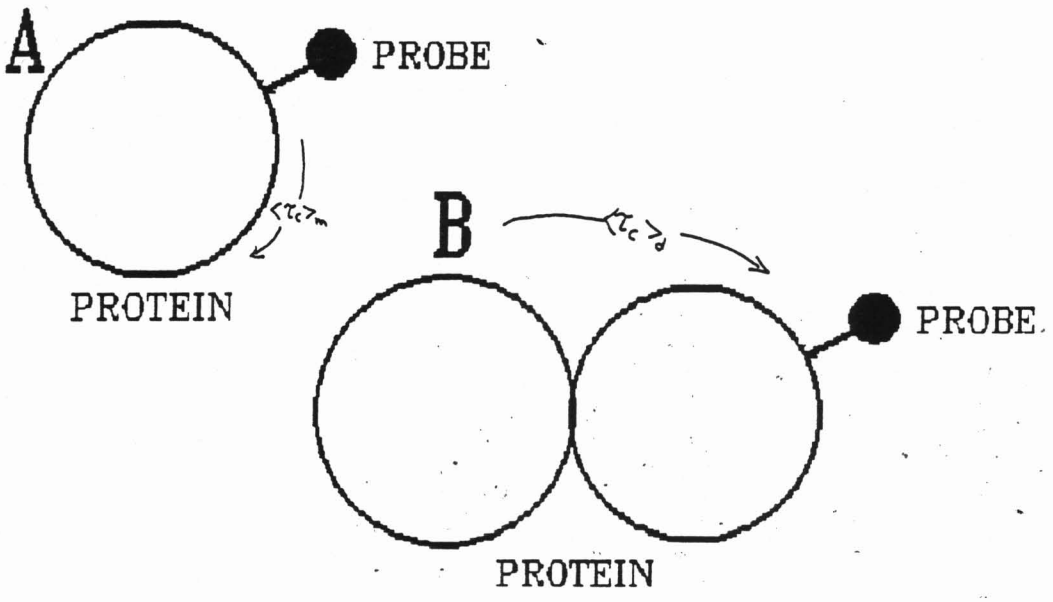

Figure 9. Schematic representation of the correlation time, $< \tau_c >$ and how , from differences in $< \tau_c >$, variation in protein size or aggregation state can be observed. (A) depicts a monomeric protein, with an attached fluorescence probe. The correlation time for the monomeric protein is $< \tau_c >_m$ (B) shows the same protein as a dimeric complex following association with another protein. The correlation time for the dimer is $< \tau_c >_d$. $< \tau_c >_m > < \tau_c >_d$, because the size of the monomer is less than that of the dimeric complex, allowing the smaller protein to rotate more freely in solution.

B. Harmonic Fluorescence Spectroscopy and Multi-exponential Lifetime Determinations

When fluorescence is excited by a sinusoidally modulated signal at high frequency, the fluorescence signal is also modulated sinusoidally. The finite persistence of the excited state (or lifetime) of the fluorophore results in a phase delay and demodulation of the fluorescence relative to the excitation (Figure 10). The emission is delayed (by the timespan of the fluorophore lifetime) relative to the excitation light. Because of the delay, the emission is out of phase with the excitation light. The value of this phase shift is Φ. The emission is also prevented from returning fully to the unexcited intensity because the fluorophore is excited again by another incident pulse of light before all the energy can be released. The emission signal is demodulated relative to the excitation signal for this reason. This means the emission intensity is decreased in amplitude relative to the excitation signal intensity. Demodulation increases as the incident modulated signal frequency increases. The modulation ratio, **M**, is the ratio of the signal amplitude at frequency ω to the average signal (the AC/DC ratio).

The impulse response function of the fluorescence decay determines the frequency-dependent phase angle and

modulation of the emission. Both are measured relative to the modulated excitation at a number of frequencies chosen to allow these quantities to change gradually over the widest possible range. The choice of excitation frequencies is important. The time scale of the emission process in the fluorescence system dictates the number and choice of frequencies used. The inverse of the lifetime of the fluorophore is included in the modulation frequency range. In the case of heterogeneous decay, the inverse of all component lifetimes should be within the range of frequencies used. In phase fluorometry, data are accumulated and averaged at a given frequency until the established standard deviation is obtained. From the phase and modulation of the emission relative to the incident light, the fluorophore lifetime or lifetime components can be calculated.

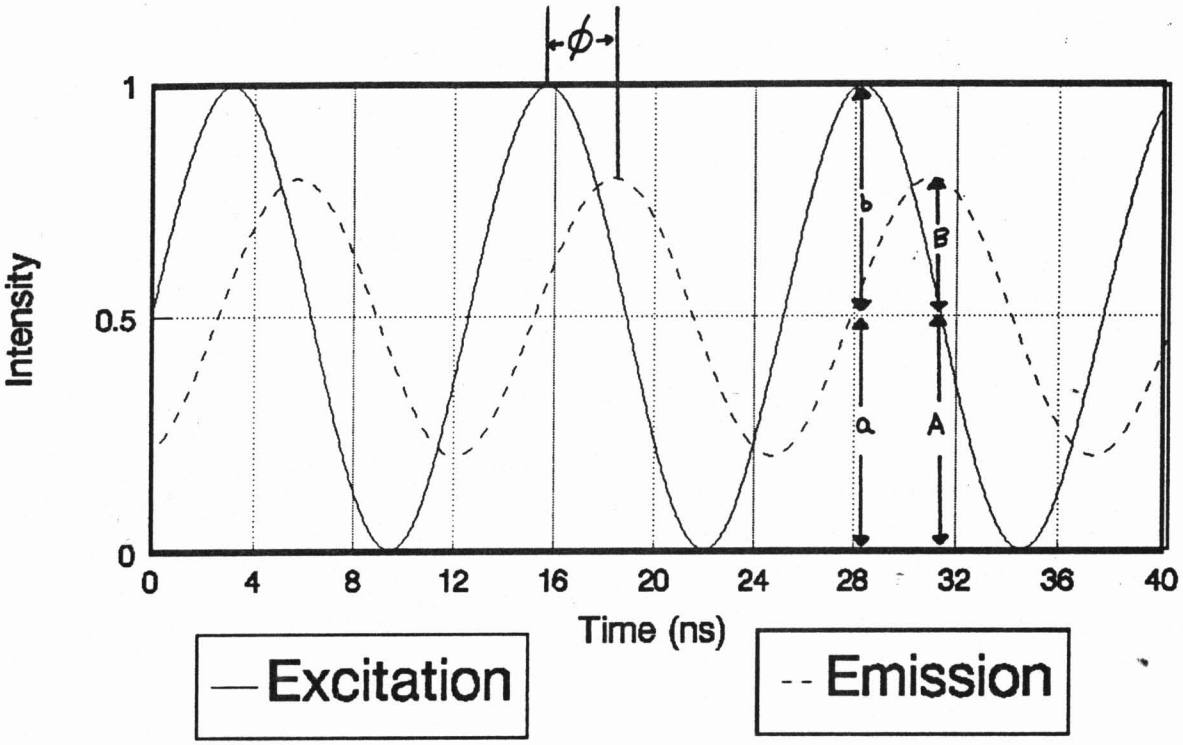

Figure 10. Illustration of phase shift and demodulation between sinusoidally modulated exitation light (-) and the subsequent emission light (--). Because of the finite fluorophore lifetime, there is a shift in the phase angle Φ (in degrees) and the emission light is demodulated, or diminished in overall intensity, as illustrated by the modulation ratio, M=(B/A)/(b/a).

The impulse response function or intensity decay function for a fluorophore with a single exponential decay is:

$$I(t) = I_0 \exp(-t/\tau) \qquad (4)$$

where I_0 is the initial intensity (at time 0), **t** is the time following excitation, and τ is the fluorophore lifetime. The phase angle, Φ , and modulation ratio, **M** are related to the fluorescence intensity decay function at a given modulation frequency ω by:

$$\tan \Phi = \omega\tau_p \qquad (5)$$

$$M = [1+\omega^2\tau_m^2]^{-1/2} \qquad (6)$$

where the measurable quantities Φ and **M** are related to the lifetime of the fluorophore. These relationships for Φ and **M** are obtained from the Fourier transform of the intensity decay function, **I(t)**. The Fourier transform gives the frequency response of the fluorophore, which is separated into real and imaginary parts, **G** and **S** , respectively:

$$G = \int^{\infty} I(t) \cos \omega t dt / \int^{\infty} I(t)\, dt \qquad (7)$$

$$S = \int^{\infty} I(t) \sin \omega t dt / \int^{\infty} I(t)\, dt \qquad (8)$$

The calculated values of the phase angle, Φ_c, and modulation, M_c, at each modulation frequency are given by:

$$\tan \Phi_c = S/G \qquad (9)$$

$$M_c = (S^2 + G^2)^{1/2} \qquad (10)$$

(Weber, 1977). Equations 5 and 6 are obtained by solving the integrals in equations 7 and 8 and substituting the resultant expressions into equations 9 and 10.

If the phase (τ_p) and modulation (τ_m) lifetimes at all frequencies are the same, the decay is a single exponential (the coincidence of the phase and modulation lifetimes at all modulation frequencies being a necessary and sufficient condition for this to be true, Gratton *et al.*, 1984a). If the phase and modulation lifetimes differ, the data must be analyzed to fit for a multi-exponential decay.

For multi-exponential decay, the fluorescence intensity decay after an excitation pulse is expressed in the form:

$$I(t) = \sum_i \alpha_i e^{(-t/\tau_i)} \qquad (11)$$

where **I(t)** represents the fluorescence intensity observed at time t after excitation as before, however components

contributing to the observed decay are considered. α_i is the pre-exponential concentration factor and τ_i is the lifetime for the *i*th emitting component of the decay. The fractional contribution to the total fluorescence intensity, f_i, for the *i*th emitting component is related to its corresponding pre-exponential factor as follows:

$$f_i = \frac{\alpha_i \tau_i}{\sum_i \alpha_i \tau_i} \qquad (12)$$

The average fluorescence lifetime $<\tau>$ of the DNS is given by:

$$<\tau> = \sum_i f_i \tau_i \qquad (13)$$

and can vary with changes in test conditions if the probe environment is altered.

The phase and modulation data collected at each modulation frequency are used to calculate the lifetime or lifetime components and their fractional intensity contributions. This enables calculation of the lifetime/lifetime components in the frequency domain rather than the time domain. For a multi-exponential decay, Equation 11 can be substituted into

Equations 7 and 8 to obtain expressions for **G** and **S** in terms of the preexponential factors and component lifetimes:

$$G = \sum_i \alpha_i \tau_i (1 + \omega^2 \tau_i^2)^{-1} / \sum_i \alpha_i \tau_i \qquad (14)$$

$$S = \sum_i \alpha_i \omega \tau_i^2 (1 + \omega^2 \tau_i^2)^{-1} / \sum_i \alpha_i \tau_i \qquad (15)$$

The phase and modulation data are analyzed by simulation with the estimated values of α_i and τ_i being those which minimize chi-square, the error weighted sum of the squared deviations between the measured and calculated values. The function which is minimized is:

$$\chi^2 = \sum_{\omega} [(\Phi_{m,\omega} - \Phi_c)^2 / (\sigma\Phi_{m,\omega})^2 + (M_{m,\omega} - M_c)^2 / (\sigma_{M_{m,\omega}})^2] \qquad (16)$$

(Gratton, *et al.*, 1984b), where $\Phi_{m,\omega}$ and $M_{m,\omega}$ are the measured values of the phase and modulation at frequency ω; $\sigma\Phi_{m,\omega}$ and $\sigma_{M_{m,\omega}}$ are the random errors (standard deviations) of the phase and modulation measurements, respectively, and are selected based on the experimental conditions (input parameters). Φ_c and M_c are calculated phase angle and modulation values at each frequency ω and are obtained from the curve fit. For a good fit, the value of the reduced χ^2 (χ^2_R) should be close to one, where:

$$\chi^2_R = \chi^2/\upsilon \qquad (17)$$

υ is the degrees of freedom, defined as 2Nq-p

N is the number of modulation frequencies,

q is the number of emission wavelengths (q=1 in this work) and

p is the number of parameters used for the fit.

V. DATA PRESENTATION

In all cases, unless otherwise noted, the TR concentrations are given in terms of dimer. Unless otherwise noted in figure legends, the data represent the average +/- 1 standard deviation of 3 experiments. The composite $<\tau_c>$ results, +/- one standard deviation, have been used to depict the variability arising from differences in TR preparation, TR handling and the stability of the protein subunit interactions under the buffer conditions investigated. The standard deviations in studies which involve biological macromolecules are meaningful in the context of evaluation of variability between experimental days only in a very general sense. Small differences in protein handling and differences between protein purifications can alter the protein performance in dilution studies. The error bars in this presentation of the study results demonstrated the consistency of handling the protein and in the protein purifications. The error bars can also be interpreted as evidence that, under certain solution conditions, the protein was subject to more variability in oligomeric state (as will be discussed in the Results section). No attempt has been made to use the standard deviations outside of these general interpretations. Error bars are shown in Figures 20 to 24 and omitted thereafter.

VI. RESULTS

A. Characterization of TR-DNS

TR was purified and labeled as described. All of the TR aliquots used for these experiments had labeling ratios of 0.5-1.5 DNS molecules per TR dimer. The labeling ratio was kept low to minimize the effect of the chemical modification on the complex (approximately 1 DNS per TR dimer). DNS labeling of the *lac* repressor has been studied to ascertain the influence of the covalently bound probe on the protein (Hsieh and Matthews, 1985); this study demonstrated that high labeling ratios altered protein activity (4.5 molecules DNS per *lac* monomer decreased non-specific binding; 0.5 molecules DNS per *lac* monomer decreased specific DNA binding. The labeled lysine residues in the *lac* repressor were found to be in the DNA binding region, explaining the observed loss in activity.). Work in the laboratory of K. Matthews (Rice University) was done to test the binding of TR and TR-DNS to operator DNA fragments. The method of Carey (1988) was used. No differences in binding were found based on visual observation of P^{32} autoradiograms in either the band mobility, band width, or band intensity (personal communication), indicating no observable detrimental changes in the DNA binding result from the DNS label. Fernando and Royer (1992) compared unlabeled and labeled TR in an HPLC

size exclusion experiment and ascertained that the DNS, at a labeling ratio of less than or equal to 1 DNS per TR dimer did not induce aggregation.

In light of the various experiments done on TR, it was important to ascertain where the DNS label covalently bound to TR. To evaluate the DNS labeling, a mild α-chymotryptic digest was carried out to divide TR into sections, allowing isolation of TR fragments containing the DNS label by observation of the fluorescence of each fragment. The eluate of the 250 mL Sephadex G-50 (fine) (molecular sieve) column and the fractions were evaluated using absorbance data at 280 nm to identify protein fractions. Fluorescence intensity data were used to determine fractions bearing the dansyl chloride label. Under the conditions of the digest (Carey, 1989, and Figures 11 and 12) the number of potential digest sites is reduced from all the possible α-chymotrypsin sites, presumably the result of the folded conformation of the native TR dimer affording protection from cleavage to many sites. This protection could result from sites buried in the protein core or sites sterically inaccessible to the enzyme. The digest proceeds in a time-dependent manner on the ApoR (Carey, 1988). Cleavage of TR was therefore expected to occur first between residues 6 and 7. After cleavage between residues 6 and 7 was almost complete, cleavage between residues 70 and 71 began.

Therefore, five protein fragments were anticipated: (1) the native (undigested) TR; (2) the "armless TR" (TR missing the first 6 amino acid residues); (3) a fragment of about 64 amino acids (the "N" fragment, residues 7 to 70; Tasayco and Carey, 1992); (4) a fragment of 37 amino acids (the "C" fragment, residues 71 to 108; Tasayco and Carey, 1992) and (5) the 6 amino acid amino terminal "TR arms". Five maxima were observed by absorption spectroscopy at 280 nm, with the last peak eluting far beyond the other four. This last peak also had a fluorescence intensity that far exceeded the peaks attributed to the two largest cleavage fragments (Figures 11 and 12). Comparison of the armless TR peak (peak 2) between Figures 11 and 12 shows that increased enzyme digestion of TR diminishes the fluorescence observed relative to native TR (peak 1), further supporting the amino termini of TR as the primary binding site for DNS. The lack of fluorescence observed for the N and C TR fragments and the loss of fluorescence observed for the armless TR relative to native TR concommitant with increasing absorbance (Figures 11 and 12) are consistent with DNS being bound to the TR amino termini. SDS-PAGE (denaturing gel electrophoresis) was run to further characterize the products of the digest. The gels run demonstrated loss of a band with the mobility of the native TR and could be interpreted as showing the three large fragments expected from the digest (Figure 13). Further characterization of

the digest products will require the use of a less common polyacrylamide gel technique which was developed to obtain molecular weight estimations of smaller protein fragments, but has not been used with TR. This gel system will be optimized in future experiments.

These experiments demonstrate that the bulk of the DNS labeling is on the amino terminus rather than the lysine residues in the protein interior. Our initial hypothesis was that a lysine residue within the TR polypeptide was labeled. In support of the findings from the present work, Molecular Probes, Inc (Eugene, Oregon) identifies DNS as an amino-terminal labeling probe. In addition, at physiological pH, the α-amino group of a polypeptide chain is a much weaker base (pK_a about 7) than the ε-amino group of lysine (pK_a about 10). At pH 7, more than 99% of the lysine residues are protonated nucleophiles, which are totally unreactive. Therefore, the effective concentration of lysine decreases as the pH is lowered from 10. The pH must be greater than 9.0 to increase the concentration of unprotonated lysine amines to any significant extent (Haugland, 1983). Since labeling is done at pH 8.0, the amino terminus would be largely unprotonated, the lysines being largely protonated, leaving the amino terminus to react most readily with DNS under the labeling conditions used.

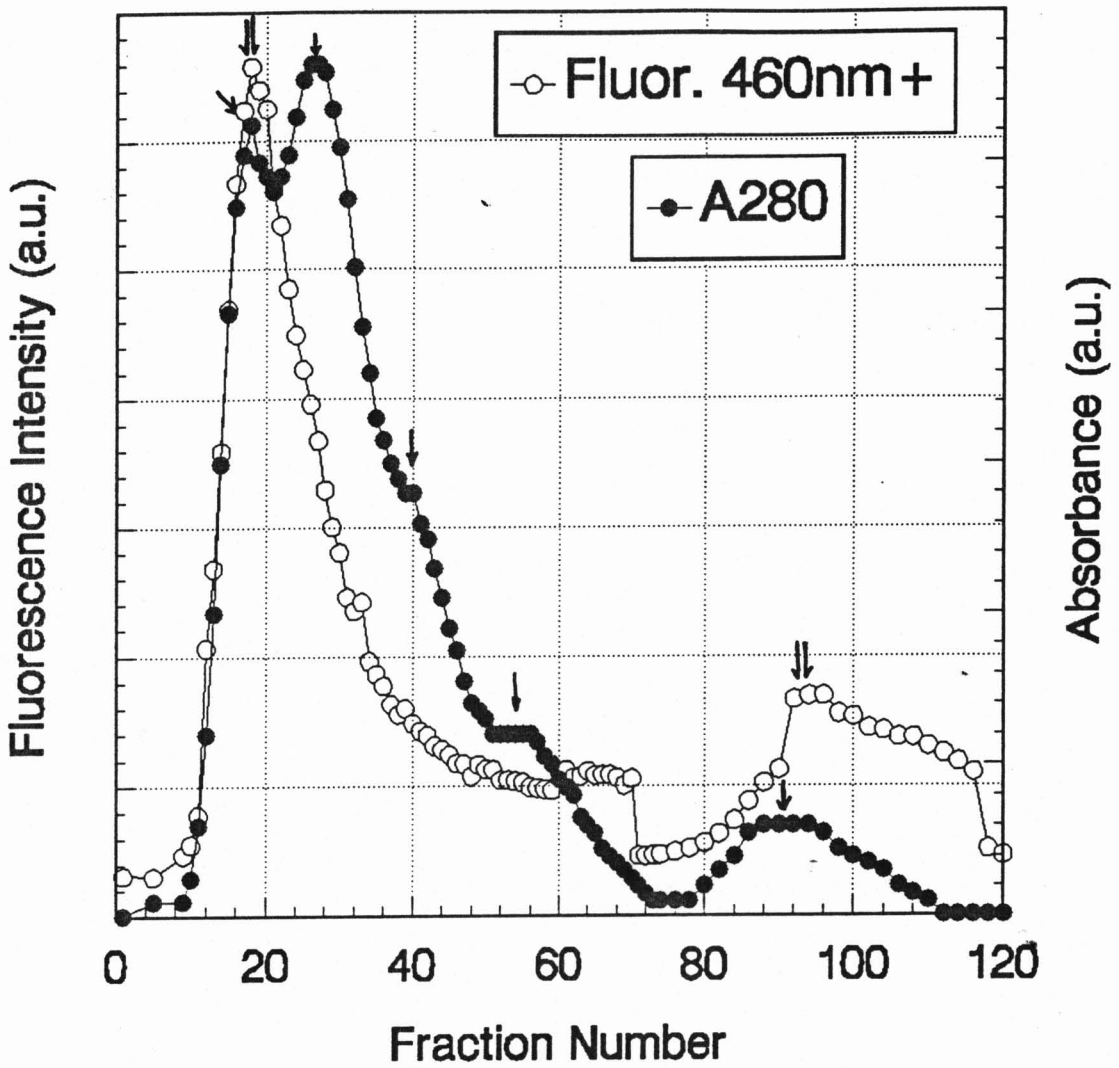

Figure 11. Elution profile from Sephadex G-50 (fine) molecular sieve column separation of TR-DNS following mild α-chymotrypsin digestion. DNS labeling of TR was carried out as described in Materials and Methods using four 1-mL TR aliquots. Each 1-mL aliqout was labeled individually. The labeled TR fractions from the Sephadex G-25 column (separating free DNS from TR-DNS) were collected and concentrated. The labeling ratio was 0.96 for the combined sample. TR-DNS was dialyzed overnight in 10 mM sodium phosphate buffer with 100 mM NaCl, pH 7.6. α-chymotrypsin which had an $A_{280} \approx 0.27$ was added to the protein and the digestion was allowed to proceed for 2 hours. 7.6 M urea (0.5 mL urea per 1 mL protein) was added. The protein was then run over the Sephadex G-50 column to separate the digest products. The eluate was collected in 2-mL fractions.

Black circles denote the absorbance profile of the eluate fractions, which shows 5 absorbance maxima (see single arrows). Open circles show the fluorescence profile whcih has only two maxima (double arrows). 1 = TR-DNS, undigested. 2 = TR-DNS, minus 6 amino terminal amino acids (des-6 TR). 3 = N fragment (residues 7-70). 4 = C fragment (residues 71-108). 5 = 6 amino acid amino terminal "arms". Fluorescence maxima are centered over peaks 1 and 5, corresponding to intact TR-DNS and the amino terminal arms, respectively.

a.u. arbitrary units

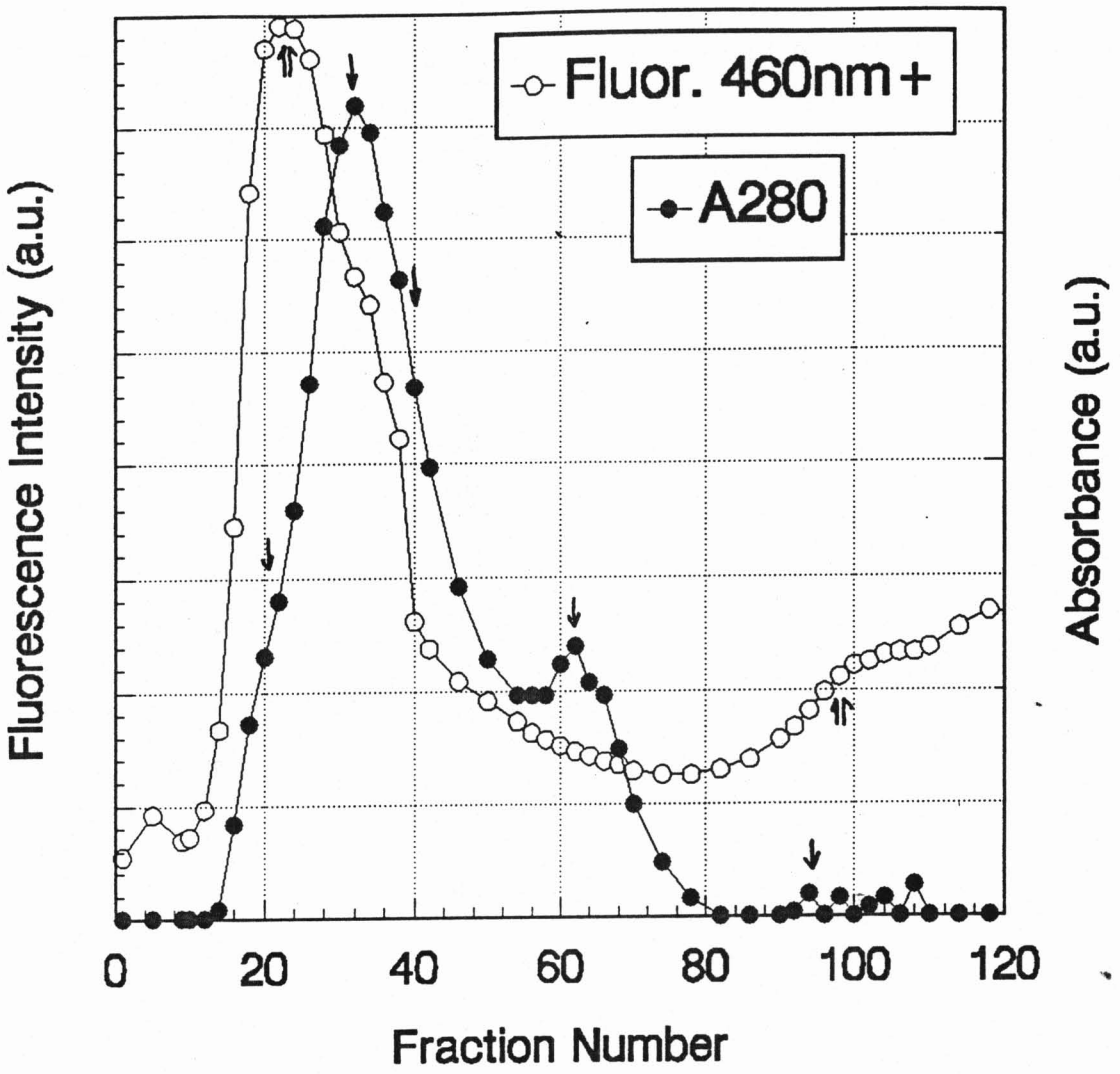

Figure 12. Elution profile from Sephadex G-50 (fine) column separation of TR-DNS following mild α-chymotrypsin digestion. Experimental procedures and conditions are described in Figure 27 legend. The labeling ratio of the composite TR sample was 1.0. In this experiment the amount of α-chymotrypsin used was increased: the A_{280} was ≈ 0.54. The digestion time was the same, 2 hours. This experiment was done to show that intact TR (Peak 1) and des-6 TR (Peak 2) would be diminished in absorbance intensity with increased enzyme.

Black circles denote the absorbance profile of the eluate fractions. Peak 1 is diminished to a shoulder, the largest peak being assymetrical and coveringthe areas of peaks 2 and 3 , which were distinct peaks in Figure 27. Peak 4 is well defined and peak 5 is diminished relative to the peak in Figure 27. Although it seems contradictory that Peak 5 is smaller, rather than larger (as more cleavage of the arms occurs from the intact repressor with increased enzyme) the 6 amino acid arm is a target for the α-chymotrypsin once it is cleaved from the protein and is subject to rapid degradation. Open circles show the fluorescence profile.

Note there is little intact TR remaining and that the absorbance intensity of des-6 TR is reduced ralative to the fluorescence profile. Fluorescence maxima remain centered over the intact TR-DNS (Peak 1) and the amino terminal arms (Peak 5).

a.u. arbitrary units

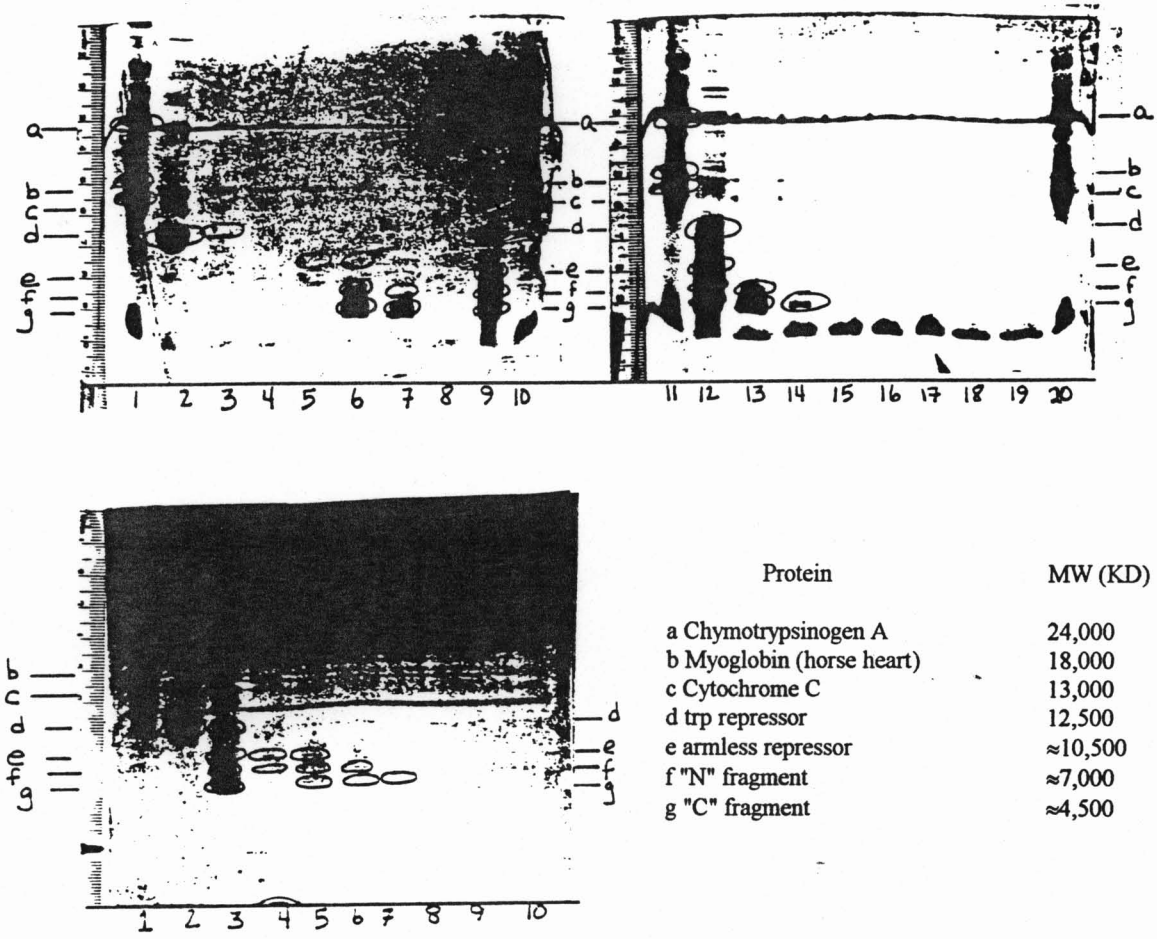

Protein	MW (KD)
a Chymotrypsinogen A	24,000
b Myoglobin (horse heart)	18,000
c Cytochrome C	13,000
d trp repressor	12,500
e armless repressor	≈10,500
f "N" fragment	≈7,000
g "C" fragment	≈4,500

Figure 13. Photographs of polyacrylamide electrophoresis gels, bands stained with silver. Discontinuous gels, (3% acrylamide stacking and 15% acrylamide resolving gels) with sodium dodecyl sulfate buffer (pH 8.3), were used.

A: Gel from chymotryptic digest shown in Figure 27. Lanes 1, 10, 11, and 20: molecular weight standards. Lane 2: TR-DNS, undigested. Lanes 9 and 12: digested TR-DNS, not run over molecular sieve column. Lanes 3-8 and 13-19: Fractions from Sephadex G-50 column, the fraction numbers can be compared directly with fraction numbers on the x-axis of Figure 27. Lane 3: Fraction 18. Lane 4: Fraction 20. Lane 5: Fraction 28. Lane 6: Fraction 39. Lanes 7 and 13: Fraction 49. Lanes 8 and 15: Fraction 57. Lane 14: Fraction 54. Lane 16: Fraction 64. Lane 17: Fraction 67. Lane 18: Fraction 88. Lane 19: Fraction 90.

B: Gel from digest shown in Figure 28. Fraction numbers can be compared directly to Figure 28. Lane 1: molecular weight standard. Lane 2: TR-DNS, undigested. Lane 3: TR-DNS following digestion, no separation of fragments on molecular sieve column. Lane 4: Fraction 26. Lane 5: Fraction 32. Lane 6: Fraction 40. Lane 7: Fraction 50. Lane 8: Fraction 62. Lane 9: Fraction 64. Lane 10: Fraction 100.

Note that there is one main band for undigested TR-DNS (lane 2, A and B). This band is greatly diminished in intensity and width following digestion (A, Lanes 9 and 12. B, Lane 3.) Two bands of lesser intensity are observed in different fractions from the chymotryptic digests (Labeled f and g on the gel photographs). The 6 amino acid amino terminal arms are of insufficient molecular weight to be retained on the gels.

B. Dilution Studies with TR-DNS

1. Anisotropy Experiments

Anisotropy values arise from depolarization of the emission dipole from the limiting value due to the global tumbling of the TR as well as local motions of the DNS probe. In all cases, under all conditions, dilution of TR-DNS in the concentration of 0.05 - 60 μM TR-DNS resulted in a decrease in the anisotropy, indicating oligomer dissociation, except at very high concentrations of corepressor, L-tryptophan (4.0 mM), and salt (200 mM KCl) where the anisotropy remained relatively unchanged. The dilution/anisotropy profiles are influenced by the probe lifetime, which indicates the local environment of the DNS changes. Determination of the DNS lifetime under the different solution conditions and upon TR dilution is required to allow evaluation of the macromolecular size of the complex. Therefore, dilution/anisotropy profiles do not provide results which can be compared among different solution test conditions. Figures 14 and 15 illustrate typical dilution/anisotropy curves for TR-DNS in the presence and absence of corepressor tryptophan. The results of the individual anisotropy experiments are shown graphically in Appendix A arranged by pH, salt concentration and date of experiment.

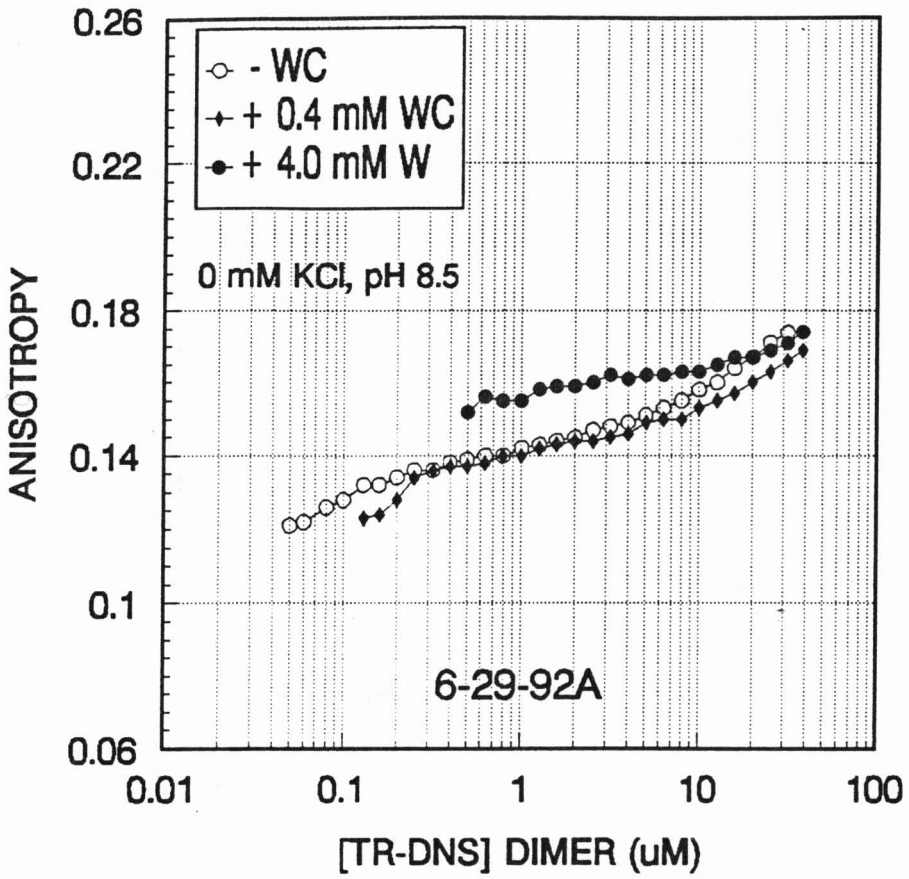

Figure 14. Dilution/anisotropy curve for TR-DNS in a 10 mM potassium phosphate buffer, 0.1 mM EDTA (standard buffer), pH 8.5, no added KCl, in the absence (-W), and presence (+0.4 mM W and + 4.0 mM W) of corepressor. Note that the curves are fairly similar in shape and the overall change in anisotropy under these conditions is relatively small.

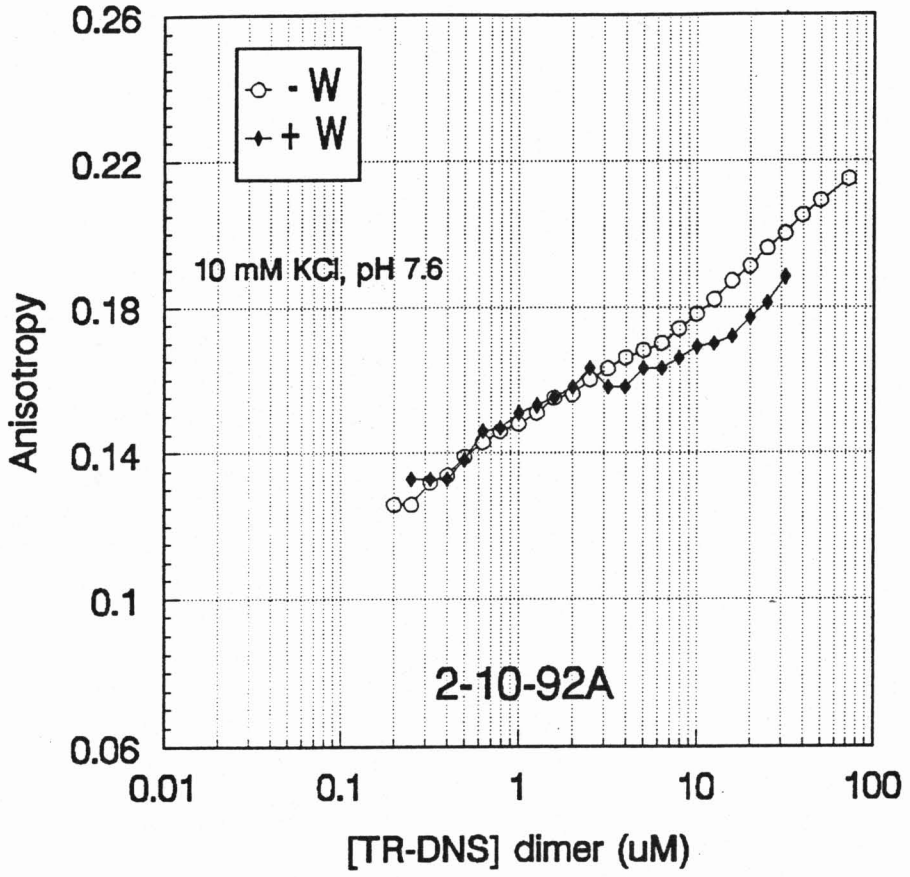

Figure 15. Dilution/anisotropy curves for TR-DNS in the standard buffer (see Figure 14), pH 7.6, 10 mM KCl, in the absence (-W) and presence (+ 0.4 mM W) of corepressor. In comparison with Figure 14, note the wider spread in anisotropy values with dilution of the protein and in the presence of corepressor.

2. Lifetime Experiments

Lifetimes were measured as a function of TR-DNS concentration under all of the test buffer conditions investigated. The TR-DNS data fit well to a triple-exponential intensity decay function in which the lifetimes were linked for three concentrations for each sample and the relative contributions of the three exponential components to the lifetimes were allowed to vary. The triple-exponential decay results were compared to double-exponential decay results. The chi-square values were improved (decreased) with use of a triple-exponential decay and the data fit was also better as evidenced by residuals which were randomly distributed and closer to zero. This is consistent with previous work using other DNS labeled proteins (Royer, *et al.*, 1989 and 1990). Multi-exponential decays of fluorescence are not generally understood and can have origins related to conformational isomers of the protein, time-dependent relaxation around the fluorophore, or intrinsic heterogeneity of the probe (Lakowicz, 1983). Heterogeneous emitting populations are expected in biological systems (Jameson and Gratton, 1983). Although the photophysics of DNS decay are not completely understood, it is understood that the polarity of the DNS environment affects its emission. The DNS lifetime is shortened in water or other polar environments relative to more apolar

solvents. This allows the probe to be used to monitor changes in DNS environment polarity (Royer, *et al.*, 1990). The triple-exponential intensity decay observed for DNS bound to macromolecules is thought to arise both from solvent-induced heterogeneity of the electronic states of the DNS (Lambooy, et al., 1982; Guest et al., 1991) as well as the intrinsic dynamically based heterogeneity of fluorophores in macromolecules (Alcala et al., 1987). Changes in the environment of the DNS probe which are dependent upon the protein concentration, regardless of their photophysical origin, result from the change in the environment of the probe upon dissociation of subunits.

The fractional contributions and three lifetime components contributing to the DNS lifetime decay are calculated using the Globals Unlimited software. The triple-exponential decay results (f_i and τ_i values), as well as the calculated average DNS lifetimes for all the experimental conditions investigated, are in Appendix B.

Increasing both L-tryptophan and salt concentration resulted in a decrease in the DNS lifetime (Table I). DNS lifetime generally decreased as a function of decreasing TR-DNS concentration, although the effect was smaller than that observed for either increasing salt or added corepressor (Table II). The decrease in DNS lifetime indicates an

Table I. Effect of pH, salt concentration (KCl) and corepressor (W) on DNS lifetime at TR-DNS concentration of 10 μM. The mean $<\tau>$ (+/- 1 SD) of three to four experiments are reported for the 0 and 0.4 mM corepressor tests. Single experiments were carried out for solutions containing 4.0 mM corepressor, hence, no standard deviations are reported. Results for individual experiments are given in Appendix B.

		$<\tau>$ (ns)		
pH	**[KCl] (mM)**	**0 mM W**	**0.4 mM W**	**4.0 mM W**
6.0	0	16.79 (0.199)	14.29 (0.832)	11.29
	50	16.28 (0.127)	12.49 (0.887)	10.41
	200	13.90 (0.113)	9.40 (0.135)	8.67
7.6	0	16.24 (0.026)	14.26 (0.493)	11.58
	50	15.30 (0.108)	11.48 (0.115)	10.43
	200	13.79 (0.191)	9.84 (0.914)	9.40
8.5	0	15.96 (0.249)	14.26 (a)	11.30
	50	15.51 (0.194)	12.75 (0.116)	10.60
	200	13.76 (0.700)	10.21 (0.513)	6.97

(a) Sample lost in preparation; mean of two values reported.
SD Standard Deviation

Table II. Effect of TR-DNS concentration on DNS lifetime in the absence and presence of corepressor, W. Results are from one experiment because the high sample concentration used for lifetime measurements was determined by the available protein. Therefore, average results could not be computed. A complete tabulation of all experimental lifetime data is in Appendix B.

		No Salt		50 mM KCl		200 mM KCl	
pH	[Corepressor] (mM)	[TR-DNS]	$\langle\tau\rangle$ (ns)	[TR-DNS]	$\langle\tau\rangle$ (ns)	[TR-DNS]	$\langle\tau\rangle$ (ns)
6.0	0	27.1	16.68	9.70	16.28	31.4	14.24
		10.0	16.56	5.00	16.17	10.0	13.97
		2.00	16.10	1.94	15.76	2.00	13.71
	0.4	28.3	13.89	20.0	12.49	25.0	9.53
		10.0	13.71	9.12	13.34	10.0	9.39
		2.00	13.19	1.82	11.28	2.00	9.25
7.6	0	30.0	16.34	28.0	15.61	34.1	13.86
		10.0	16.25	10.0	15.42	10.0	14.01
		2.00	15.63	2.00	14.98	2.00	13.72
	0.4	24.3	14.41	21.1	11.71	26.9	10.08
		10.0	14.82	10.0	11.47	10.0	10.84
		2.00	14.67	2.00	11.11	2.00	11.12
8.5	0	31.8	16.31	31.4	16.02	28.1	14.24
		10.0	16.01	10.0	15.73	10.0	14.12
		2.00	15.75	1.00	15.26	2.00	14.01
	0.4	27.8	14.41	30.5	13.04	20.0	10.19
		10.0	14.57	10.0	12.86	10.0	10.34
		2.00	14.28	1.00	12.43	2.00	10.10

increase in the solvent exposure of the probe, which is consistent with oligomer dissociation. This implicates a change in the amino termini environment with changes in the concentration of TR-DNS and salt, as well as with added corepressor.

Increasing pH did not affect the DNS lifetime until 200 mM KCl was present in the test buffer, hence the anisotropy profiles were not influenced. At this salt concentration, in the absence of corepressor and in the presence of 0.4 mM corepressor, lifetimes were 0.5 to 1 ns *longer* for DNS in pH 8.5 solutions compared to solutions of pH 6.0 or pH 7.6. This indicates less exposure of the DNS to solvent at pH 8.5. However, in solutions containing both 200 mM KCl and 4.0 mM L-tryptophan, the DNS lifetimes were approximately 2 ns *shorter* at pH 8.5 than in solutions of pH 6.0 or 7.6. This means that the influence of the corepressor concentration in solution overcomes the influence of salt in the latter case, enhancing oligomer dissociation.

Representative multi-frequency dilution/lifetime data for TR-DNS in the absence and presence of corepressor (0.4 mM L-tryptophan) are in Figures 16 and 17 for the same samples whose anisotropy data are shown in Figures 14 and 15. Note the shift of both the phase and modulation curves to higher frequency for tests done in the presence of L-tryptophan.

This indicates a shorter lifetime for the DNS in the presence of corepressor. The influence of the lifetimes on the anisotropy results can be observed by comparison of Figures 14 and 15 with Figures 18 and 19. Note that the curve shapes are preserved, but the dilution/correlation time curves with L-tryptophan in the test buffer system shift to significantly lower values of $<\tau_c>$ relative to the dilution curve in the absence of L-tryptophan as a result of the shorter DNS lifetime in the presence of the corepressor. There is a substantial difference in the the correlation times of TR-DNS in the presence of L-tryptophan at high TR concentrations relative to the correlation times of high TR-DNS concentrations in the absence of L-tryptophan, which is not evident in the dilution/anisotropy profiles. The dilution/ correlation time curves in both the absence and presence of corepressor have essentially the same plateaus at the low TR_d concentrations.

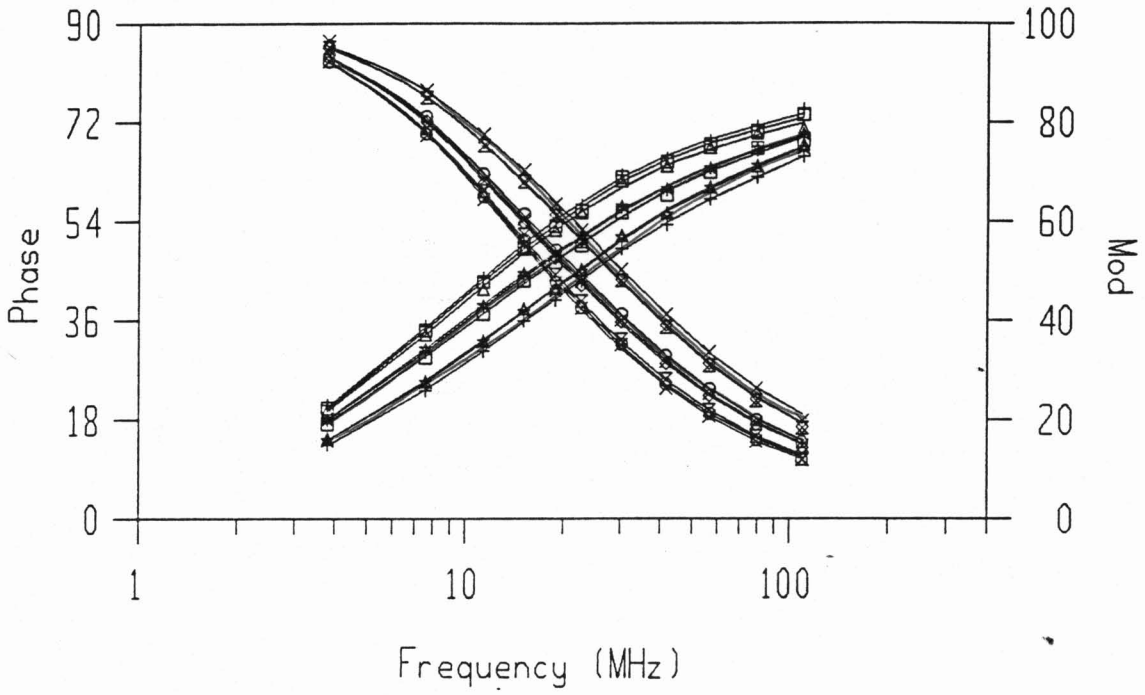

Figure 16. Phase and modulation curves for the protein sample whose dilution/anisotropy curves are shown in Figure 14. Note the 3 distinct groups of curves. The curves shifted farthest to the left (black) are the result of the dilution/lifetime experiments without corepressor in the test buffer (ApoR). The middle group of curves (red), are from dilution/lifetime experiments with test buffer containing 0.4 mM W. The curves shifted farthest to the right (blue) are from dilution/lifetime experiments with 4.0 mM W in the test buffer. Note the shift to higher frequencies of the curves with addition of corepressor and increasing corepressor concentration. This indicates the DNS lifetime is shorter in the presence of L-tryptophan.

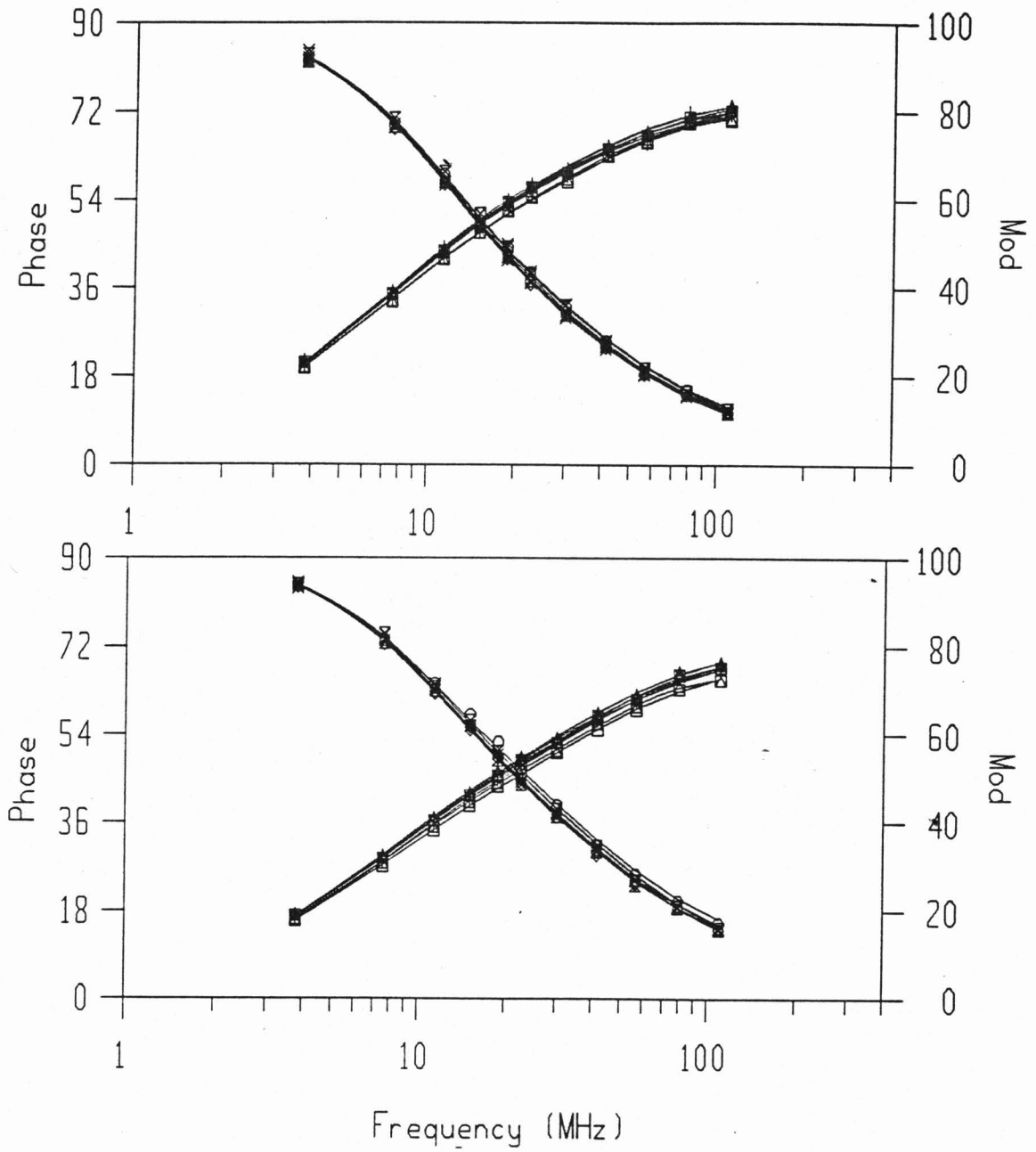

Figure 17. Phase and modulation curves for the protein sample with dilution/anisotropy results shown in Figure 15. Here the TR-DNS profiles in the absence **(A)** and presence **(B)** of corepressor are shown separately to allow evaluation of the variability in the dilution/lifetime experiments. There is more spread to the curves in the presence of W (0.4 mM) than in the absence. Nine curves are included on both **(A)** and **(B)**, 3 curves from each of 3 separate dilution/lifetime experiments carried out on different days and with different protein fractions. The phase shifts are increasing (as shown by the curves denoted C) and the emission light is decreasing (curves denoted D) with increasing frequency.

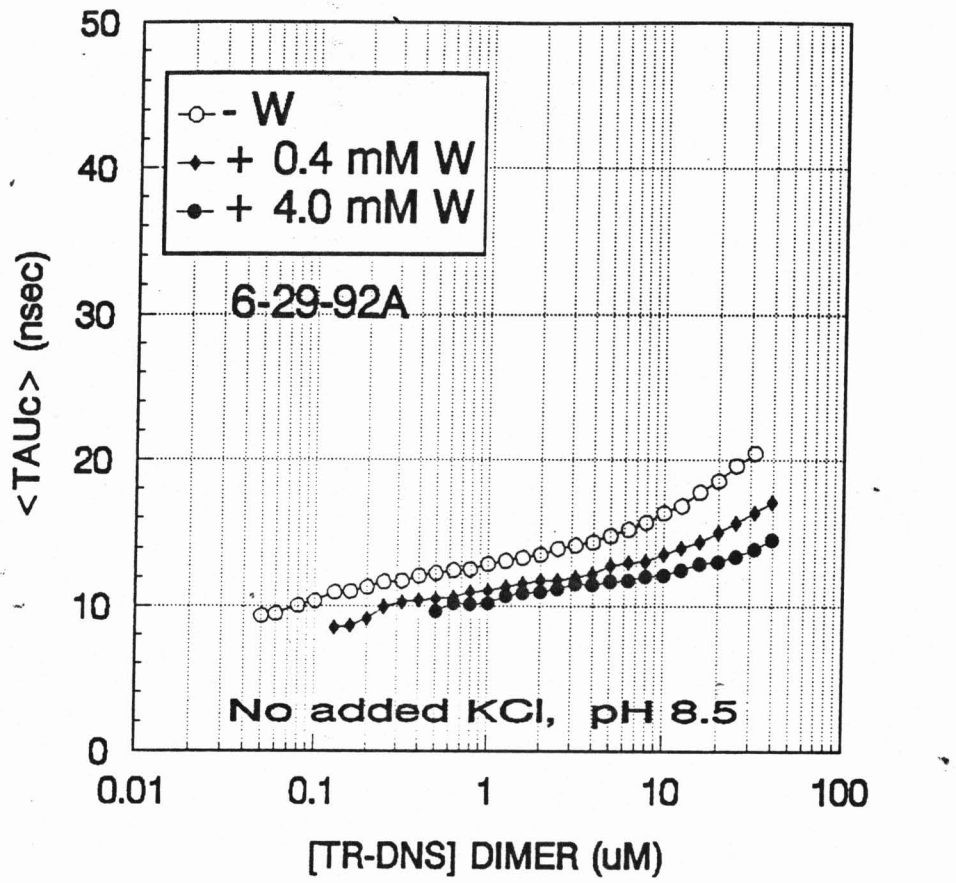

Figure 18. Correlation times as a function of TR concentration for the same sample as described in Figures 14 and 16. The anisotropy values and probe lifetimes are used (see text) to calculate $<\tau_c>$.(<TAUc>). Note the curves in the presence of corepressor (TR, + W curves) are shifted to lower correlation times with respect to the ApoR (- W curve). Compare with Figure 14 to observe this shift. At low concentrations of TR, the curves appear to converge at $<\tau_c> \approx$ 10 ns.

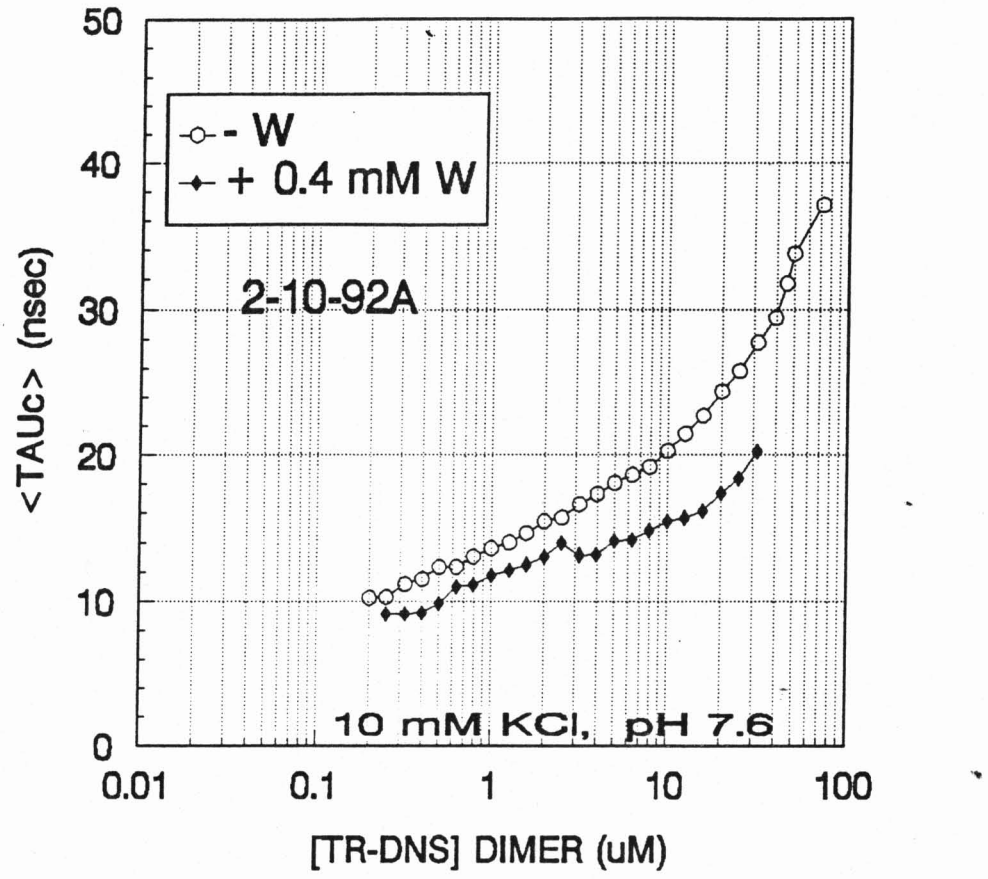

Figure 19. Correlation times as a function of TR concentration for the same sample as described in Figures 15 and 17. See discussion in Figure 18 legend. Compare with Figure 15 to observe the shift in TR profile to lower correlation times with 0.4 mM W in the test buffer, relative to ApoR (- W curve). As observed for the results in Figure 18, both curves appear to converge at $< \tau_c, > \approx$ 10 ns.

3. Correlation Times

Dilution of TR results in a decrease in correlation time under all conditions except high salt or high L-tryptophan concentrations. Correlation times greater than approximately 17 ns indicate the presence of oligomers of order greater than dimer in solution, based on a 10-17 ns correlation time range for low and high estimates of TR shape using hydrodynamic property calculations (Fernando and Royer, 1992). This is the case for all profiles at pH 6.0 and most of the profiles with pH 7.6 buffers. Figures 20-24 show composite dilution/average correlation time ($<\tau_c>$) results under all test conditions. Correlation times calculated in solution are the average of all the species present. Therefore the value of the correlation time calculated using the Perrin equation is the average of all the multimeric TR species present at the particular TR-DNS concentration, under the specific test conditions. The mean of 3 to 4 experiments was used to generate the composite dilution/average correlation time profiles shown in Figures 20-24. Average correlation time versus TR_d concentration profiles for individual experiments are in Appendix C, presented by pH, salt concentration and the date of experiment.

The highest correlation times (50-65 ns) are observed in the absence of corepressor for $[TR]_{dimer}$ in the range of 30-40 μM, in solution conditions pH 6.0 and in low salt (0 or 10 mM added KCl). Under these same conditions, the differences between experimental results was large, resulting in wide error bars (Figures 20 and 21). Correlation time for the aporepressor at pH 7.6 in the absence of KCl was approximately 30 ns (at 40 μM TR_d). Standard deviations were high under these conditions, too. In general the addition of 0.4 mM L-tryptophan did not diminish the variability observed. The data for solution condition experiments for which increased variability was observed are presented graphically in Appendix D. Except for these particular experimental conditions, the standard deviations for the mean $<\tau_c>$ of multiple experiments were small, often within the designating symbol.

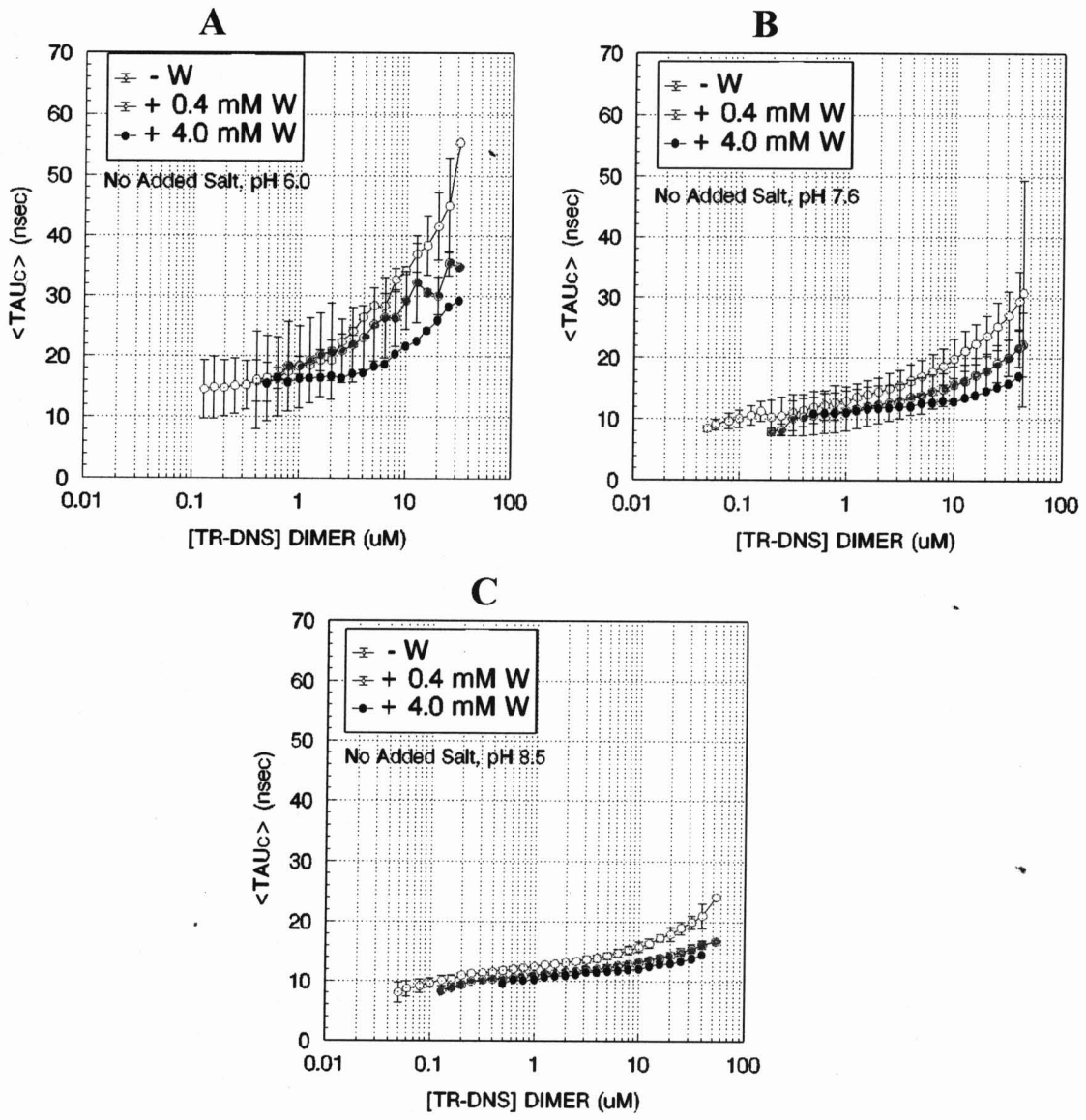

Figure 20. The influence of corepressor, L-tryptophan (W), on the correlation times of TR is shown at pH 6.0 **(A)**, pH 7.6 **(B)**, and pH 8.8 **(C)** in the absence of added KCl in the standard (10 mM potassium phosphate, 0.1 mM EDTA) test buffer. Open circles: aporepressor (3 experiments). Red circles: TR in the presence of 0.4 mM W (3 experiments). Black circles: TR in the presence of 4.0 mM W (one experiment). Where shown, error bars indicate +/- one standard deviation about the mean. Note the evidence of higher order oligomers as indicated by higher correlation times at the higher concentrations of TR. The correlation times decrease with increasing pH in the absence of salt. The wide error bars suggest instability in the oligomeric form in the absence of salt at pH 6.0. At pH 8.5, the oligomeric state is stabilized at correlation times consistent with dimeric TR throughout the TR concentration range.

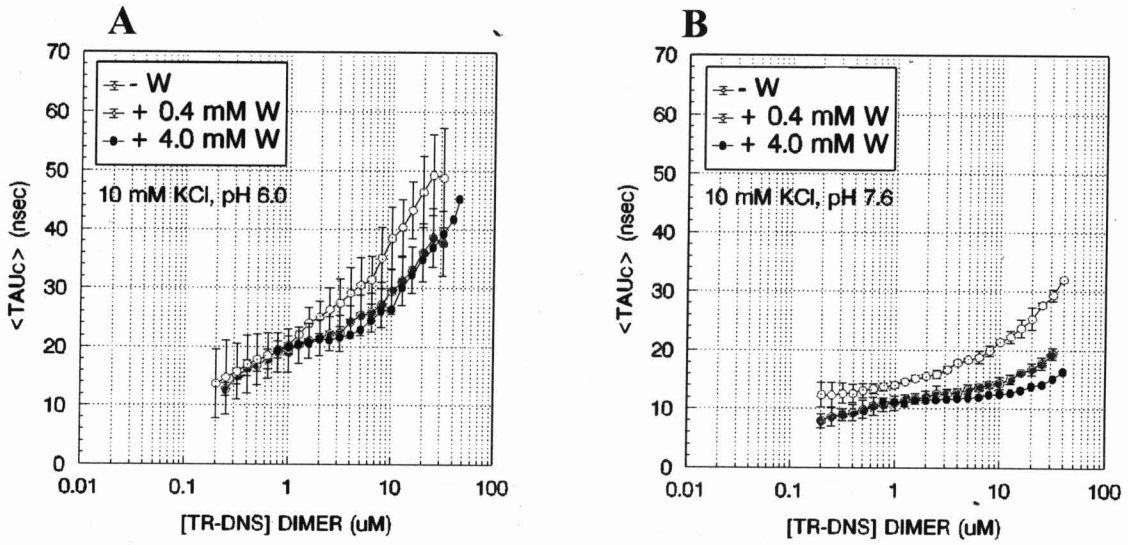

Figure 21. The influence of corepressor (W) on the TR correlation time at pH 6.0 (**A**) and pH 7.6 (**B**), with 10 mM KCl in the standard test buffer. Standard test buffer, symbols and error bars are as in Figure 20. At pH 6.0 (**A**), the correlation times are higher at high concentrations of TR_d than at pH 7.6 (**B**), indicating the presence of a larger population of higher order oligomers at pH 6.0. Note also the higher variability observed at pH 6.0. This may indicate the presence of alternate conformations of TR or instability of the higher order oligomers at that pH.

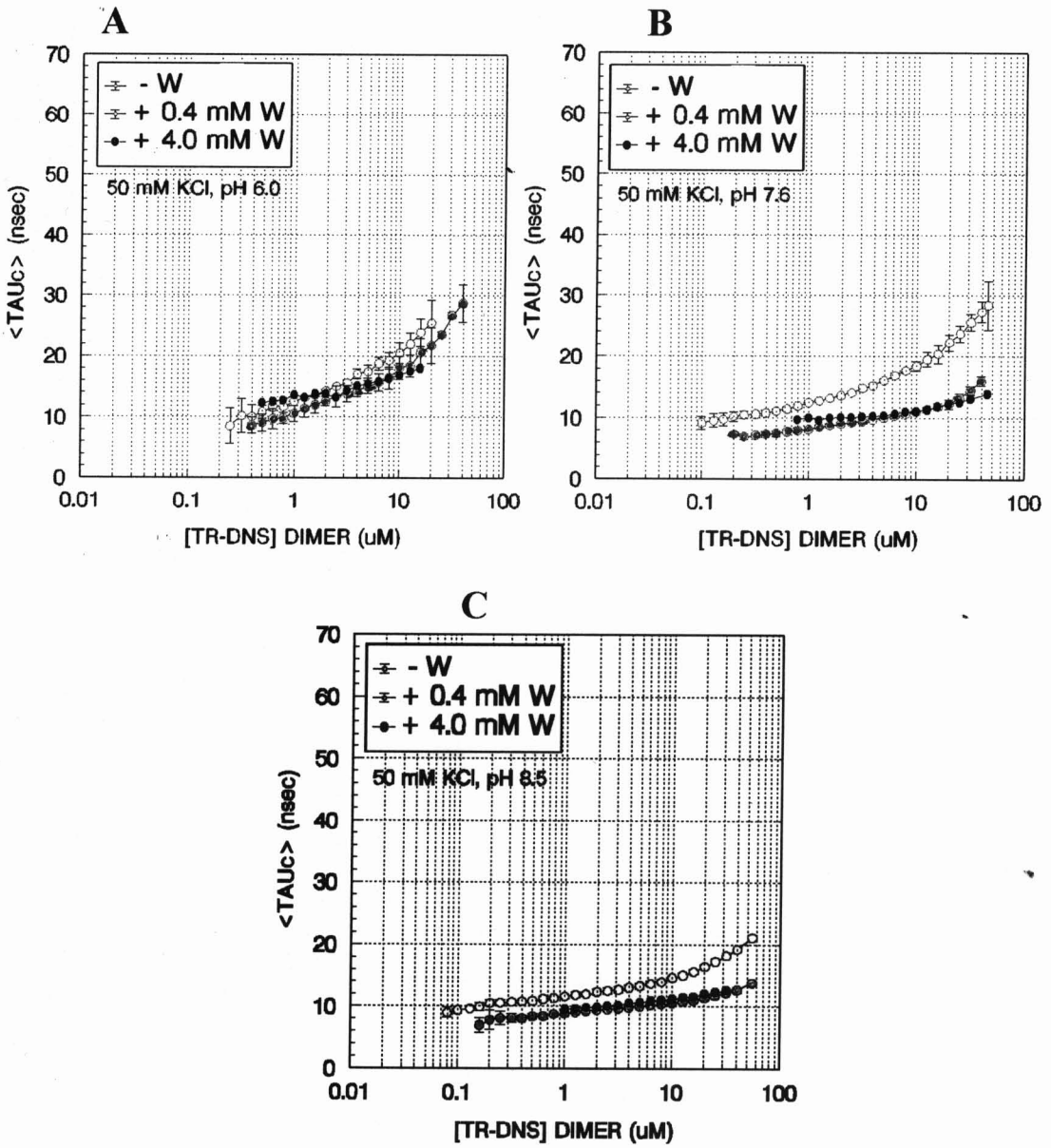

Figure 22. The influence of corepressor (W) on the TR correlation times at pH 6.0 (**A**), pH 7.6 (**B**), and pH 8.5 (**C**) in the standard test buffer with 50 mM KCl. Standard test buffer, symbols and error bars are as in Figure 20. In 50 mM KCl, the TR is largely present in an oligomeric state with a correlation time consistent with TR_d at and below concentrations of TR_d =10 μM.

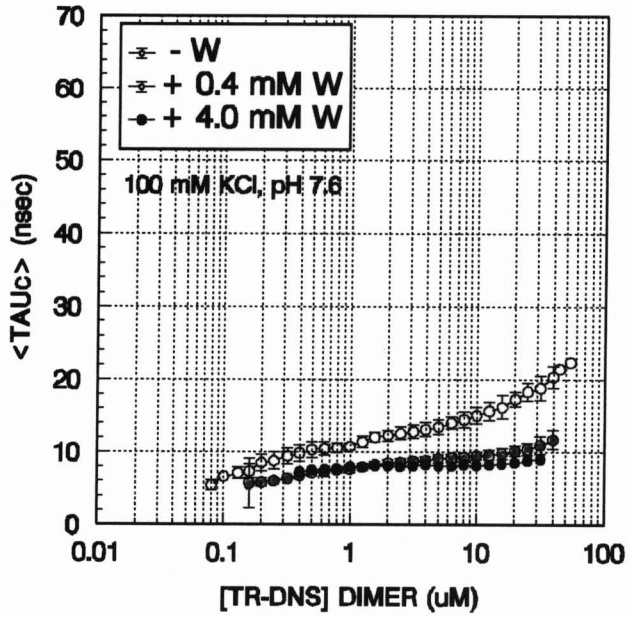

Figure 23. The influence of corepressor (W) on the TR correlation times at pH 7.6 in the standard buffer with 100 mM KCl. Standard test buffer, symbols and error bars are as in Figure 20. Comparison of this graph with Figure 22 (**B**) shows that the correlation times at pH 7.6 at the highest concentrations of TR_d are diminished by 7-8 ns in 100 mM KCl as compared to 50 mM KCl. The overall dilution profiles, however, are similar.

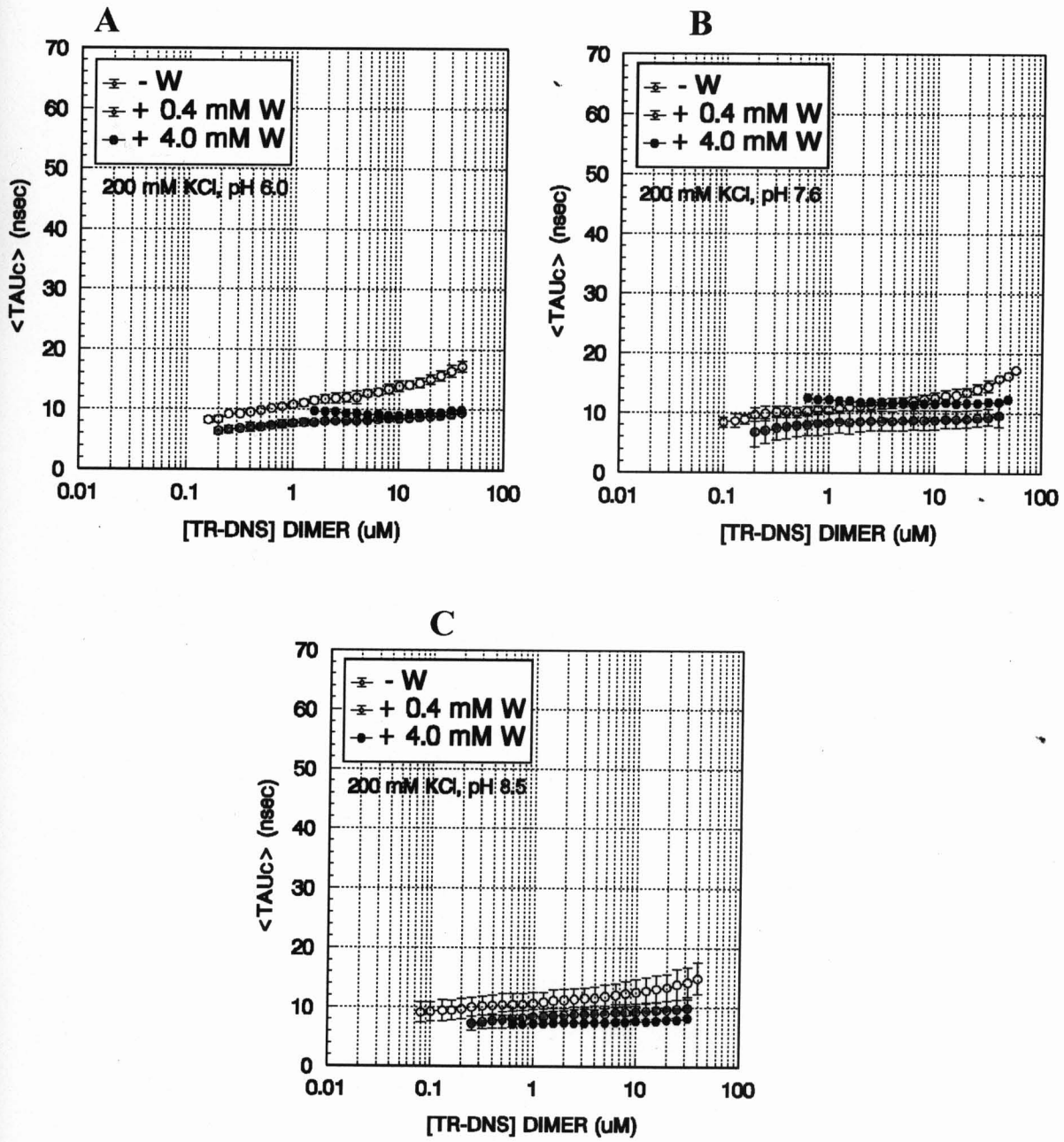

Figure 24. The influence of corepressor (W) on the TR correlation times in pH 6.0 (**A**), pH 7.6 (**B**), and pH 8.5 (**C**) in the standard test buffer with 200 mM KCl. Standard test buffer, symbols, and error bars ar as in Figure 20. All of the correlation times are in or near the range predicted to correspond to TR_d (Fernando and Royer, 1992).

VII. DISCUSSION

A. Oligomerization of TR Dimers in the Absence of DNA

1. Role of Electrostatic Interactions in the Association of TR Dimers

Higher order oligomers are present under essentially all solution conditions studied with the possible exception of solutions with both saturating corepressor and high salt (Figures 20 and 21) at each pH studied. All other solution condition tests resulted in $<\tau_c>$ values for TR greater than 10-17 ns, indicating the presence of complexes larger than dimeric TR. Under some solution conditions studied, the correlation times were significantly greater than that of dimeric TR. Destabilization of higher order oligomers to dimeric TR is demonstrated in the presence of corepressor, by the addition of KCl and by increasing pH in the range of 6.0 to 8.5. Higher order oligomers are also destabilized by decreasing TR-DNS concentration.

Correlation times were diminished for all solutions studied with increasing concentration of KCl, demonstrating destabilization by salt of higher order TR oligomers to dimeric TR. An electrostatic component is therefore indicated to the association of higher order TR oligomers,

which can be disrupted by shielding the protein charges with high salt concentrations. The strength of the electrostatic interaction decreased with increasing pH. In the absence of corepressor, increasing KCl at pH 6.0 caused reduction in TR oligomeric size (Figure 25). Dilution/correlation time profiles in buffers containing 0 and 10 mM added KCl (low salt) were indistinguishable within error; the correlation times were much higher than 17 ns at high TR concentrations. The profiles in low salt are higher throughout the TR concentration range studied (0.05-60 μM) than the profiles in solutions containing 50 and 200 mM KCl, indicating higher populations of TR oligomers larger than dimers. Correlation times for TR-DNS in buffers at pH 6.0 in the presence of 200 mM KCl were all below 18 ns, indicating that the average TR complex size is dimeric. In pH 7.6 solutions, in the absence of corepressor, the spread of the correlation time results at high TR concentrations in 0-200 mM KCl solutions was much less than at pH 6.0, hence there is less change in oligomeric size with increasing salt concentration at this pH (Figure 25). Correlation times for concentrations of TR-DNS = 30 μM ranged from 32 ns (10 mM KCl) to 12 ns (500 mM KCl). In 0, 10 and 50 mM KCl, the profiles were indistinguishable within error, however, decreasing correlation times with increasing salt concentration was observed. At pH 8.5 very little influence of salt was noted over the range of 0 to 200 mM KCl (Figure 25). Any

differences in the dilution curves were evident only above 20 μM TR. Below that TR concentration, correlation times were all approximately 10 ns, consistent with dimeric TR.

In the presence of 0.4 mM corepressor at pH 6.0 there is still an observable influence of salt on the size of TR oligomers (Figure 26). The profiles of the dilution curves in the absence of KCl and in 10 mM added KCl are the same within experimental error. The 10 mM KCl curve appears to result in higher correlation times than those obtained in the absence of salt, but the error bars (Figure 21) indicate that this may be an artifact. At 200 mM KCl, the dilution curve is flat near a 10 ns correlation time, indicating dimeric TR as the primary oligomer present. The same qualitative result is observed in solution containing 4.0 mM L-tryptophan (Figure 27), with slightly lower correlation times at the higher TR concentrations than the profiles in the presence of 0.4 mM corepressor for all salt concentrations except 200 mM KCl.

Dilution study results at pH 7.6 in the presence of the corepressor (0.4 mM and 4.0 mM) show results qualitatively the same as in the absence of corepressor, but the correlation time spread for high TR concentrations for 0 to 500 mM KCl is diminished as compared to the pH 6.0 results

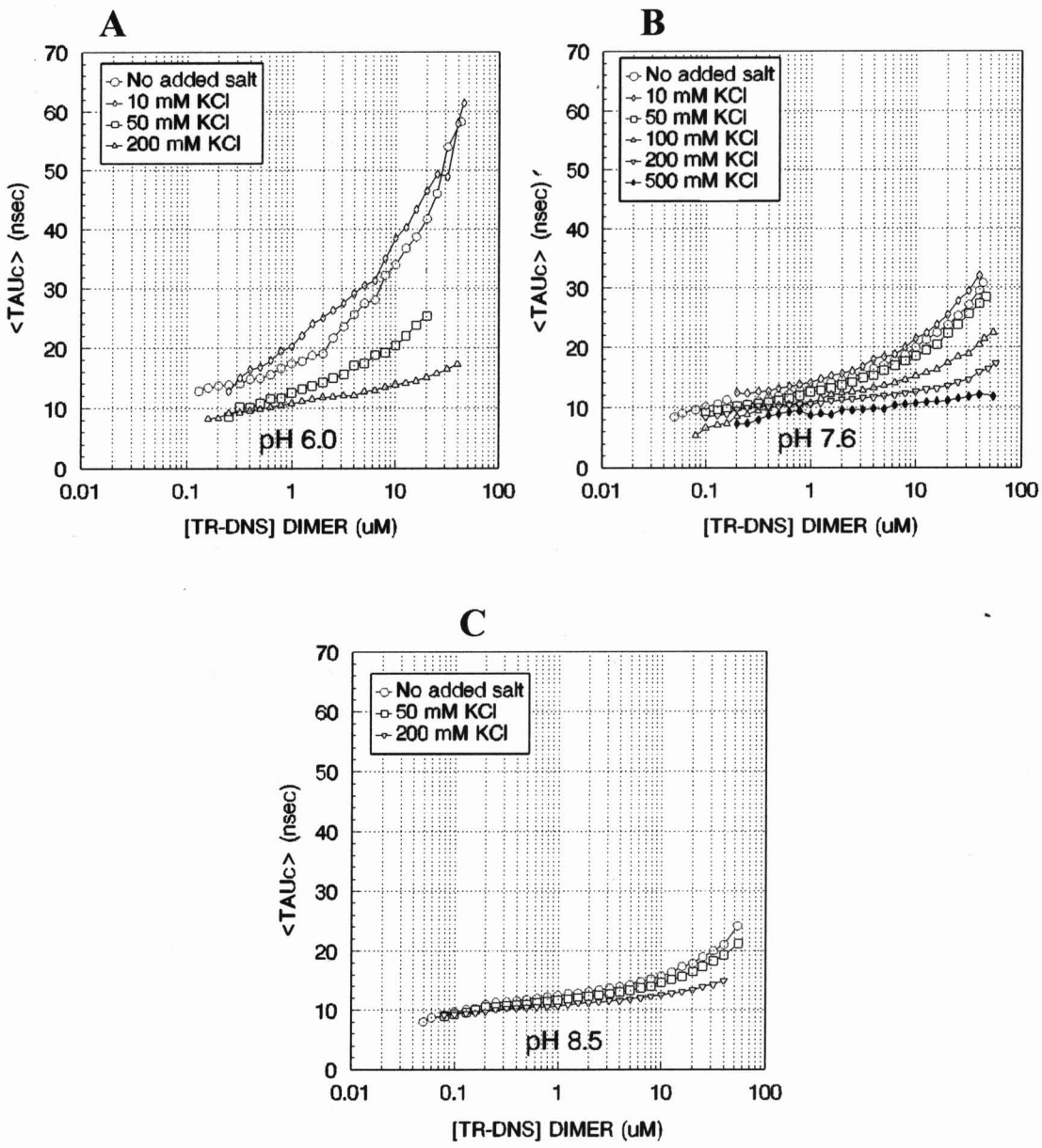

Figure 25. The influence of salt, in the absence of corepressor, on TR correlation times in pH 6.0 (**A**), pH 7.6 (**B**), and pH 8.5 (**C**) test buffers. The effect of salt is greatest at pH 6.0, which is close to the pI of TR (pI = 5.9, Joachimiak, *et al.*, 1983). Although the overall TR complex is uncharged, there is an electrostatic component to the protein-protein interactions at pH 6.0. With increasing pH (and therefore increasing negative charge on TR), this effect is diminished.

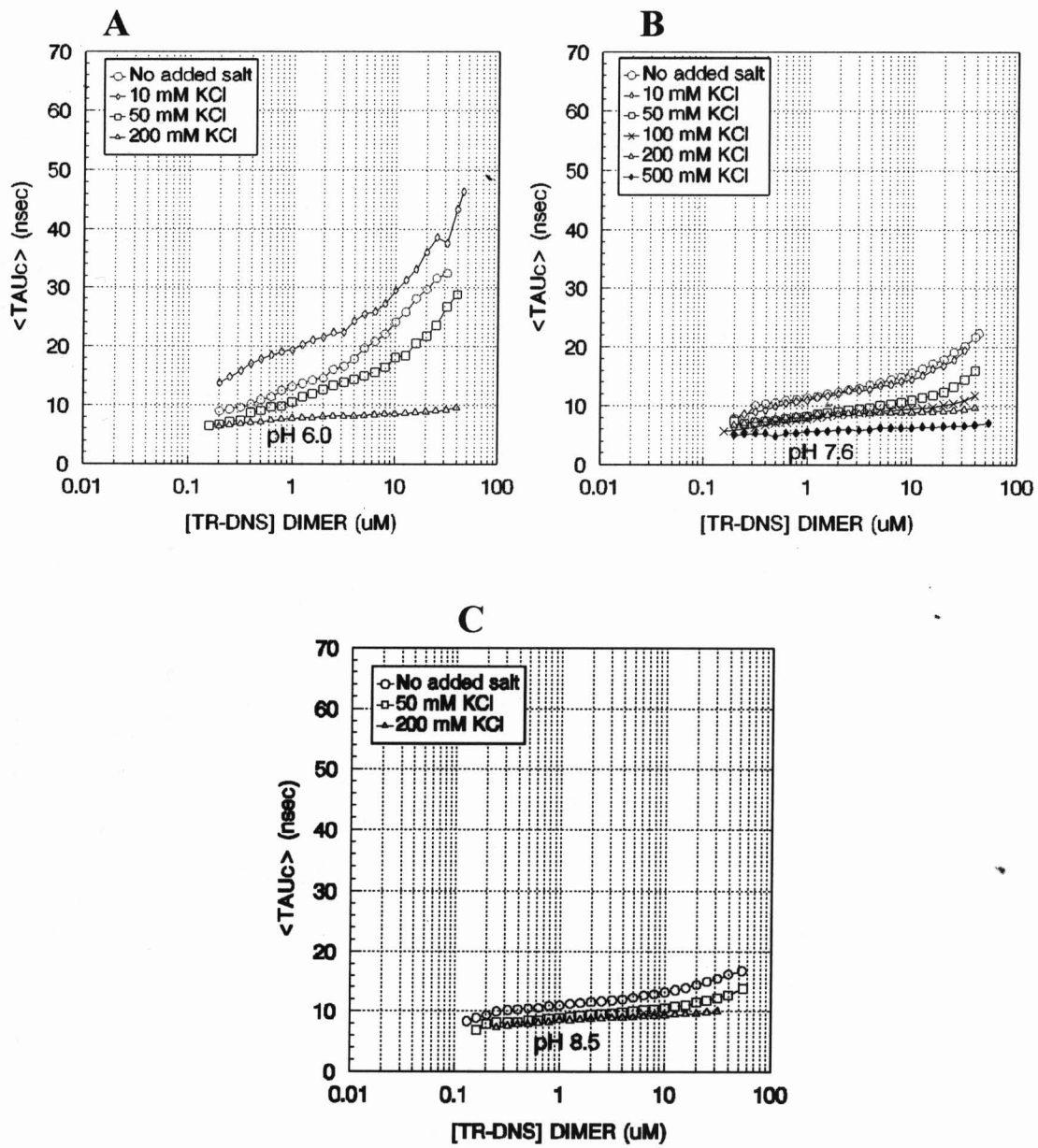

Figure 26. The influence of salt on the correlation times of TR in the presence of 0.4 mM corepressor (W) in test buffers of pH 6.0 (**A**), pH 7.6 (**B**), and pH 8.5 (**C**). See discussion in Figure 25 legend. The effect of salt at the various pH is qualitatively the same. The magnitude of the spread of correlation times in the range of 0 to 200 mM KCl is diminished.

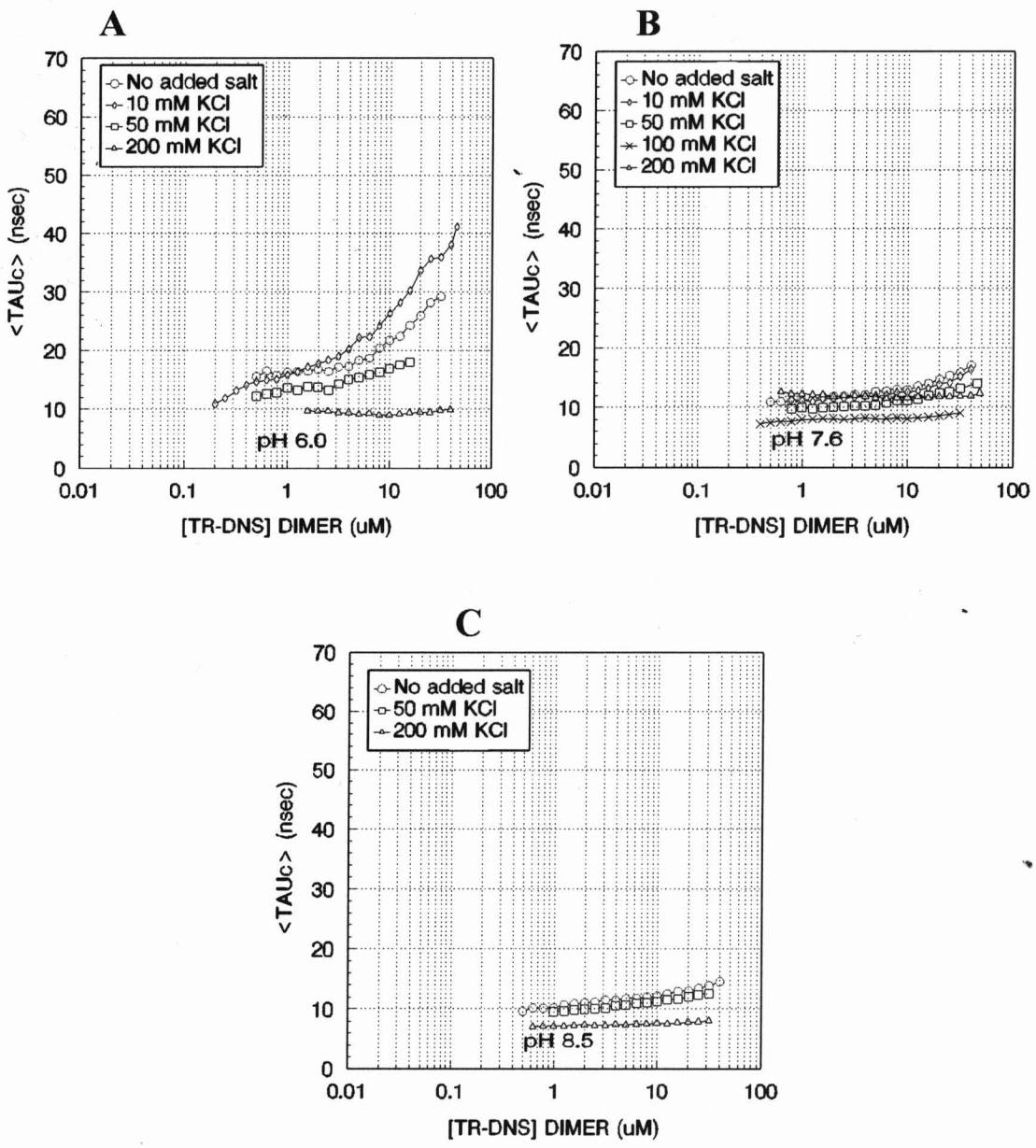

Figure 27. The influence of salt on the correlation times of TR in the presence of 4.0 mM corepressor (W) at pH 6.0 (**A**), pH 7.6 (**B**), and pH 8.5 (**C**). The only remaining evidence of higher order oligomers in the presence of 4.0 mM W is at pH 6.0, as shown by the spread in correlation times in (**A**). In pH 7.6 and pH 8.5, the correlation times correspond with that calculated for TR_d (Fernando and Royer, 1992).

(Figures 26 and 27). In the presence of 4.0 mM L-tryptophan the curves are essentially indistinguishable and flat near 10 ns at all concentrations of TR and salt concentrations. For both concentrations of corepressor, the effect of salt at pH 8.5 on the oligomeric state of TR is minimal. The correlation times remain below 18 ns at all concentrations of TR-DNS, indicating that TR dimers are the primary oligomer present.

Figures 28 and 29 depict the effect of pH on TR. In the absence of salt and corepressor, an obvious destabilization of higher order oligomers to dimeric TR is observed with increasing pH from 6.0 to 8.5 over the range of [TR]=0.5nM to 40 μM (Figure 28). Correlation times change from 60 ns (pH 6.0) to 30 ns (pH 7.6) to 24 ns (pH 8.5) at 40 μM TR_d. Considering the correlation time of dimeric TR to be 10 ns, a 60 ns correlation time exceeds that of the dimer by a factor of six. This means the solution contains multimers which are larger than tetrameric TR. Below 1 μM TR, all curves are nearly flat and have correlation times ≤ 20 ns, indicating the complexes have largely dissociated to TR dimers. The same result is obtained in the presence of 50 mM KCl but the effect is much smaller: at [TR]= 20 μM, correlation times were 24, 22 and 16 ns for pH 6, 7.6 and 8.5, respectively (Figure 29). At 200 mM KCl, all effect of pH on the correlation times has vanished. Within error, all

curves are identical, with all correlation times below 16 ns, indicating the TR dimer is the dominant species present in solution (Figure 28).

In the presence of 0.4 mM corepressor (Figures 28 and 29), the effect of pH is also diminished, but a distinct trend remains. At [TR]= 30 μM, correlation times are 32, 20, and 16 ns for pH 6.0, 7.6, and 8.5, respectively, indicating the presence of TR oligomers larger than dimers at pH 6.0 and pH 7.6. In the presence of corepressor and 50 mM KCl, pH 7.6 and 8.5 results become indistinguishable, but the pH 6.0 dilution profile shows higher correlation times at high $[TR_d]$ (> 20 ns). Complexes larger than expected for dimeric TR (Figure 29) are indicated at pH 6.0 under these test conditions. In a solution containing 200 mM KCl and 0.4 mM corepressor, all influence of pH is eliminated as demonstrated by the unchanging correlation times near that of the TR dimer, 10 ns (Figure 28). In the presence of 4.0 mM L-tryptophan, the results are similar to those observed for 0.4 mM L-tryptophan (Figures 28 and 29). However, in the absence of salt, $<\tau_c>$ results at pH 7.6 are indistinguishable from the pH 8.5 results, indicating further destabilization of higher order complexes to dimeric TR by the higher concentration of corepressor.

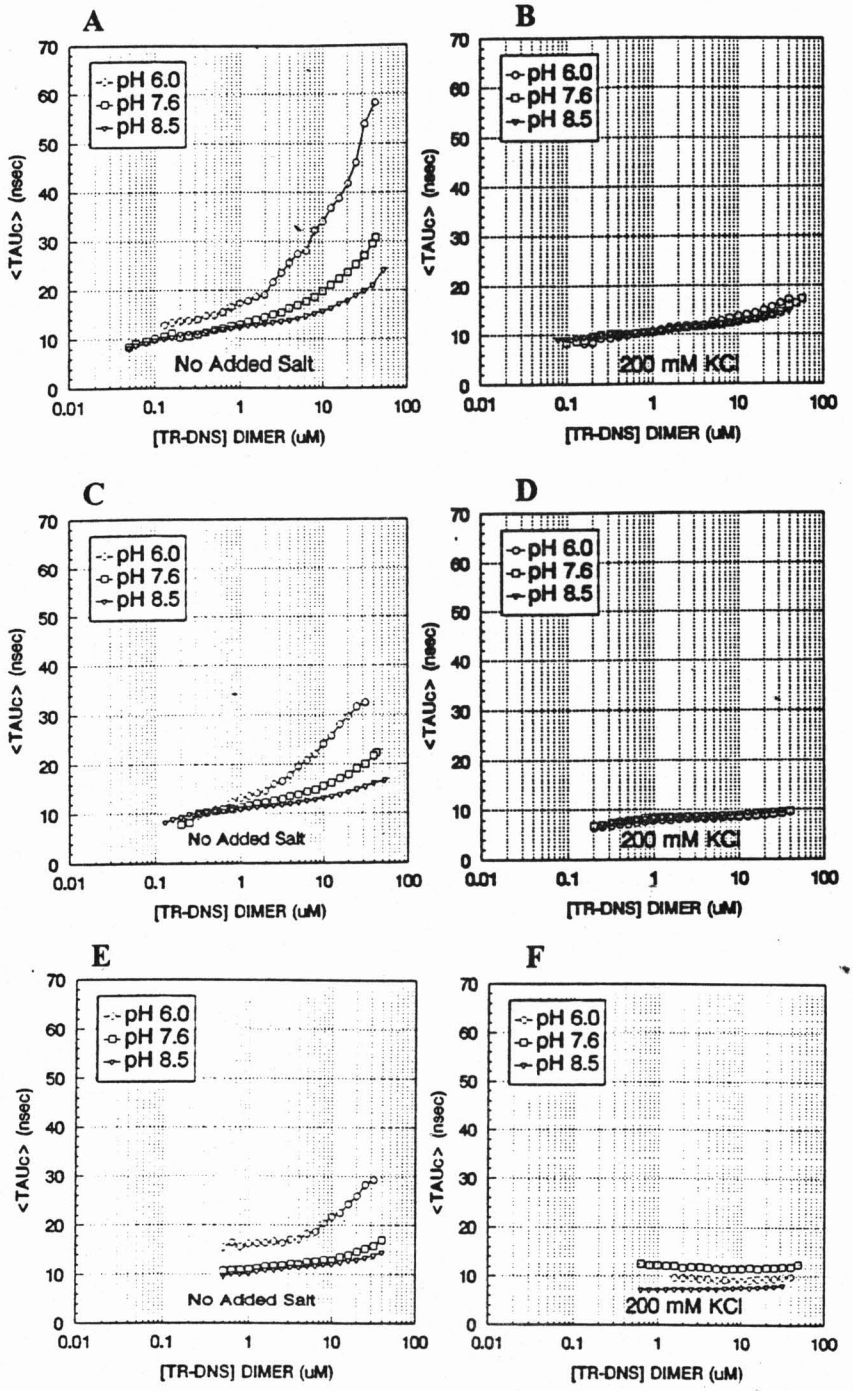

Figure 28. The influence of pH on TR correlation times in standard test buffer. **(A)** No added KCl, No corepressor. **(B)** 200 mM KCl, No corepressor. **(C)** No added KCl, 0.4 mM W. **(D)** 200 mM KCl, 0.4 mM W. **(E)** No added KCl, 4.0 mM W. **(F)** 200 mM KCl, 4.0 mM W. The destabilization of oligomers of order greater than dimer at different pH with added salt is evident by comparison of **(A)**, **(C)**, and **(E)** with **(B)**, **(D)**, and **(F)**. The destabilization of higher order oligomers at different pH with addition of corepressor is observed by comparing the graphs pairwise down the page: **(A)** and **(B)** (-W); **(C)** and **(D)** (0.4 mM W); **(E)** and **(F)** (4.0 mM W).

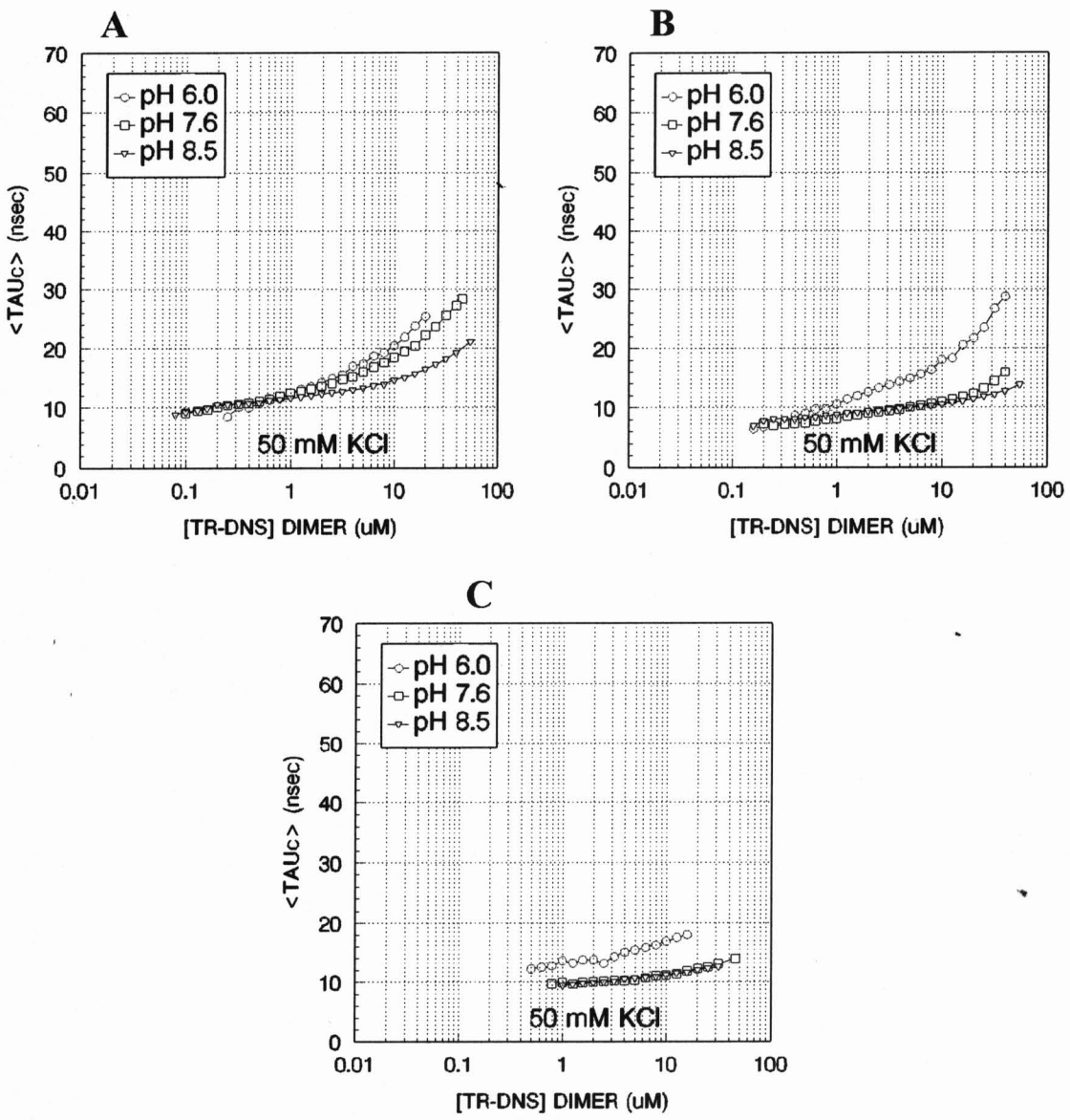

Figure 29. The influence of pH on TR correlation times in standard test buffer with 50 mM KCl. (**A**) No added corepressor, (W); (**B**) 0.4 mM W, and (**C**) 4.0 mM W. Note that ApoR shows some destabilization of higher order oligomers with increasing pH. The influence of pH diminishes as concentration of corepressor increases. The origin of the shift in correlation time between pH 6.0 and pH 7.6/8.5 in (**C**) is unknown; in all cases a plateau was reached, indicating a stable form of TR, which corresponds to dimeric TR correlation times.

The ionic nature of the interaction between TR dimers to form higher order oligomers is corroborated by the work of Liu (1991) who, using molecular sieve chromatography, determined that the addition of salt (500 mM KCl) to high concentrations of TR destabilized a TR complex of molecular weight approximately two times that of the dimer to the molecular weight of the dimer. Investigation of the TR using molecular sieve chromatography (Sephacryl S-200 HR C10/40 column) revealed increasing molecular weight complexes with increasing concentration of TR in the range of 0.004 mg/mL (0.32 μM) to 1.92 mg/mL (154 μM). At the highest concentration of TR (as monomer) tested, the molecular weight was approximately that of tetrameric TR. No upper limit to the correlation time has been established for TR in the present work as no upper plateau in the dilution curves was seen or even hinted at by the generally steeply falling anisotropy at high TR concentrations. SDS-PAGE experiments carried out in this laboratory to examine the purity of TR fractions resulted in multiple bands (visualized by silver staining) of molecular weight greater than TR dimer for concentrations as TR (dimer) above 2 mg/mL (data not shown), further supporting the presence of several higher order oligomers. The bands were discreet, not smeared, suggesting complexes of specific stoichiometries. The protein preparations used in this work were more dilute than those of Liu (1991), and insufficient to obtain TR_d

concentrations at or above 80 μM. Future preparations can be concentrated sufficiently to allow the determination of a plateau, if it exists, near these concentrations of TR using the fluorescence spectroscopic techniques applied here. In any case, observation of the TR equilibrium shifted toward tetramer is suggested by the work of Liu at TR dimer concentrations above 80 μM.

Recent NMR data (Arrowsmith, *et al.*, 1991b) suggested that TR existed as a population of conformers in solution. Arrowsmith and coworkers suggested that this population was the result of structural variability in the D and E helices, with added influence of the interhelical packing changes of helix C upon binding of the corepressor, L-tryptophan. Evidence of the variation of TR oligomeric state in solution included broadened lines at concentrations of TR in the range of 1-3 mM (monomer). Hyde, *et al.*, (1989) interpreted the spectral characteristics observed to be an indication of the self-association of TR, consistent with the results of the current study.

The intracellular environment of *Escherichia Coli* is not static. Changes in the composition of the extracellular environment have been shown to modulate the composition of the intracellular environment (Richey, *et al.*, 1987). The intracellular ionic environment of *E. coli* was reproducibly

changed by modification of the osmolarity of the growth medium. Both the concentration of ions and the pH were modified in this manner. Concentrations of K^+ and glutamate ions were changed in the growth medium and found to influence *in vivo lac* repressor-DNA interactions only weakly. Because of the large *in vitro* salt effects observed for this protein system, Richey and coworkers proposed chemical and/or physical mechanisms used by *E. coli* to reduce the sensitivity of non-covalent macromolecular assembly interactions to intracellular electrolyte concentration changes. The study suggested a role for changes in the intracellular environment influencing the activity and oligomeric state of proteins within the cell.

pH and salt effects have been extensively studied on systems involving effector binding and protein binding to DNA (Record, *et al.*, 1976 and 1978; Revzin and von Hippel, 1977; Barkley, *et al.*, 1981; Senear and Ackers, 1990, among others) to obtain information on binding interfaces. However, very little work has been done to characterize the same for protein-protein interactions which are energetically coupled to effector-protein and protein-DNA binding (Weber 1966 and 1972). Koblan and Ackers (1991) and Fernando and Royer (1992) have considered the role of protein-protein interactions on the overall thermodynamics of transcriptional regulatory protein systems.

pH and salt dependence studies are done to assess the contributions of electrostatics and hydrophobicity to oligomerization. Koblan and Ackers (1991) investigated the subunit-subunit energetics in the bacteriophage λ *cI* repressor system under conditions of varying temperature, salt concentration and pH to understand the linkage between reversible protein oligomerization and DNA binding. The complex was stabilized by increasing concentrations of KCl, indicating that formation of the dimer interface had a hydrophobic component, mediated by screening of repulsive interactions from charged side chains. This is in direct contrast to the results obtained in the current study. TR oligomers are not stabilized by increasing salt concentration, but are destabilized, indicating that the interactions between TR dimers are ionic in nature, rather than hydrophobic.

The effect of salt is generally considered as a screening effect, destabilizing associations driven by electrostatic charge interactions. Monovalent ions neutralize exposed charges on the protein which are solvent accessible, screening the charges from other charged portions of the protein. pH effects are generally considered in terms of protonation or deprotonation of surface charged groups. Both biochemical and structural evidence indicate that the

stability of biomacromolecular complexes involves key long- and short-range electrostatic interactions. Salt effects are monitored to establish the magnitude of electrostatic free energy which arises from the entropy of proton and H_2O release rather than from charge energetics which are shown by pH effects (Jaenicke, 1991). The overall charge state of a protein in solution depends on the pKa's of the ionizable amino acids and/or the extent of ion binding to specific sites. The pI of TR is 5.9 (measured by isoelectric focusing, Joachimiak, *et al.*, 1983), therefore at pH 6.0, the protein has no net charge. Proteins at the isoelectric point are subject to mutual attraction because there is an equal number of positively and negatively charged amino acid residues. If many charged amino acids of opposite sign are at opposing poles of the polypeptide or complex, the dipole moment of the protein is further enhanced and association is favored to a greater degree. Proton or pH effects have been extensivly studied in the interactions of small oppositely charged electron transfer proteins. Mauk and coworkers (1990) cite the significant contribution of titratable group protonation to the electrostatic potential surface of a protein. Changes in the surface potential influences remote sites on the protein by transfer of charge through the protein structure (Mauk, *et al.*, 1990). The central hydrophobic core of the TR appears to have the necessary architecture to mediate long-range influences of proton

exchange (Luisi and Sigler, 1990). Hyde and coworkers (1991) monitored the binding of corepressor and inducer by observing the indole NH signal of Trp19, a residue far from the binding site, further supporting the ability of the TR dimeric structure to mediate long range signals through the complex. Greater association of TR occurs at pH 6.0 than at pH 7.6 or pH 8.5, which is consistent with enhancement of the protein dipole at the protein's pI.

Higher order TR oligomers would be largely destabilized by the high salt concentrations used in buffers of previous studies. Work by Lane (1986) using electronic spectra (fluorescence, circular dichroism, and absorption difference) to evaluate TR was carried out in 100 mM sodium phosphate, pH 7.5 at 25° C. Filter binding studies (Klig, *et al.*, 1987) on the TR-operator interactions have been done with buffer containing 10 mM TRIS-HCl, pH 7.6 and an optimal salt concentration of 1.5 M $(NH_4)_2SO_4$. NMR work was done in 25-50 mM sodium phosphate, pH 5.8 or 7.5, with 200-500 mM KCl or NaCl, at concentrations of TR in the range of 1-4 mM (monomer). In tests where active TR was studied (Hyde, *et al.*, 1991) rather than the aporepressor, 0.1-10 mM L-tryptophan was also added to the test buffer (Hyde, *et al.*, 1989).

Crystals for x-ray analysis were grown under differing conditions, depending on the desired product. Examples of growth conditions are:

- 2.37 M ammonium sulfate, 50 mM sodium acetate, pH 5.4, with 0.4 M NaCl amd 2.4 mM corepressor (Schevitz, *et al.*, 1985).

- 10 mM cacodylate, pH 6.8 in 35% 2,4-dimethylpentanediol with 50 mM NaCl amd 11 mM calcium chloride (Otwinowski, *et al.*, 1988).

Note the high salt concentrations as well as the additives necessary to allow crystal growth. Clearly interactions in the crystal structures may be influenced by the growth conditions.

Table III summarizes a selection of the varied experimental methods and solution conditions which have been used to study TR. A key point to note is the total concentration of salt in each study. In all cases but possibly one[4], at least one salt was present in a quantity of 50 mM or greater, which is the only common feature to these studies. The present work shows the TR oligomeric equilibrium would be greatly shifted toward dimeric TR in buffers containing 50 mM (or higher) KCl concentrations and clearly illustrates

[4] The one method which cites a low salt concentration was a gel filtration experiment. The salt concentrations may have been reported in error. This is believed to be the case because other experiments done in the same work used higher salt concentrations and the results indicated "essentially no monomer or higher multimeric species" were detected (the concentration of TR under test was not given), which would be consistent with a higher salt concentration. Therefore, these results are taken as consistent with the other work presented, not as an anomaly.

that acceptance of a static TR dimer was established by studies with TR in solution environments in which the oligomeric equilibrium was shifted toward dimeric TR.

The solution conditions listed in Table III also illustrate the lack of consistency in the choice of salts used for the various tests. In some cases, as noted for the crystallographic data, the salt is chosen to optimize the crystal growth. In other cases, there is some disagreement in what is considered "physiological". Several of the published reports cited their conditions as "physiological", yet no two sets of conditions are the same. The salt used for this work was KCl. K^+ is the principal cation in the cell and is a cofactor for certain enzymes. Inorganic anion composition varies to some extent with the anionic composition of the medium, but always includes phosphate and usually glutamate, sulfate and chloride (Ingraham, *et al.*, 1983). The purpose of this inquiry was to evaluate the salt effects and approximate the magnitude of the effects, therefore Cl^- was selected to maintain consistency with the work done previously in this lab and with collaborators, such that results could be compared directly.

Table III. Summary of solution conditions used for TR studies. See text for discussion of the solution conditions. NS = [TR] was not specified. GPC = Gel Permeation Chromatography. BSA = Bovine Serum Albumin

Method	Buffer	pH	Salt A	Salt B	Salt C	[W]	Other	Refer.	$[TR]_d$
NMR	25-100 mM (a, Na,f)	5.8, 7.5, or 7.6	100 - 500mM (b ,i)	3 mM (c)	2 mM (d)	0.1-10 mM	2 mM DTT	1,2	0.5-2 mM
Filter Binding	10 mM (a)	7.6	1.5 (e)	0.1 mM (d)	10 mM (g)		5% DMSO	3	1-14 ng in 25 uL
Gel fil-tration	20 mM (Na,f)	6.8	0.1 mM (h)					4	92.5 uM
Equil. Dialysis	10 mM (K,f)	7.6	200 mM (b)			1 mM	5% glycerol	4	92.5 uM
Alkaline Phosph-atase	10 mM (a)	7.4	250 mM (i)					5	2.5-70 uM
PAGE	12.5 mM (Na,f)	6.0	125 mM (i)			0.4 mM		6	2-250 nM
Fluor.	10 mM (K,f)	7.5	100 mM (b)	1 mM (d)				7	1 uM
Electron Spectra.	100 mM (Na,f)	7.5						8	12.5-22.5 uM
RsaI	6 mM (a)	7.5	50 mM (Na,f)	6 mM (c)		1 mM	6 mM (j),BSA	9	NS
PAGE	50 mM (Na,f))	6.8						9	NS
GPC	100 mM (K,f)	6.8						9	1.5 µg ApoR

a TRIS-HCl
b KCl
c $MgCl_2$
d EDTA
e $(NH_4)_2SO_4$
f phosphate: K,g = potassium phosphate, Na,g = sodium phosphate
g $Mg(C_2H_3O_2)_2$
h Na_2SO_4
i NaCl
j 2-mercaptoethanol
k $Na(C_2H_3O_2)_2$

1. Arrowsmith, et al., 1989, 1991a,b
2. Hyde, et al., 1989, 1991
3. Klig, et al., 1987
4. Arvidson, et al., 1986
5. Marmorstein, et al., 1986
6. Carey, 1988
7. Chou, et al., 1989
8. Lane, 1986
9. Joachimiak, et al., 1983

2. Role of Corepressor Binding in the Association of TR Dimers.

The present work clearly demonstrates the destabilization of higher order oligomers to dimeric TR by addition of corepressor. In the presence of corepressor, a dramatic decrease in TR-DNS correlation time is observed at high concentrations of TR-DNS in all cases relative to the correlation times of the ApoR under the same solution conditions (but in the absence of corepressor) (Figures 20 to 24). 4.0 mM corepressor destabilizes the dimer $\leftrightarrow$ higher order oligomer equilibrium substantially toward the dimer even at concentrations of TR_d up to 40 μM, with the exception of pH 6.0 solution work in the absence of salt. This shows a greater destabilizing effect than 0.4 mM corepressor on TR oligomers. Under the latter conditions, correlation times above 17 ns are maintained until 5 μM [TR]. The final valley in all cases remained near a correlation time of 10 ns, indicating dimeric TR.

At pH 7.5 (100 mM potassium phosphate), Liu (1991) found that addition of 4 μM corepressor to TR (TR concentration range of 0.004 to 1.92 mg/mL) decreased the apparent molecular weight of TR complexes from 40 to 26 kD, suggesting a shift in the equilibrium from tetrameric TR to dimeric TR. It is possible that in the absence of

corepressor, higher order oligomers form to keep free ApoR from binding randomly with operator sites. Once the concentration of corepressor in the cell increases sufficiently, oligomers dissociate to dimer to allow repression. Oligomerization of the TR in this role provides an additional level of control within the cell.

The intracellular concentration of TR in *E. coli* has been determined to vary in the range of 270-850 nM in response to extracellular concentrations of L-tryptophan (corepressor) (range: 0 to 100 μg/mL or 0 to 8 μM corepressor) (Gunsalus, *et al.*, 1986). This concentration range of TR was within that tested, potentially allowing direct evaluation of the effects of corepressor on the TR. (Note: As a result of macromolecular crowding in the cell, the concentration of corepressor may be the same, but the activities may be altered (Jarvis, et al., 1990.)) With addition of corepressor at either concentration of 0.4 mM or 4.0 mM, the dilution profiles showed a final plateau near a 10 ns correlation time (concentrations of TR_d to 0.05 μM or 50 nM).

For TR, the binding of the corepressor ligand to ApoR was evaluated in the crystal structures and found to involve mainly hydrophobic contacts (Schevitz, *et al.*, 1985). The stabilizing influence of corepressor on the ApoR dimer is

very strong. In the presence of corepressor, no heterodimers, composed of a wild-type TR polypeptide chain and a mutant TR polypeptide chain, were formed upon mixing the two types of homodimers and heating to 65° C (Graddis, *et al.*, 1988). In one mutant system studied, the heterodimer formed in the absence of corepressor was resistant to dissociation in the presence of corepressor, in spite of having only one wild-type corepressor binding site. These findings indicate the magnitude of stabilization afforded by binding of corepressor to the aporepressor. Once the corepressor binds to a TR or mutant TR dimer, the dimeric complex stability is greatly enhanced. In the absence of corepressor, the stability of ApoR was diminished over that of the active complex. Arvidson and coworkers (1986) also noted that, in low salt concentrations, the ApoR was unstable in storage, as evidenced by decreased corepressor binding following a storage period. The ApoR was found to be more sensitive to handling during the dilution study (data not shown), than was TR in the presence of corepressor. Carey (1988) has also commented on the influence of handling on TR activity. These observations corroborate the stabilizing influence of corepressor on the TR dimer.

The putative hydrophobic nature of the interaction of corepressor with the TR dimer is supported by the increased

stability of the TR dimer in the presence of salt, both in the presence and absence of L-tryptophan. This is demonstrated in this work by correlation time plateaus at low concentrations of TR-DNS in the presence of high KCl concentrations (Figures 28 and 29). In some test buffers, specifically those containing low salt and no corepressor, at the low concentrations of TR_d, the correlation times appeared to start to decrease following a plateau (Figures 20 and 21). A dimer to monomer equilibrium cannot be definitively concluded by this work, because the further decreases in anisotropy occurred near the limit of the available emission signal. However, at the low concentrations of TR_d, once the anisotropy began to fall following the plateau, the drop was precipitous (data not shown). A dimer to monomer transition for TR is supported by the results of Fernando (1991), Fernando and Royer (1992), and in TR-DNA binding studies in this laboratory, (LeTilly and Royer, manuscript submitted to *Science*).

B. Role of TR Oligomerization in TR-DNA Binding

The study of TR oligomerization is not complete without linking the oligomerization of TR to TR-DNA binding, as understanding the mechanisms involved in the transcription of the genes in the operators modulated by TR is the primary goal of the research in this laboratory. We believe the TR

subunit interactions are energetically coupled with the corepressor-TR interactions and TR-DNA binding.

Carey (1988) used gel retardation to study TR-DNA binding (12.5 mM NaH_2PO_4 buffer, pH 6.0, 125 mM NaCl, 1 pM DNA, [TR] range 0-250 nM, 0.4 mM L-tryptophan). The DNA used was a 75 base pair (bp) non-specific fragment, and a 415-bp fragment containing a *trp*EDCBA operator site. Bands with greatly retarded mobility relative to the free DNA were observed at concentrations of TR greater than 100 nM (dimer), in addition to one band found to have a stoichiometry of one TR dimer per operator site. Recently Liu (1991) investigated TR-DNA binding assays using various DNS fragments and the method of Carey (1988), finding two bands with decreased mobility relative to the free DNA on a DNA fragment 40 bp in length. One band was identified as the DNA bound repressor dimer and a second band with higher mobility and affinity was observed following overexposure of the autoradiogram. The higher mobility band was replaced by the "normal" mobility band as the concentration of free DNA decreased, strongly suggesting sequential binding of multiple TR dimers or binding of multimeric TR to DNA. With the enhanced association of TR subunits at pH 6.0, higher order TR oligomers would be expected, and binding of a larger TR complex to DNA would certainly retard mobility relative to free DNA. Carey notes in her paper that she does not

believe the retardation of mobility is solely a result of the increased positive charge on TR. The results of Carey (1988) and Liu (1991) show more than one binding stoichiometry exists for TR binding to DNA. The difference in the operator fragments chosen may account for the differences in bands observed. The salient point from these gel electrophoresis studies is that binding of TR to DNA is shown to occur in multiple, specific stoichiometries. This demonstrates multiple TR subunits in the presence of DNA, complementing the findings of this work, which clearly demonstrate TR subunit interactions in the absence of DNA.

Other studies to date have shown DNA binding stoichiometries other than one dimer per operator DNA site. Haydock and Somerville (1984) concluded (using a gel procedure called Protein Distribution Analysis) that a significant fraction of TR was inert to operator binding, observing only one stable TR-DNA complex (with a ratio of 4 TR monomers per DNA operator). The experimental conditions were not extraordinary (10 mM TRIS-HCl, pH 7.4; 1 mM EDTA, 50 mM NaCl, 0.5 mM L-tryptophan, concentration of operator DNA = 2.17×10^{-7} M, TR concentration range was 0 to 1.81 μM; similar to conditions for other studies as noted in Table II). From the study results, it was concluded that, although the nature of the inactive protein was unknown, it was not denatured. Further, they determined using

immunological studies that only a minor fraction of the aporepressor was unable to bind L-tryptophan. The existence of TR in a conformation which was bound to DNA in a stoichiometry greater than dimeric TR is suggested by these findings. The solution conditions are similar to the 10 mM phosphate, 0.1 mM EDTA, 50 mM KCl, pH 7.6 investigations in this work, where TR oligomers greater than dimer are observed. The TR concentration range for Haydock and Somerville's work was approximately 0 to 1.8 μM (as monomer).

Tandem binding has been proposed (Kumamoto, *et al.*, 1987) as a mechanism to explain differential repression observed at the various TR operators *in vivo*, which cannot be explained by differences in operator affinity for TR (Klig, *et al.*, 1988). Tandem binding has been accepted as structurally feasible based on modelling of the crystal structure (Otwinowski, *et al.*, 1988) and has gained acceptance (Luisi and Sigler, 1990; Haran, *et al.*, 1992). Tandem binding, as proposed by Kumamoto and coworkers (1987) would not necessarily indict higher order TR oligomers in the absence of DNA or protein-protein interactions between DNA bound TR. Crystallography would not have revealed tandem binding because the short operator (18 bp) used, rather than the entire promoter, precluded many of the contacts implicated in tandem binding. The binding of TR_d to operators in

stoichiometries of 1:1, 2:1, and 3:1 was demonstrated by the work of Haran and coworkers (1992). These authors also employed modelling of the results of Otwinowski, *et al.*,(1988), showing the possibility of attractive protein-protein interactions between reading heads of tandemly bound repressors. Gel retardation studies suggested cooperativity in tandem binding to the wild type *trp*EDCBA promoter (Haran, *et al.*, 1992); attractive interactions between TR subunits would be one possible source of cooperativity in DNA binding. Other systems have been identified which required overlapping binding patterns for repression (MetJ protein, Phillips, 1991). In these reports, oligomeric association between TR dimers was not considered.

Much of the literature discussion on the influence of experimental conditions on TR-DNA binding has centered around the differences between the work of Carey (1988) and Marmorstein and coworkers (1991): pH 6.0 vs pH 7.4. Marmorstein proposed that the lower pH used by Carey would favor electrostatic interaction with DNA phosphates because the amino termini of the polypeptide chains would become more positively charged at pH 6.0. It is suggested that this interaction enhances energetic contributions to DNA binding through contacts with the DNA phosphate backbone, accounting for the lower dissociation constant observed in Carey's work (K_D = 0.5 nM for Carey, and K_D = 2 nM for

Marmorstein and coworkers). Clearly, in light of the results of this work, there is more to the influence of solution conditions to be considered than simply pH. The enhancement of affinity resulting from contact between the amino terminus and the DNA phosphates is not supported by experiments carried out in the laboratory of K. Matthews (Rice University). Using the gel binding assay of Carey (1988), the mobility of TR and TR-DNS were compared using a 26-mer operator DNA fragment. Visualization of bands on the gel revealed no difference in band mobility or intensity with either TR or TR-DNS bound to the 26-mer (K. Matthews, personal communication). This suggests that the charge on the amino terminus is not highly influential in the protein's affinity for the DNA. The DNS label has been shown to be largely bound to the amino terminus, eliminating the positive charge on the amino terminus at pH 6.0. If the positive charge contributed significantly to stabilizing DNA binding, TR-DNS would be expected to show decreased binding over unlabeled TR. Therefore, binding enhancement of TR to DNA at pH 6.0 over binding at pH 7.4 is not solely the result of contact between negative DNA phosphates and a positively charged TR amino terminus.

C. Models for TR Subunit Interactions

1. The TR Dimer Surface

The DNA binding surface of TR, specifically the DNA contacts in the D and E helices, is positively charged and/or polar (Figure 30). Crystallographic data suggest that the major contributor to the association energy is through contacts with the negatively charged DNA phosphate backbone or contacts mediated through hydrogen bonds with water molecules. The corepressor binding sites are also oriented toward the DNA binding surface of TR. Binding of TR to DNA essentially blocks the L-tryptophan into the pocket, as suggested by a contact reported between the L-tryptophan and the DNA (Otwinowski, *et al.*, 1988). How is this related to protein-protein interactions? In the absence of corepressor, this same face is available in the TR dimer. The two "flexible reading heads" are not positioned for contact with DNA major groove sites but still have essentially the same electrostatically positive surface (Zhang, *et al.*, 1987), available for protein-protein interactions. The balance of the TR surface contacts to DNA involves residues in helix C and the positively charged amino terminus of helix A. Therefore, the ApoR has an available surface which is positively charged and contains the L-tryptophan binding site. In the absence of L-

tryptophan, the ApoR dimers could interact with a surface which had a partial negative charge. The backside of the TR dimer, which would face away from the DNA when the protein was DNA bound, contains many negative groups. Some residues from helix F and F' (the prime denoting the second monomer in the dimer) are negatively charged at pH 6.0 (3 residues per helix). Many of the hydrophobic residues in helix F would be involved in the central hydrophobic core, orienting the negatively charged residues away from the core to the surface of the TR dimer. The carboxy-termini of helices A, E, A' and E' are negatively charged and would project away from the DNA binding surface (Figure 3). Other possible exposed areas would be residues toward the carboxy ends of the A and A' helices and the amino-termini of helices B and B'. Based on this charge evaluation, the backside of the TR dimer is negatively charged with respect to the front side, especially at pH 6.0.

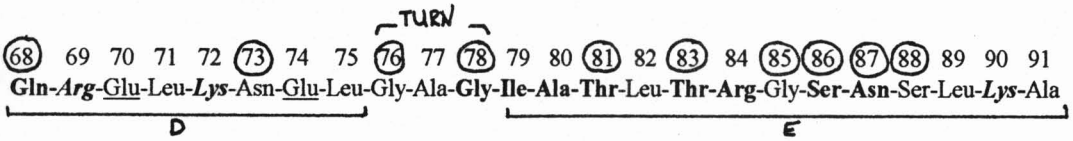

Figure 30. Amino acid sequence in the HTH region of the TR monomer polypeptide. The numbers indicate the amino acid residue numbers. The D and E helices are indicated, as well as the 3 amino acid "turn". Residues which make direct contact with DNA in the crystal structure based on the results of Otwinowski and coworkers (1988) are highlighted in bold lettering. Positively charged residues are shown in italics. Negatively charged residues are underlined. The residue numbers of polar, uncharged amino acids are circled.

Some interesting studies relating to the role of electrostatic interactions involve the so called *trp* "superrepressors" (Kelley and Yanofsky, 1985; Klig, *et al.*, 1987; Luisi and Sigler, 1990; Hurlburt and Yanofsky, 1992). Three of four "superrepressors" involve glutamic acid to lysine mutations (replacing a negatively charged amino acid with a positively charged amino acid). The mutants changing the negative charges to positive charges (EK13, EK18 and EK49) occur on the DNA binding face of the dimer (Schevitz, *et al.*, 1985). However, none of the three mutations involve sites reported to contact the DNA. Interestingly, at high salt concentration (0.4 M NaCl), corepressor liganded EK49 binds ten times more tightly to operator DNA than does wild type TR, but at 0.2 M NaCl, corepressor liganded EK49 binds only marginally better than wild type TR. This suggests that the stabilizing influence of the lysine substitution cannot be screened. In other words, a counterion doesn't influence the improved electrostatic attraction resulting from the substitution for specific binding. Unliganded EK49 binds 100 times better than wild type ApoR (non-specific DNA binding), indicating that the improved binding is not simply a matter of increased electrostatic attraction. The mutations increase the positive electrostatic charge on the DNA binding surface, enhancing binding in a more global manner, rather than in a direct, local electrostatic effect. This is

strongly supported by the increased binding of EK18 to DNA, which Otwinowski and coworkers (1988) judge to be in a position which could not directly contact B-DNA. The enhanced affinities of the superrepressors both for oligomerization and DNA binding further support interactions mediated by the protein's dipole.

2. Oligomerization of ApoR

The results of this work, considered with the TR dimer surface charges and protein dipole, suggest a simple mechanism that would be feasible in the cell for maintaining a minimum of DNA binding sites under conditions where no repression of TR operons is needed. The positively charged DNA binding face could be envisioned to bind electrostatically with the more negatively charged backside of another TR dimer, forming a "stack". This proposed model would not favor tetrameric TR over multimeric complexes. Destabilization of the complexes would occur when the corepressor concentration is sufficient for cellular activity and repression of transcription would be warranted. The L-tryptophan binding site is buried in the proposed contact region between TR dimers of the stacked multimer, requiring the dissociation of the multimer to allow corepressor binding. The attraction between the corepressor and its binding site is energetically favorable, as demonstated by

Zhang and coworkers (1987). Upon addition of corepressor to TR crystals, the crystals shattered. The destabilization of TR multimers in such a manner is supported by the results of this current study. The aporepressor under all conditions of salt concentration and pH examined shows evidence of higher order oligomers by the elevated correlation times at high concentrations (30 μM and higher). This is especially evident at pH 6.0 in solutions of no added or 10 mM KCl. A significant decrease in $<\tau_c>$ is observed for TR relative to ApoR. These results suggest a physiological role for oligomerization of TR *in vivo*. Once the cell manufactures sufficient L-tryptophan, dimeric TR, which has been held in a stacked oligomeric conformation, can be released to bind DNA as the active species.

A model of stacked ApoR dimers is further supported by Carey's 1988 finding that the specificity ratio for site specific binding over non-specific binding was only 200, whereas in the *lac* repressor it has been determined to be 10^6. If no factors influenced the binding of the TR to DNA other than the presence of co-repressor, it is possible that with this low selectivity the aporepressor could bind the operator sites by random action. With such a low selectivity, other regulatory factors would be implicated to keep TR available but not actively repressing transcription. Fewer DNA binding surfaces are available as a result of the

proposed stacking of TR dimers, keeping the number of ApoR DNA binding sites low and minimizing non-specific binding of TR to DNA. It was previously suggested that an experiment could be done to ascertain if tetrameric TR was present in solution at high TR concentrations, using high concentrations of TR (concentrations of TR, as dimer, exceeding 80 μM are necessary) to identify a correlation time plateau corresponding to tetrameric TR. Modification to the anticipated outcome of such an experiment could be suggested by the proposed stacking model. If several dimers stacked, either no plateau would be found at or above 80 μM TR_d or a plateau as well as further increases in correlation times at higher TR might be observed. A hypothesis of stacked TR dimers may be consistent with the results of Carey (1988), who found that TR bound to nonspecific DNA in an apparently very large complex (gel retardation assays at pH 6.0). Under conditions of low pH, the TR surfaces may remain sufficiently charged that excess TR can stack even with one TR dimer bound to DNA. In the presence of high ratios of TR to DNA, stacking may even be possible in the presence of corepressor.

The high concentrations of TR found in the cell (Gunsalus, *et al.*, 1986) also suggest that a mechanism must exist to keep ApoR bound and inactive when it's not needed. This model would also explain the observed salt effect on the TR

correlation time. The ionic association is screened by increasing salt concentration, and TR oligomers then dissociate. pH 6.0 would enhance the ionic charge of both sides of the TR dimer. At both pH 7.6 and 8.5 there would still remain some residual charge difference between dimer faces, which would diminish as the pH increased, largely by deprotonation of amine groups in the amino acid side chains.

3. Role of TR Oligomers in DNA Binding

A stacking model for the ApoR which is destabilized by corepressor would appear to contradict binding of TR to DNA in more than one stoichiometry, as higher order oligomers would dissociate to enable TR dimer binding to DNA to occur. The findings do not have to be incongruous, if <u>two</u> models are envisioned for TR association. One model can explain, as above, the association of ApoR, keeping the TR from binding to DNA when repression is not required. A second model could address the influence of TR subunit interactions on the differing stoichiometries observed for binding of TR dimers to the operator regions of DNA.

The role of the amino terminal arms (TA) of the TR have been a point of some study and may have involvement in TR interactions in the presence of DNA. The amino terminal arms are generally considered the first 6 to 15 amino acids

in the TR monomer polypeptide chain. Otwinowski and coworkers (1988), found the first 15 amino acids to be disordered, as was the case in the previous two crystallographic studies of ApoR and TR (Schevitz, *et al.*, 1985; Zhang, *et al.*, 1987). Zhang and coworkers concluded that the position of the arms was not defined by intramolecular interactions but rather by the neighboring molecules in the crystal lattice. Otwinowski and coworkers (1988) suggested that the failure of the TA to form a part of the repressor-operator interface in the crystal might reflect an important difference between natural interactions and those in the crystal. Because the evaluation of crystallographic data involves computer analysis and molecular modelling, four independent copies of each half operator are compared to define contacts involved. Evidence from our laboratory also shows that a six amino acid arm (amino acid sequence: ALA-GLN-GLN-SER-PRO-TRP[5]) does not bind to calf thymus (non-specific) DNA (data not shown). This provides some evidence that the arms do not make non-specific contacts with the DNA thus enhancing stability.

The TA have been suggested to be important in the facilitation of dimer folding (Schevitz, *et al.*, 1985 and

---

[5] ALA=alanine, non-polar residue; GLN=glutamine, uncharged, polar residue; SER=serine, uncharged, polar residue; PRO=proline, non-polar residue, TRP=tryptophan, non-polar residue that was substituted for the wild type residue TYR=tyrosine, uncharged, polar residue. The substitution of TRP for TYR was done to allow fluorescence studies on the six amino acid peptide, TRP providing a stronger emission signal.

Marmorstein, *et al.*, 1991), facilitation of diffusion (Zhang, *et al.*, 1987 and Hurlburt and Yanofsky, 1992) and promotion of protein-protein interactions (Kumamoto, *et al.*, 1987 and Otwinowski, *et al.*, 1988). In peptides synthesized from genes missing codons for amino acids 2-8 of the TR monomer polypeptide, no protein or repressor activity was found, possibly suggesting a role in protein folding or protection from degradation (Hurlburt and Yanofsky, 1992). NMR data (Arrowsmith, *et al.*, 1989) suggest that the energetic contribution of the arms to DNA binding is derived from stabilizing the first α-helix (the helix denoted A). Contribution of the arms to overall stability of TR is questioned because intact and armless TR shows essentially the same midpoint for urea-induced denaturation (Carey, 1989), which would indicate no difference in stability. Arrowsmith and coworkers (1989) support promiscuous DNA contacts with backbone phosphates (as proposed from crystallographic studies). Recall from Table III that NMR data were taken under conditions of high salt. Specific conditions included 100 mM NaH_2PO_4, pD 7.3, 500 mM KCl, TR concentration ≈ 1 mM and L-tryptophan concentration of +/- 1 mM (Arrowsmith, *et al.*, 1989). Under these conditions, TR oligomer equilibria have been shown in the present work to be shifted toward dimeric TR. With the TR equilibrium shifted toward the dimer, observation of interactions between TR dimers would not be expected. This conclusion

can also be considered in light of the TR/DNA and TR-DNS/DNA binding experiments done in the K. Matthews' laboratory (Rice University). If no difference between binding in the absence or presence of the positive amino terminus is observed, the role of the TA in contacting negatively charged DNA contacts cannot be critical to the DNA binding reaction.

The TA project out from the TR globular fold (Otwinowski, *et al.*, 1988). These results are corroborated by the NMR work of Lane,1986; Arrowsmith, *et al.*, 1989, 1991a and 1991b; Hyde, *et al.*, 1989 and 1991. Harrison and Aggarwal (1990) used the tandem binding proposal of Kumamoto and coworkers (1987) and found no elements of the central portion of the bound dimer interfering with an adjacent dimer in their modelling studies. In addition to the potential positive interaction between reading heads (Harrison and Aggarwal, 1990), an interaction between dimers via the amino terminal arms may exist. The arms are uncharged but some amino acids in the sequence are polar and can participate in hydrogen bonding. The positive charge of the amino terminus itself would be a factor in interactions between dimers via the "arms", but would not be the sole contributing interaction. It was reported from modelling of the crystallography data that the arms were sufficiently long to wrap around the DNA, allowing contacts with the minor groove bases (Schevitz, *et*

al., 1985), although protection experiments to date do not show protection in these areas. Schevitz and coworkers (1985) suggested that the arms may be positioned folded back along the A helix from their interpretation of the crystallographic data. This would position the TA in roughly the central region of the TR dimer/operator complex. The TA may be long enough to reach around the DNA and contact negatively charged and/or polar groups on the backside of a tandemly bound TR dimer, which would explain to some degree the cooperativity noted by LeTilly and Royer (evidenced by the sigmoidal curve shapes obtained in the TR-DNA binding fluorescence experiments, manuscript submitted to *Science*). A model of interaction between TR dimers bound to DNA involving the TA would provide a mechanism for protein-protein interactions between TR dimers on DNA, as well as a possible explanation for the loss of binding energy of the armless TR compared with intact TR observed by Carey (1989).

VIII. CONCLUSIONS

The oligomeric state of TR in the absence of DNA has been characterized as a function of TR concentration, pH, salt concentration and the concentration of corepressor, L-tryptophan. TR oligomers dissociate to dimers with decreasing TR concentration under all solution conditions studied. Both ApoR and TR form oligomers larger than dimer which are destabilized to dimeric TR by increasing salt concentration and increasing pH in the range of 6.0 to 8.5, indicating ionic interactions between dimers in TR oligomers. Oligomers are also destabilized by corepressor to dimeric TR. This demonstrates a link between ligand binding and TR protein subunit interactions, which may have implications in DNA binding. The electrostatic component of oligomerization together with the destabilization of ApoR multimers by corepressor suggests a physiological role for ApoR oligomers. The DNS label used to monitor the oligomeric state of the *trp* repressor has been found to bind primarily to the amino terminus of the TR monomer polypeptide. Therefore, changes in the probe lifetime upon dilution of TR suggest that the amino terminal arms are in or near the binding interface between ApoR dimers.

Energetic coupling of TR oligomerization with DNA binding is suggested by the present study results. The physiological

significance of TR subunit interactions in the differential modulation of transcription at DNA operons controlled by TR is supported by the high intracellular TR concentrations in *E. coli*. Taken collectively with previous work, this systematic evaluation of the influence of solution conditions on the oligomeric state of TR provides insight into the linked equilibria involved in the regulation of transcription by TR. These results demonstrate that TR exists as oligomers much larger than a dimer under a variety of solution conditions. In addition, the subunit interactions observed in this *in vitro* study provide evidence for an *in vivo* role for TR oligomerization. Regulation of transcription at operons controlled by TR may be modulated in part by differences in solution conditions through effects on protein-protein, protein-ligand and protein-DNA equilibria. This suggests complex and subtle contributions to transcriptional regulation *in vivo*.

VIII. BIBLIOGRAPHY

Alcala, J.R., Gratton, E., and Prendergast, F.G. (1987) *Biophys. J.* **51**, 597-604.

Arrowsmith, C.H., Carey, J., Treat-Clemons, L., and Jardetzky, O. (1989) Biochemistry **28**(9), 3875-3879.

Arrowsmith, C.H., Czaplicki, J., Iyer, S.B., and Jardetzky, O. (1991a) *J. Am. Chem. Soc.* **113**, 4020-4022.

Arrowsmith, C.H., Pachter, R., Altman, R., and Jardetzky, O. (1991b) *Eur. J. Biochem.* **202**, 53-66.

Arvidson, D.N., Bruce, C., and Gunsalus, R.P. (1986) *J. Biol. Chem.* **261**(1), 238-243.

Barkley, M.D., Lewis, P.A., and Sulliven, G.E. (1981) *Biochemistry* **20**, 3842-3851.

Bass, S., Sugioro, P., Arvidson, D.N., Gunsalus, R.P., and Youderian, P. (1987) *Genes Dev.* **1**, 565-572.

Beechem, J. M., Gratton, E., Ameloot, M., Knutson, J. R. & Brand, L. (1989) in *Fluorescence Spectroscopy: Principles and Techniques*, Vol. I, ed: Joseph R. Lakowicz, Plenum Press, New York.

Bennett, G.N., Schweingruber, M.E., Brown, K.D., Squires, C., and Yanofsky, C. (1976) *Proc. Natl. Acad. Sci. USA* **73**, 2351-2355.

Blackwood, E.M. and Eisenman, R.N. (1991) *Science* **251**, 1211-1217.

Carey, J. (1988) *Proc. Natl. Acad. Sci. USA* **85**, 975-979.

Carey, J. (1989) *J. Biol. Chem.* **264**(4),1941-1945.

Fernando, T.M. (1991) PhD Thesis, University of Illinois at Urbana-Champaign.

Fernando, T. and Royer, C., (1992) *Biochemistry* **31**, 3429-3441.

Gartenberg, M.R., Ampe, C., Steitz, T.A., and Crothers, D.M. (1990) *Proc. Natl. Acad. Sci. USA* **87**, 6034-6038.

Graddis, T.J., Klig, L.S., Yanofsky, C., and Oxender, D.L. (1988) *Proteins* **4**, 173-181.

Gratton, E., Jameson, D.M., and Hall, R.D. (1984a) *Ann. Rev. Biophys. Bioeng.* **13**, 105-124.

Gratton, E., Limkeman, M., Lakowicz, J., Maliwal, B. P., Cherek, H. & Laczko, G. (1984b) *Biophys. J.* **46**, 479-486.

Gratton, E. & Limkeman, M. (1983) *Biophys. J.* **44**, 315-323.

Guest, C.R., Hochstrasser, R.A., Dupuy, C.G., Allen, D.J., Benkovic, S.J., and Millar, D.P. (1991) *Biochemistry* **30**, 8759-8770.

Gunsalus, R.P., Gunsalus-Miquel, A., and Gunsalus, G.L. (1986) *J. Bacteriol.* **167**(1), 272-278.

Gunsalus, R.P. and Yanofsky, C. (1980) *Proc. Natl. Acad. Sci. USA* **77**(12), 7117-7121.

Haran, T.E., Joachimiak, A., and Sigler, P.B. (1992) *EMBO J.* **11**(8), 3021-3030.

Harrison, S.C. and Aggarwal, A.K. (1990) *Annu. Rev. Biochem.* **59**, 933-969.

Haugland, R.P. (1983) in *Excited States of Biopolymers* (Steiner, R.F., Ed.), Plenum Press, NY.

Haydock, P.V., and Somerville, R.L. (1984) *Biochem. Biophys. Res. Comm.* **119**(3), 926-932.

Hsieh, W-T. and Matthews, K.S. (1985) *Biochemistry* **24**(12), 3043-3049.

Hurlburt, B.K. and Yanofsky, C. (1992) *Nucleic Acids Res.* **20**(2), 337-341.

Hyde, E.I., Ramesh, V., Roberts, G.C.K., Arrowsmith, C.H., Treat-Clemons, L., Klaic, B., and Jardetzky, O. (1989) *Eur. J. Biochem.* **183**, 545-553.

Hyde E.I., Ramesh, V., Frederick, R., and Roberts, G.C.K. (1991) *Eur. J. Biochem.* **201**, 569-579.

Ingraham, J.L., Maaloe, O., and Neidhardt, F.C. (1983) *Growth of the Bacterial Cell*, Sinauer Associates, Sunderland, MA.

Jaenicke, R. (1991) *Biochemistry* **30**(13), 3147-3161.

Jameson, D. M. (1978) Ph.D. Dissertation, University of Illinois, Urbana,IL.

Jameson D.M. and Gratton, E. (1983) in *New Directions in Molecular Luminescence*, ASTM STP822 (Eastwooe, D., Ed.) pp 67-81.

Janin, J., Miller, S., and Chothia, C. (1988) *J. Mol. Biol.* **204**, 155-164.

Jarvis, T.C., Ring, D.M., Daube, S.S., and von Hippel, P.H. (1990) *J. Biol Chem.* **265**(25), 15160-15167.

Joachimiak, A., Kelley, R.L., Gunsalus, R.P., Yanofsky, C., and Sigler, P.B. (1983) *Proc. Natl. Acad. Sci. USA* **80**, 668-672.

Johnson, P.F. and McKnight, S.L. (1989) *Annu. Rev. Biochem.* **58**, 799-839.

Kelley, R.L. and Yanofsky, C. (1985) *Proc. Natl. Acad. Sci. USA* **82**, 483-487.

Klig, L.S., Carey, J., and Yanofsky, C. (1988) *J. Mol. Biol.* **202**, 769-777.

Klig, L.S., Crawford, I.P., and Yanofsky, C. (1987) *Nucleic Acids Res.* **15**(13), 5339-5351.

Koblan, K.S. and Ackers, G.K. (1991) *Biochemistry* **30**(31), 7817-7821.

Kouzarides, T. and Ziff,E. (1989) *Nature* **340**, 568-571.

Kumamoto, A.A., Miller, W.G., and Gunsalus, R.P. (1987) *Genes Dev.* **1**, 556-564.

Lakowicz, J.R. (1983) *Principles of Fluorescence Spectroscopy*, Plenum Press, NY.

Lambooy, P.K., Steiner, R.F., and Sternberg, H. (1982) *Arch. Biochem. Biophys.* **217**,517-528.

Lane, A.N. (1986) *Eur. J. Biochem.* **157**, 405-413.

Lawson, C.L., Zhang, R-G., Schevitz, R.W., Otwinowski, Z., Joachimiak, A., and Sigler, P.B. (1988) *Proteins* **3**,18-31.

Liu, Y-C. (1991), PhD Thesis, Rice University.

Luisi, B.F. and Sigler, P.B. (1990) *Biochim. Biophys. Acta* **1048**, 113-126.

Marmorstein, R.Q., Joachimiak, A., Sprinzl, M., and Sigler, P.B. (1987) *J. Biol. Chem.* **262**(10), 4922-4927.

Marmorstein, R.Q., Sprinzl, M., and Sigler, P.B. (1991) *Biochemistry* **30**, 1141-1148.

Mauk, M.R., Barker, P.D., and Mauk, A.G. (1990) *Biochemistry* **30**(41), 9873-9881.

Murre, C., McCaw, P.S., Vaessin, H., Caudy, M., Jan, L.Y., Jan, V.N., Cabrera, C.V., Buskin, J.N., Huruschka,S.D., Lassar, A.B., Weintraub, H., and Baltimore, D. (1989) *Cell* **58**, 537-544.

Otwinowski, Z., Schevitz, R.W., Zhang, R-G., Lawson, C.L., Joachimiak, A., Marmorstein, R.Q., Luisi, B.F., and Sigler, P.B. (1988) *Nature* **335**, 321-329.

Paluh, J.L. and Yanofsky, C. (1986) *Nucleic Acids Res.* **14**, 7851-7860.

Perrin, F. (1926) *J. Phys. Radium* **7**, 390-401.

Phillips, S.E.V. (1991) *Curr. Opin. Struct. Biol.* **1**, 89-98.

Record, M.T., Jr., Anderson, C.F. and Lohman, T.M. (1978) *Quart. Rev. Biophys.* **11**(2), 103-178.

Record, M.T., Jr., Lohman, T.M., and deHaseth, P., (1976) *J. Mol. Biol.* **107**, 145-158.

Richey, B., Cayley, D.S., Mossing, M.C., Kolka, C., Anderson, C.F., Farran, T.C., and Record, M.T. Jr. (1987) *J. Biol. Chem.* **262**(15), 7157-7164.

Revzin, A. and von Hippel, P.H. (1977) *Biochemistry* **16**(22), 4769-4776.

Royer, C.A., Chakerian, A.E., and Matthews, K.S. (1990) *Biochemistry* **29**,4959-4966.

Royer, C.A., Rusch, R.M., and Scarlatta, S.F. (1989) *Biochemistry* **28**, 6631-6637.

Schevitz, R.W., Otwinowski, Z., Joachimiak, A., Lawson, C.L., and Sigler, P.B. (1985) *Nature* **317**, 782-786.

Senear, D.F. and Ackers, G.K. (1990) *Biochemistry* **29**, 6568-6577.

Tasayco, M.L. and Carey, J. (1992) *Science* **255**, 594-597.

Tsapakos, M., Haydock, P.V., Hermodson, M., and Somerville, R.L. (1985) *J. Biol. Chem.* **260**, 16383-16394.

Turner, R. and Tjian, R. (1989) *Science* **243**, 1689-1694.

Weber, G. (1953) *Adv. in Protein Chem.* **8**, 415-459.

Weber, G. (1966) in *Fluorescence and Phosphorescence Analysis* (Chapter 8) (Hercules, D.M., Ed.) Interscience Publishers, div. of John Wiley & Sons, NY.

Weber, G. (1972) *Biochemistry* **11**, 864-878.

Weber, G. (1977) *J. Chem. Phys.* **66**, 4081-4091.

Weber, G. (1981) *J. Phys. Chem.* **85**, 949-953.

Weber, G. (1992) *Protein Interactions*, Chapman and Hall, NY.

Zhang, R-G., Joachimiak, A., Lawson, C.L., Schevitz, R.W., Otwinowski, Z., and Sigler, P.B. (1987) *Nature* **327**, 591-596.

Zubay, G., Morse, D.E., Schrenk, W.J., and Miller, J.H.M. (1972) *Proc. Natl. Acad. Sci. USA* **69**(5), 1100-1103.

Zurawski, G., Gunsalus, R.P., Brown, K.D., and Yanofsky, C. (1981) *J. Mol. Biol.* **145**, 47-73.

APPENDIX A

Anisotropy Results by pH and Salt Concentration

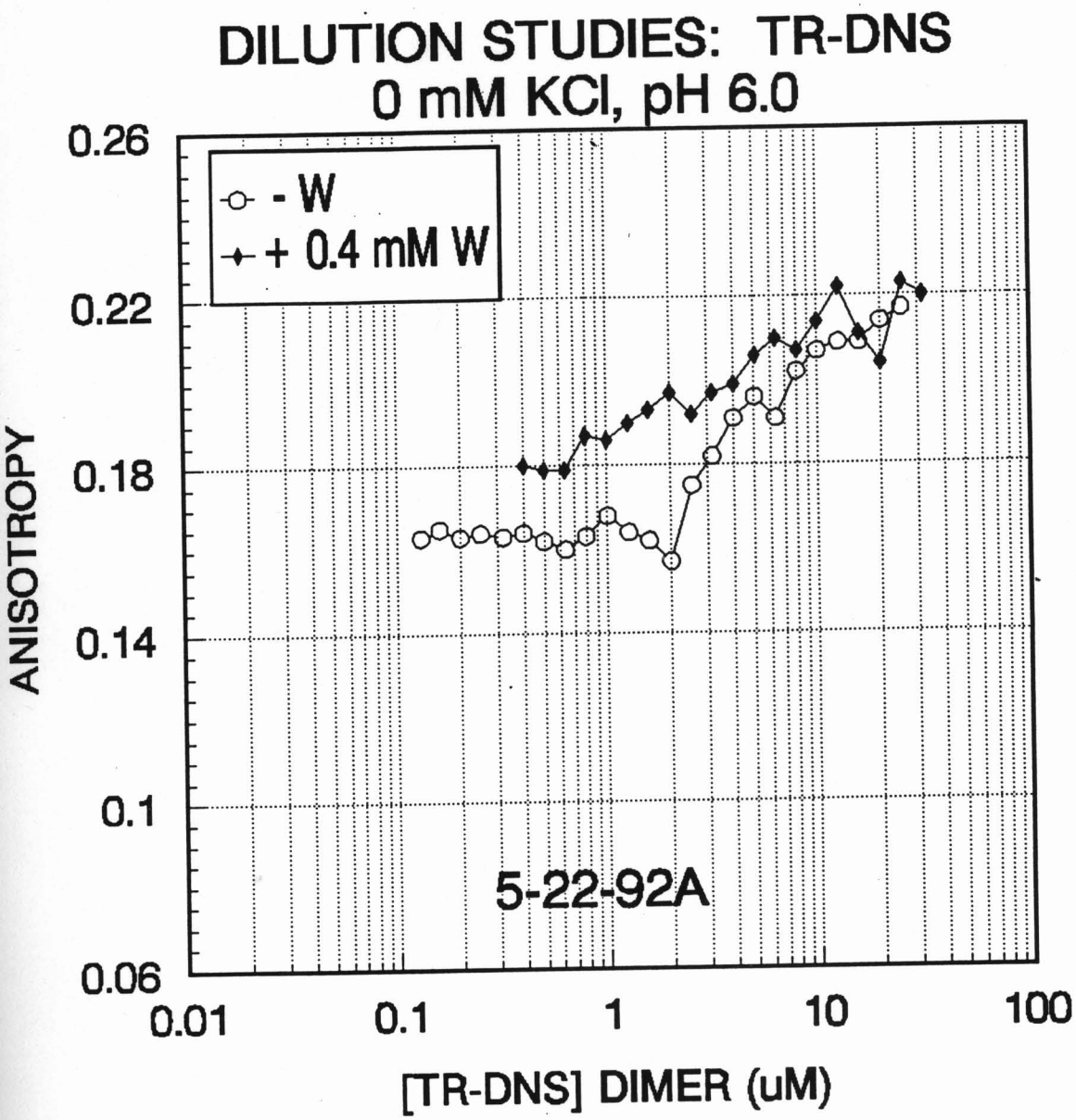
DILUTION STUDIES: TR-DNS
0 mM KCl, pH 6.0
- W
+ 0.4 mM W
0.26
0.22
0.18
0.14
0.1
0.06
ANISOTROPY
5-22-92A
0.01
0.1
1
10
100
[TR-DNS] DIMER (uM)

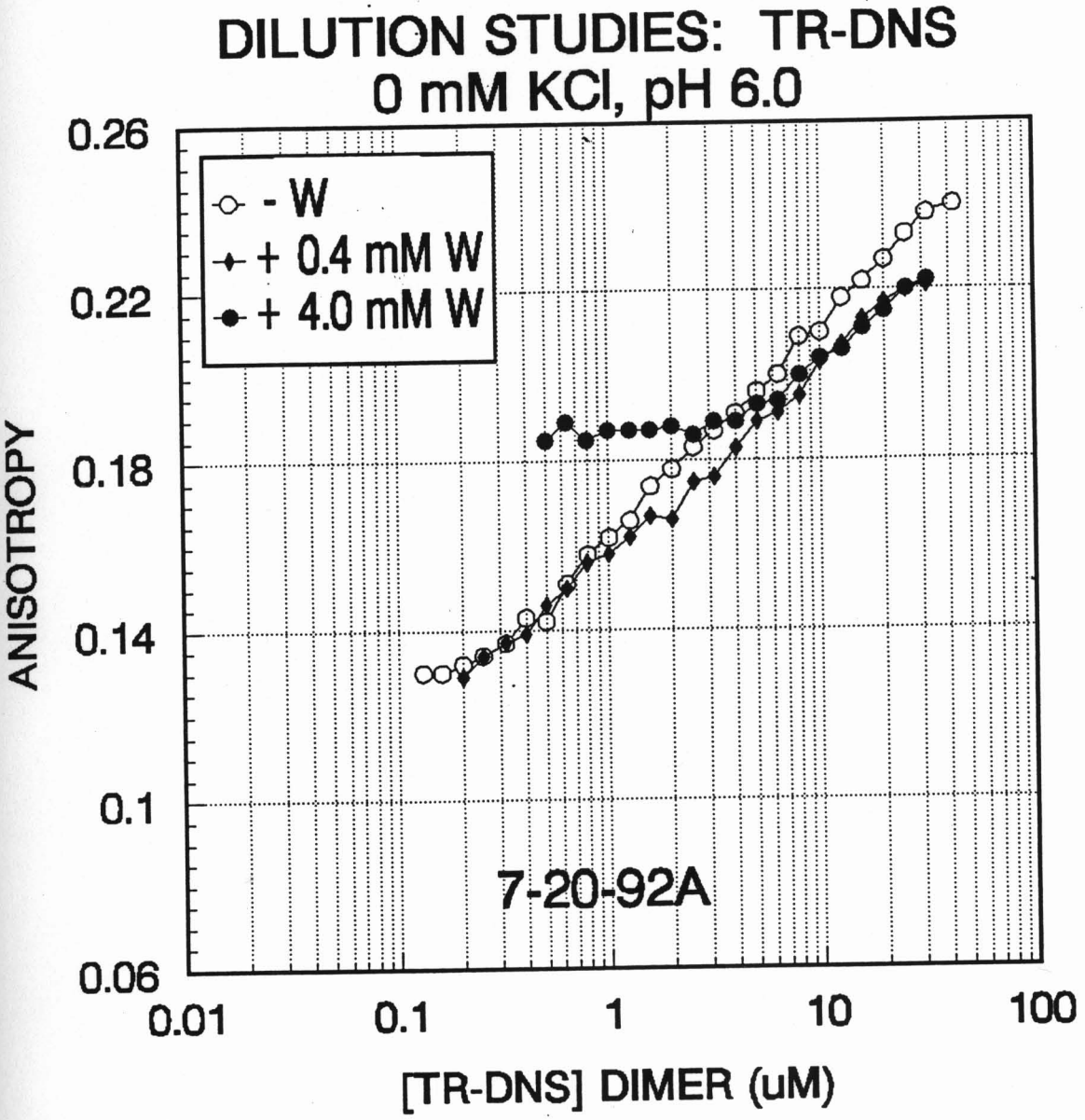
DILUTION STUDIES: TR-DNS
0 mM KCl, pH 6.0
- W
+ 0.4 mM W
+ 4.0 mM W
7-20-92A
ANISOTROPY
0.26
0.22
0.18
0.14
0.1
0.06
0.01
0.1
1
10
100
[TR-DNS] DIMER (uM)

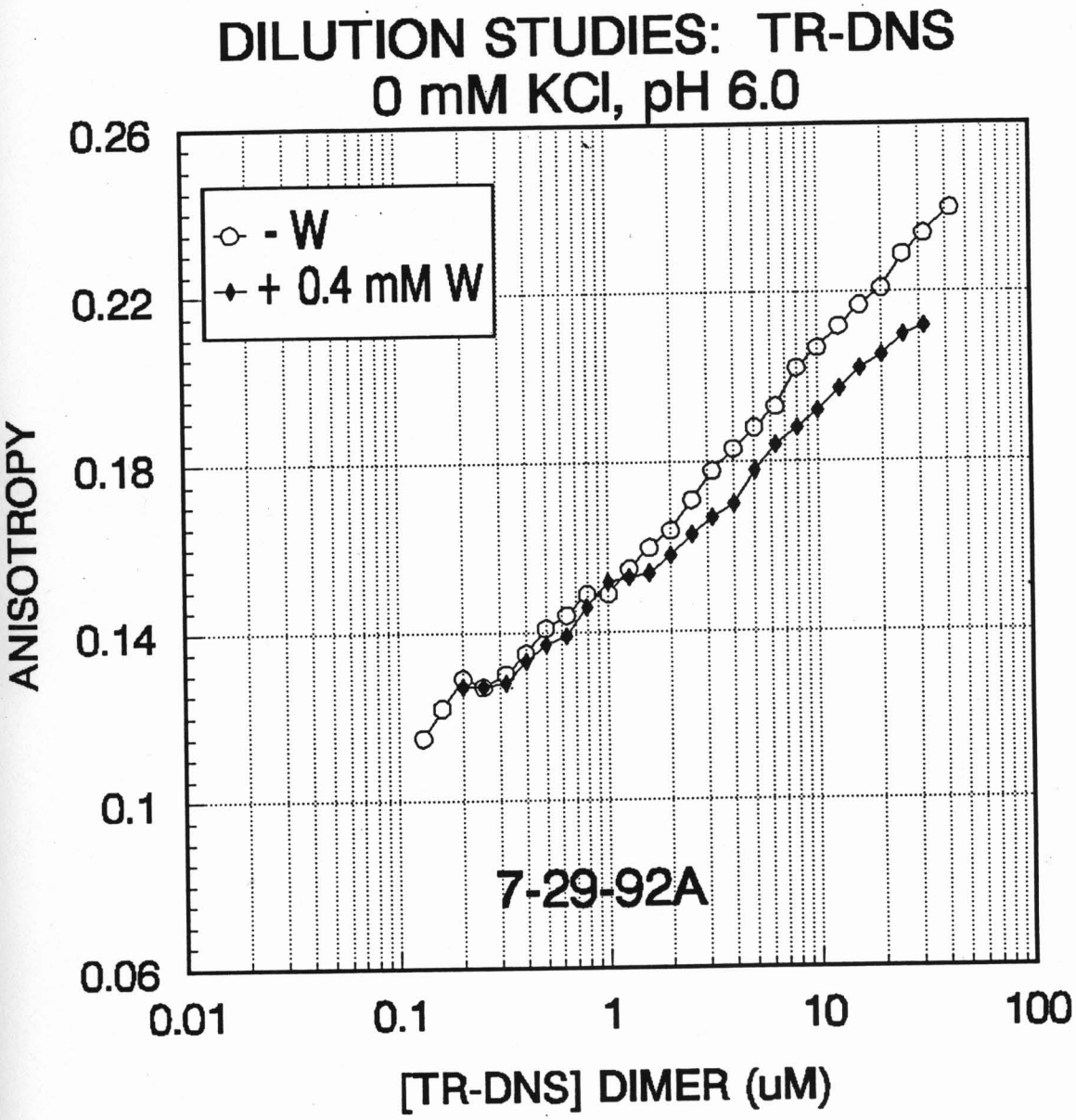
DILUTION STUDIES: TR-DNS
0 mM KCl, pH 6.0
- W
+ 0.4 mM W
7-29-92A
ANISOTROPY
0.26
0.22
0.18
0.14
0.1
0.06
0.01
0.1
1
10
100
[TR-DNS] DIMER (uM)

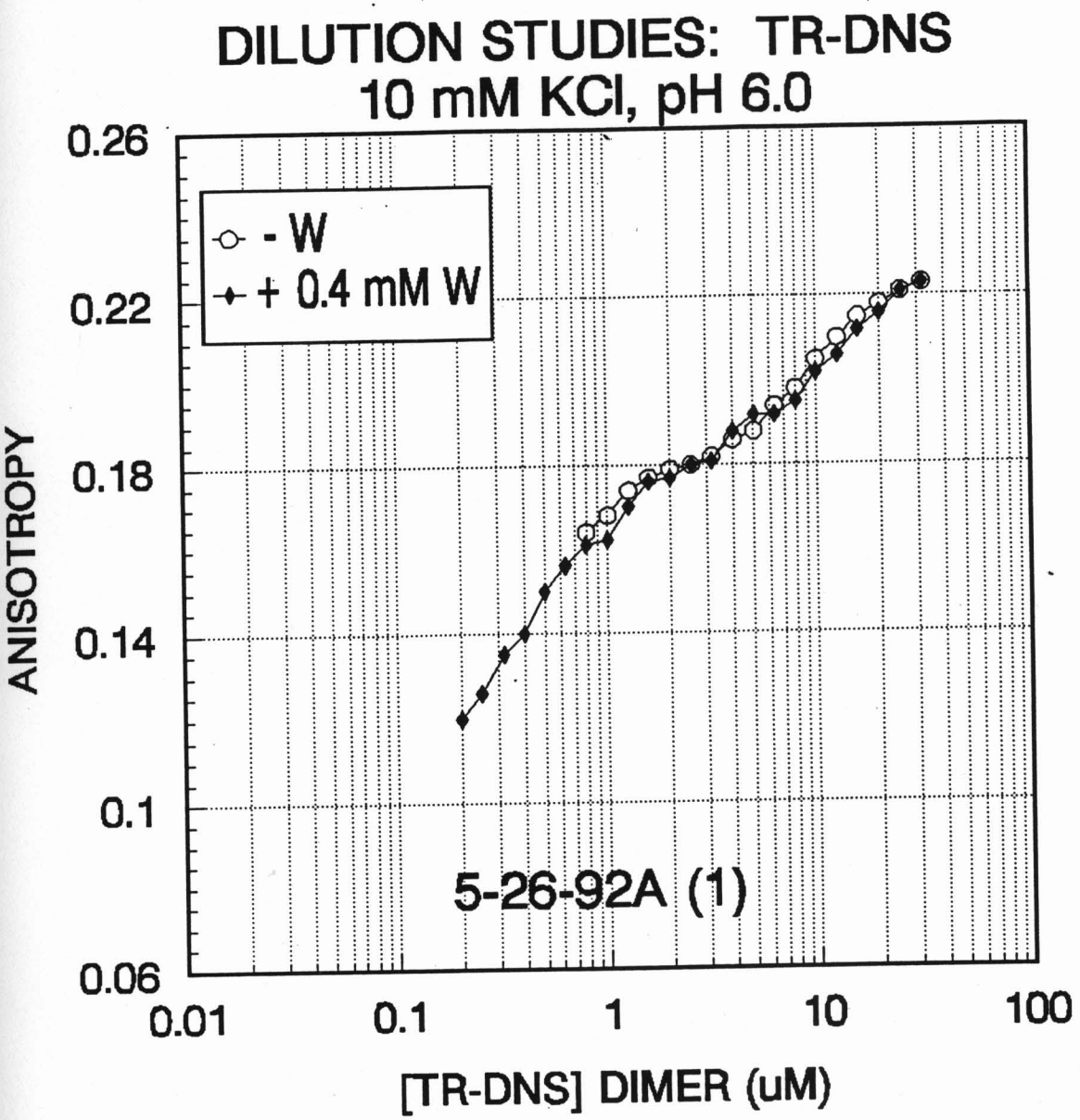
DILUTION STUDIES: TR-DNS
10 mM KCl, pH 6.0
- W
+ 0.4 mM W
5-26-92A (1)
ANISOTROPY
0.26
0.22
0.18
0.14
0.1
0.06
0.01
0.1
1
10
100
[TR-DNS] DIMER (uM)

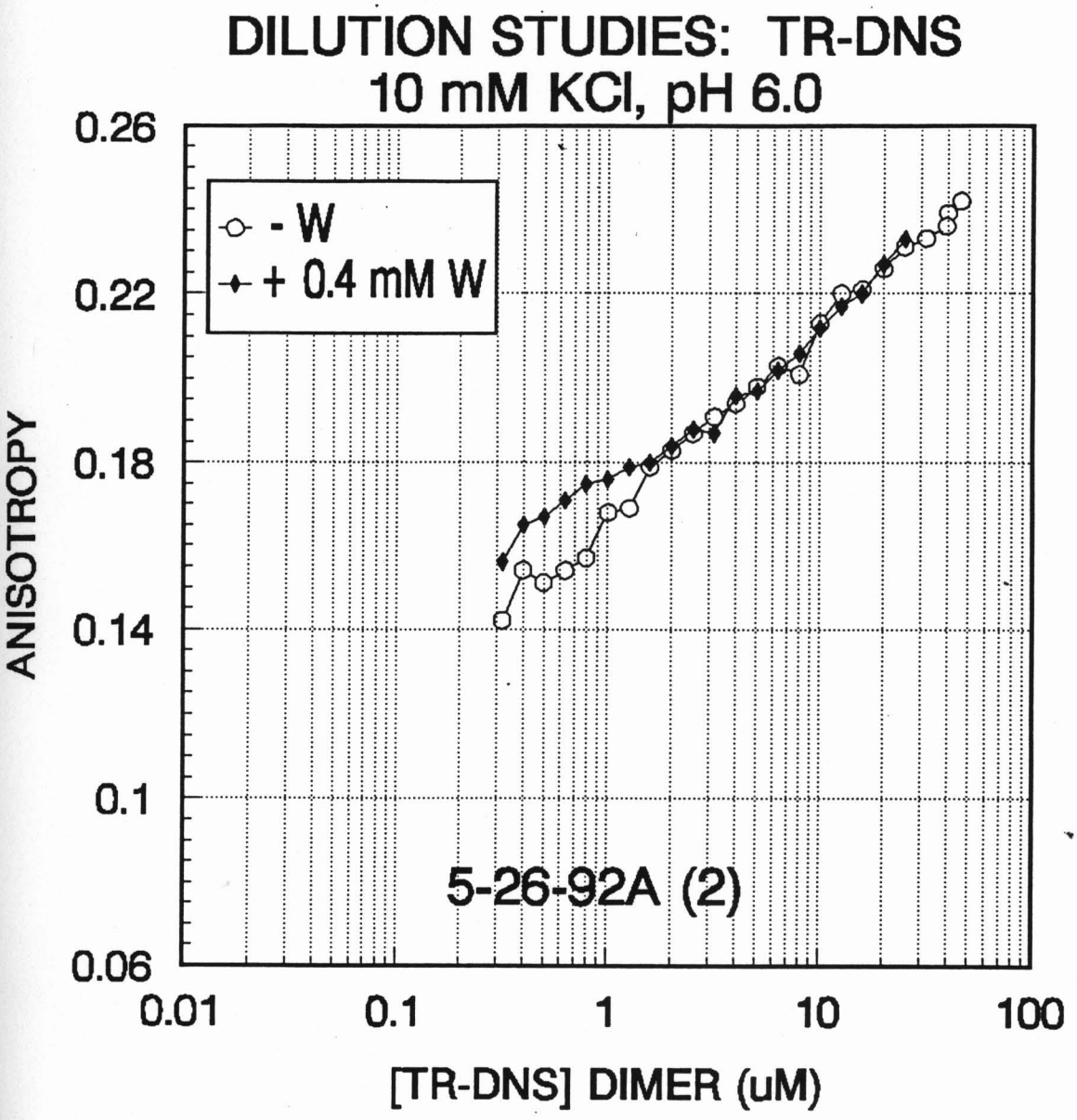
DILUTION STUDIES: TR-DNS
10 mM KCl, pH 6.0
- W
+ 0.4 mM W
5-26-92A (2)
ANISOTROPY
0.26
0.22
0.18
0.14
0.1
0.06
0.01
0.1
1
10
100
[TR-DNS] DIMER (uM)

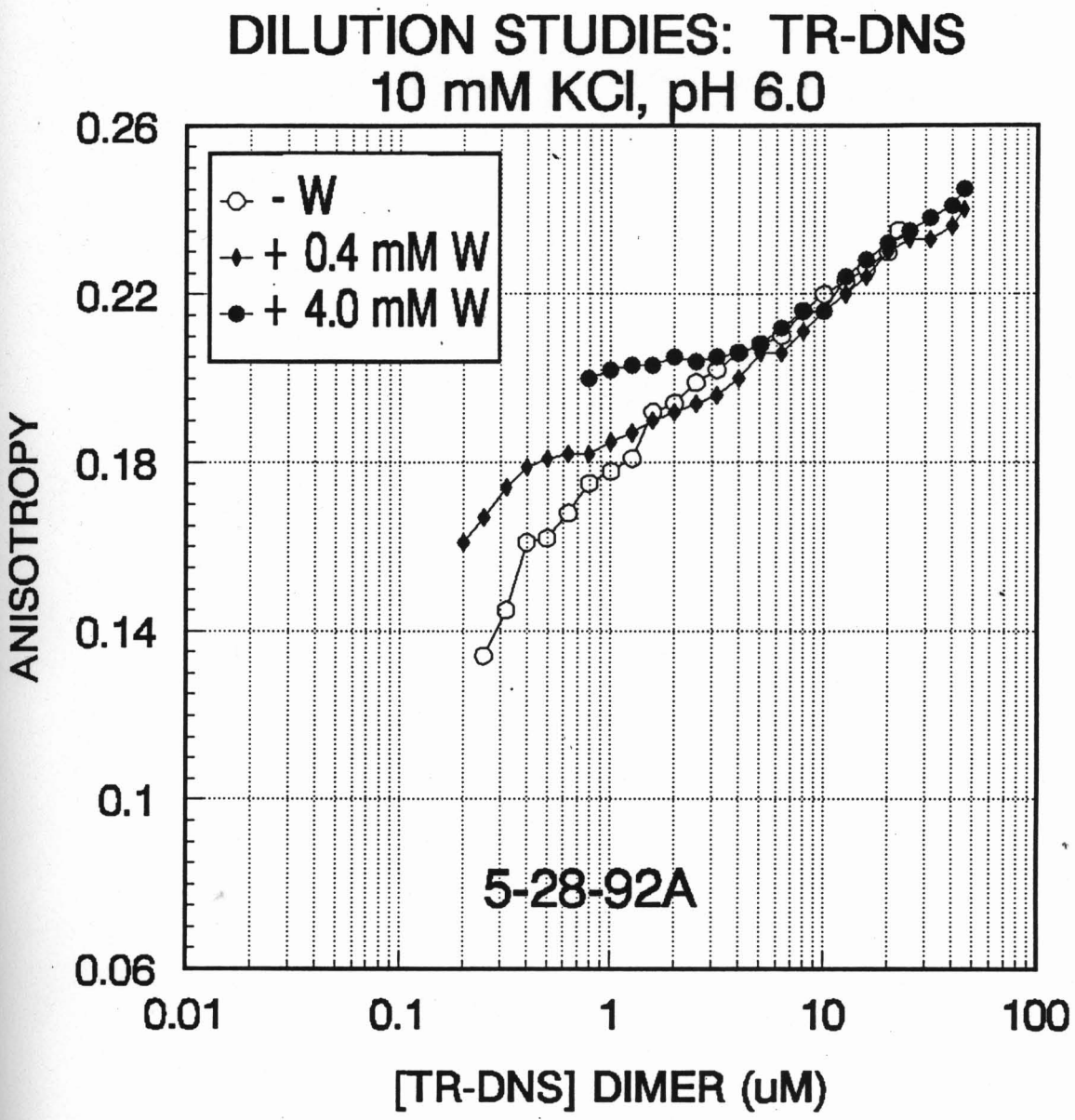
DILUTION STUDIES: TR-DNS
10 mM KCl, pH 6.0
- W
+ 0.4 mM W
+ 4.0 mM W
5-28-92A
ANISOTROPY
0.26
0.22
0.18
0.14
0.1
0.06
0.01
0.1
1
10
100
[TR-DNS] DIMER (uM)

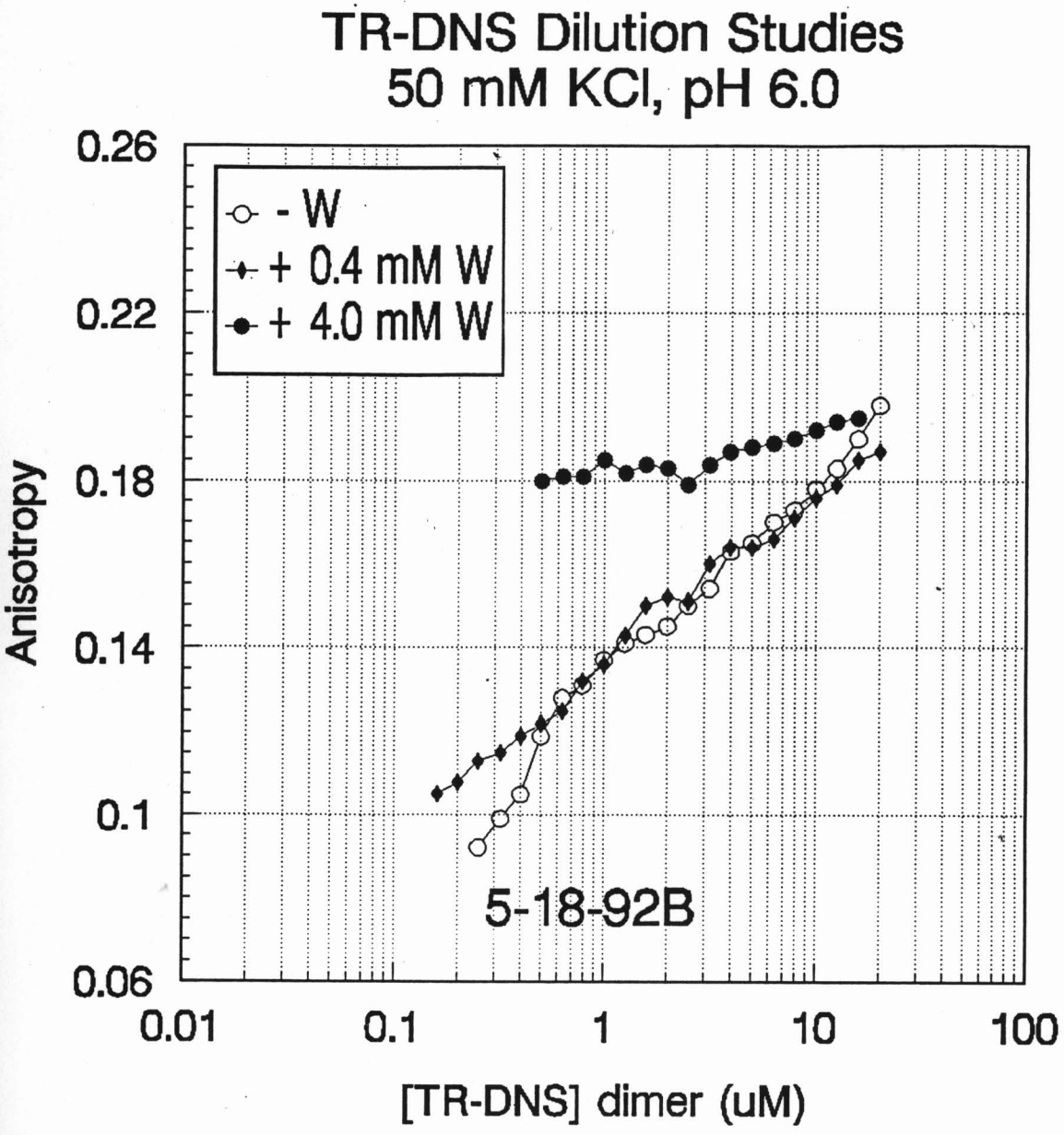
TR-DNS Dilution Studies
50 mM KCl, pH 6.0
- W
+ 0.4 mM W
+ 4.0 mM W
Anisotropy
0.26
0.22
0.18
0.14
0.1
0.06
0.01
0.1
1
10
100
[TR-DNS] dimer (uM)
5-18-92B

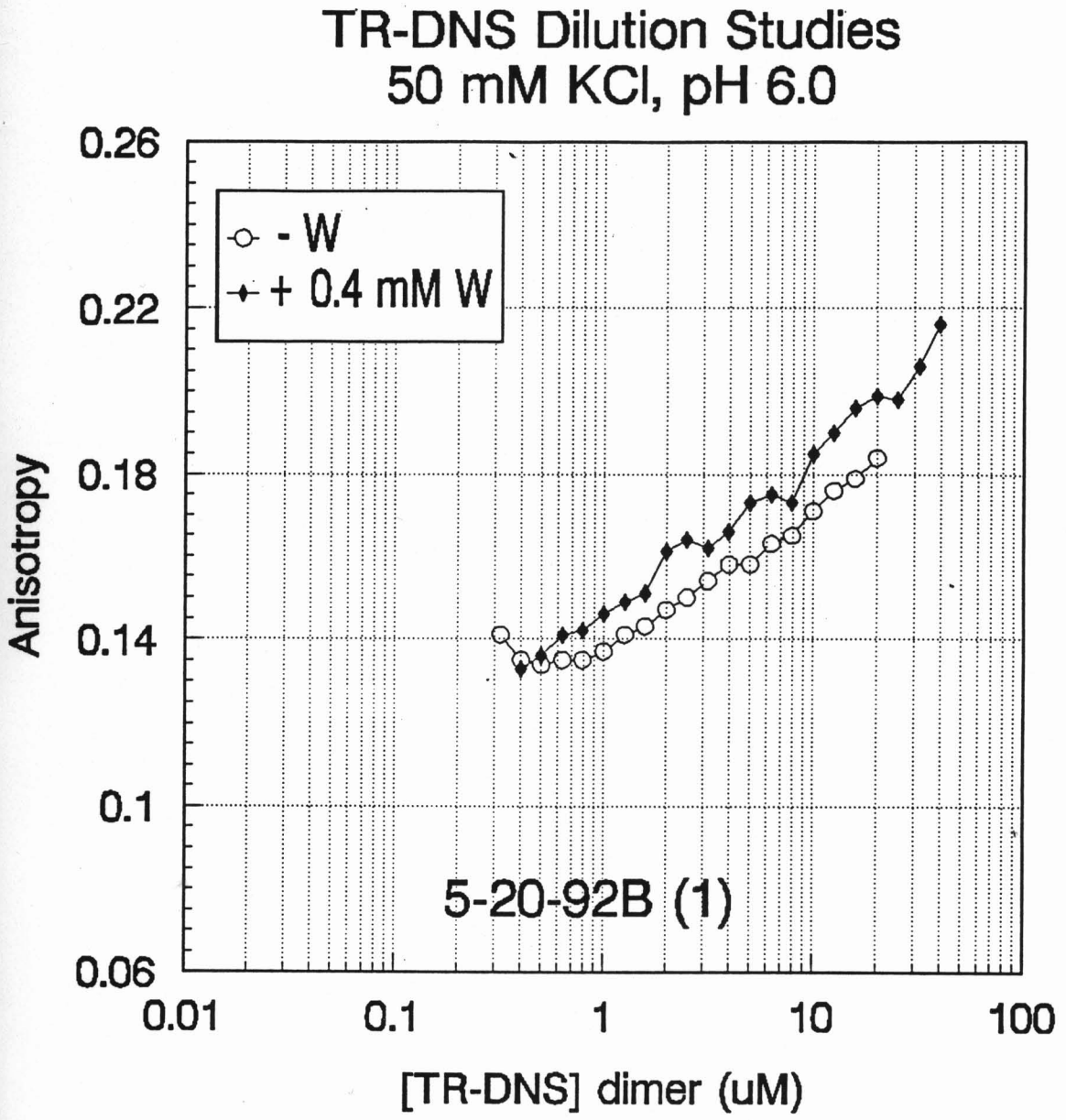
TR-DNS Dilution Studies
50 mM KCl, pH 6.0
- W
+ 0.4 mM W
5-20-92B (1)
Anisotropy
0.26
0.22
0.18
0.14
0.1
0.06
0.01
0.1
1
10
100
[TR-DNS] dimer (uM)

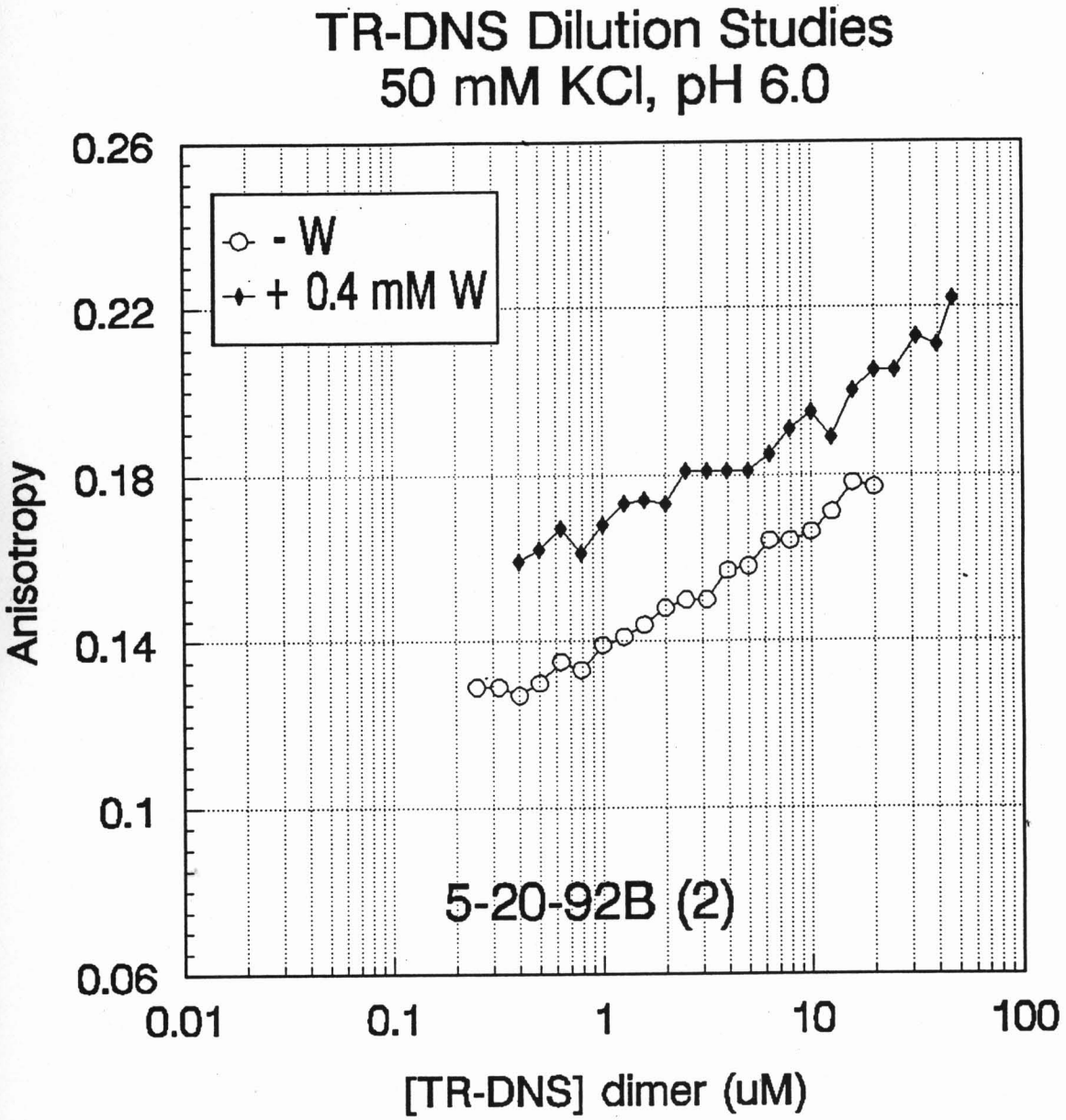
TR-DNS Dilution Studies
50 mM KCl, pH 6.0
- W
+ 0.4 mM W
5-20-92B (2)
Anisotropy
0.26
0.22
0.18
0.14
0.1
0.06
0.01
0.1
1
10
100
[TR-DNS] dimer (uM)

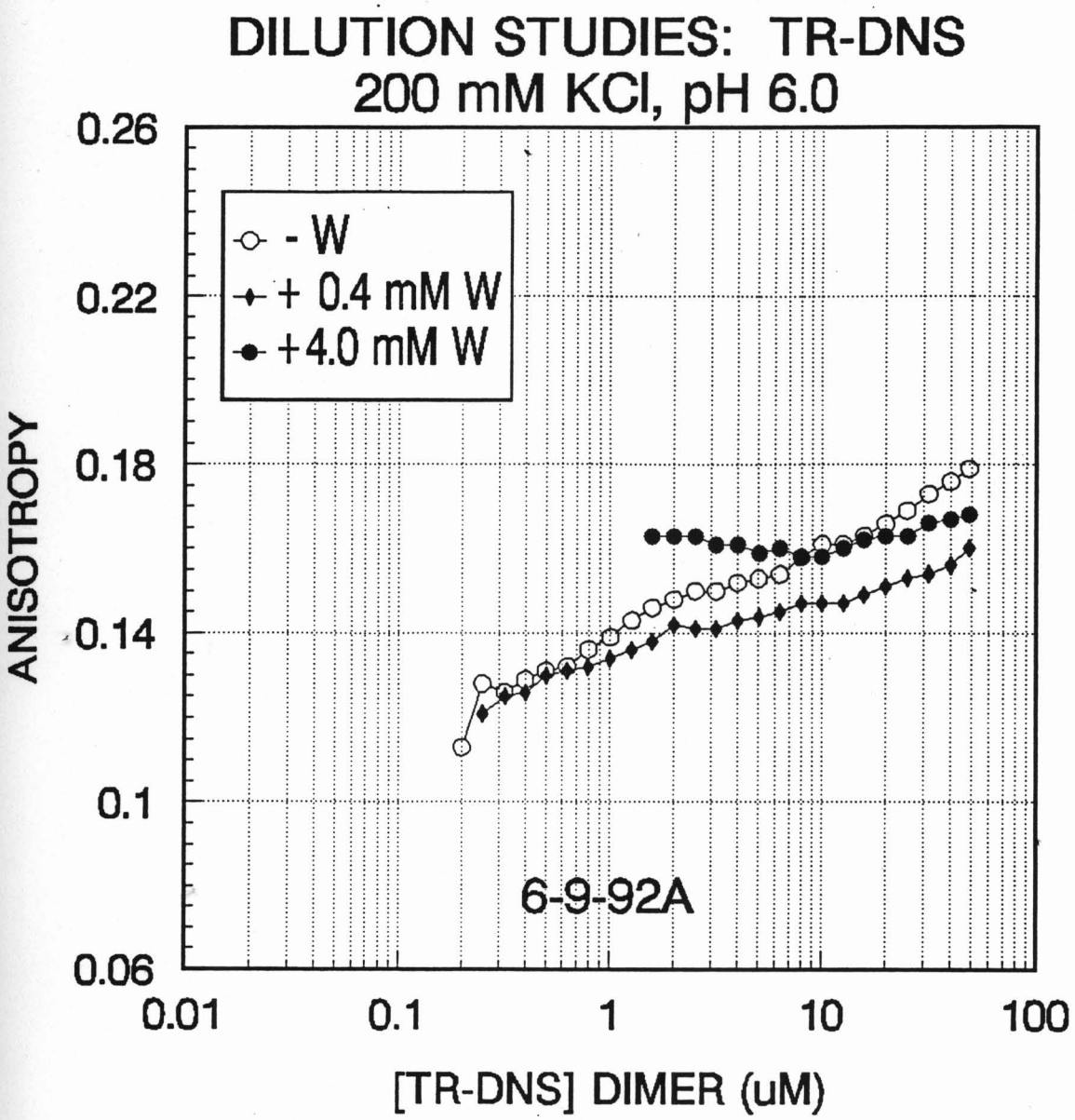
DILUTION STUDIES: TR-DNS
200 mM KCl, pH 6.0
- W
+ 0.4 mM W
+4.0 mM W
6-9-92A
ANISOTROPY
0.26
0.22
0.18
0.14
0.1
0.06
0.01
0.1
1
10
100
[TR-DNS] DIMER (uM)

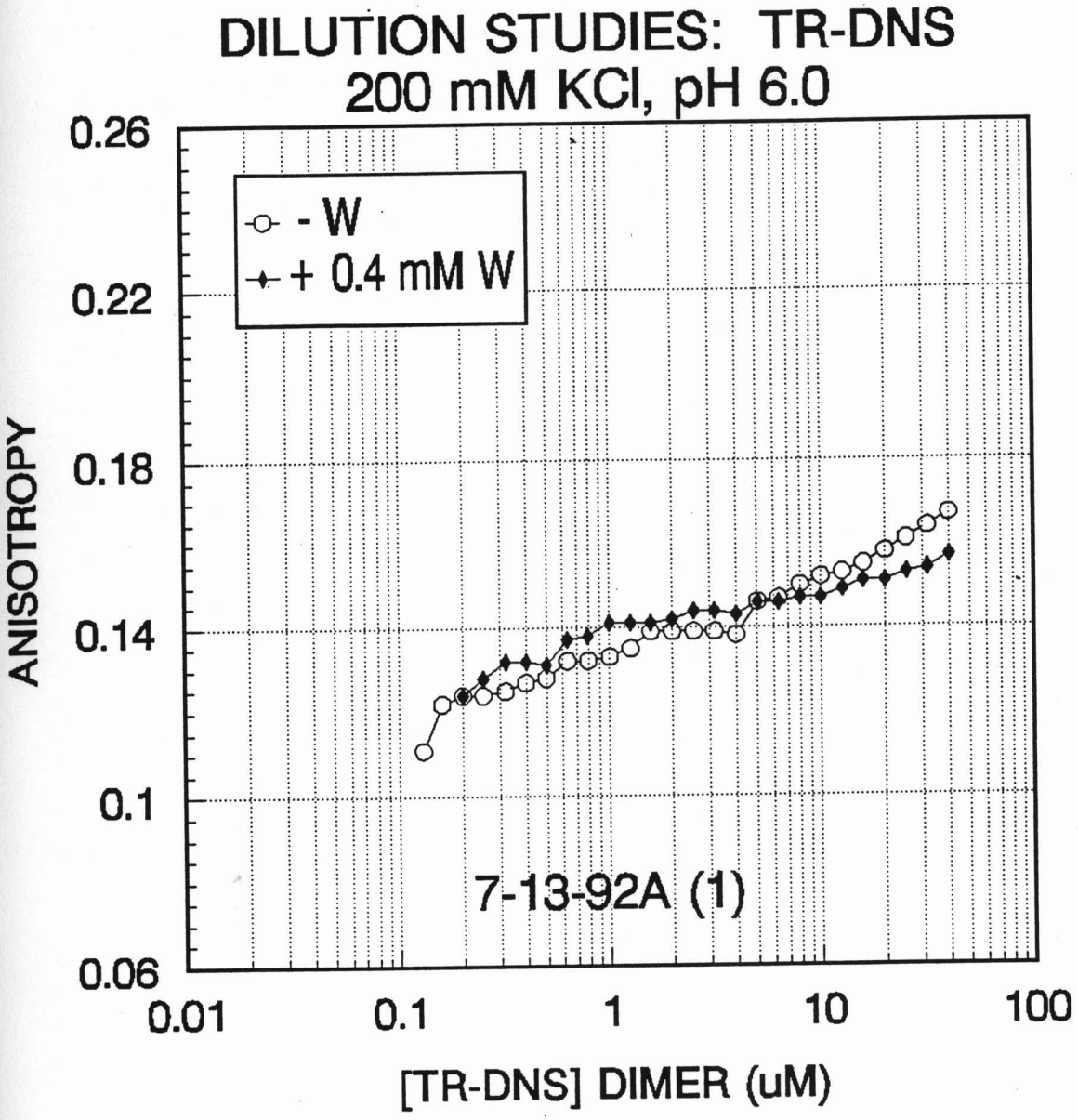
DILUTION STUDIES: TR-DNS
200 mM KCl, pH 6.0
- W
+ 0.4 mM W
7-13-92A (1)
ANISOTROPY
0.26
0.22
0.18
0.14
0.1
0.06
0.01
0.1
1
10
100
[TR-DNS] DIMER (uM)

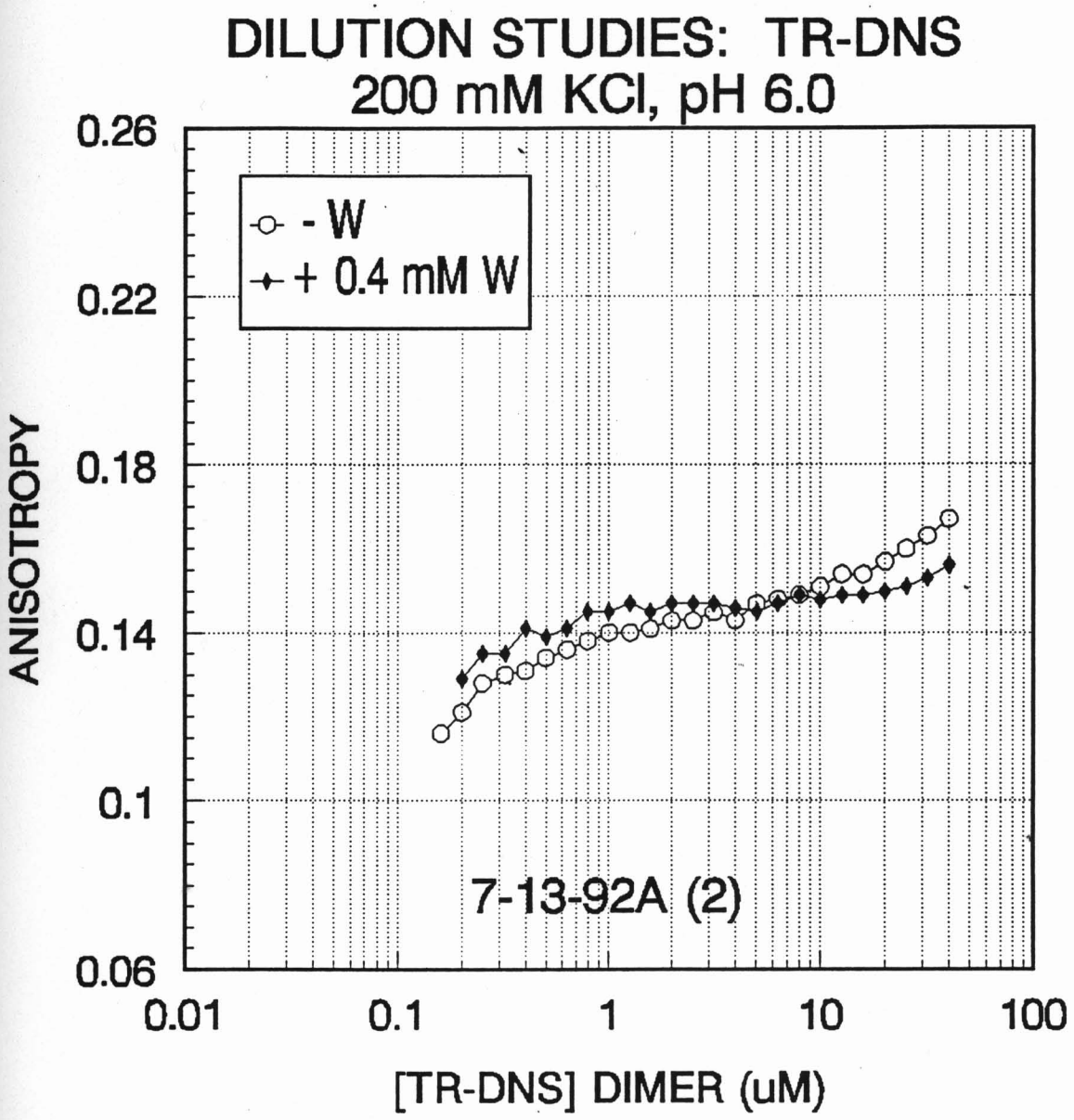
DILUTION STUDIES: TR-DNS
200 mM KCl, pH 6.0
- W
+ 0.4 mM W
ANISOTROPY
0.26
0.22
0.18
0.14
0.1
0.06
0.01
0.1
1
10
100
7-13-92A (2)
[TR-DNS] DIMER (uM)

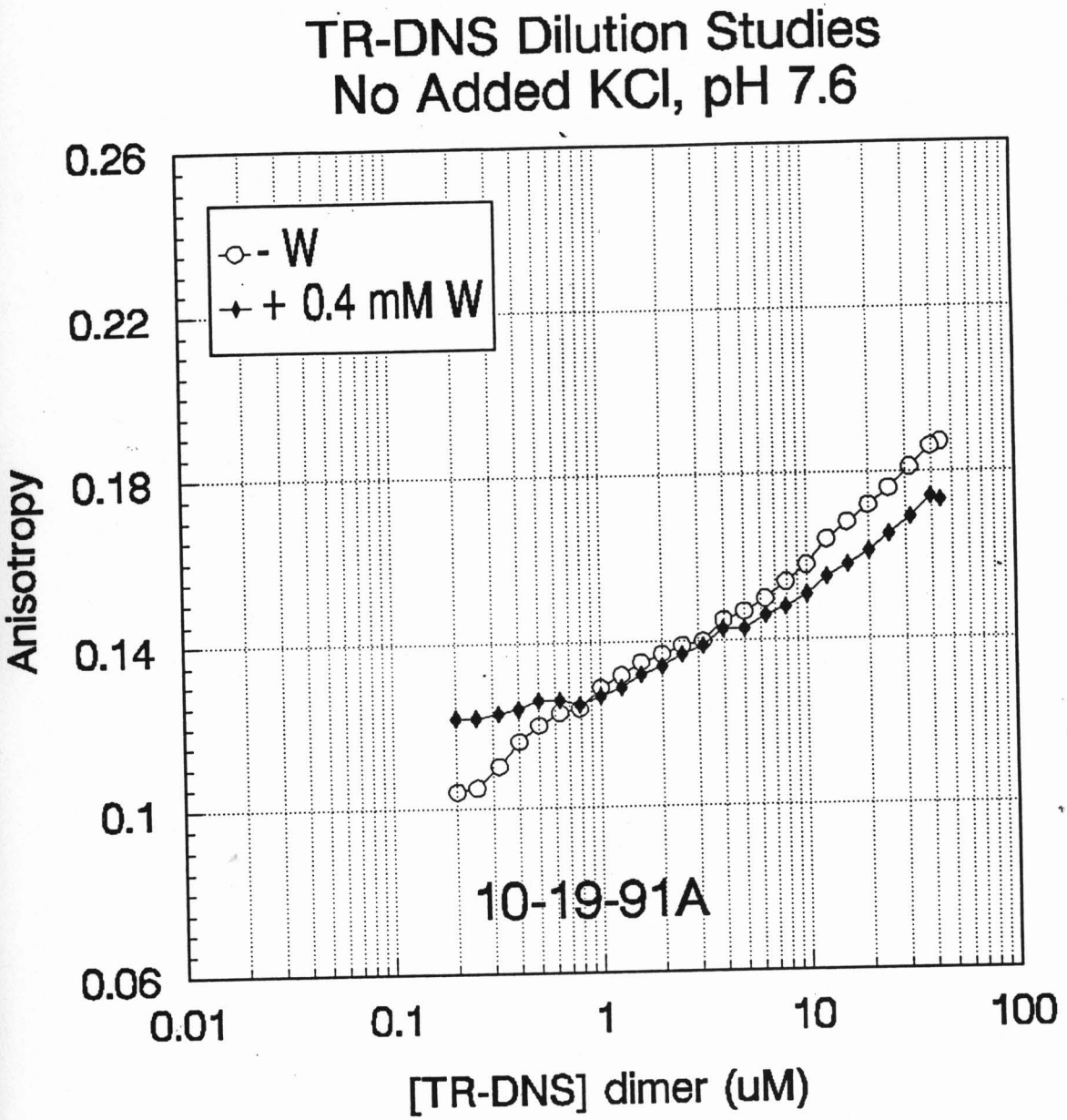
TR-DNS Dilution Studies
No Added KCl, pH 7.6
- W
+ 0.4 mM W
0.26
0.22
0.18
0.14
0.1
0.06
Anisotropy
10-19-91A
0.01
0.1
1
10
100
[TR-DNS] dimer (uM)

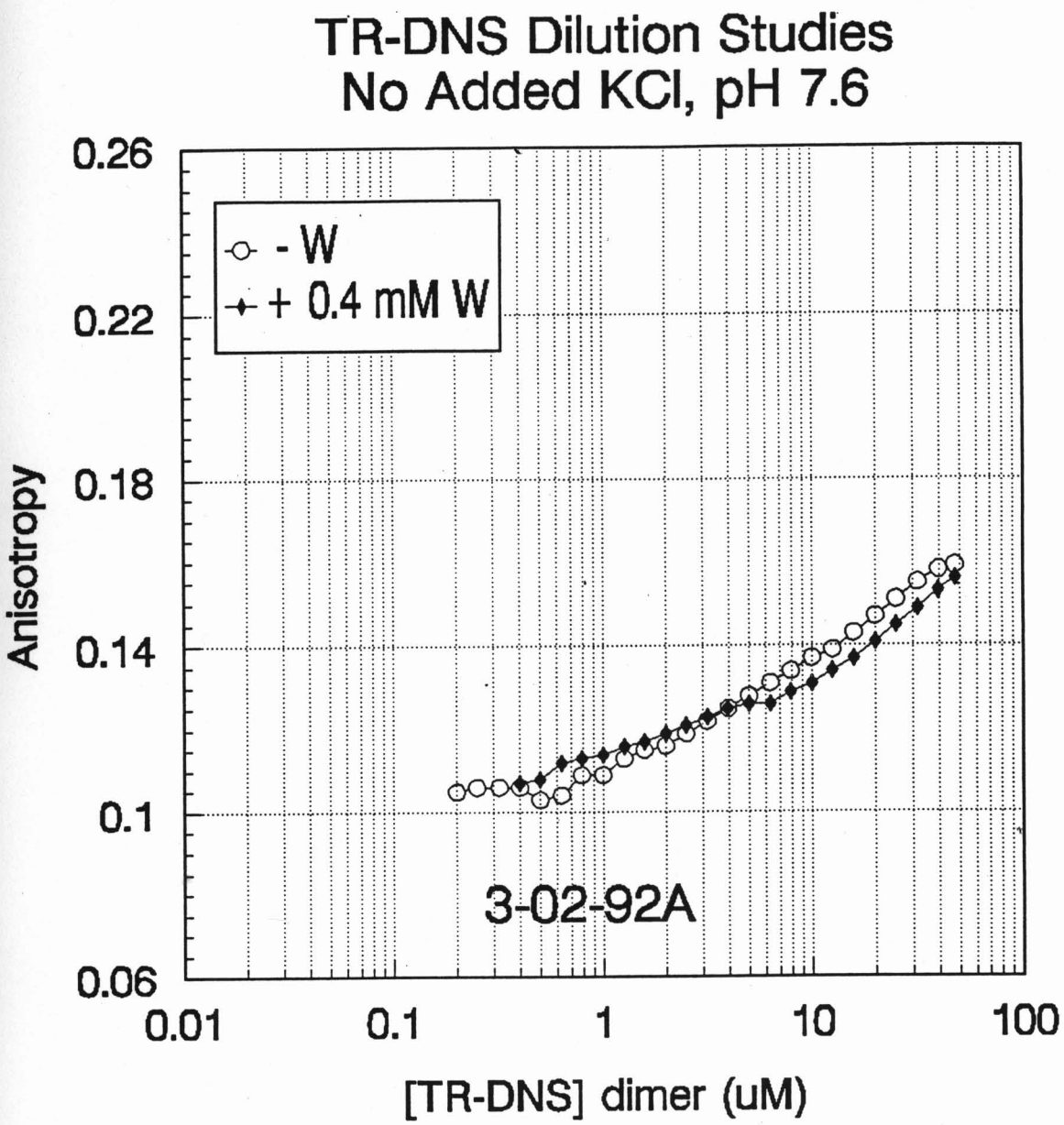
TR-DNS Dilution Studies
No Added KCl, pH 7.6
- W
+ 0.4 mM W
3-02-92A
Anisotropy
0.26
0.22
0.18
0.14
0.1
0.06
0.01
0.1
1
10
100
[TR-DNS] dimer (uM)

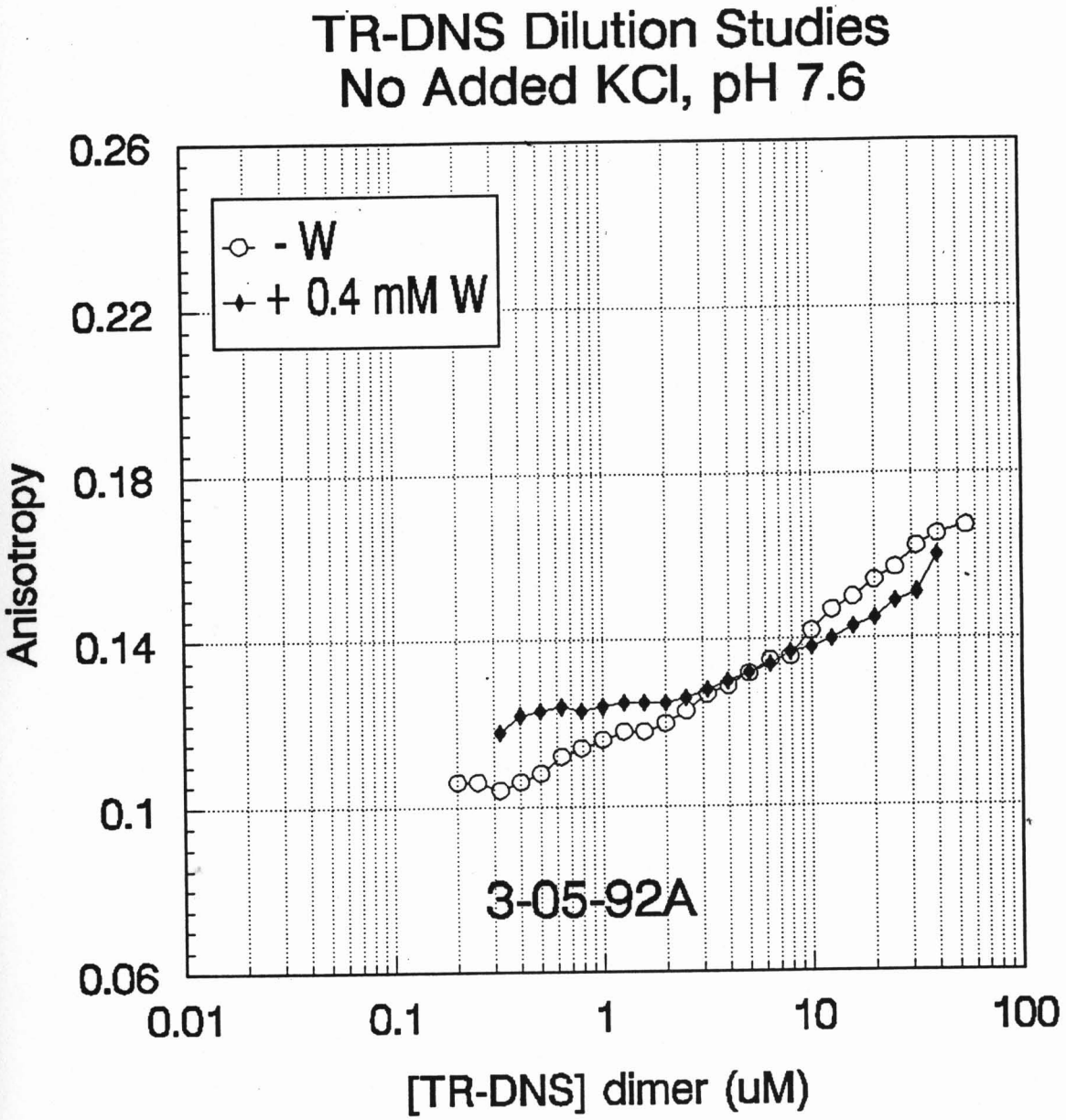
TR-DNS Dilution Studies
No Added KCl, pH 7.6
- W
+ 0.4 mM W
Anisotropy
0.26
0.22
0.18
0.14
0.1
0.06
0.01
0.1
1
10
100
3-05-92A
[TR-DNS] dimer (uM)

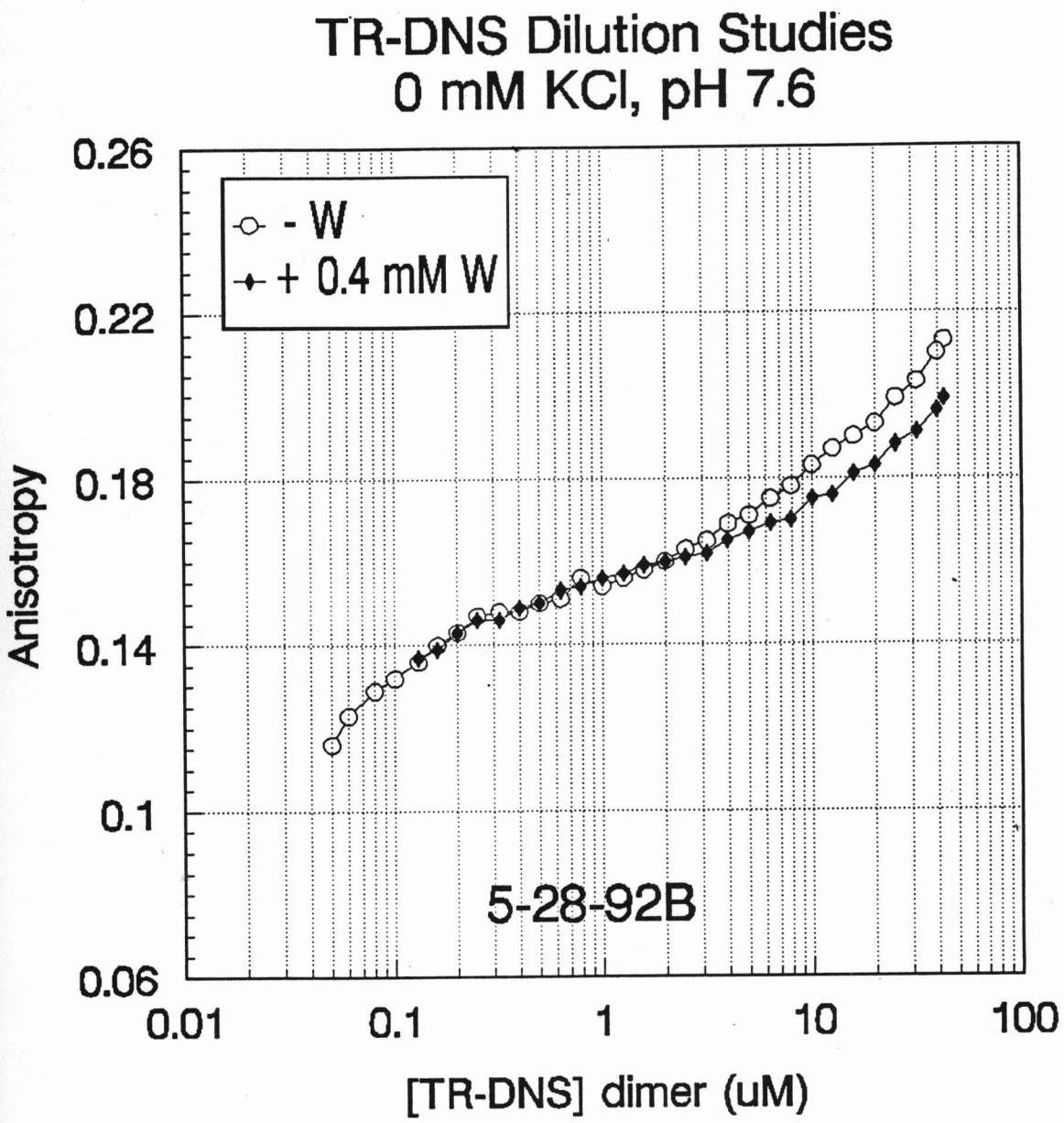
TR-DNS Dilution Studies
0 mM KCl, pH 7.6
- W
+ 0.4 mM W
0.26
0.22
0.18
0.14
0.1
0.06
Anisotropy
5-28-92B
0.01
0.1
1
10
100
[TR-DNS] dimer (uM)

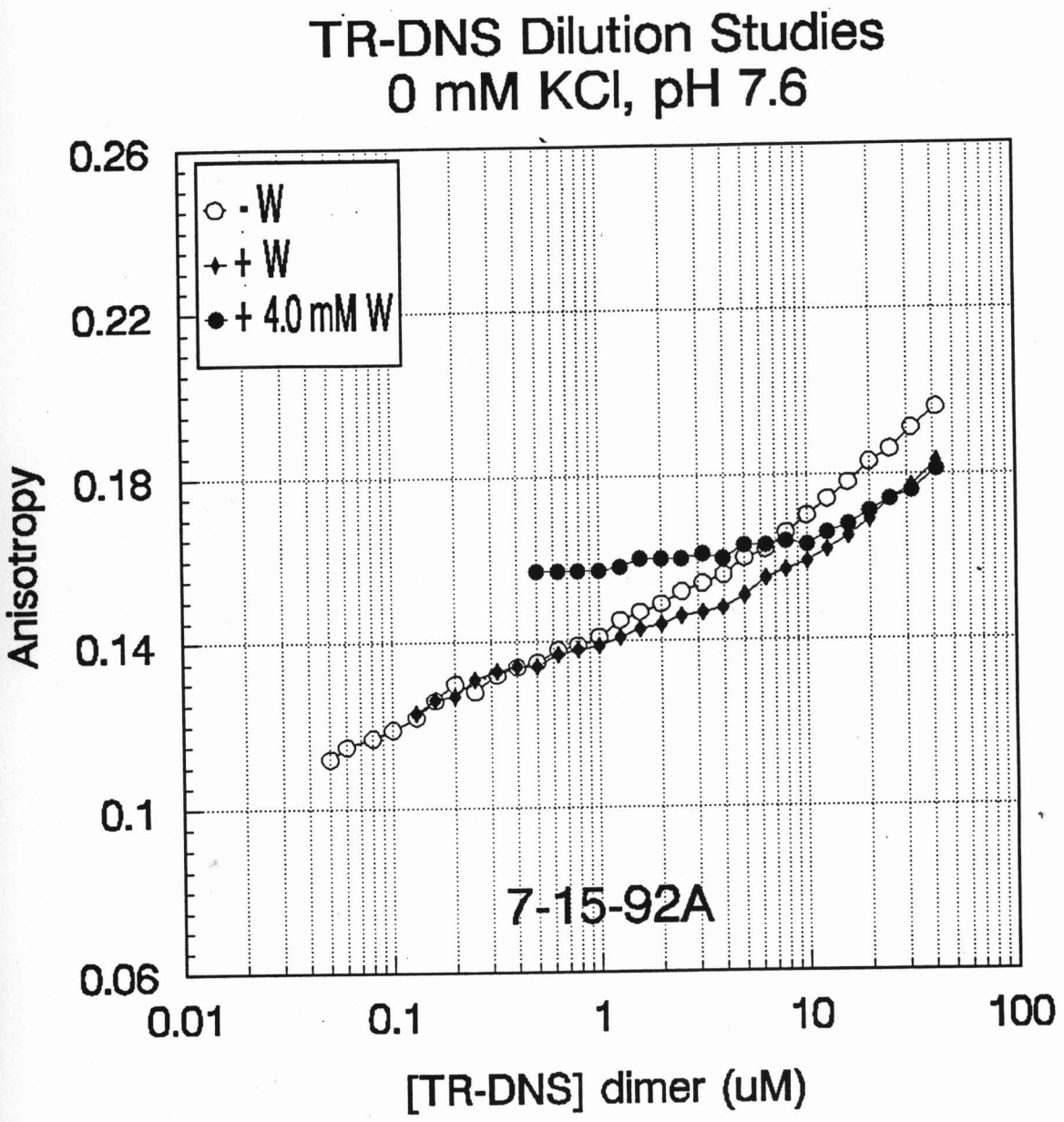
TR-DNS Dilution Studies
0 mM KCl, pH 7.6
- W
+ W
+ 4.0 mM W
Anisotropy
0.26
0.22
0.18
0.14
0.1
0.06
0.01
0.1
1
10
100
[TR-DNS] dimer (uM)
7-15-92A

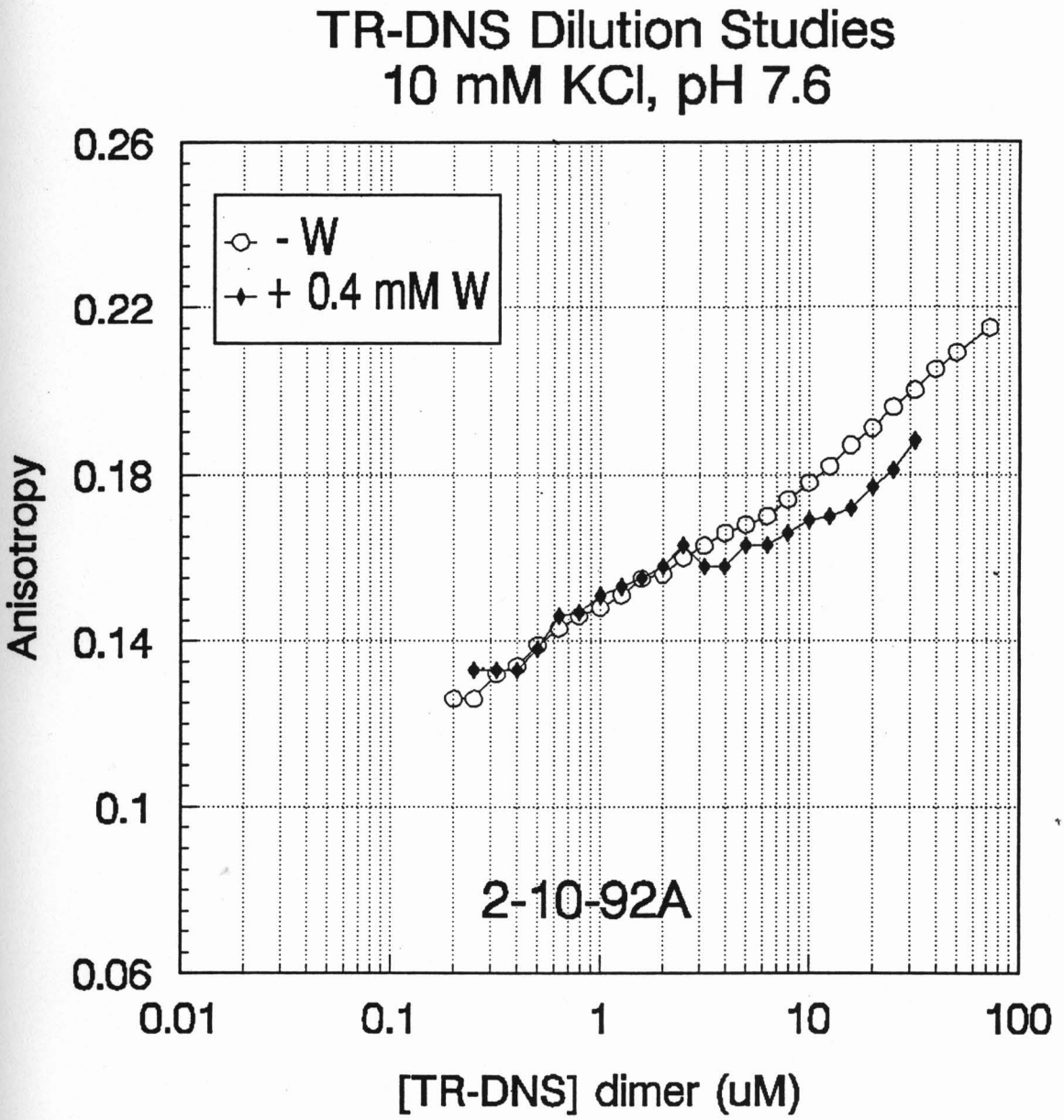
TR-DNS Dilution Studies
10 mM KCl, pH 7.6
- W
+ 0.4 mM W
2-10-92A
Anisotropy
0.26
0.22
0.18
0.14
0.1
0.06
0.01
0.1
1
10
100
[TR-DNS] dimer (uM)

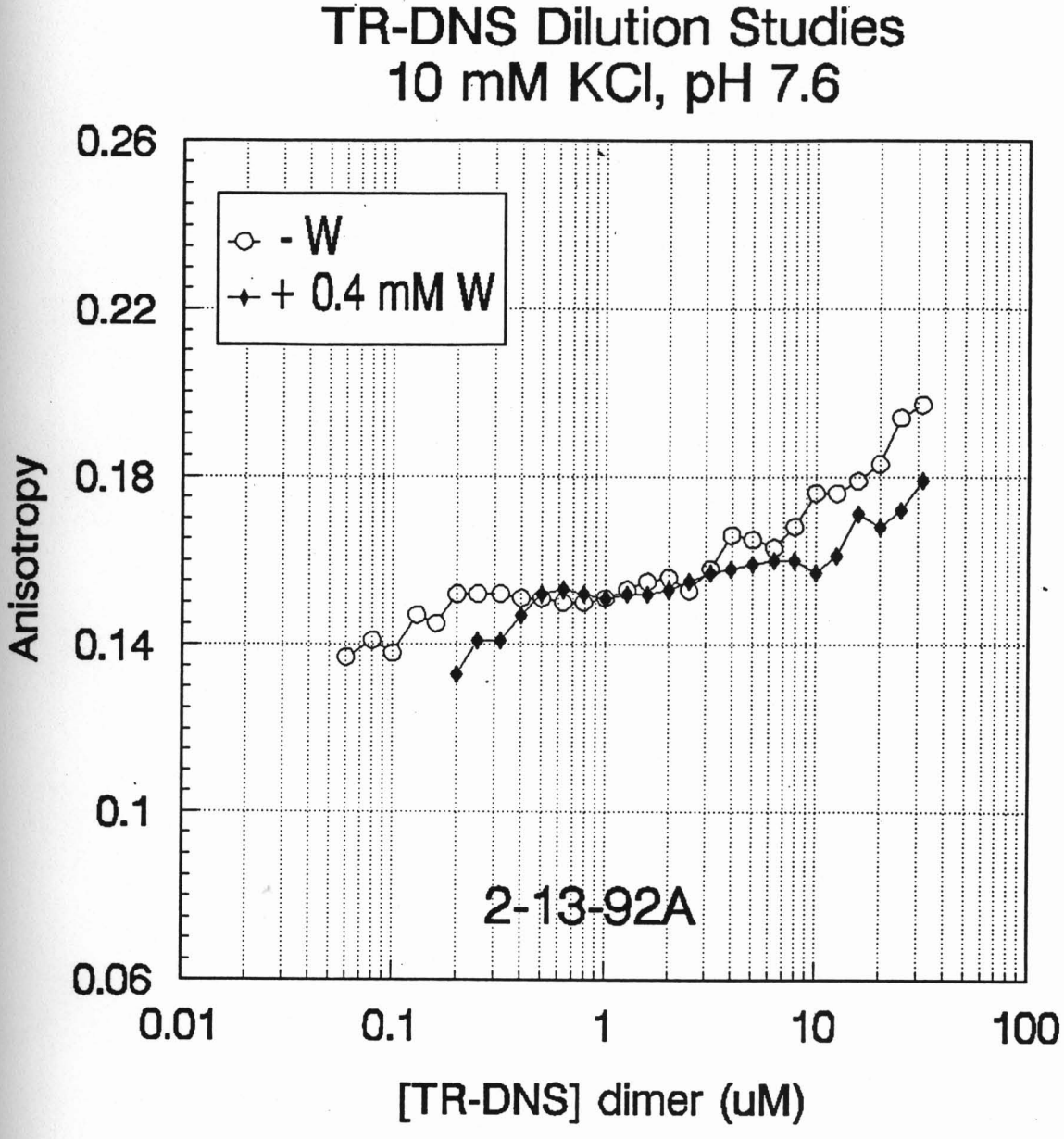
TR-DNS Dilution Studies
10 mM KCl, pH 7.6
- W
+ 0.4 mM W
2-13-92A
Anisotropy
0.26
0.22
0.18
0.14
0.1
0.06
0.01
0.1
1
10
100
[TR-DNS] dimer (uM)

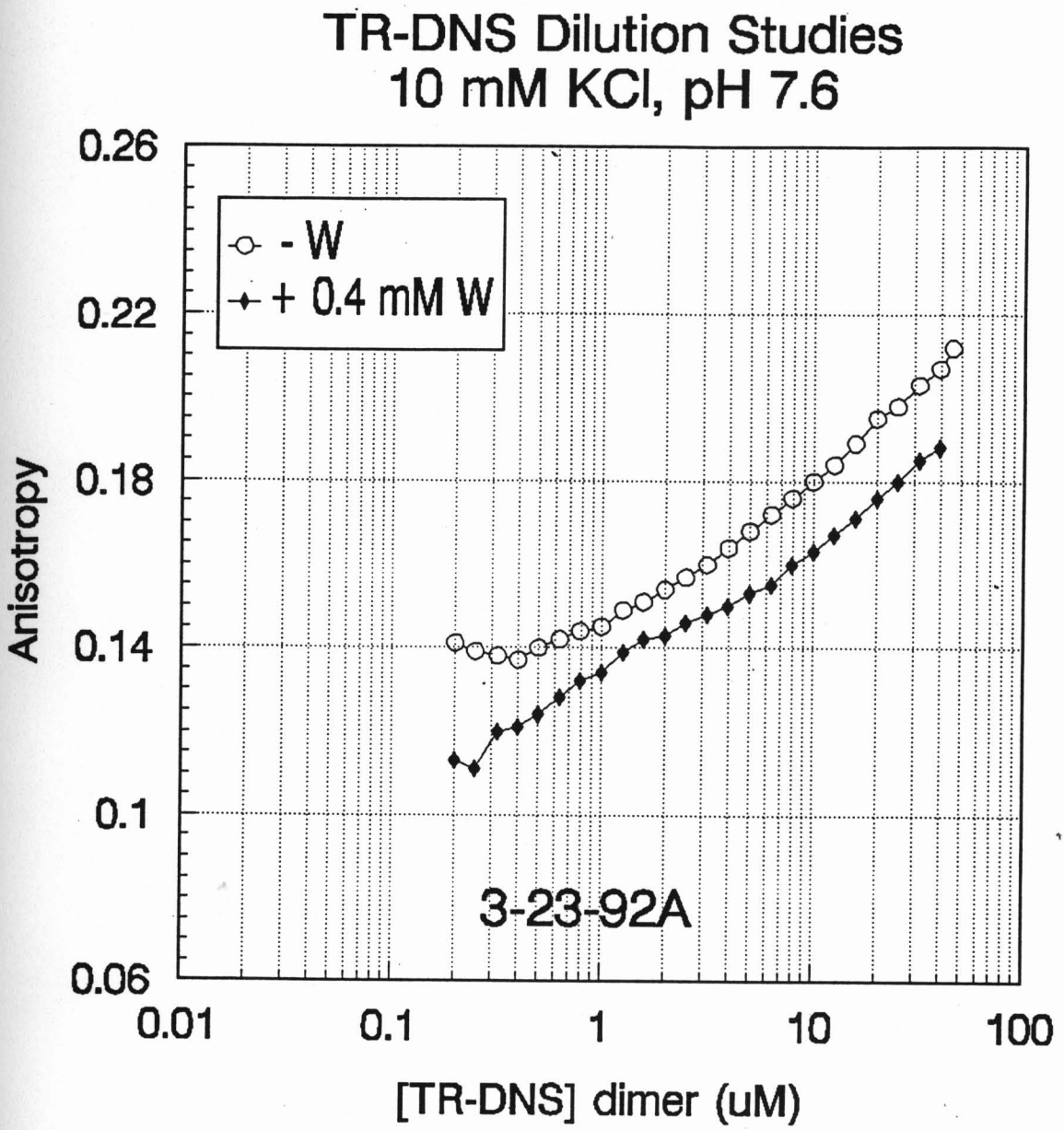
TR-DNS Dilution Studies
10 mM KCl, pH 7.6
- W
+ 0.4 mM W
3-23-92A
Anisotropy
0.26
0.22
0.18
0.14
0.1
0.06
0.01
0.1
1
10
100
[TR-DNS] dimer (uM)

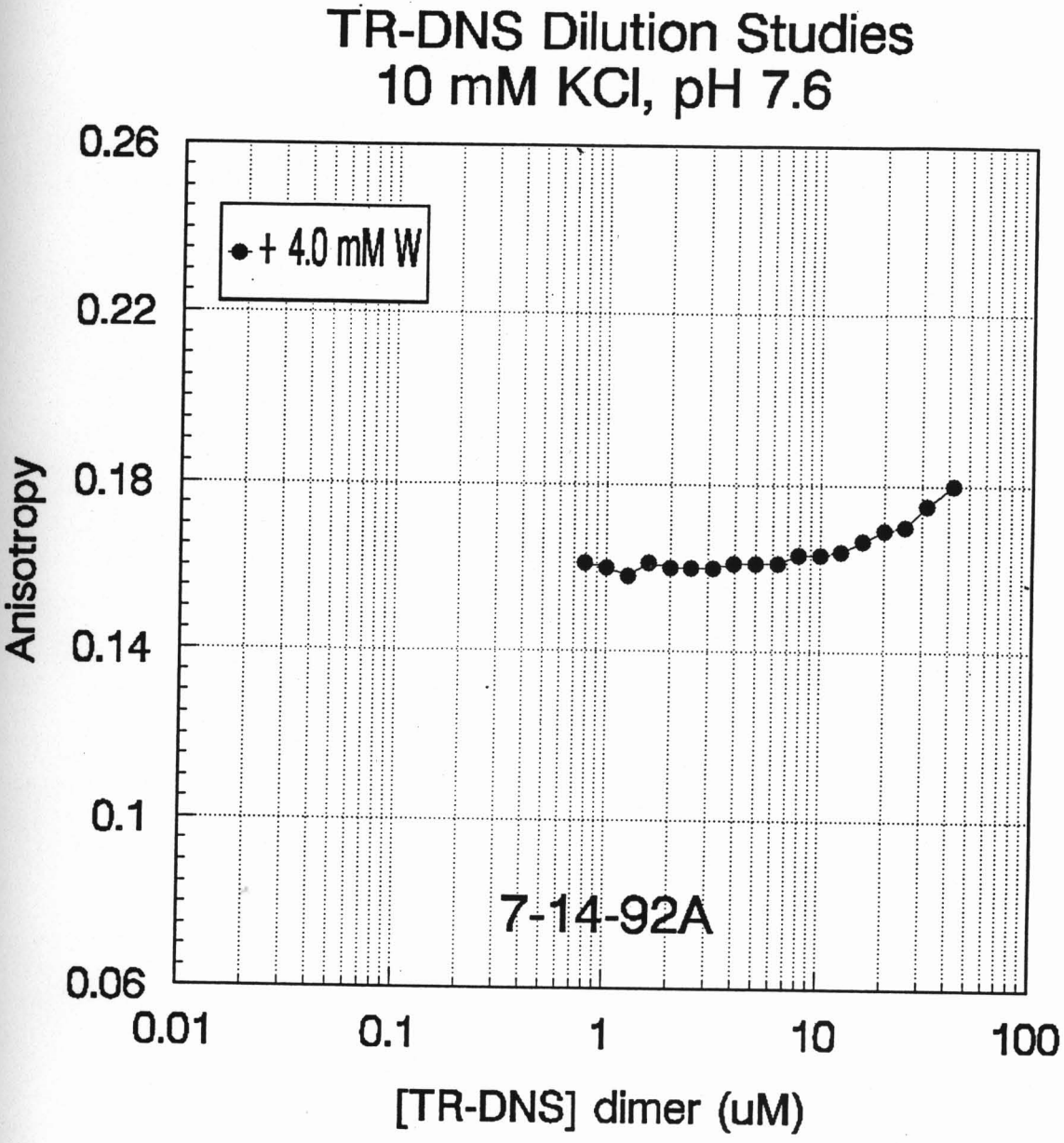
TR-DNS Dilution Studies
10 mM KCl, pH 7.6
+ 4.0 mM W
0.26
0.22
0.18
0.14
0.1
0.06
Anisotropy
7-14-92A
0.01
0.1
1
10
100
[TR-DNS] dimer (uM)

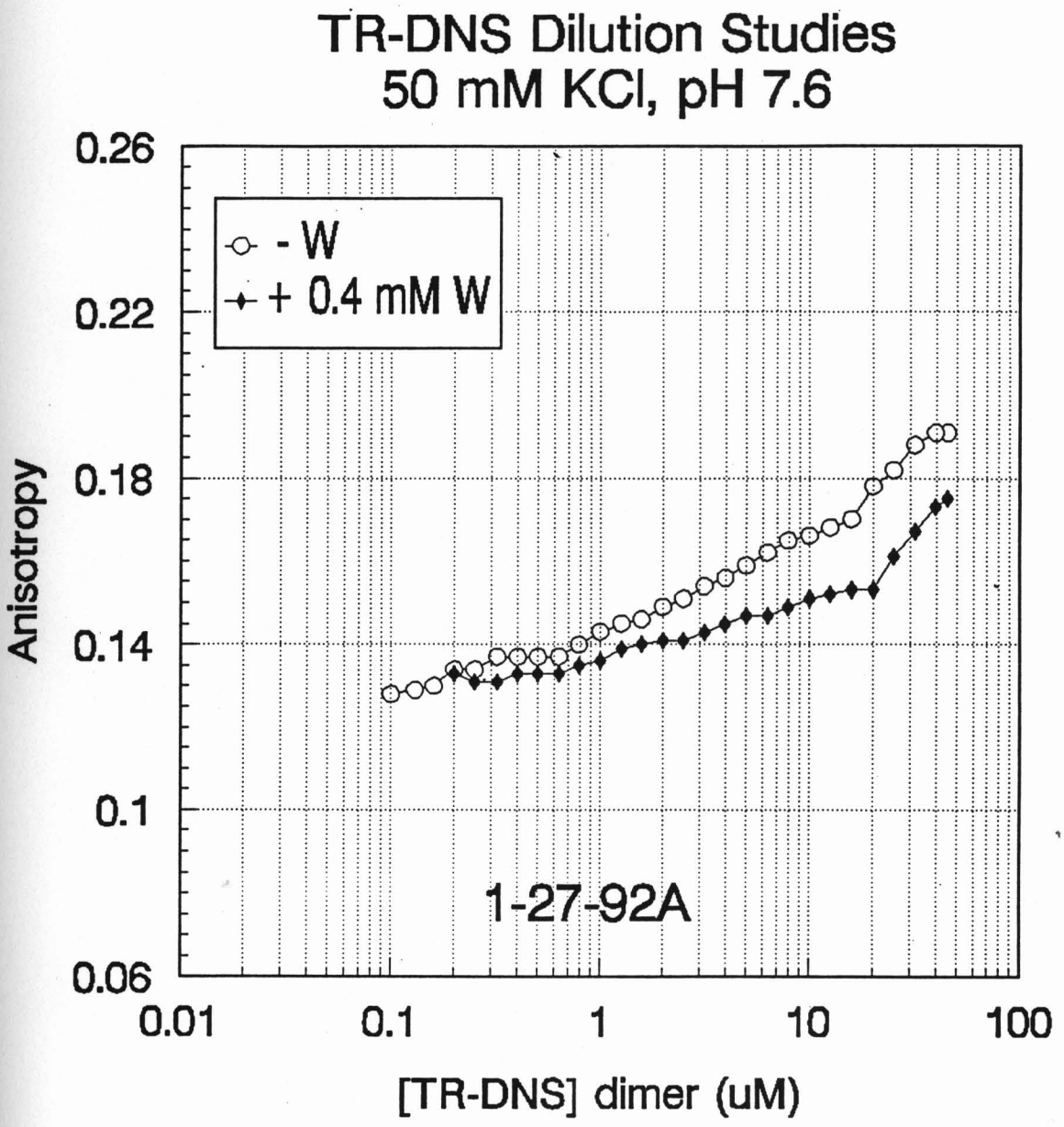
TR-DNS Dilution Studies
50 mM KCl, pH 7.6
- W
+ 0.4 mM W
Anisotropy
0.26
0.22
0.18
0.14
0.1
0.06
0.01
0.1
1
10
100
1-27-92A
[TR-DNS] dimer (uM)

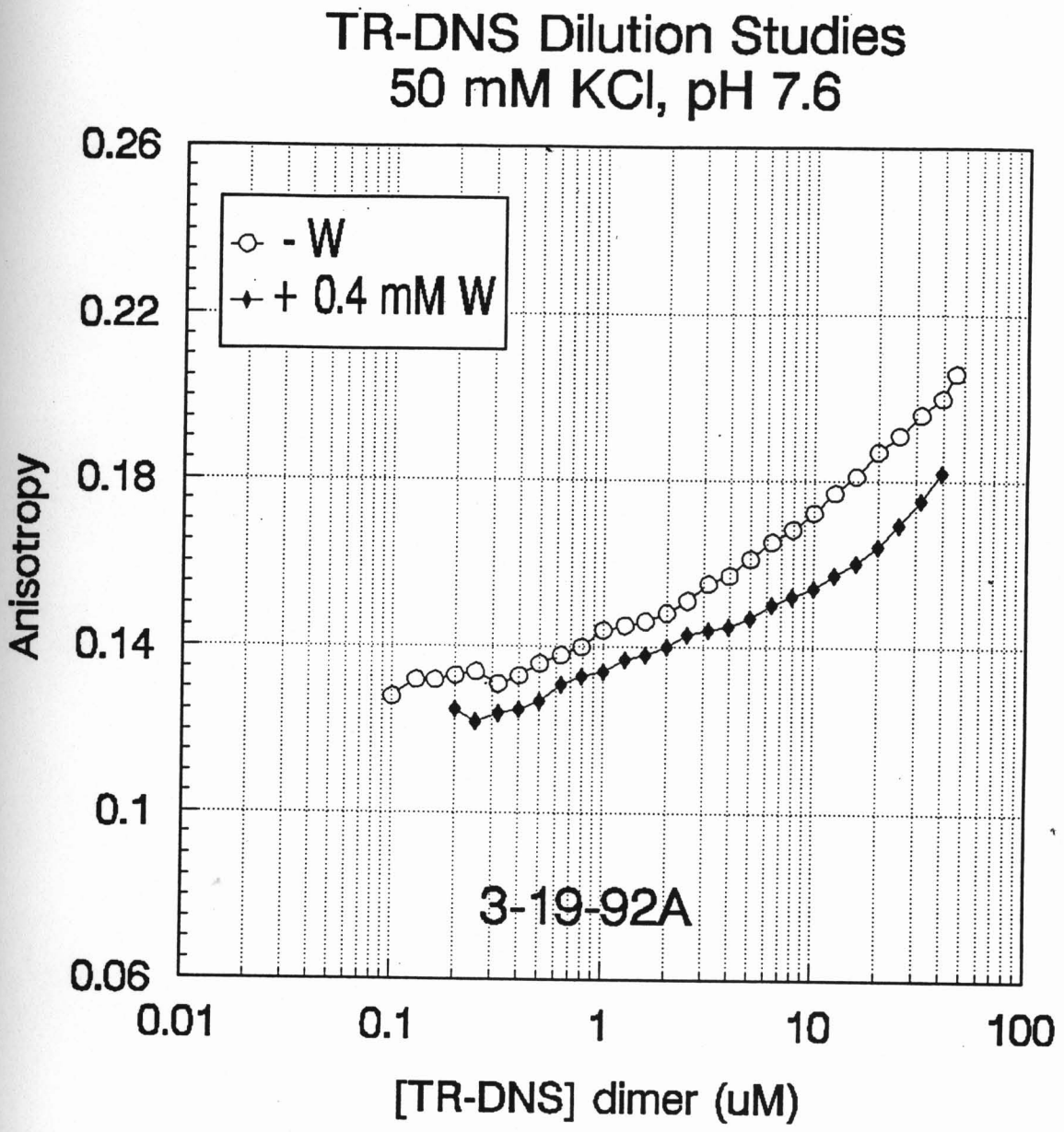
TR-DNS Dilution Studies
50 mM KCl, pH 7.6
- W
+ 0.4 mM W
Anisotropy
0.26
0.22
0.18
0.14
0.1
0.06
3-19-92A
0.01
0.1
1
10
100
[TR-DNS] dimer (uM)

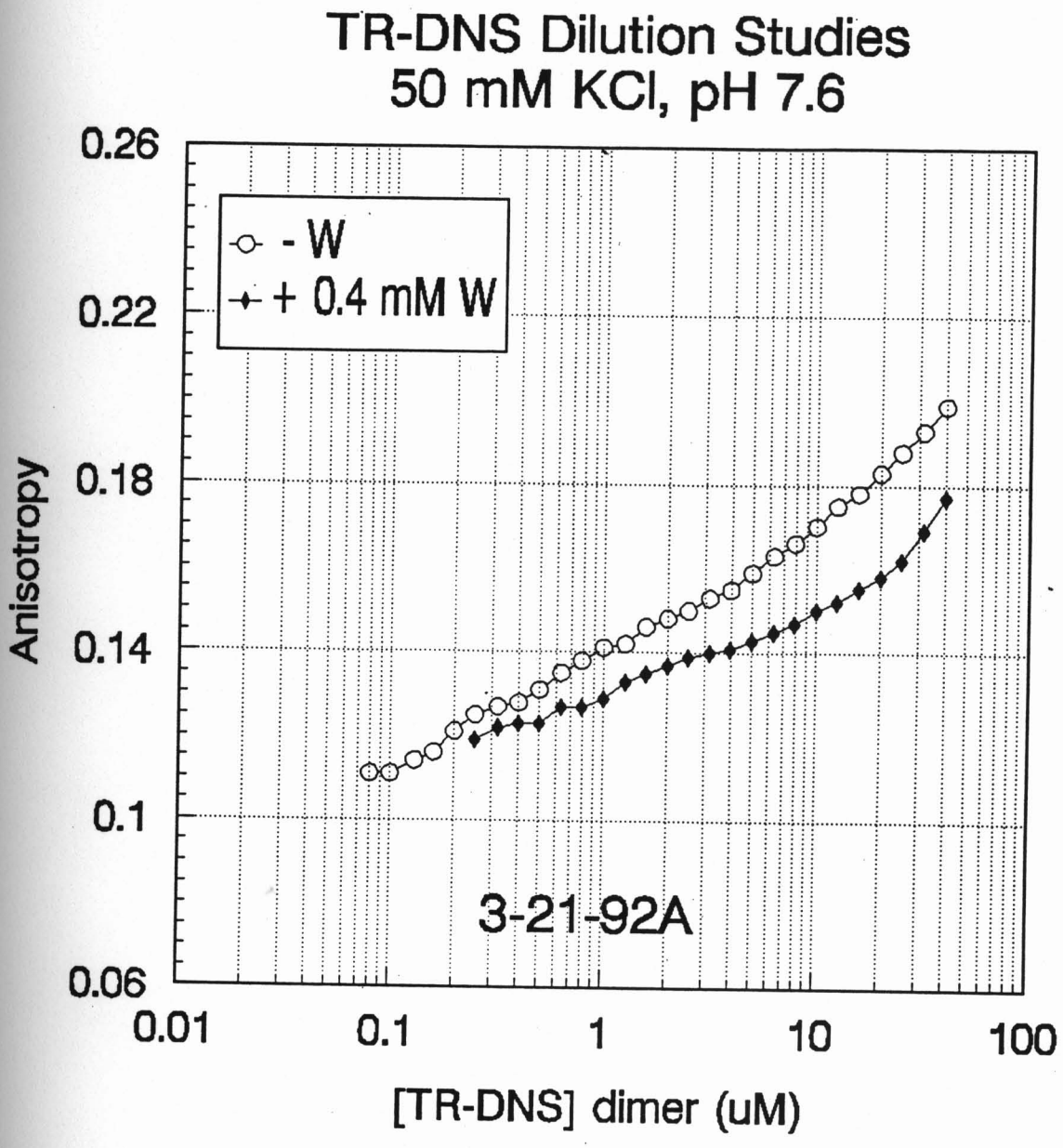
TR-DNS Dilution Studies
50 mM KCl, pH 7.6
- W
+ 0.4 mM W
Anisotropy
0.26
0.22
0.18
0.14
0.1
0.06
3-21-92A
0.01
0.1
1
10
100
[TR-DNS] dimer (uM)

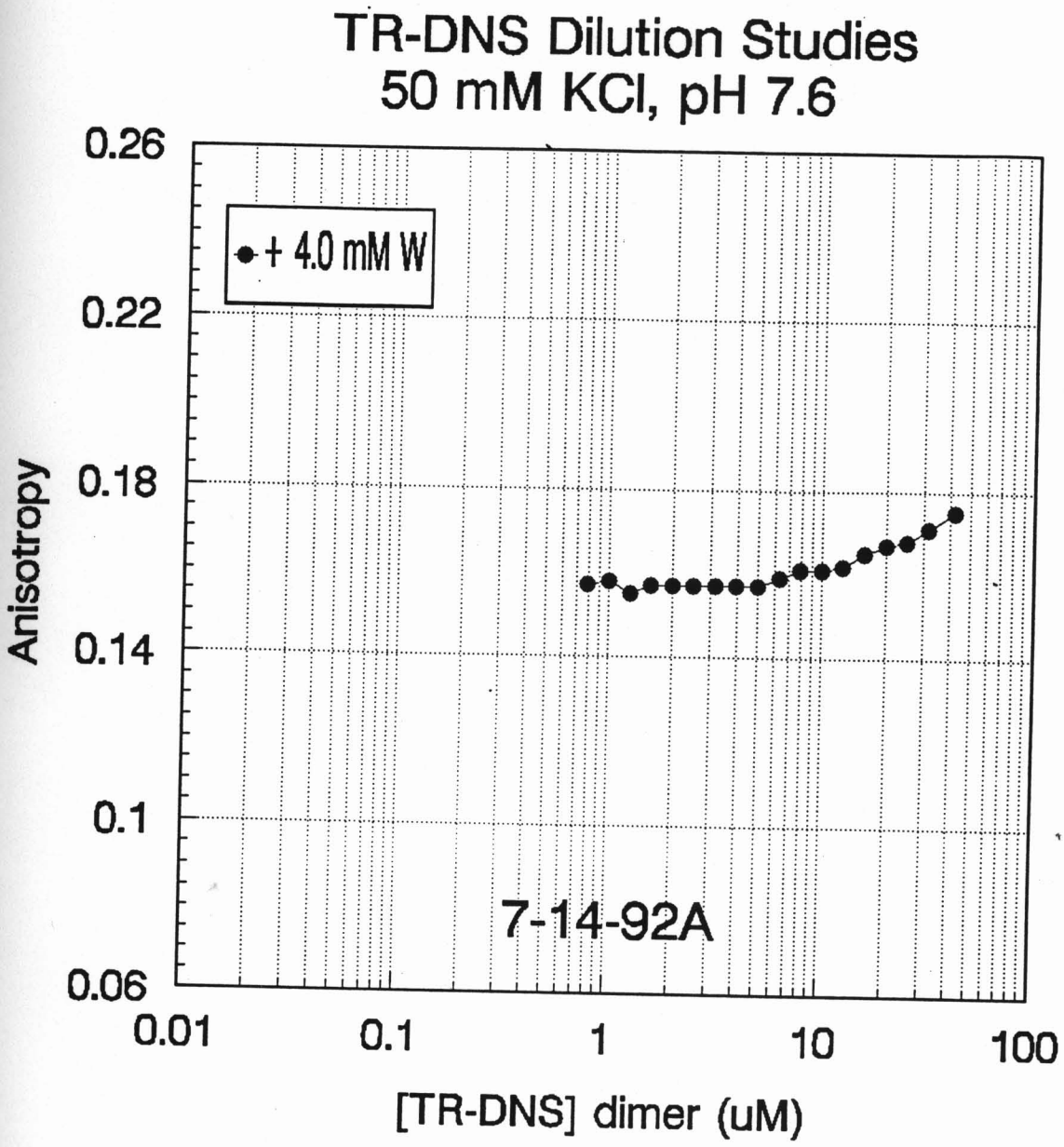
TR-DNS Dilution Studies
50 mM KCl, pH 7.6
+ 4.0 mM W
0.26
0.22
0.18
0.14
0.1
0.06
Anisotropy
7-14-92A
0.01
0.1
1
10
100
[TR-DNS] dimer (uM)

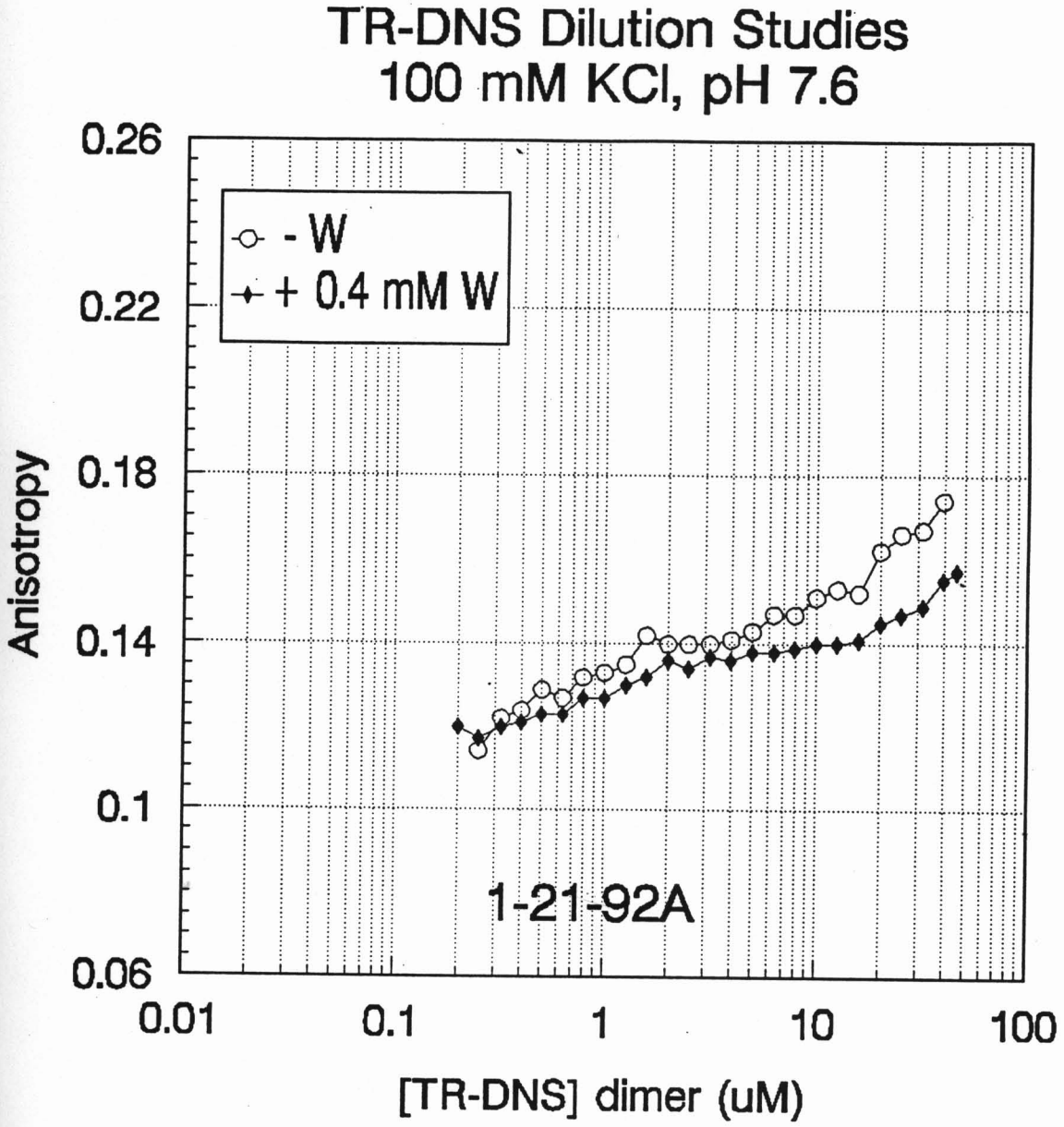
TR-DNS Dilution Studies
100 mM KCl, pH 7.6
- W
+ 0.4 mM W
1-21-92A
Anisotropy
0.26
0.22
0.18
0.14
0.1
0.06
0.01
0.1
1
10
100
[TR-DNS] dimer (uM)

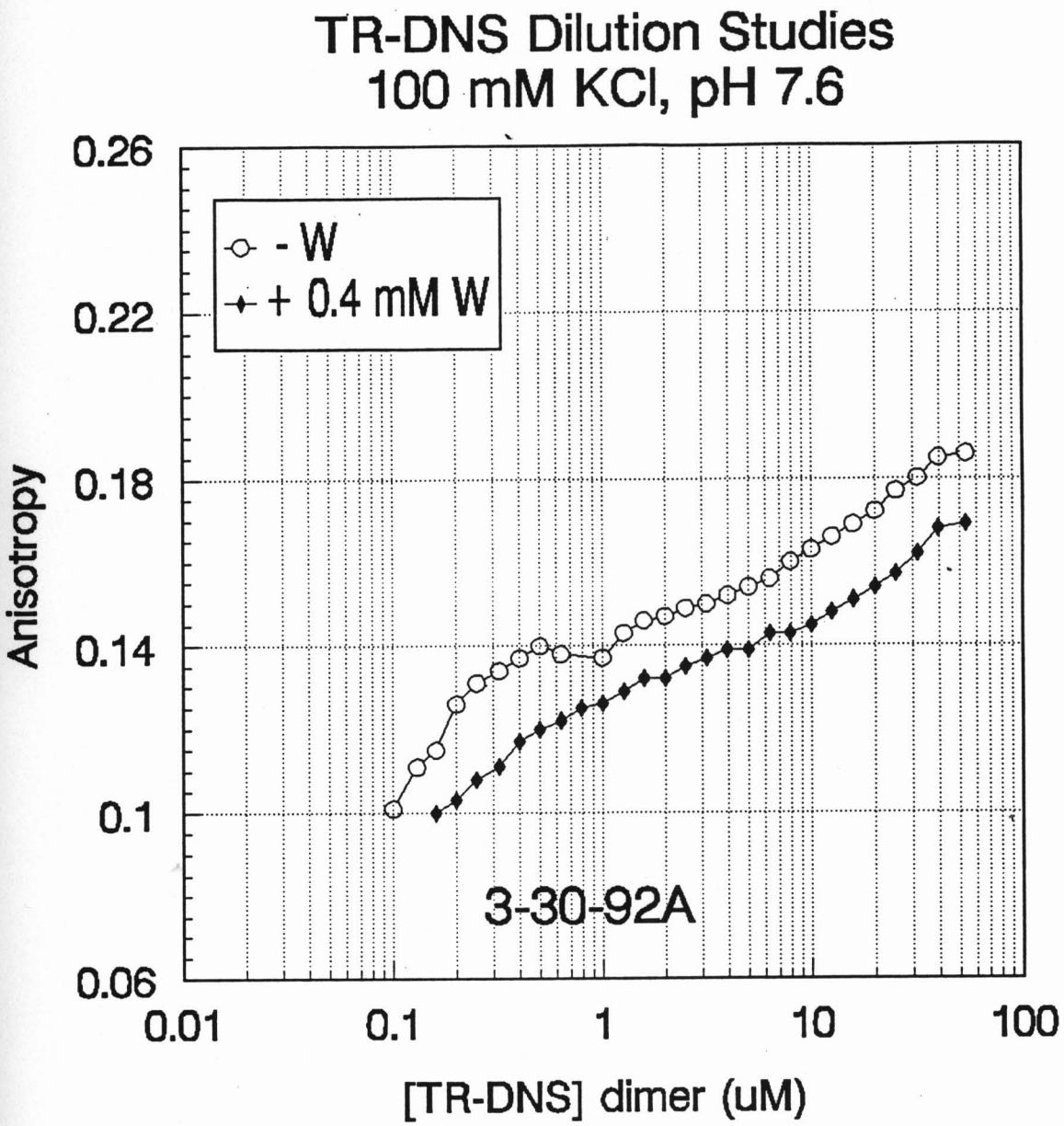
TR-DNS Dilution Studies
100 mM KCl, pH 7.6
- W
+ 0.4 mM W
3-30-92A
Anisotropy
0.26
0.22
0.18
0.14
0.1
0.06
0.01
0.1
1
10
100
[TR-DNS] dimer (uM)

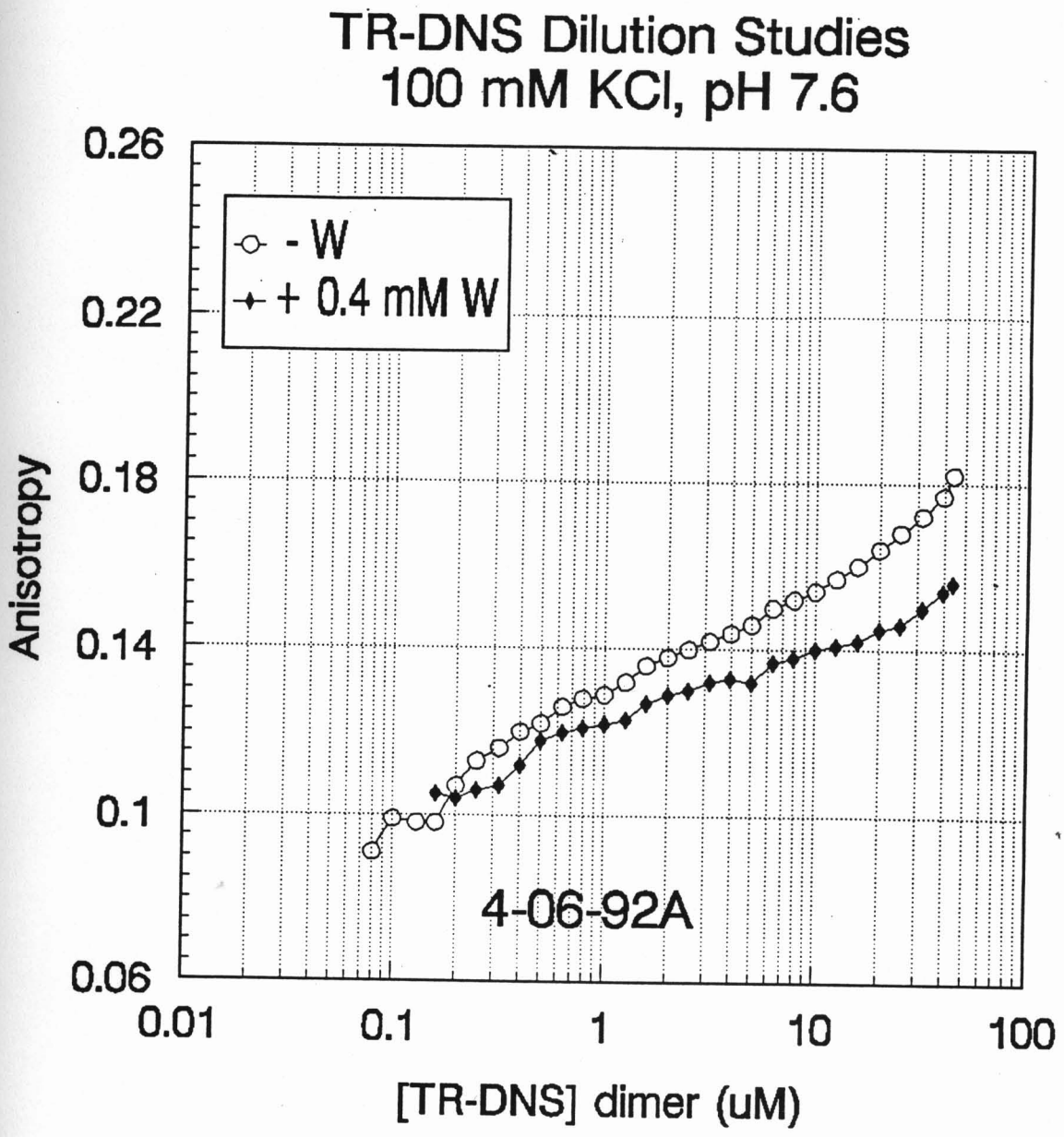
TR-DNS Dilution Studies
100 mM KCl, pH 7.6
- W
+ 0.4 mM W
4-06-92A
Anisotropy
0.26
0.22
0.18
0.14
0.1
0.06
0.01
0.1
1
10
100
[TR-DNS] dimer (uM)

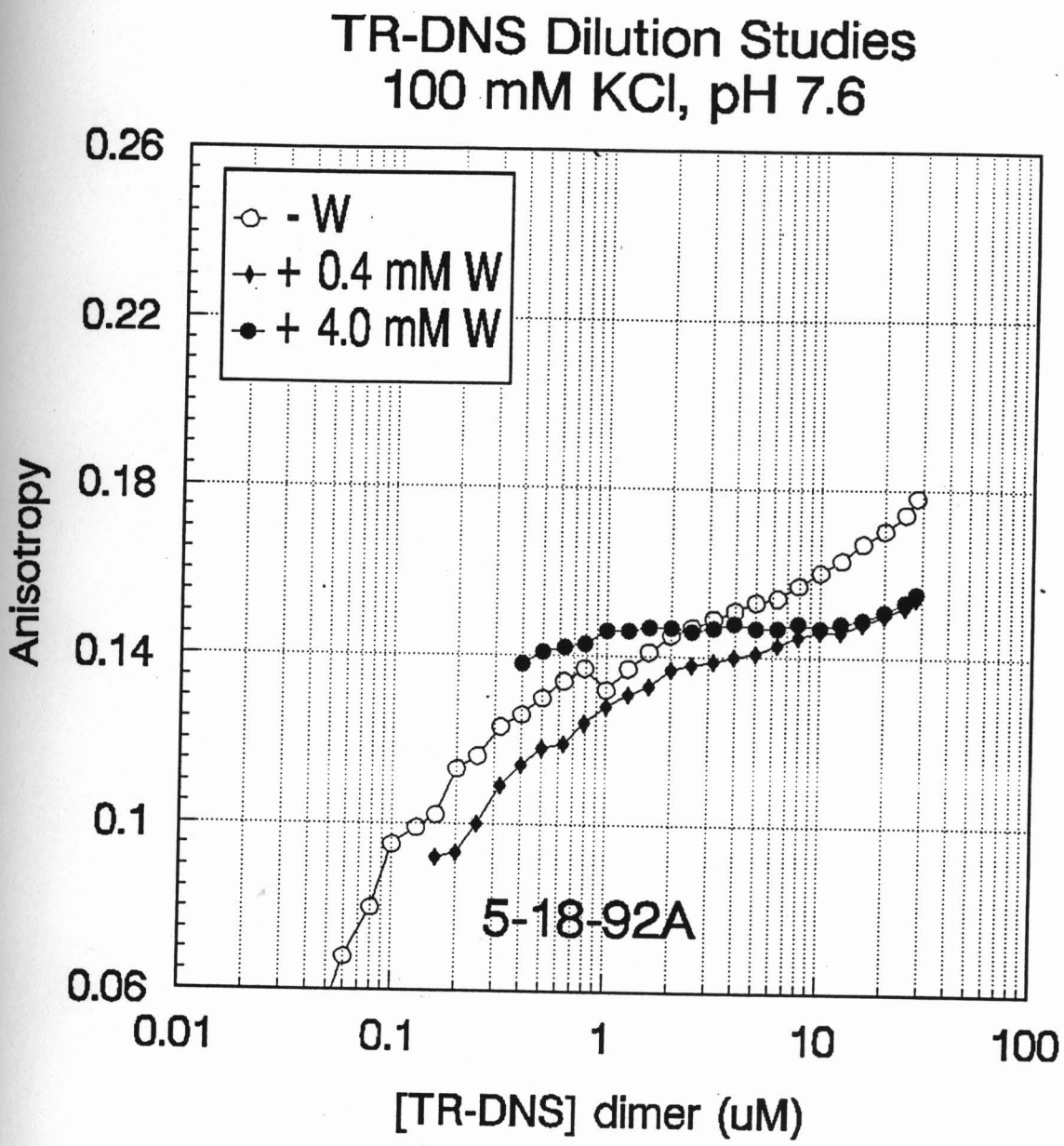
TR-DNS Dilution Studies
100 mM KCl, pH 7.6
- W
+ 0.4 mM W
+ 4.0 mM W
5-18-92A
Anisotropy
0.26
0.22
0.18
0.14
0.1
0.06
0.01
0.1
1
10
100
[TR-DNS] dimer (uM)

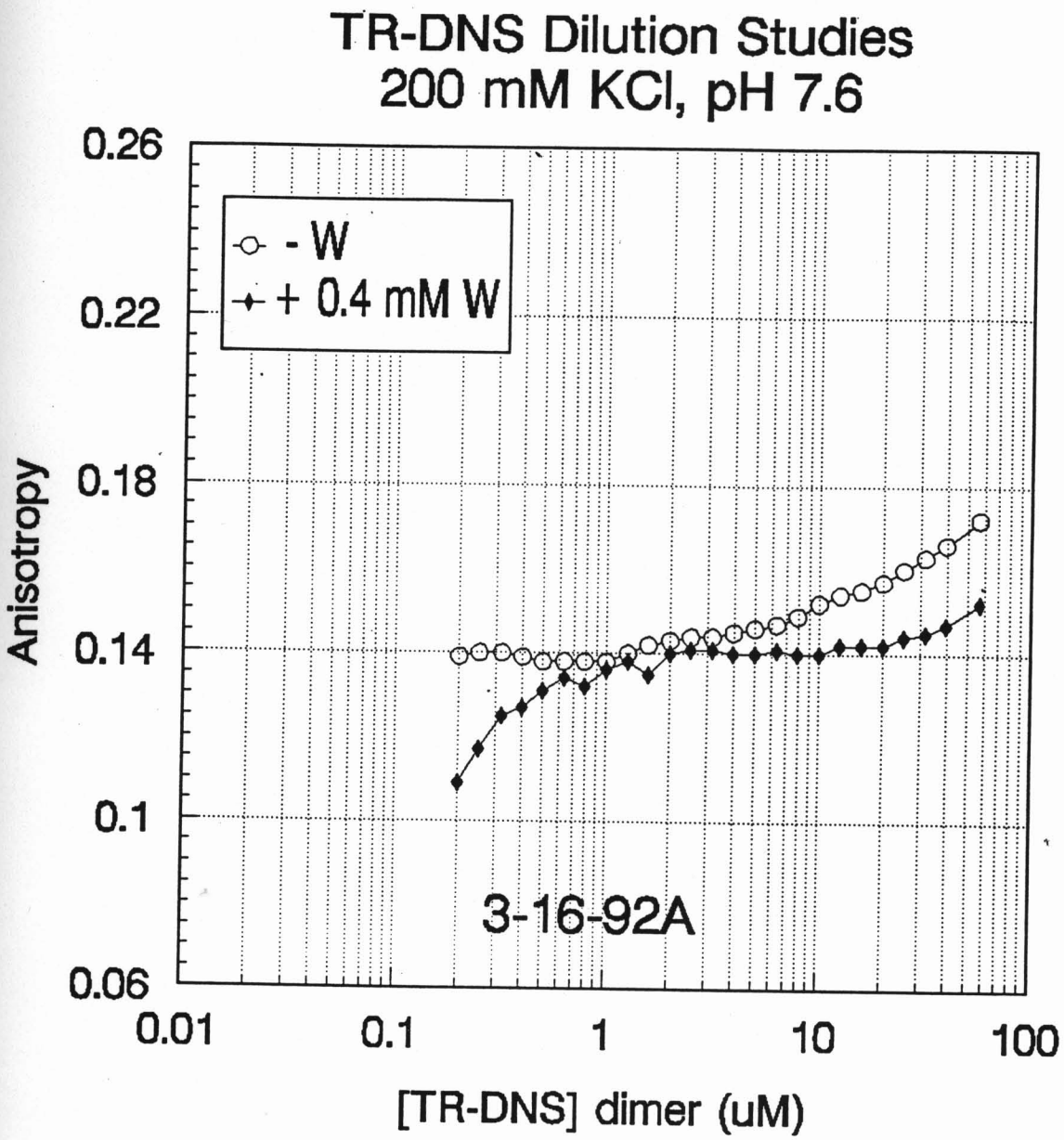
TR-DNS Dilution Studies
200 mM KCl, pH 7.6
- W
+ 0.4 mM W
Anisotropy
0.26
0.22
0.18
0.14
0.1
0.06
0.01
0.1
1
10
100
3-16-92A
[TR-DNS] dimer (uM)

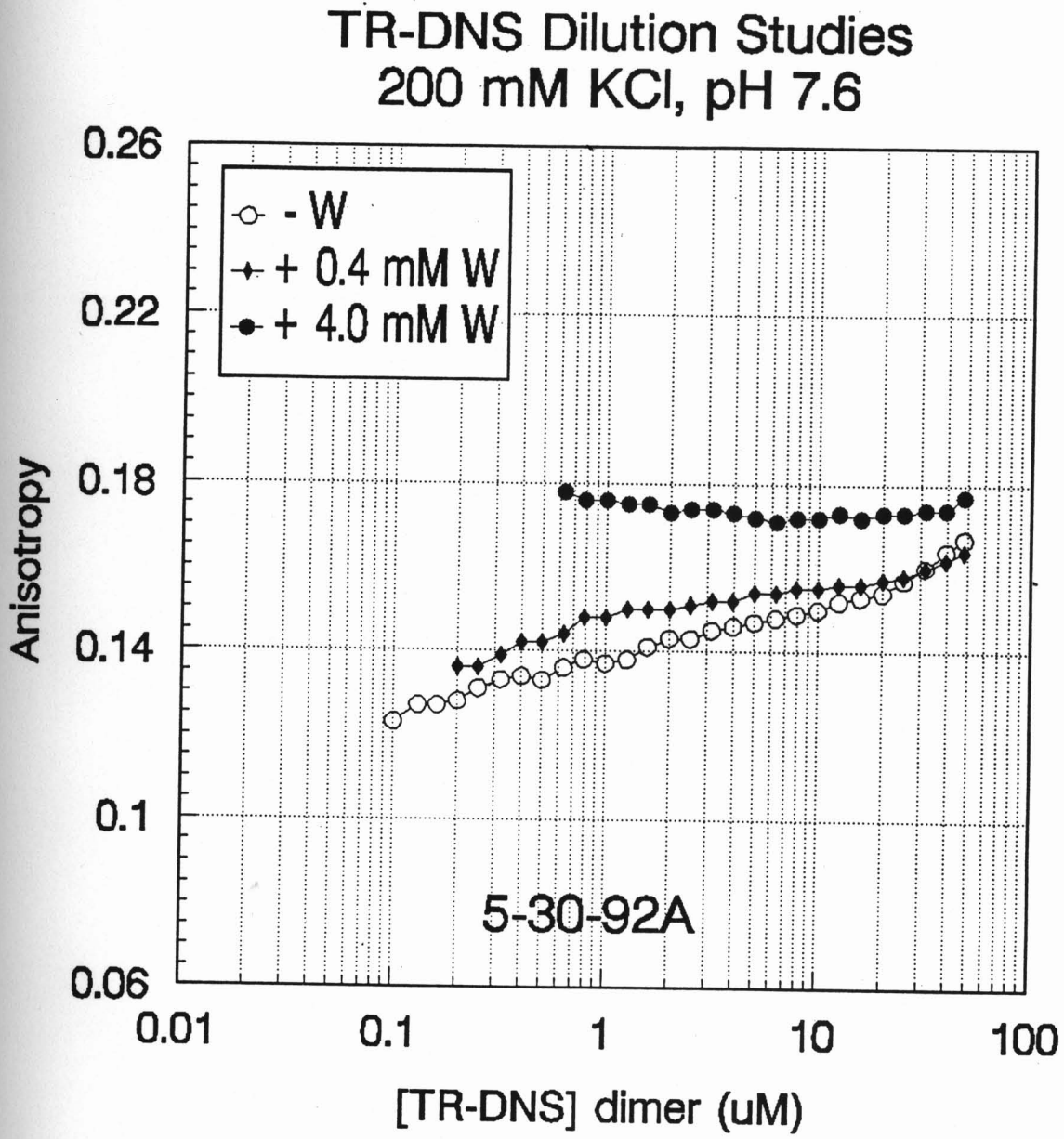
TR-DNS Dilution Studies
200 mM KCl, pH 7.6
- W
+ 0.4 mM W
+ 4.0 mM W
0.26
0.22
0.18
0.14
0.1
0.06
Anisotropy
5-30-92A
0.01
0.1
1
10
100
[TR-DNS] dimer (uM)

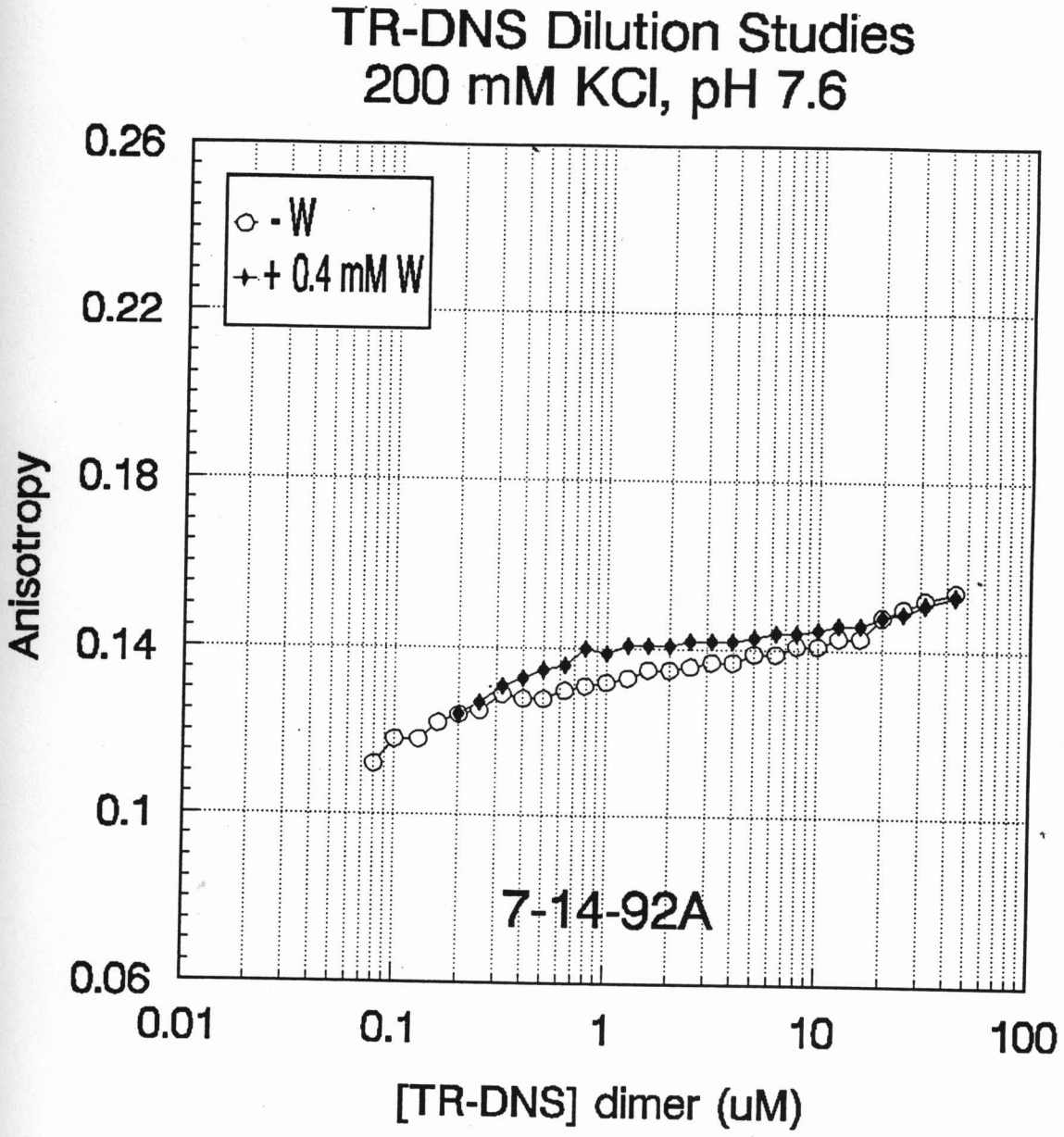
TR-DNS Dilution Studies
200 mM KCl, pH 7.6
- W
+ 0.4 mM W
7-14-92A
Anisotropy
0.26
0.22
0.18
0.14
0.1
0.06
0.01
0.1
1
10
100
[TR-DNS] dimer (uM)

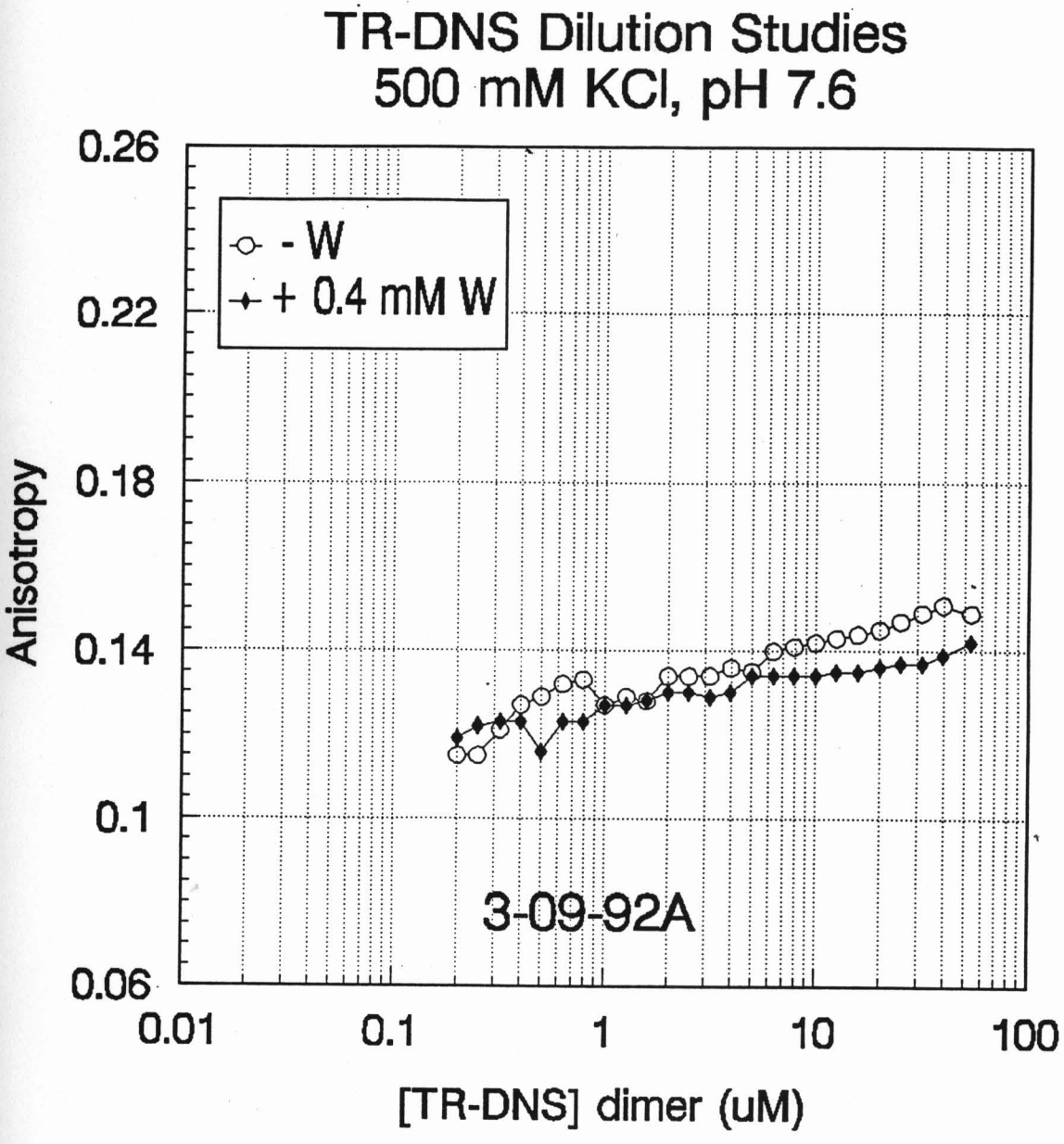
TR-DNS Dilution Studies
500 mM KCl, pH 7.6
- W
+ 0.4 mM W
3-09-92A
Anisotropy
0.26
0.22
0.18
0.14
0.1
0.06
0.01
0.1
1
10
100
[TR-DNS] dimer (uM)

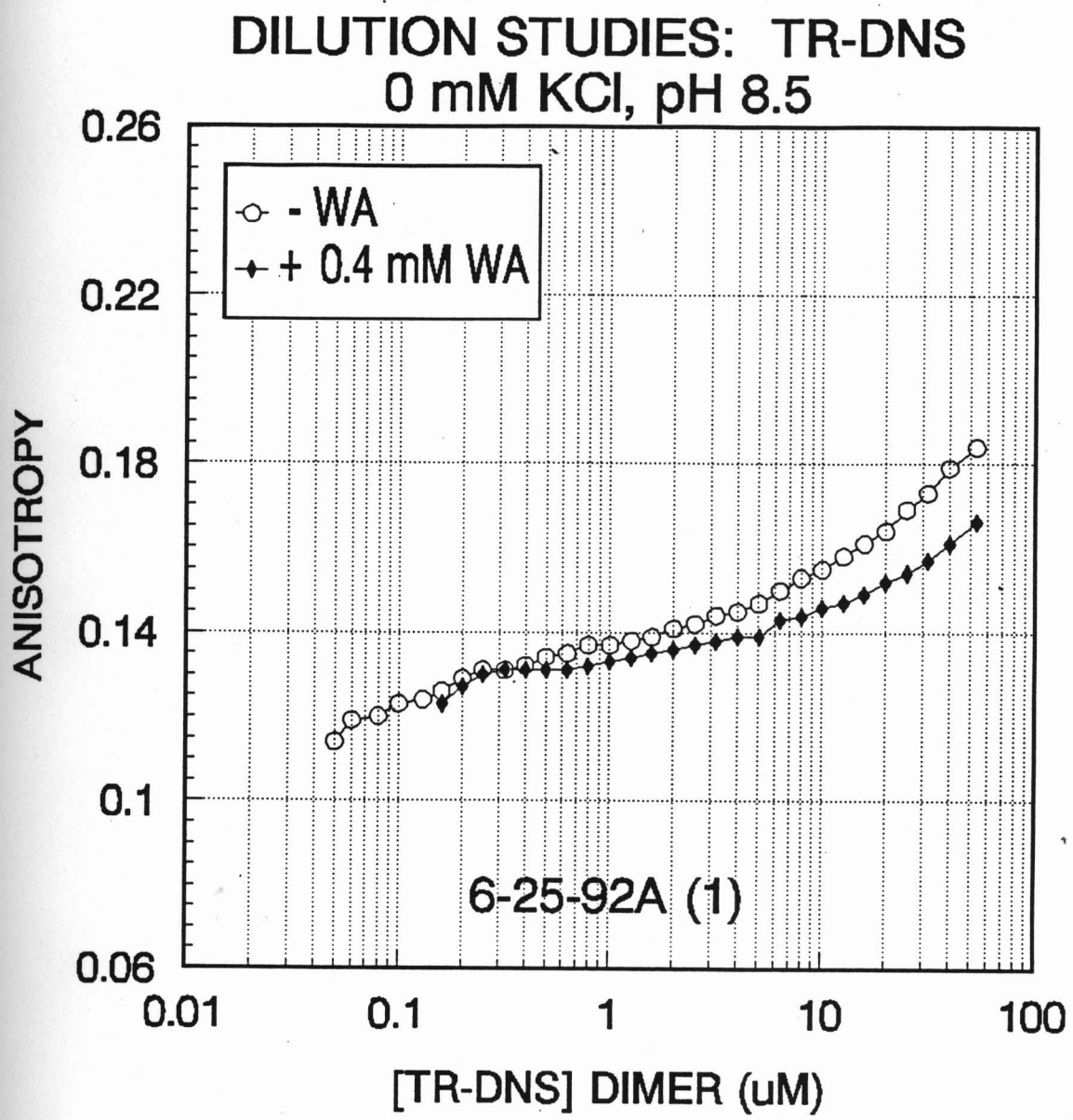
DILUTION STUDIES: TR-DNS
0 mM KCl, pH 8.5
- WA
+ 0.4 mM WA
6-25-92A (1)
ANISOTROPY
0.26
0.22
0.18
0.14
0.1
0.06
0.01
0.1
1
10
100
[TR-DNS] DIMER (uM)

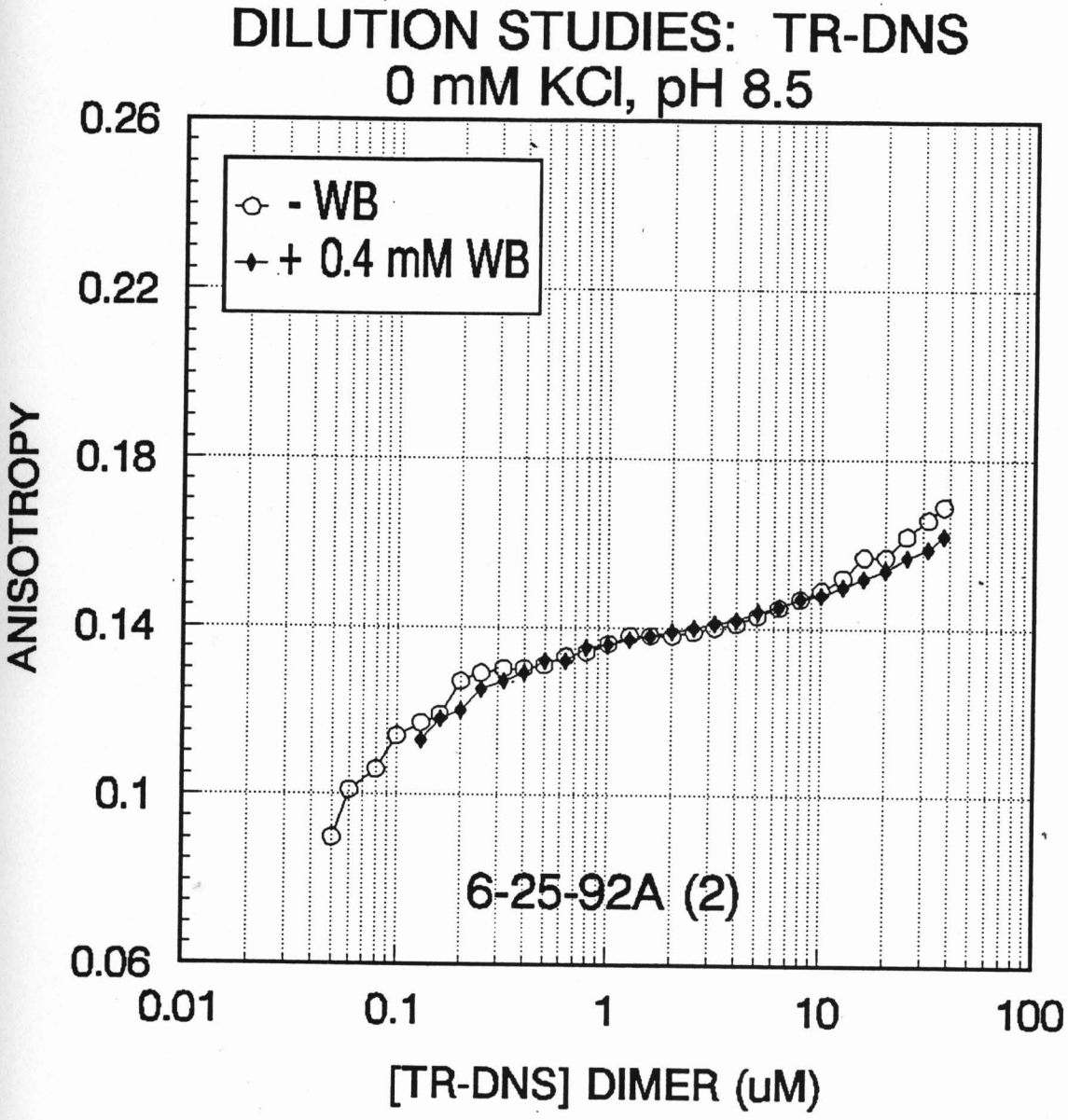
DILUTION STUDIES: TR-DNS
0 mM KCl, pH 8.5
- WB
+ 0.4 mM WB
6-25-92A (2)
ANISOTROPY
0.26
0.22
0.18
0.14
0.1
0.06
0.01
0.1
1
10
100
[TR-DNS] DIMER (uM)

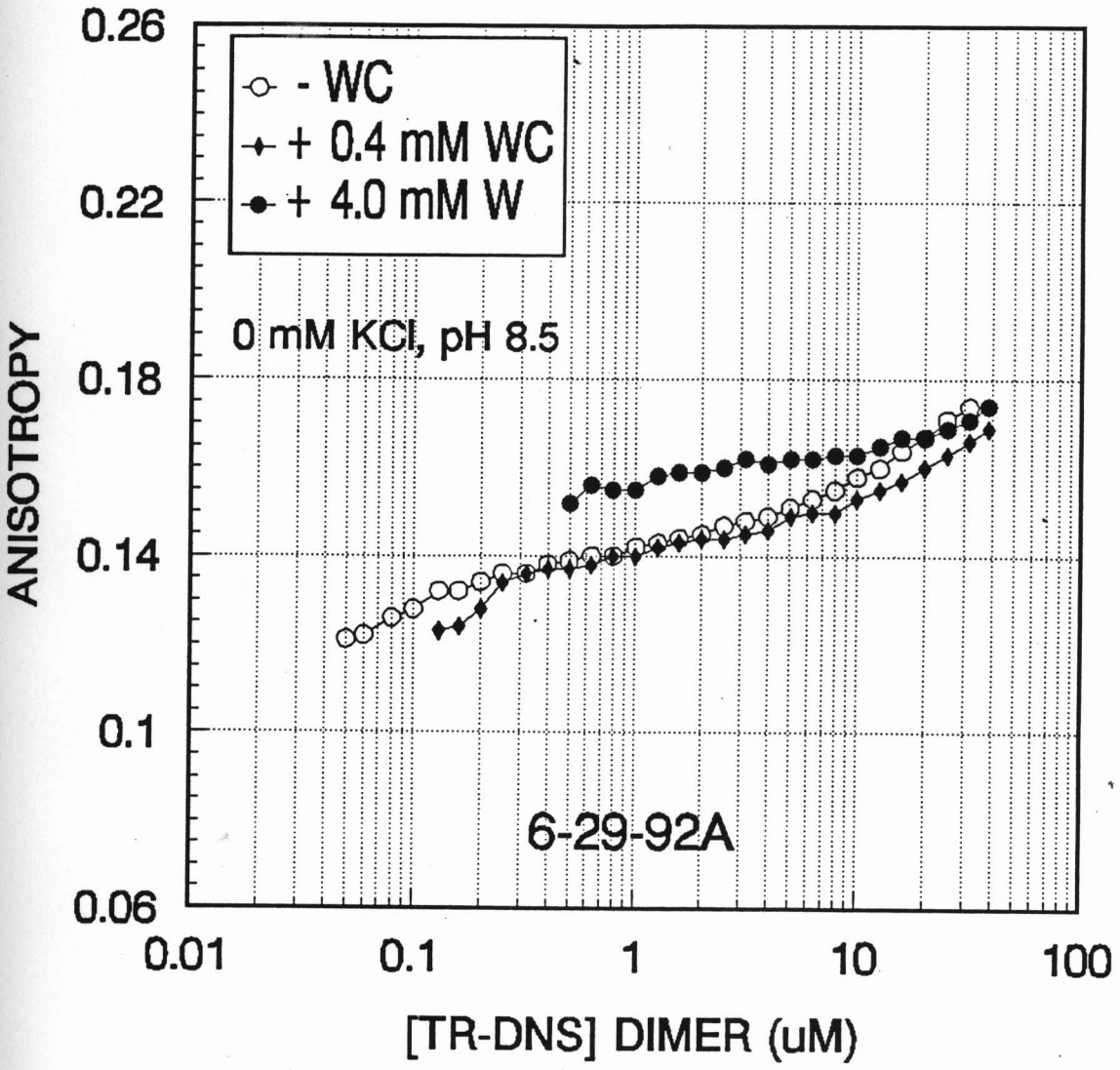
0.26
0.22
0.18
0.14
0.1
0.06
ANISOTROPY
- WC
+ 0.4 mM WC
+ 4.0 mM W
0 mM KCl, pH 8.5
6-29-92A
0.01
0.1
1
10
100
[TR-DNS] DIMER (uM)

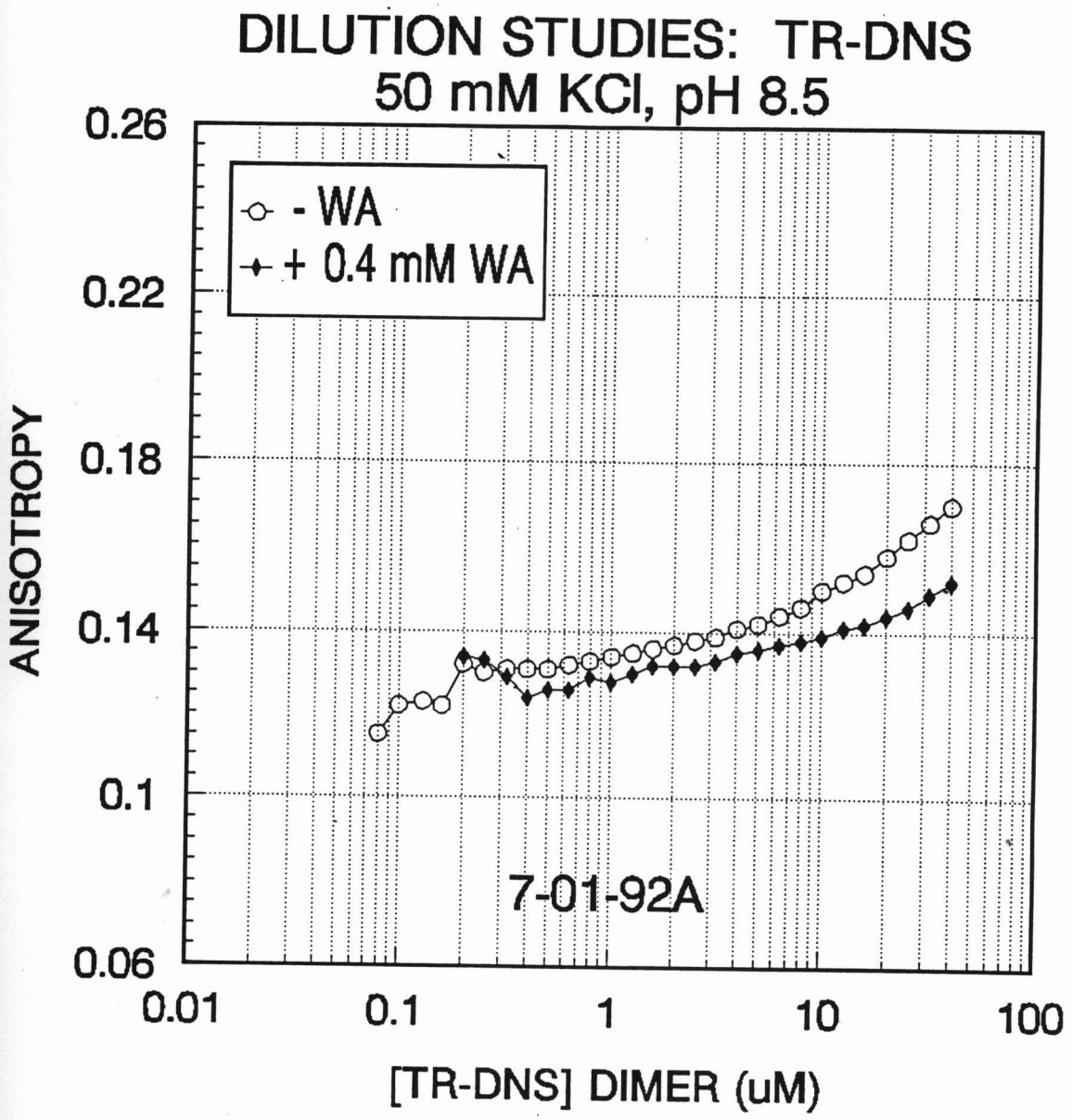
DILUTION STUDIES: TR-DNS
50 mM KCl, pH 8.5
- WA
+ 0.4 mM WA
ANISOTROPY
0.26
0.22
0.18
0.14
0.1
0.06
7-01-92A
0.01
0.1
1
10
100
[TR-DNS] DIMER (uM)

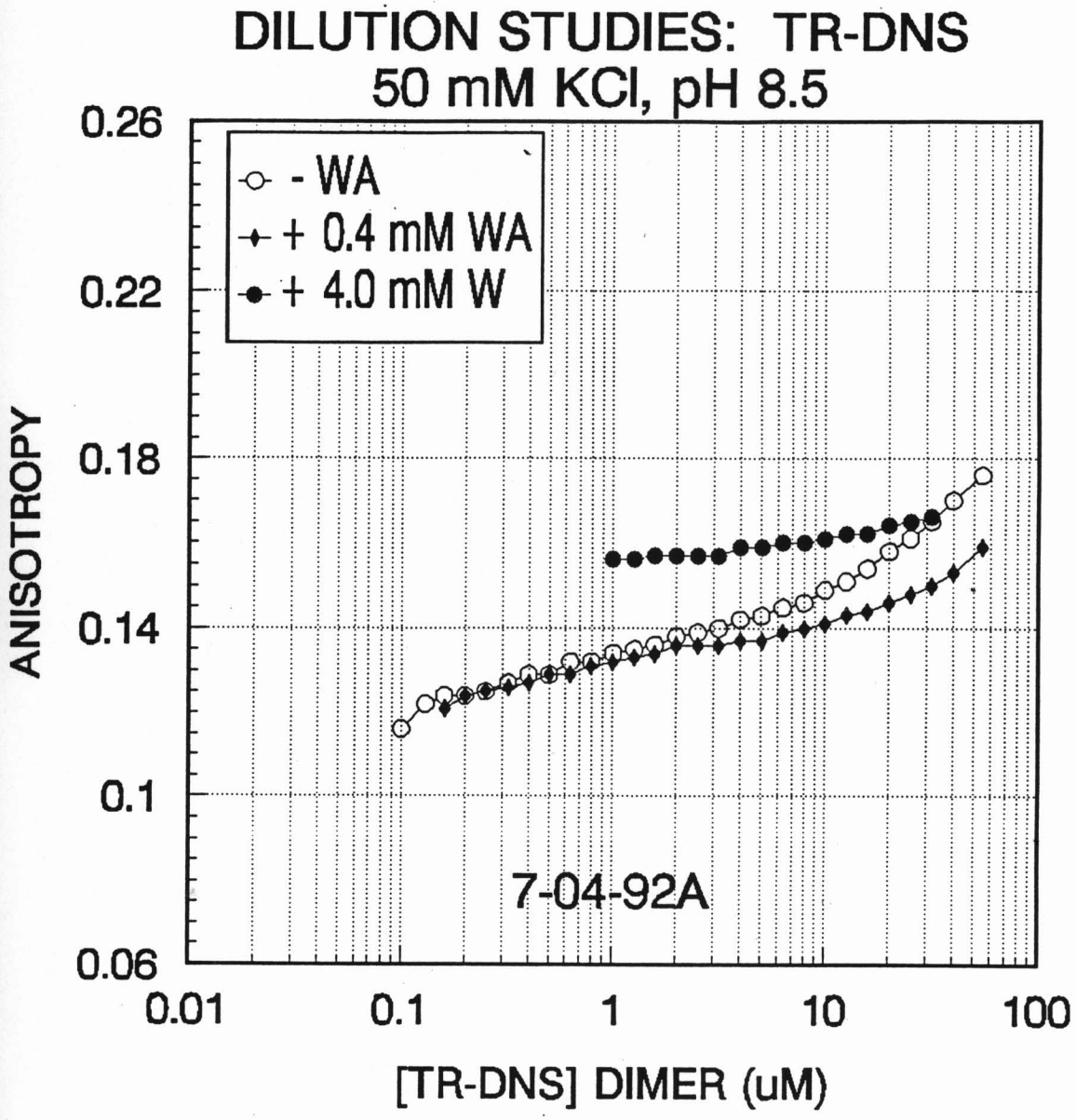
DILUTION STUDIES: TR-DNS
50 mM KCl, pH 8.5
- WA
+ 0.4 mM WA
+ 4.0 mM W
0.26
0.22
0.18
0.14
0.1
0.06
ANISOTROPY
7-04-92A
0.01
0.1
1
10
100
[TR-DNS] DIMER (uM)

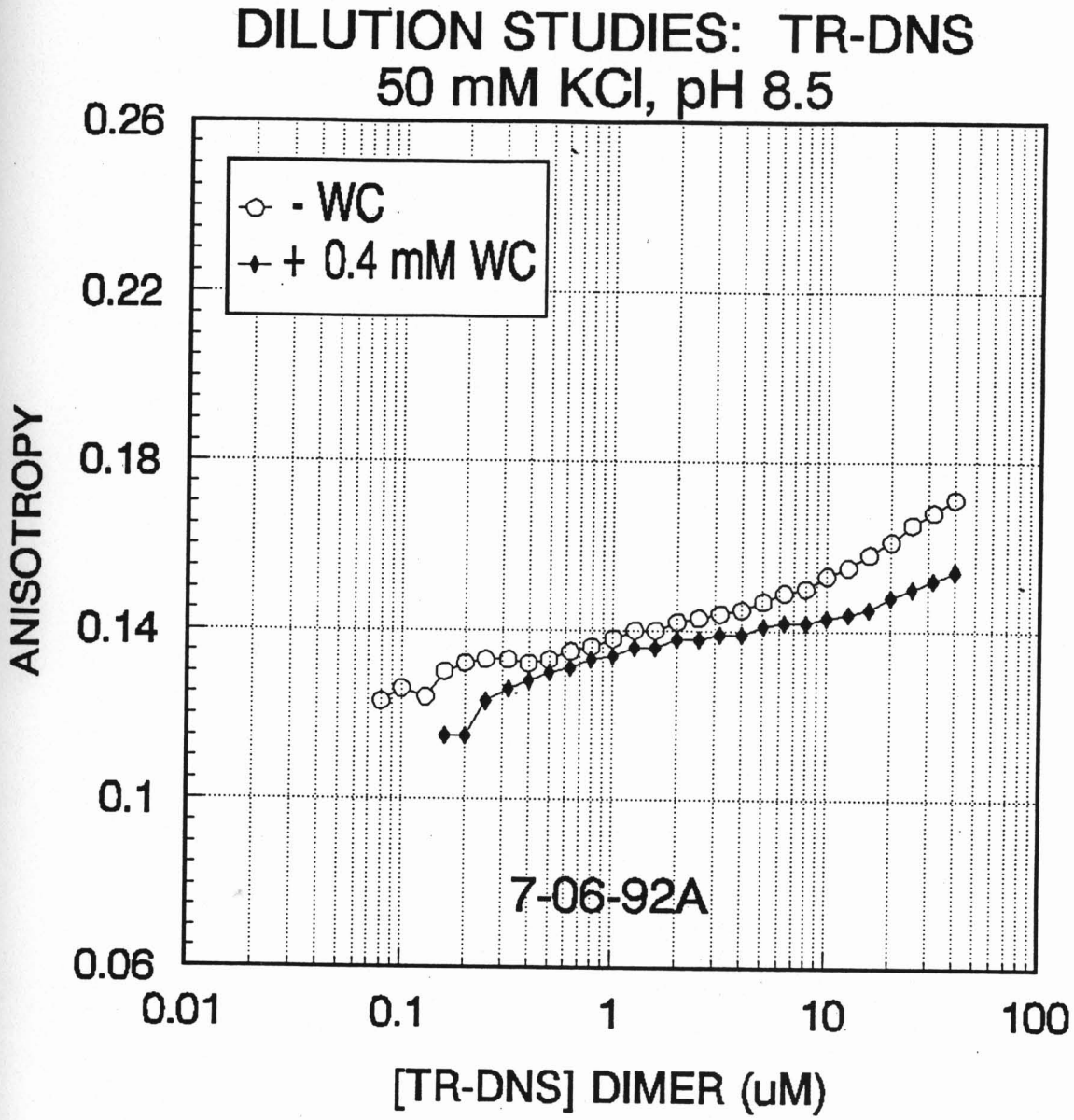
DILUTION STUDIES: TR-DNS
50 mM KCl, pH 8.5
- WC
+ 0.4 mM WC
7-06-92A
ANISOTROPY
0.26
0.22
0.18
0.14
0.1
0.06
0.01
0.1
1
10
100
[TR-DNS] DIMER (uM)

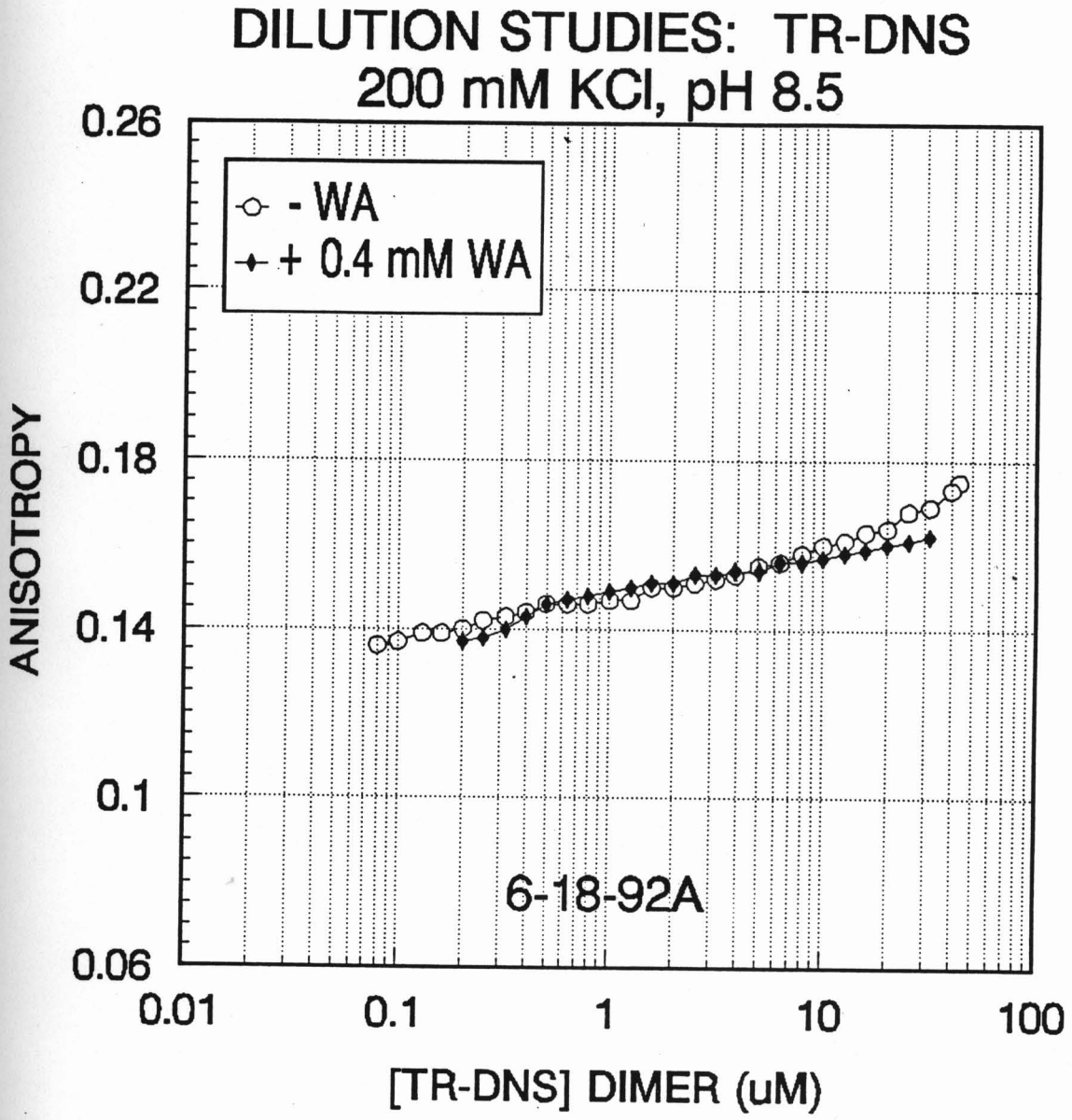
DILUTION STUDIES: TR-DNS
200 mM KCl, pH 8.5
- WA
+ 0.4 mM WA
6-18-92A
ANISOTROPY
0.26
0.22
0.18
0.14
0.1
0.06
0.01
0.1
1
10
100
[TR-DNS] DIMER (uM)

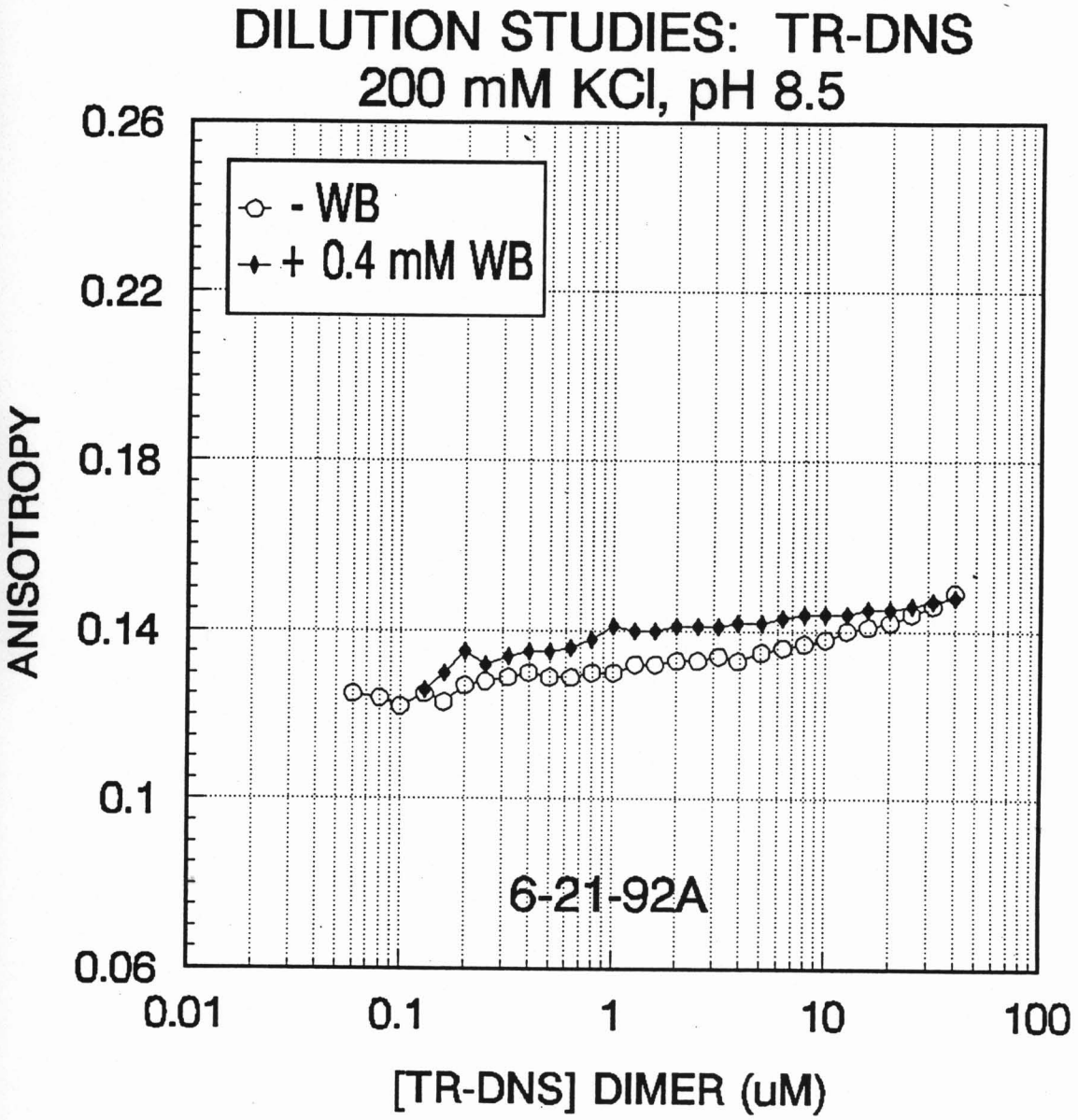
DILUTION STUDIES: TR-DNS
200 mM KCl, pH 8.5
- WB
+ 0.4 mM WB
6-21-92A
ANISOTROPY
0.26
0.22
0.18
0.14
0.1
0.06
0.01
0.1
1
10
100
[TR-DNS] DIMER (uM)

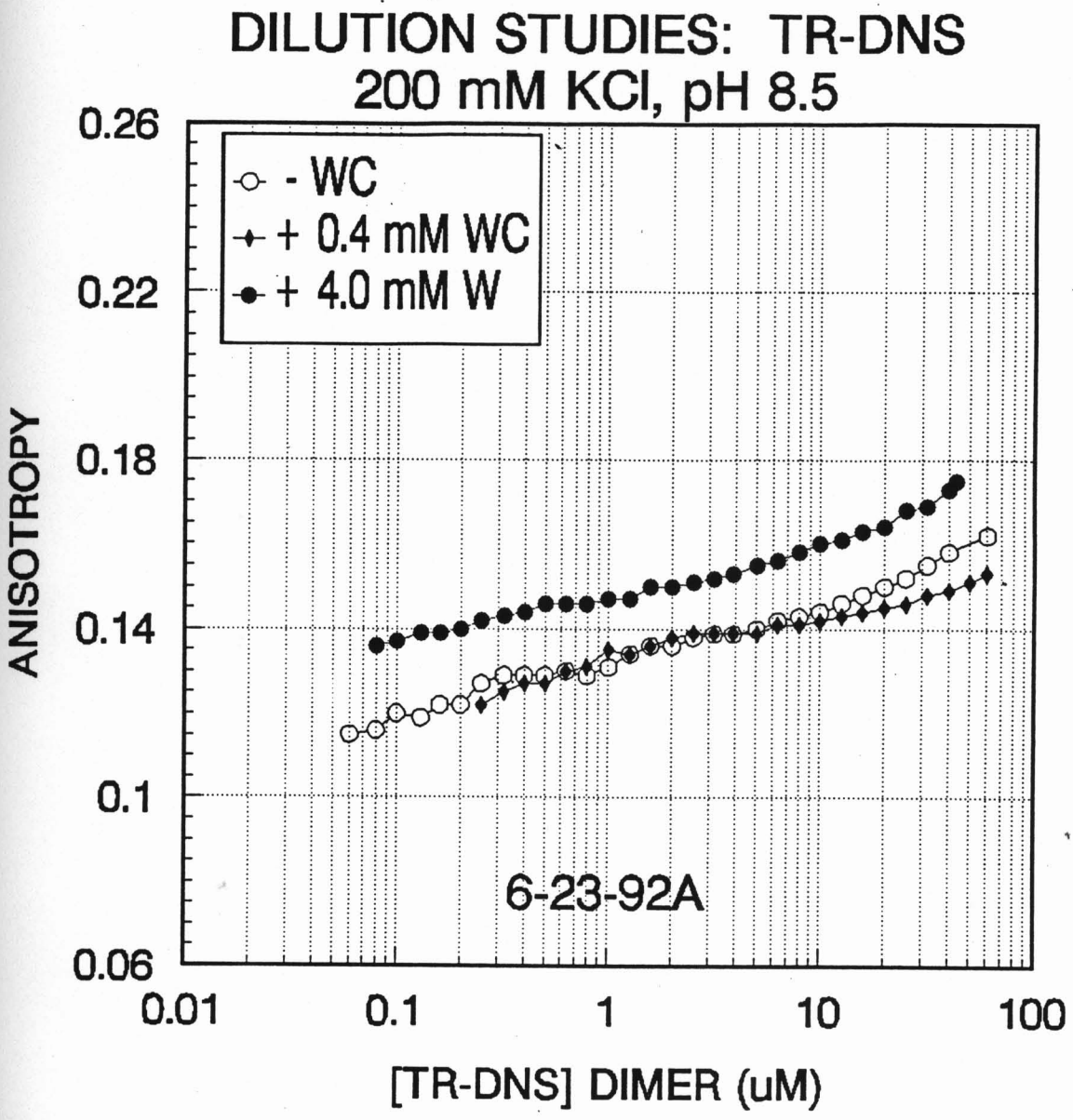
DILUTION STUDIES: TR-DNS
200 mM KCl, pH 8.5
- WC
+ 0.4 mM WC
+ 4.0 mM W
6-23-92A
ANISOTROPY
0.26
0.22
0.18
0.14
0.1
0.06
0.01
0.1
1
10
100
[TR-DNS] DIMER (uM)

APPENDIX B

Fractional and Average Lifetime Data

Table B-I. Tabulated lifetimes and fractional lifetime contributions for pH 6.0 experiments.

No Added KCl

Experiment	L.R.	[W] (mM)	[TR-DNS] (μM)	f_1	τ_1	f_2	τ_2	f_3	τ_3	$\langle\tau\rangle$ (ns)
5-22-92A	1.18	0	20.1	0.782	19.851	0.188	6.651	0.029	1.118	16.81
			10	0.788		0.185		0.027		16.90
			2	0.762		0.206		0.032		16.53
5-22-92A		0.4	21.8	0.592	19.646	0.340	6.948	0.068	1.326	14.08
			10	0.674		0.271		0.055		15.20
			2	0.660		0.285		0.055		15.02
7-20-92A	0.95	0	27.1	0.824	19.202	0.154	5.488	0.022	0.739	16.68
			10	0.815		0.163		0.022		16.56
			2	0.787		0.175		0.038		16.10
7-20-92A		0.4	28.3	0.681	18.156	0.277	5.353	0.043	0.913	13.89
			10	0.669		0.284		0.047		13.71
			2	0.634		0.302		0.064		13.19
7-20-92A		4.0	25.8	0.586	16.504	0.354	5.153	0.060	0.928	11.55
			10	0.563		0.376		0.061		11.29
			2	0.538		0.370		0.092		10.87
7-29-92A	0.94	0	30.1	0.793	19.988	0.182	6.161	0.025	0.868	16.99
			10	0.788		0.184		0.028		16.91
			2	0.755		0.212		0.033		16.43
7-29-92A		0.4	21.3	0.652	18.544	0.298	5.593	0.051	0.973	13.81
			10	0.654		0.291		0.055		13.81
			2	0.617		0.327		0.056		13.33

Table B-II. Tabulated lifetimes and fractional lifetime contributions for pH 6.0 experiments.

10 mM KCl

Experiment	L.R.	[W] (mM)	[TR-DNS] (μM)	f_1	τ_1	f_2	τ_2	f_3	τ_3	$\langle\tau\rangle$ (ns)
5-26-92A (1)	1.23	0	16.7	0.766	19.835	0.201	6.536	0.033	1.100	16.54
			10	0.775		0.193		0.032		16.67
			2	0.745		0.220		0.034		16.25
5-26-92A (1)		0.4	18.5	0.611	18.372	0.324	5.836	0.065	1.076	13.19
			10	0.658		0.283		0.059		13.80
			2	0.683		0.263		0.054		14.14
5-26-92A (2)	0.61	0	24.2	0.784	20.093	0.185	6.564	0.031	1.101	17.00
			10	0.790		0.179		0.031		17.08
			2	0.746		0.221		0.034		16.48
5-26-92A (2)		0.4	18.9	0.593	19.010	0.331	6.380	0.076	1.223	13.48
			10	0.637		0.298		0.065		14.09
			2	0.647		0.288		0.065		14.22
5-28-92A	0.62	0	14.2	0.780	20.254	0.192	6.858	0.028	1.091	17.15
			10	0.787		0.188		0.025		17.26
			2	0.734		0.238		0.028		16.53
5-28-92A		0.4	23.2	0.580	19.271	0.354	6.660	0.066	1.271	13.62
			10	0.668		0.279		0.054		14.80
			2	0.692		0.257		0.050		15.11
5-28-92A		4.0	27.4	0.5995	16.433	0.338	5.650	0.067	1.167	11.77
			10	0.577		0.350		0.073		11.54
			2	0.524		0.380		0.096		10.87

Table B-III. Tabulated lifetimes and fractional lifetime contributions for pH 6.0 experiments.

50 mM KCl

Experiment	L.R.	[W] (mM)	[TR-DNS] (μM)	f_1	τ_1	f_2	τ_2	f_3	τ_3	$\langle\tau\rangle$ (ns)
5-18-92B	1.47	0	9.07	0.796	19.383	0.185	5.510	0.019	0.629	16.46
			5	0.793		0.188		0.020		16.42
			1.81	0.760		0.222		0.018		15.97
5-18-92B		0.4	16.3	0.508	18.156	0.422	5.855	0.070	1.119	11.77
			10	0.569		0.372		0.059		12.57
			2	0.544		0.392		0.063		12.24
5-18-92B		4.0	14.6	0.542	15.693	0.381	5.083	0.077	1.175	10.53
			10	0.532		0.387		0.081		10.41
			2	0.462		0.425		0.113		9.54
5-20-92A (1)	0.85	0	9.70	0.806	19.004	0.170	5.592	0.024	0.703	16.28
			5	0.796		0.183		0.022		16.17
			1.94	0.766		0.213		0.021		15.76
5-20-92A (1)		0.4	20	0.536	18.465	0.389	6.427	0.075	1.24	12.49
			9.12	0.603		0.330		0.068		13.34
			1.82	0.443		0.464		0.093		11.28
5-20-92A (2)	1.12	0	9.90	0.766	19.603	0.190	7.331	0.045	1.499	16.48
			5.0	0.749		0.207		0.043		16.26
			1.98	0.707		0.252		0.042		15.77
5-20-92A (2)		0.4	19.6	0.559	17.624	0.370	5.778	0.072	1.130	12.07
			10	0.518		0.407		0.075		11.57
			2	0.446		0.467		0.086		10.66

Table B-IV. Tabulated lifetimes and fractional lifetime contributions for pH 6.0 experiments.

200 mM KCl

Experiment	L.R.	[W] (mM)	[TR-DNS] (μM)	f_1	τ_1	f_2	τ_2	f_3	τ_3	$\langle\tau\rangle$ (ns)
6-9-92A	1.33	0	26.4	0.761	17.017	0.217	4.233	0.022	0.124	13.87
			10	0.753		0.225		0.021		13.77
			2	0.743		0.234		0.023		13.64
6-9-92A		0.4	26.2	0.481	14.747	0.453	4.340	0.066	0.606	9.10
			10	0.496		0.441		0.063		9.27
			2	0.508		0.427		0.066		9.38
6-9-92A		4.0	23.2	0.478	13.692	0.467	4.198	0.055	0.499	8.53
			10	0.493		0.451		0.056		8.67
			2	0.502		0.434		0.063		8.73
7-13-92A (1)	0.83	0	31.4	0.609	19.592	0.327	6.851	0.063	1.114	14.24
			10	0.589		0.344		0.067		13.97
			2	0.572		0.354		0.074		13.71
7-13-92A (1)		0.4	25.0	0.407	16.817	0.501	5.218	0.092	0.817	9.53
			10	0.395		0.512		0.093		9.39
			2	0.387		0.510		0.103		9.25
7-13-92A (2)	0.85	0	36.4	0.666	18.536	0.286	6.228	0.047	0.946	14.17
			10	0.650		0.300		0.049		13.96
			2	0.622		0.326		0.052		13.61
7-13.-92A (2)		0.4	23.1	0.371	17.489	0.518	5.339	0.112	0.864	9.35
			10	0.379		0.531		0.089		9.54
			2	0.373		0.523		0.105		9.41

Table B-V. Tabulated lifetimes and fractional lifetime contributions for pH 7.6 experiments.
No Added KCl

Experiment	L.R.	[W] (mM)	[TR-DNS] (μM)	f_1	τ_1	f_2	τ_2	f_3	τ_3	$\langle\tau\rangle$ (ns)
10-19-91A	1.05	0	23.6	0.744	19.698	0.208	7.480	0.048	1.425	16.28
			8.34	0.736		0.220		0.044		16.21
			1.67	0.661		0.287		0.052		15.24
10-19-91A		0.4	34.9	0.651	19.262	0.271	6.996	0.078	1.669	14.57
			10	0.595		0.327		0.078		13.88
			2	0.516		0.387		0.097		12.81
3-2-92A[a]	1.03	0	24.6	0.783	19.047	0.182	6.266	0.035	1.134	16.09
			10	0.776		0.191		0.033		16.01
			2	0.742		0.220		0.038		15.55
3-2-92A[a]		0.4	23.2	0.605	19.432	0.326	7.394	0.069	1.451	14.27
			10	0.601		0.332		0.067		14.23
			2	0.573		0.356		0.071		13.87
3-5-92A[a]	1.04	0	32.8	0.834	18.465	0.152	4.560	0.014	0	16.09
			10	0.814		0.171		0.015		15.81
			2	0.790		0.194		0.016		15.47
3-5-92A[a]		0.4	19.9	0.703	17.424	0.255	4.998	0.042	0.780	13.56
			10	0.681		0.276		0.043		13.28
			2	0.639		0.317		0.044		12.75
5-28-92B	1.26	0	30.0	0.785	19.330	0.180	6.251	0.036	1.042	16.34
			10	0.779		0.184		0.036		16.25
			2	0.733		0.228		0.039		15.63
5-28-92B		0.4	24.3	0.634	19.441	0.299	6.710	0.067	1.208	14.41
			10	0.663		0.278		0.059		14.82
			2	0.650		0.293		0.057		14.67
7-15-92A	0.94	0	35.1	0.725	20.453	0.232	7.823	0.043	1.367	16.70
			10	0.692		0.261		0.047		16.26
			2	0.644		0.303		0.053		15.61
7-15-92A		0.4	25.8	0.633	19.719	0.308	6.641	0.059	1.250	14.60
			10	0.597		0.337		0.066		14.09
			2	0.536		0.388		0.076		13.24
7-15-92A		4.0	23.5	0.489	18.754	0.433	6.251	0.078	1.227	11.97
			10	0.458		0.463		0.079		11.58
			2	0.424		0.481		0.095		11.07

a. Dilution curve profile not consistent with other experimental results. Data from these dilution study experiments not included in averages.

Table B-VI. Tabulated lifetimes and fractional lifetime contributions for pH 7.6 experiments.

10 mM KCl

Experiment	L.R.	[W] (mM)	[TR-DNS] (μM)	f_1	τ_1	f_2	τ_2	f_3	τ_3	$\langle\tau\rangle$ (ns)
2-10-92A	0.85	0	32.0	0.832	18.593	0.153	4.565	0.014	0.001	16.17
			10	0.819		0.165		0.016		15.98
			2	0.785		0.197		0.018		15.49
2-10-92A		0.4	16.6	0.699	16.884	0.277	4.249	0.024	0	12.98
			10	0.694		0.281		0.024		12.91
			2	0.668		0.300		0.031		12.55
2-13-92A	0.86	0	23.1	0.816	18.891	0.163	4.882	0.022	0.496	16.22
			10	0.803		0.174		0.023		16.03
			2	0.771		0.204		0.024		15.57
2-13-92A		0.4	21.9	0.686	17.422	0.271	4.788	0.043	0.782	13.28
			10	0.666		0.289		0.045		13.02
			2	0.622		0.323		0.055		12.43
3-23-92A	1.28	0	31.1	0.811	18.677	0.167	5.073	0.022	0.699	16.01
			10	0.797		0.180		0.023		15.81
			2	0.769		0.206		0.025		15.23
3-23-92A		0.4	19.1	0.696	17.122	0.270	4.662	0.033	0.649	13.20
			10	0.690		0.276		0.034		13.12
			2	0.658		0.302		0.040		12.70
7-14-92A (2)	0.70	4.0	21.4	0.496	18.078	0.425	5.816	0.079	1.064	11.52
			10	0.482		0.435		0.083		11.32
			2	0.436		0.463		0.102		10.68

Table B-VII. Tabulated lifetimes and fractional lifetime contributions for pH 7.6 experiments.

50 mM KCl

Experiment	L.R.	[W] (mM)	[TR-DNS] (μM)	f_1	τ_1	f_2	τ_2	f_3	τ_3	$\langle\tau\rangle$ (ns)
1-27-92A	1.19	0	28.9	0.723	19.466	0.225	7.053	0.051	1.348	15.73
			10	0.684		0.264		0.051		15.25
			2	0.637		0.307		0.056		14.64
1-27-92A		0.4	21.9	0.604	16.945	0.331	5.340	0.064	0.998	12.07
			10	0.564		0.371		0.066		11.60
			2	0.522		0.404		0.075		11.08
3-19-92A	0.71	0	28.0	0.789	18.599	0.185	4.983	0.026	0.711	15.61
			10	0.775		0.197		0.028		15.42
			2	0.744		0.225		0.030		14.98
3-19-92A		0.4	21.1	0.598	16.699	0.342	4.903	0.060	0.784	11.71
			10	0.578		0.362		0.060		11.47
			2	0.548		0.390		0.062		11.11
3-21-92A	1.10	0	24.8	0.792	18.372	0.188	4.854	0.020	0.229	15.47
			10	0.774		0.205		0.020		15.22
			2	0.755		0.223		0.022		14.96
3-21-92A		0.4	21.9	0.611	16.338	0.338	4.775	0.050	0.700	11.63
			10	0.590		0.354		0.055		11.37
			2	0.564		0.379		0.057		11.06
7-14-92A (2)	0.70	4.0	36.8	0.445	17.761	0.478	5.625	0.077	0.945	10.67
			10	0.430		0.482		0.088		10.43
			2	0.390		0.486		0.123		9.78

Table B-VIII. Tabulated lifetimes and fractional lifetime contributions for pH 7.6 experiments.

100 mM KCl

Experiment	L.R.	[W] (mM)	[TR-DNS] (μM)	f_1	τ_1	f_2	τ_2	f_3	τ_3	$\langle\tau\rangle$ (ns)
1-21-92A	1.10	0	27.6	0.715	18.524	0.239	6.395	0.047	1.208	14.83
			10	0.683		0.271		0.046		14.44
			2	0.656		0.293		0.051		14.09
1-21-92A		0.4	23.1	0.551	16.119	0.387	5.072	0.062	0.946	10.90
			10	0.510		0.430		0.060		10.46
			2	0.490		0.442		0.068		10.20
3-30-92A	1.50	0	40.1	0.690	18.922	0.262	6.602	0.048	1.143	14.84
			10	0.690		0.261		0.049		14.84
			2	0.668		0.282		0.050		14.56
3-30-92A		0.4	28.2	0.572	16.290	0.374	5.013	0.055	0.797	11.24
			7.05	0.588		0.358		0.054		11.42
			1.41	0.585		0.358		0.057		11.37
4-6-92A	1.20	0	26.9	0.711	18.743	0.244	6.337	0.045	1.116	14.92
			10	0.715		0.243		0.042		14.99
			2	0.683		0.275		0.043		14.59
4-6-92A		0.4	24.7	0.466	17.741	0.448	6.132	0.086	1.177	11.12
			10	0.505		0.416		0.079		11.60
			2	0.520		0.404		0.076		11.79
5-18-92A	1.02	0	20.4	0.726	18.333	0.238	5.533	0.035	0.802	14.65
			10	0.725		0.245		0.031		14.67
			2	0.706		0.264		0.031		14.43
5-18-92A		0.4	17.6	0.492	16.673	0.438	5.426	0.071	0.954	10.65
			10	0.537		0.400		0.063		11.18
			2	0.554		0.384		0.062		11.38
5-18-92A		4.0	17.2	0.432	14.856	0.492	5.027	0.075	0.943	8.96
			10	0.440		0.487		0.073		9.05
			2	0.435		0.484		0.081		8.97

Table B-IX. Tabulated lifetimes and fractional lifetime contributions for pH 7.6 experiments.

200 mM KCl

Experiment	L.R.	[W] (mM)	[TR-DNS] (μM)	f_1	τ_1	f_2	τ_2	f_3	τ_3	$\langle\tau\rangle$ (ns)
3-16-92A	0.95	0	40.8	0.746	17.223	0.232	4.374	0.023	0	13.86
			10	0.732		0.246		0.022		13.68
			2	0.728		0.250		0.022		13.63
3-16-92A		0.4	29.8	0.487	14.662	0.457	4.360	0.056	0.481	9.16
			10	0.476		0.467		0.057		9.04
			2	0.464		0.475		0.060		8.90
5-30-90A	0.98	0	34.1	0.695	17.914	0.261	5.259	0.044	0.788	13.86
			10	0.705		0.257		0.038		14.01
			2	0.685		0.275		0.040		13.75
5-30-92A		0.4	26.9	0.457	16.683	0.454	5.230	0.089	0.913	10.08
			10	0.517		0.411		0.072		10.84
			2	0.540		0.391		0.070		11.12
5-30-92A		4.0	27.7	0.430	15.393	0.480	5.299	0.090	1.016	9.25
			10	0.443		0.470		0.087		9.40
			2	0.436		0.468		0.096		9.29
7-14-92A	0.89	0	37.2	0.635	18.961	0.303	6.528	0.062	1.160	14.09
			10	0.603		0.333		0.064		13.68
			2	0.583		0.348		0.070		13.41
7-14-92A		0.4	27.4	0.444	16.414	0.472	5.102	0.083	0.852	9.77
			10	0.435		0.479		0.086		9.66
			2	0.424		0.484		0.092		9.51

Table B-X. Tabulated lifetimes and fractional lifetime contributions for pH 7.6 experiments.

500 mM KCl

Experiment	L.R.	[W] (mM)	[TR-DNS] (μM)	f_1	τ_1	f_2	τ_2	f_3	τ_3	$\langle\tau\rangle$ (ns)
3-9-92A	1.35	0	39.6	0.677	16.809	0.288	4.551	0.036	0.529	12.71
			10	0.670		0.296		0.034		12.63
			2	0.664		0.300		0.037		12.55
3-9-92A		0.4	33.1	0.430	14.335	0.500	4.356	0.070	0.475	8.38
			10	0.414		0.517		0.069		8.22
			2	0.410		0.521		0.069		8.18

Table B-XI. Tabulated lifetimes and fractional lifetime contributions for pH 8.5 experiments.

No Added KCl

Experiment	L.R.	[W] (mM)	[TR-DNS] (μM)	f_1	τ_1	f_2	τ_2	f_3	τ_3	$\langle\tau\rangle$ (ns)
6-25-92A	0.66	0	47.6	0.780	19.584	0.180	6.544	0.040	1.099	16.50
(1)			10	0.757		0.200		0.043		16.18
			2	0.726		0.231		0.043		15.78
6-25-92A[a]										
(1)										
6-25-92A	0.76	0	31.8	0.767	19.580	0.190	6.576	0.043	1.065	16.31
(2)			10	0.745		0.210		0.044		16.01
			2	0.726		0.226		0.048		15.75
6-25-92A		0.4	27.8	0.660	19.133	0.282	6.153	0.058	1.103	14.41
(2)			10	0.671		0.274		0.055		14.57
			2	0.649		0.294		0.057		14.28
6-29-92A	0.93	0	21.5	0.737	19.289	0.224	7.513	0.038	1.238	15.95
			10	0.717		0.241		0.042		15.69
			2	0.695		0.258		0.047		15.40
6-29-92A		0.4	25.3	0.645	18.827	0.299	6.455	0.056	1.166	14.14
			10	0.629		0.314		0.057		13.94
			2	0.599		0.341		0.060		13.55
6-29-92A		4.0	26.6	0.481	17.350	0.438	6.193	0.081	1.230	11.16
			10	0.471		0.445		0.084		11.03
			2	0.420		0.478		0.102		10.37

[a] Sample lost in preparation. Average lifetime data from experiment 6-25-92A (2) were used to calculate the average correlation times for this dilution study experiment.

Table B-XII. Tabulated lifetimes and fractional lifetime contributions for pH 8.5 experiments

50 mM KCl

Experiment	L.R.	[W] (mM)	[TR-DNS] (μM)	f_1	τ_1	f_2	τ_2	f_3	τ_3	$\langle\tau\rangle$ (ns)
7-01-92A	0.98	0	31.6	0.722	19.332	0.233	7.000	0.045	1.160	15.641
			10	0.702		0.251		0.047		15.38
			2	0.678		0.272		0.050		15.07
			1	0.653		0.296		0.051		14.75
7-01-92A		0.4	21.9	0.585	17.995	0.351	5.778	0.064	1.046	12.62
			10	0.587		0.346		0.067		12.63
			2	0.565		0.367		0.068		12.36
			1	0.557		0.374		0.069		12.26
7-04-92A	0.69	0	31.4	0.724	19.694	0.230	7.407	0.046	1.152	16.02
			10	0.703		0.247		0.049		15.73
			1	0.667		0.278		0.055		15.26
7-04-92A		0.4	30.5	0.576	18.733	0.359	6.087	0.064	0.962	13.04
			10	0.563		0.370		0.067		12.86
			1	0.533		0.390		0.076		12.43
7-04-92A		4.0	27.1	0.449	17.519	0.467	6.022	0.085	1.162	10.78
			10	0.437		0.471		0.092		10.60
			1	0.350		0.508		0.143		9.36
7-06-92A	0.81	0	21.6	0.746	18.983	0.208	6.531	0.046	1.040	15.57
			10	0.734		0.218		0.048		15.41
			1	0.703		0.245		0.052		15.00
7-06-92A		0.4	20.1	0.571	18.507	0.347	6.109	0.081	1.091	12.78
			10	0.570		0.349		0.080		12.77
			1	0.460		0.438		0.102		11.30

Table B-XIII. Tabulated lifetimes and fractional lifetime contributions for pH 8.5 experiments.

200 mM KCl

Experiment	L.R.	[W] (mM)	[TR-DNS] (μM)	f_1	τ_1	f_2	τ_2	f_3	τ_3	$\langle\tau\rangle$ (ns)
6-18-92A	1.30	0	31.6	0.760	17.630	0.215	4.162	0.026	0.023	14.29
			10	0.753		0.221		0.026		14.20
			2	0.748		0.220		0.032		14.10
6-18-92A		0.4	21.5	0.528	16.555	0.406	4.543	0.066	0.512	10.62
			10	0.529		0.405		0.067		10.64
			2	0.520		0.408		0.072		10.50
6-21-92A	0.66	0	28.1	0.688	18.417	0.259	5.858	0.054	0.896	14.24
			10	0.680		0.265		0.054		14.12
			2	0.675		0.260		0.065		14.01
6-21-92A		0.4	20	0.431	17.426	0.475	5.474	0.094	0.890	10.19
			10	0.442		0.467		0.092		10.34
			2	0.430		0.458		0.112		10.10
6-23-92A	0.82	0	33.4	0.675	17.266	0.290	4.641	0.035	0.649	13.02
			10	0.672		0.284		0.043		12.95
			2	0.653		0.294		0.053		12.67
6-23-92A		0.4	28.4	0.503	15.667	0.432	4.258	0.065	0.400	9.75
			10	0.494		0.441		0.065		9.64
			2	0.486		0.440		0.074		9.52
6-23-92A		4.0	19.2	0.479	13.970	0.435	4.299	0.086	0.728	7.11
			10	0.469		0.448		0.083		6.97
			2	0.458		0.443		0.099		6.83

APPENDIX C

Correlation Time Results by pH and Salt Concentration

DILUTION STUDIES: TR-DNS

With and without added Tryptophan (W)

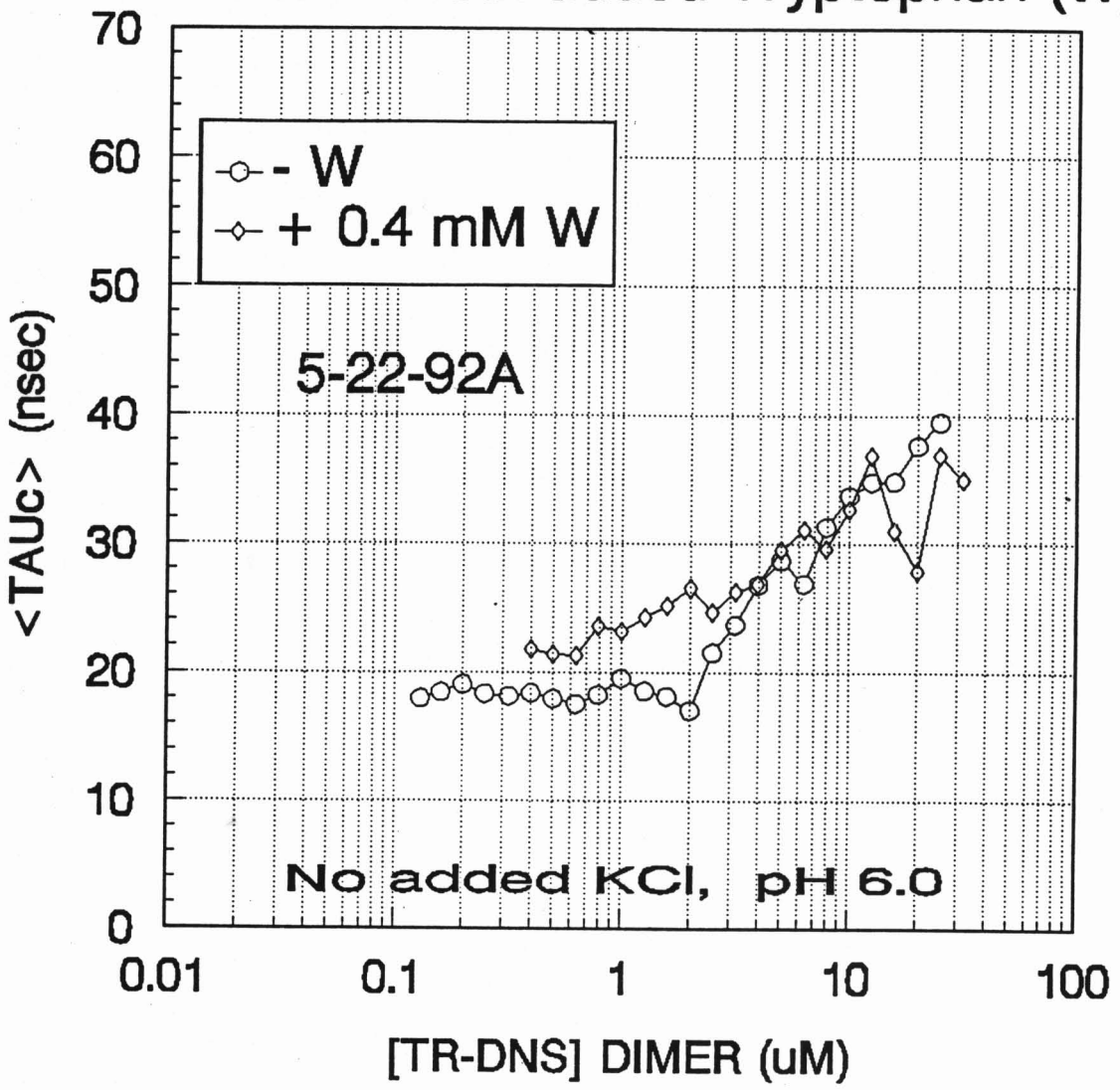

DILUTION STUDIES: TR-DNS

With and without added Tryptophan (W)

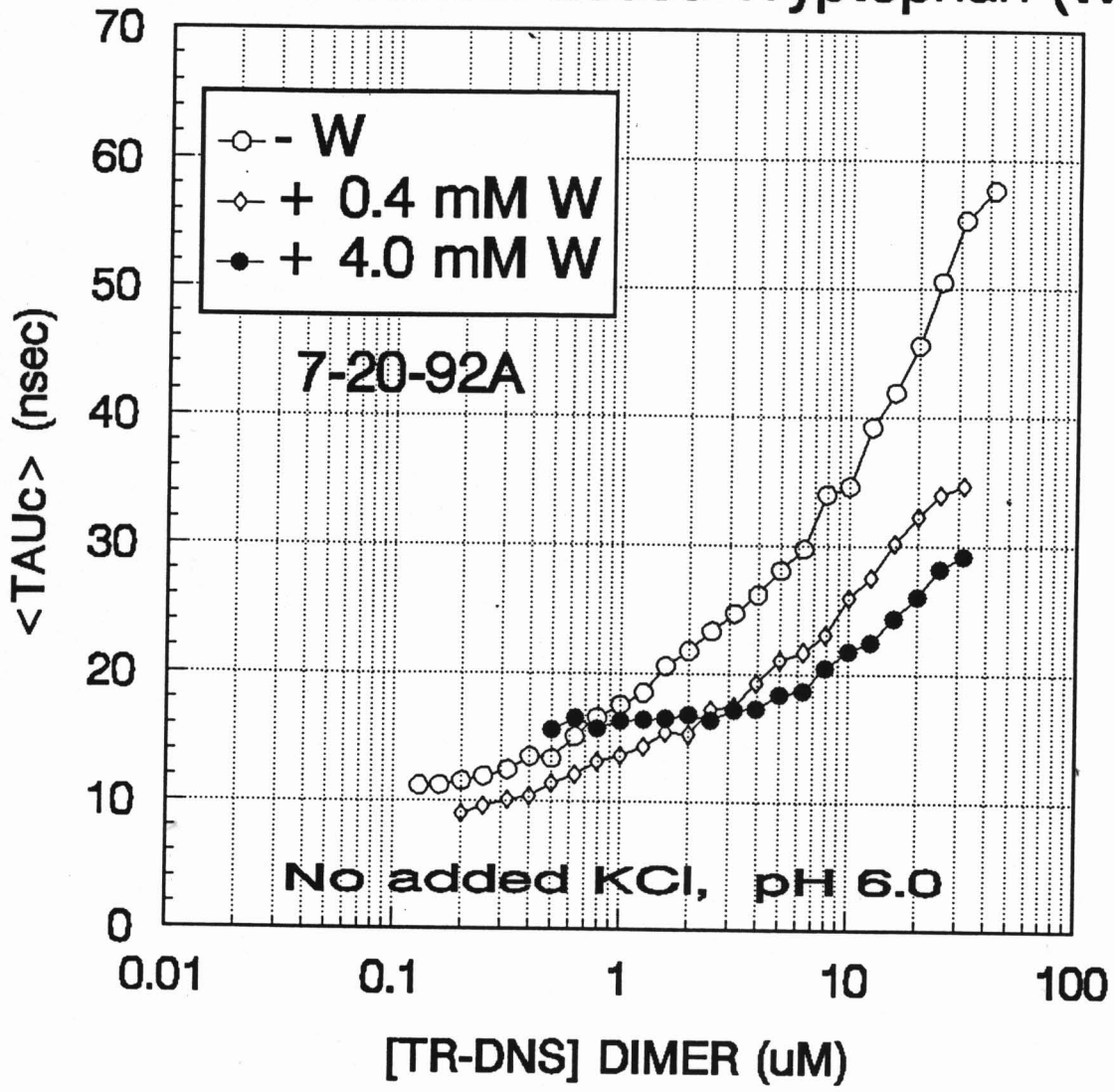

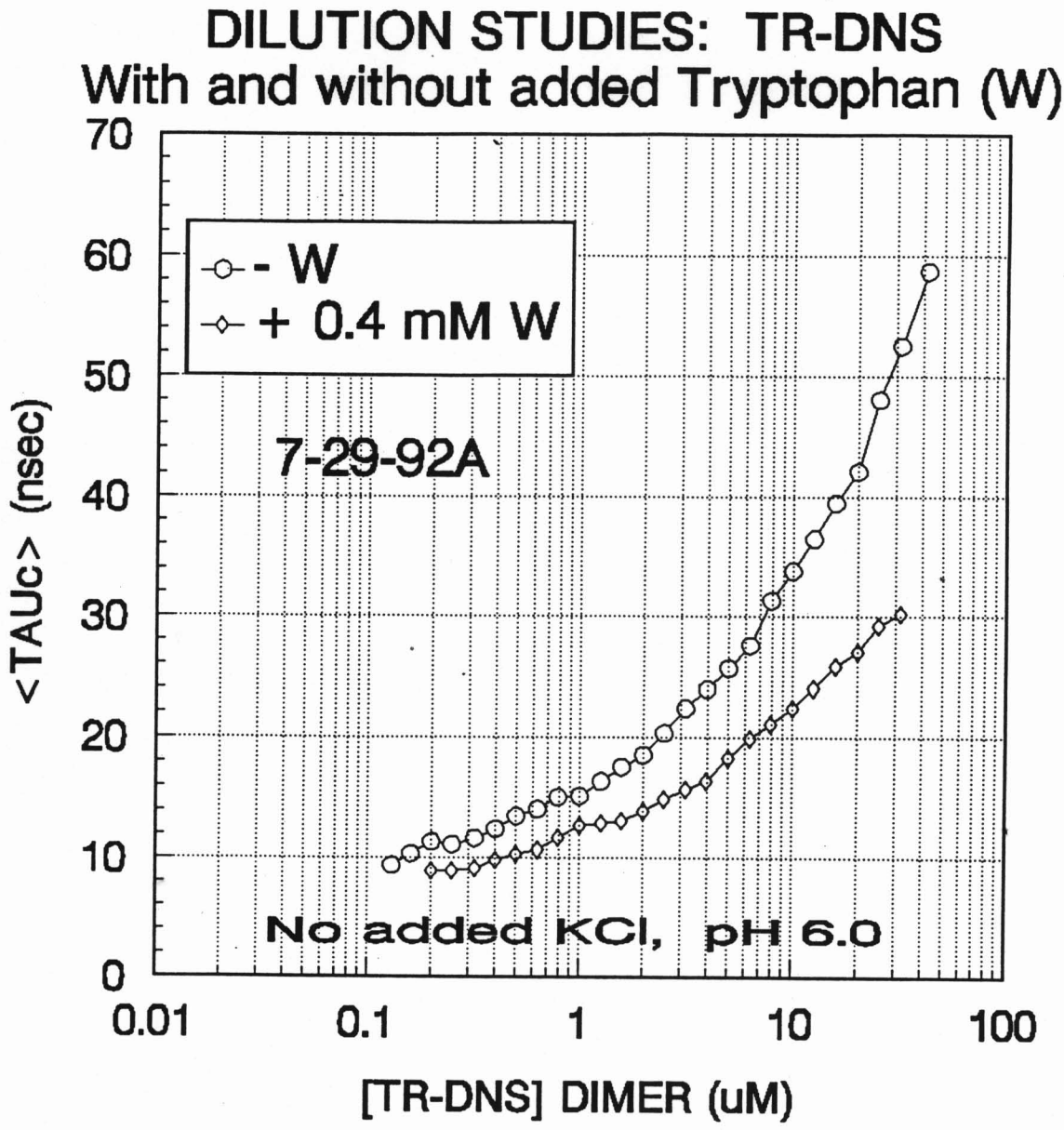
DILUTION STUDIES: TR-DNS
With and without added Tryptophan (W)
- W
+ 0.4 mM W
7-29-92A
No added KCl, pH 6.0
<TAUc> (nsec)
[TR-DNS] DIMER (uM)
0
10
20
30
40
50
60
70
0.01
0.1
1
10
100

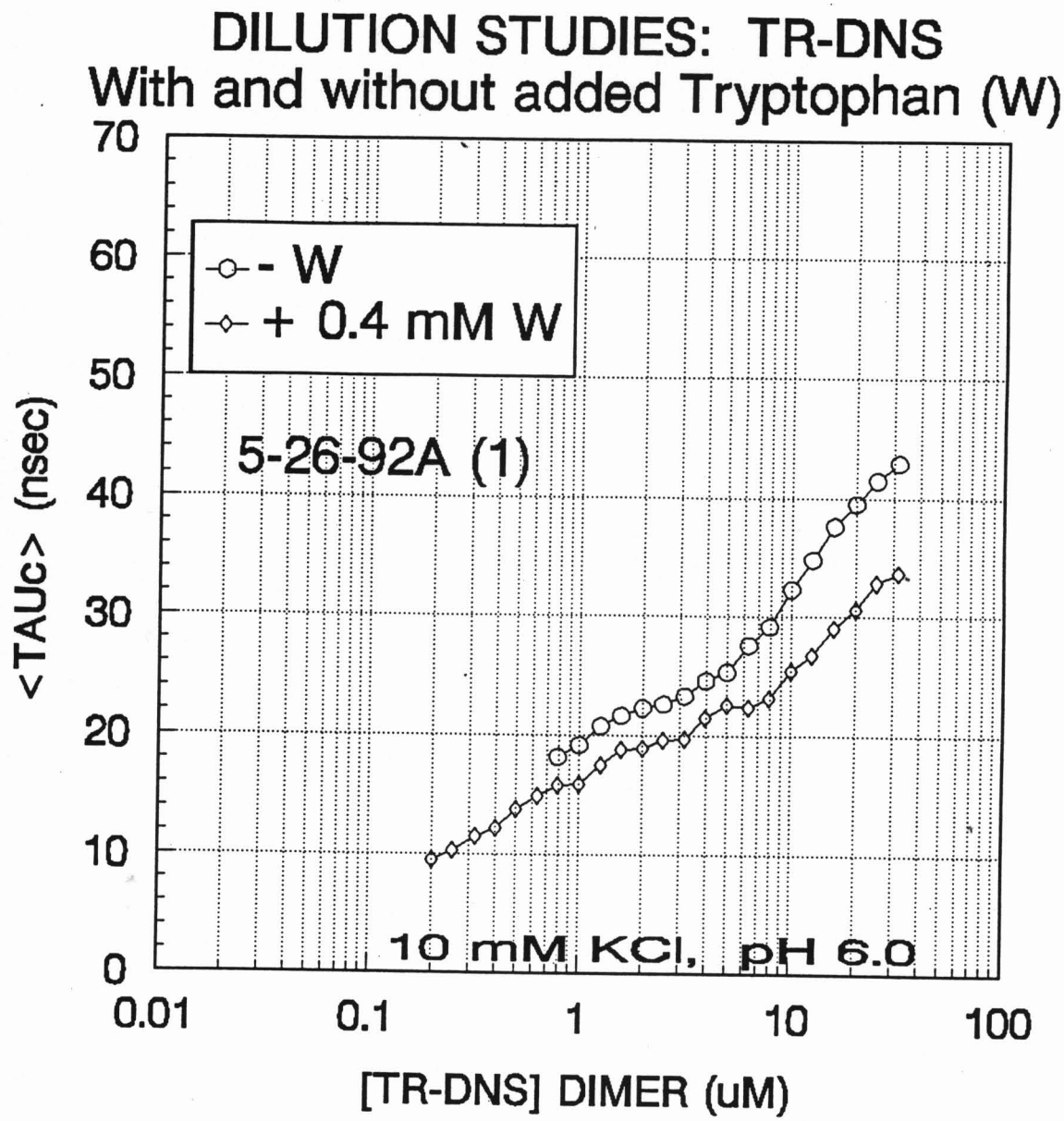
DILUTION STUDIES: TR-DNS
With and without added Tryptophan (W)
- W
+ 0.4 mM W
5-26-92A (1)
10 mM KCl, pH 6.0
<TAUc> (nsec)
[TR-DNS] DIMER (uM)
0
10
20
30
40
50
60
70
0.01
0.1
1
10
100

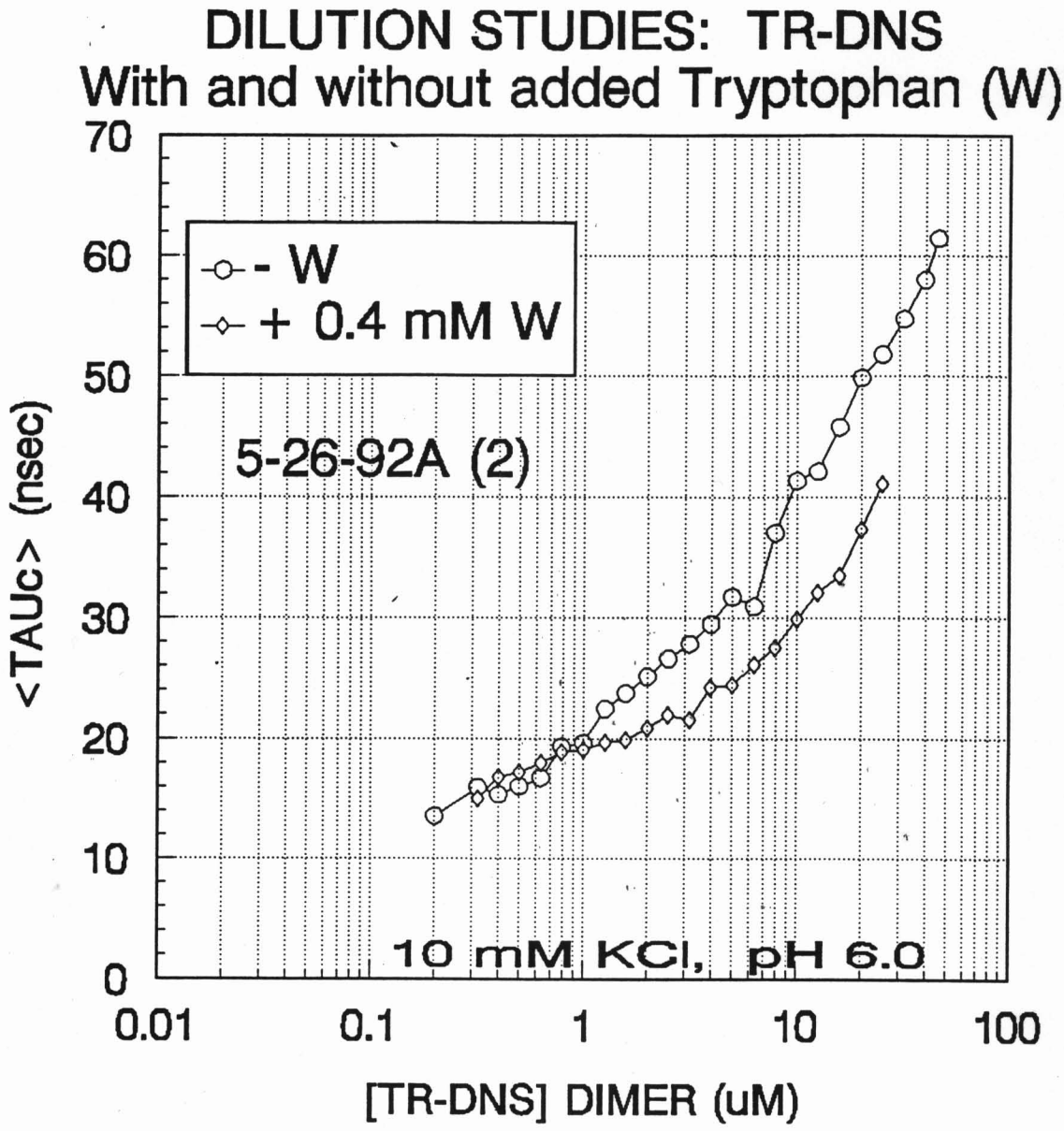
DILUTION STUDIES: TR-DNS
With and without added Tryptophan (W)
- W
+ 0.4 mM W
5-26-92A (2)
10 mM KCl, pH 6.0
<TAUc> (nsec)
[TR-DNS] DIMER (uM)
0
10
20
30
40
50
60
70
0.01
0.1
1
10
100

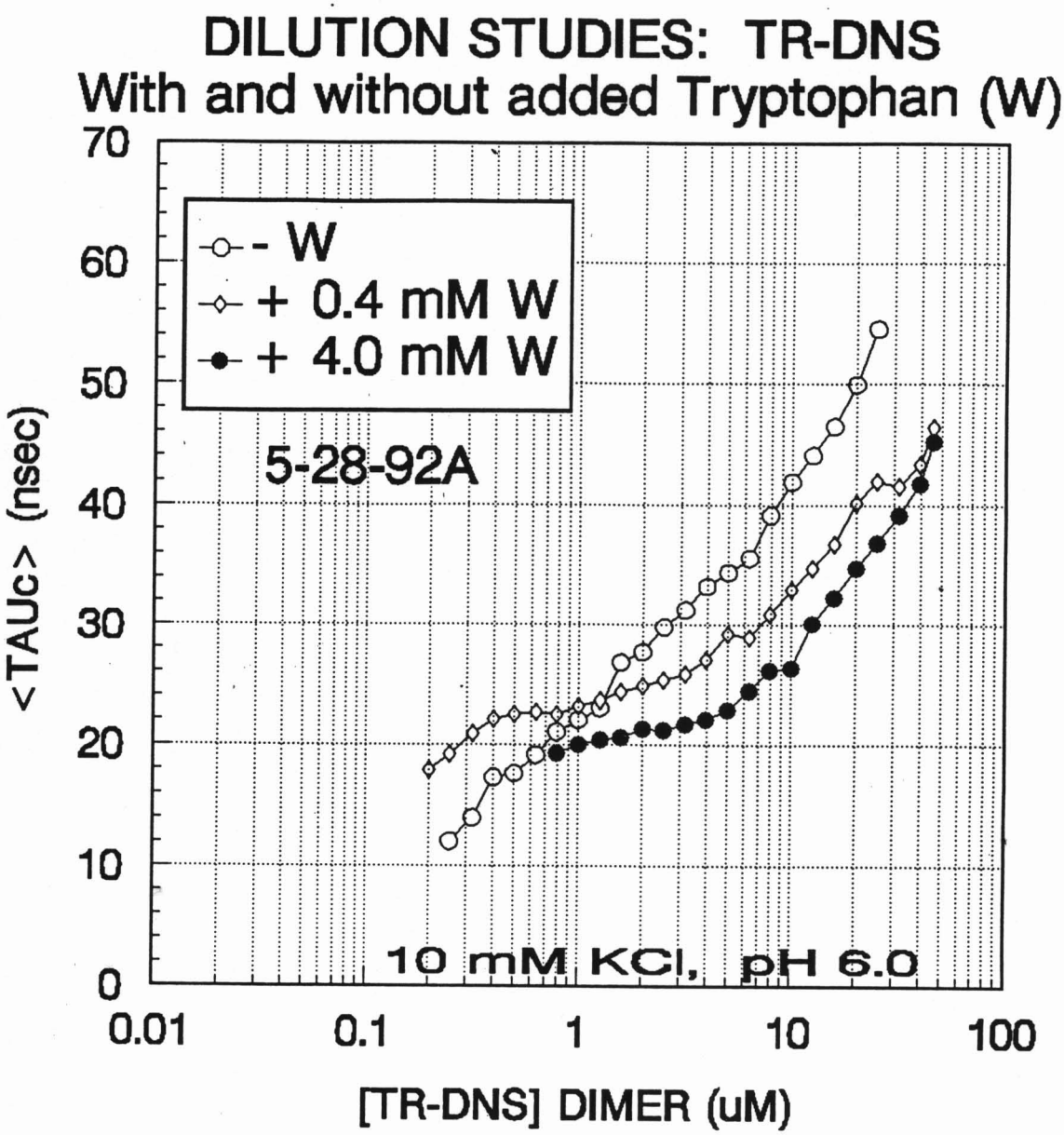
DILUTION STUDIES: TR-DNS
With and without added Tryptophan (W)
- W
+ 0.4 mM W
+ 4.0 mM W
5-28-92A
10 mM KCl, pH 6.0
<TAUc> (nsec)
[TR-DNS] DIMER (uM)
0
10
20
30
40
50
60
70
0.01
0.1
1
10
100

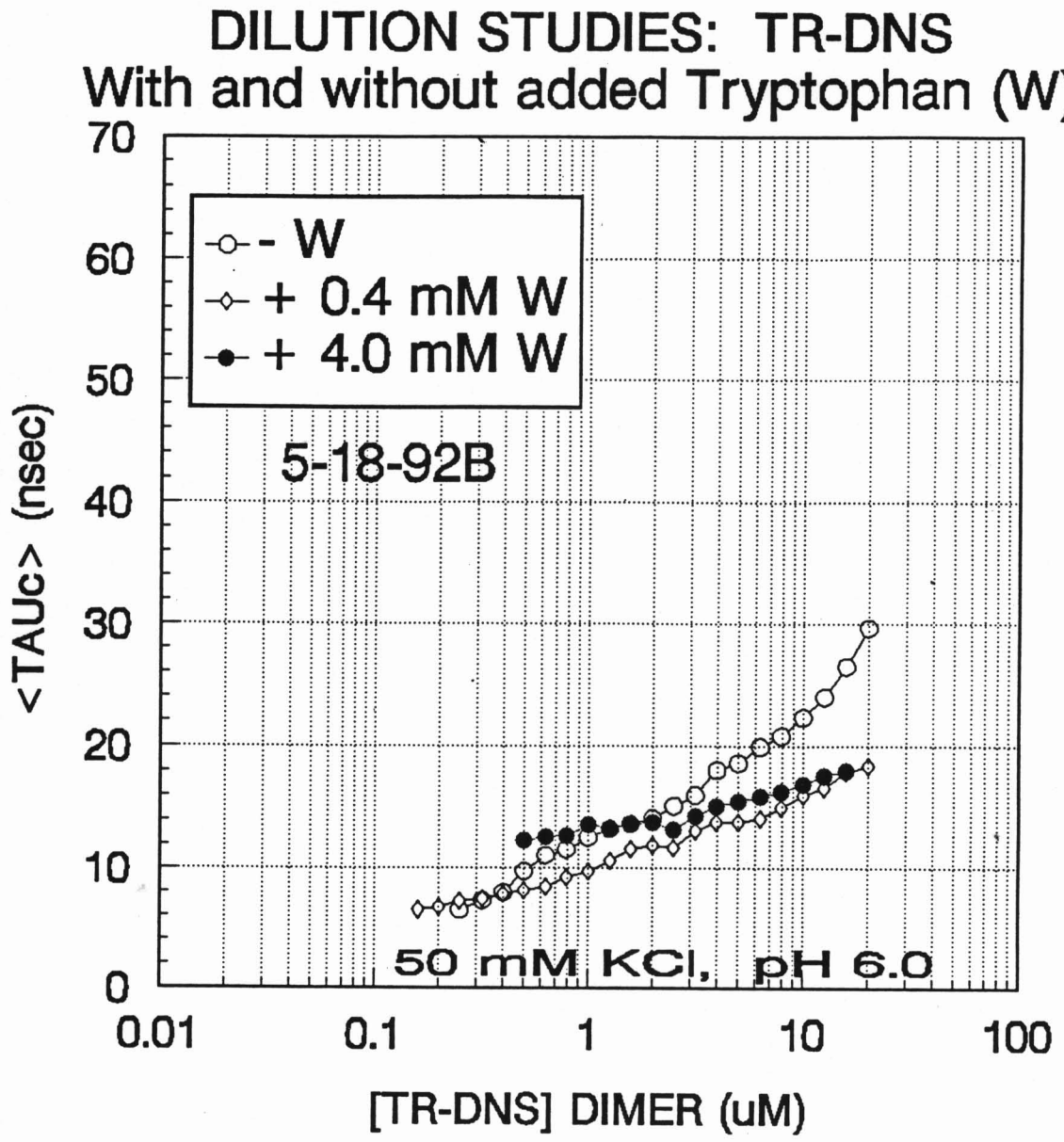
DILUTION STUDIES: TR-DNS
With and without added Tryptophan (W)
- W
+ 0.4 mM W
+ 4.0 mM W
5-18-92B
50 mM KCl, pH 6.0
<TAUc> (nsec)
[TR-DNS] DIMER (uM)
0
10
20
30
40
50
60
70
0.01
0.1
1
10
100

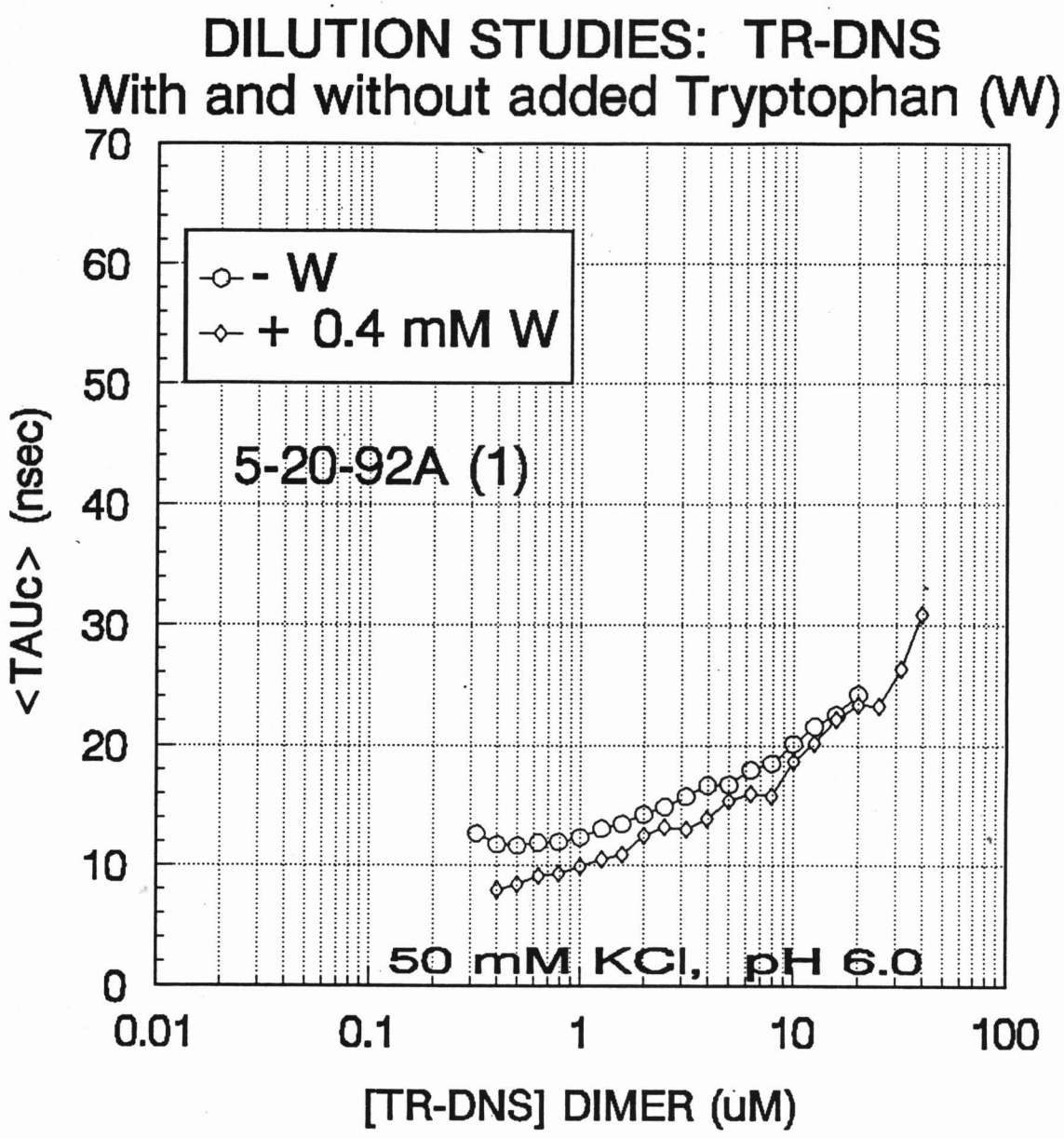
DILUTION STUDIES: TR-DNS
With and without added Tryptophan (W)
- W
+ 0.4 mM W
5-20-92A (1)
50 mM KCl, pH 6.0
<TAUc> (nsec)
[TR-DNS] DIMER (uM)
0
10
20
30
40
50
60
70
0.01
0.1
1
10
100

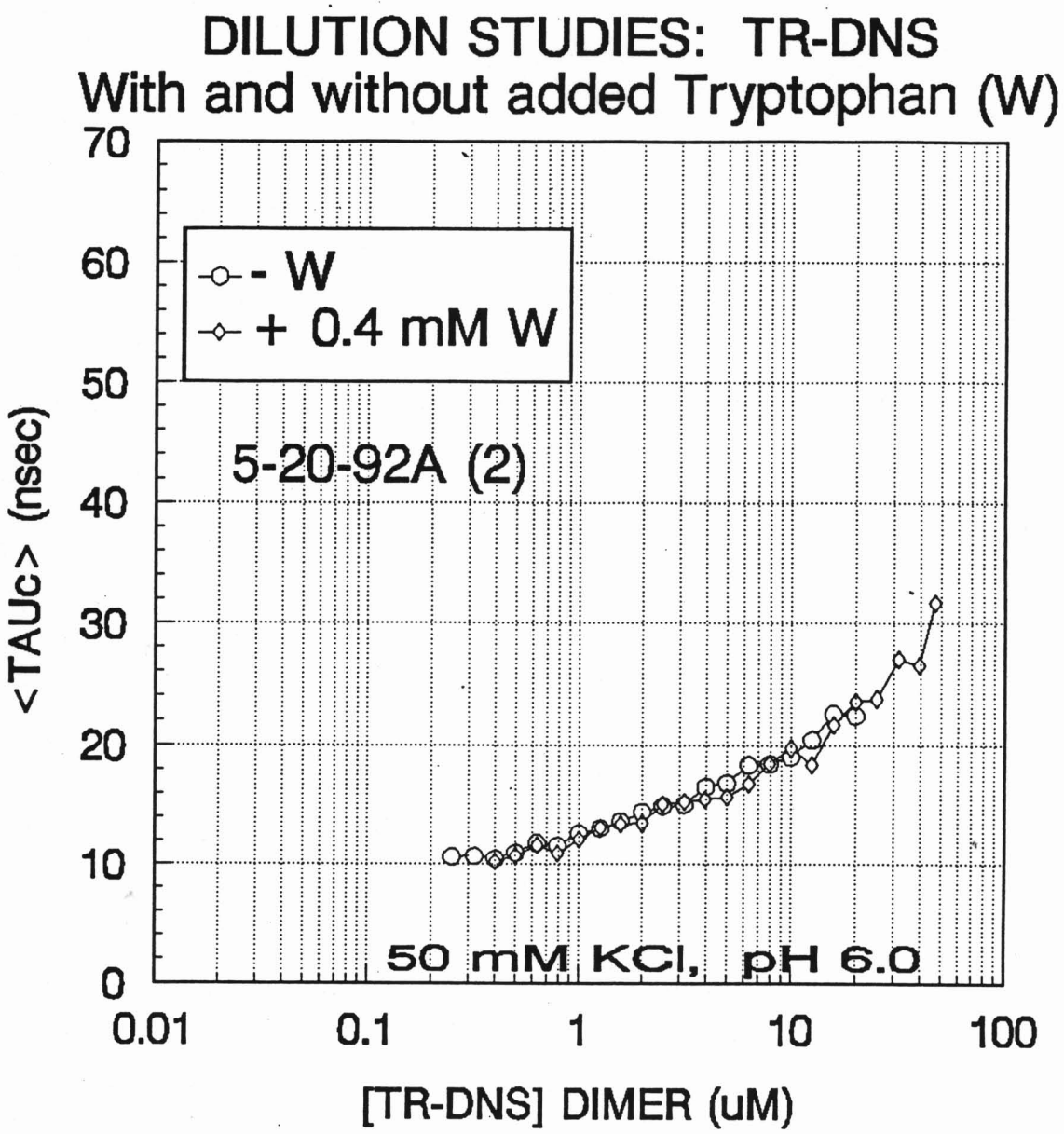
DILUTION STUDIES: TR-DNS
With and without added Tryptophan (W)
- W
+ 0.4 mM W
5-20-92A (2)
50 mM KCl, pH 6.0
<TAUc> (nsec)
[TR-DNS] DIMER (uM)
0
10
20
30
40
50
60
70
0.01
0.1
1
10
100

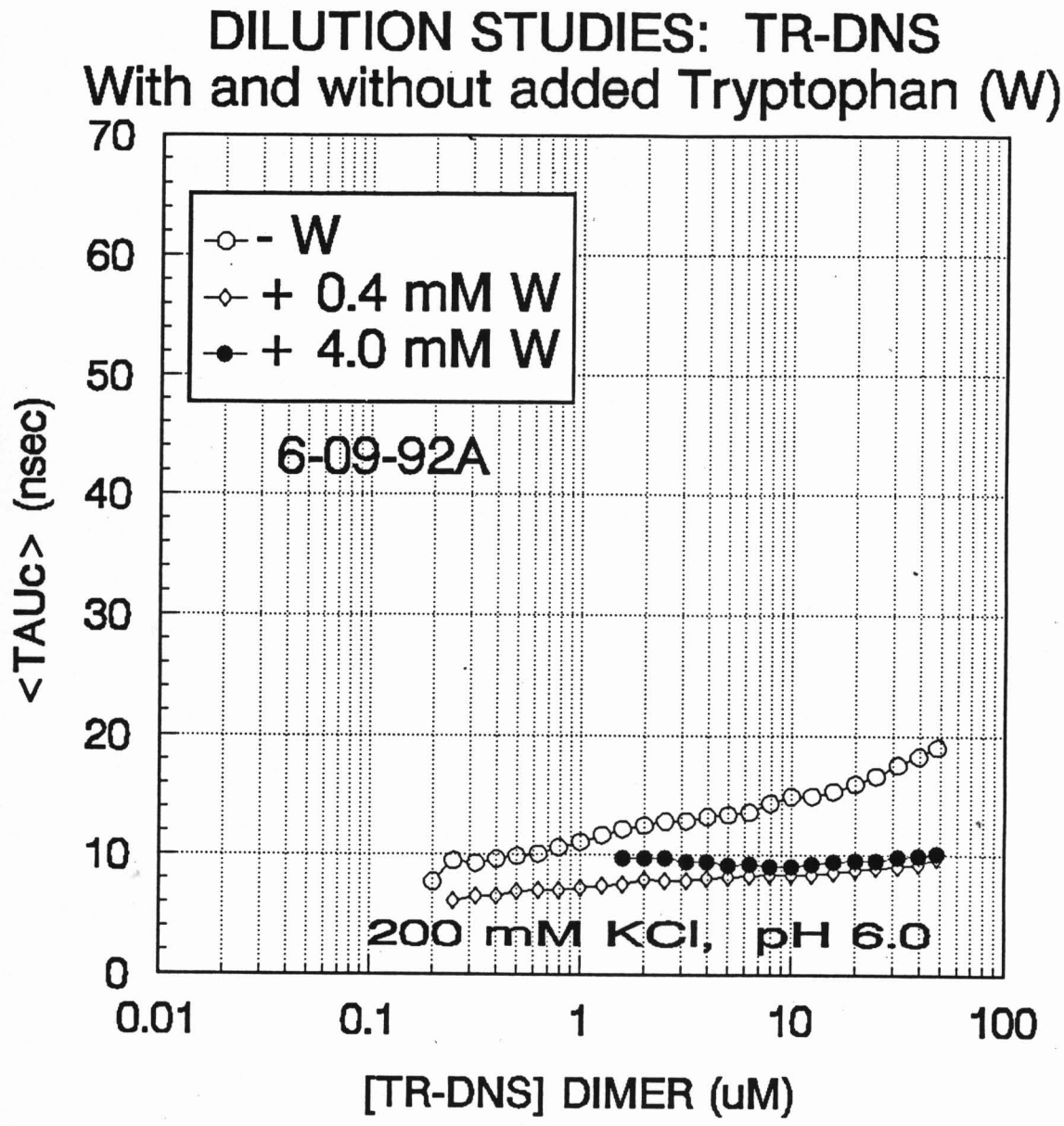
DILUTION STUDIES: TR-DNS
With and without added Tryptophan (W)
- W
+ 0.4 mM W
+ 4.0 mM W
6-09-92A
200 mM KCl, pH 6.0
<TAUc> (nsec)
[TR-DNS] DIMER (uM)
0
10
20
30
40
50
60
70
0.01
0.1
1
10
100

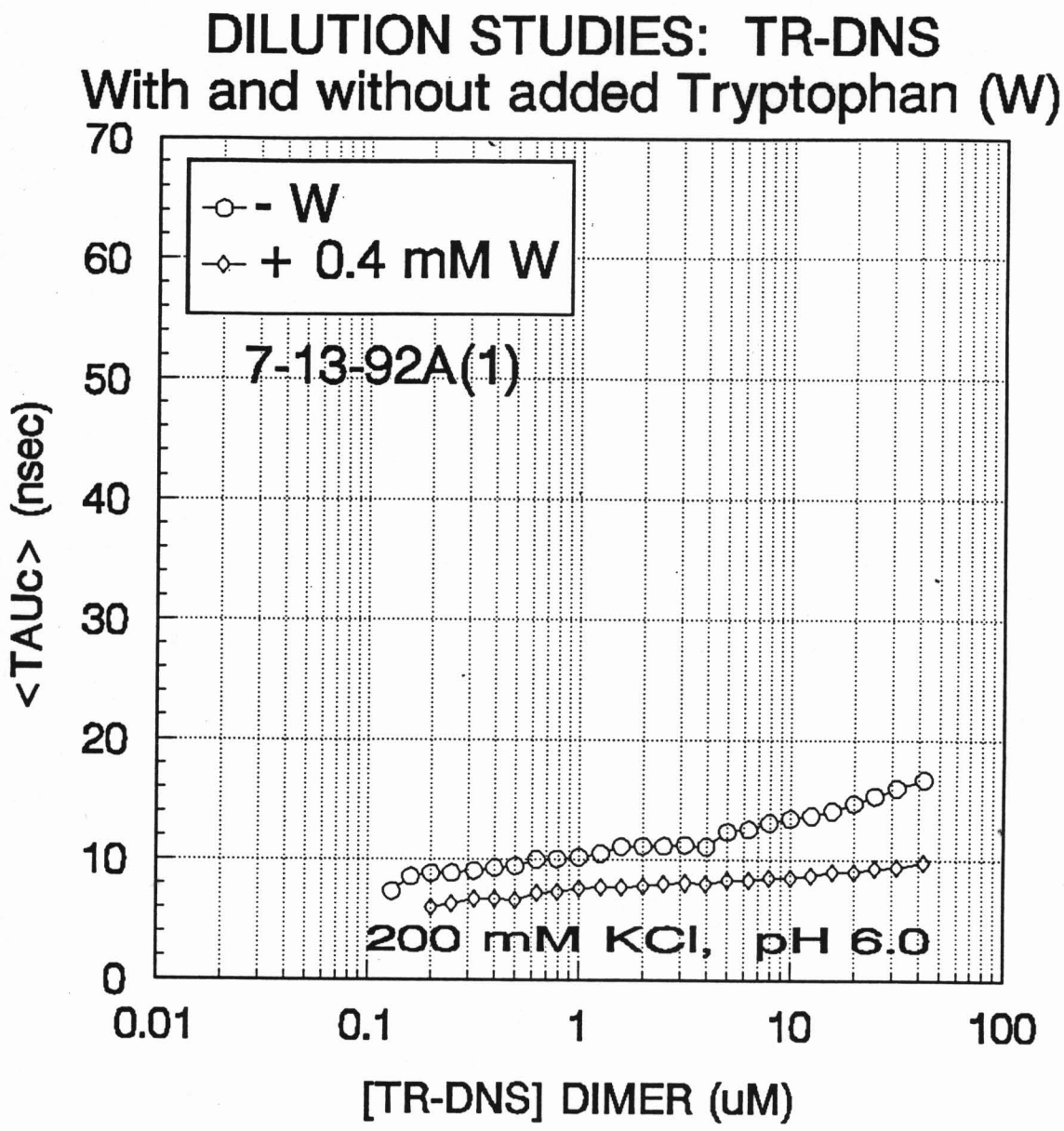
DILUTION STUDIES: TR-DNS
With and without added Tryptophan (W)
- W
+ 0.4 mM W
7-13-92A(1)
200 mM KCl, pH 6.0
<TAUc> (nsec)
[TR-DNS] DIMER (uM)
0
10
20
30
40
50
60
70
0.01
0.1
1
10
100

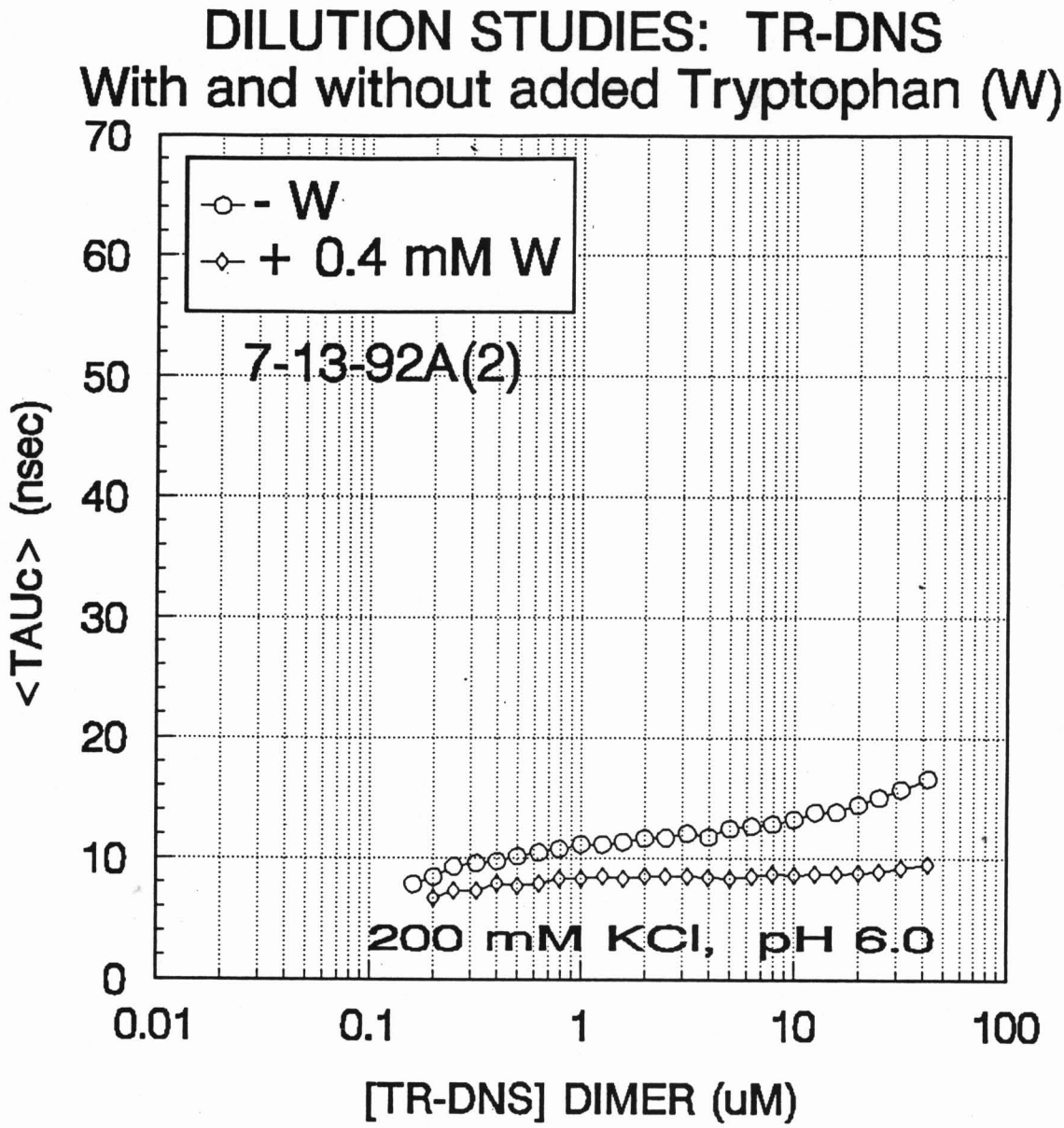
DILUTION STUDIES: TR-DNS
With and without added Tryptophan (W)
- W
+ 0.4 mM W
7-13-92A(2)
200 mM KCl, pH 6.0
<TAUc> (nsec)
[TR-DNS] DIMER (uM)
0
10
20
30
40
50
60
70
0.01
0.1
1
10
100

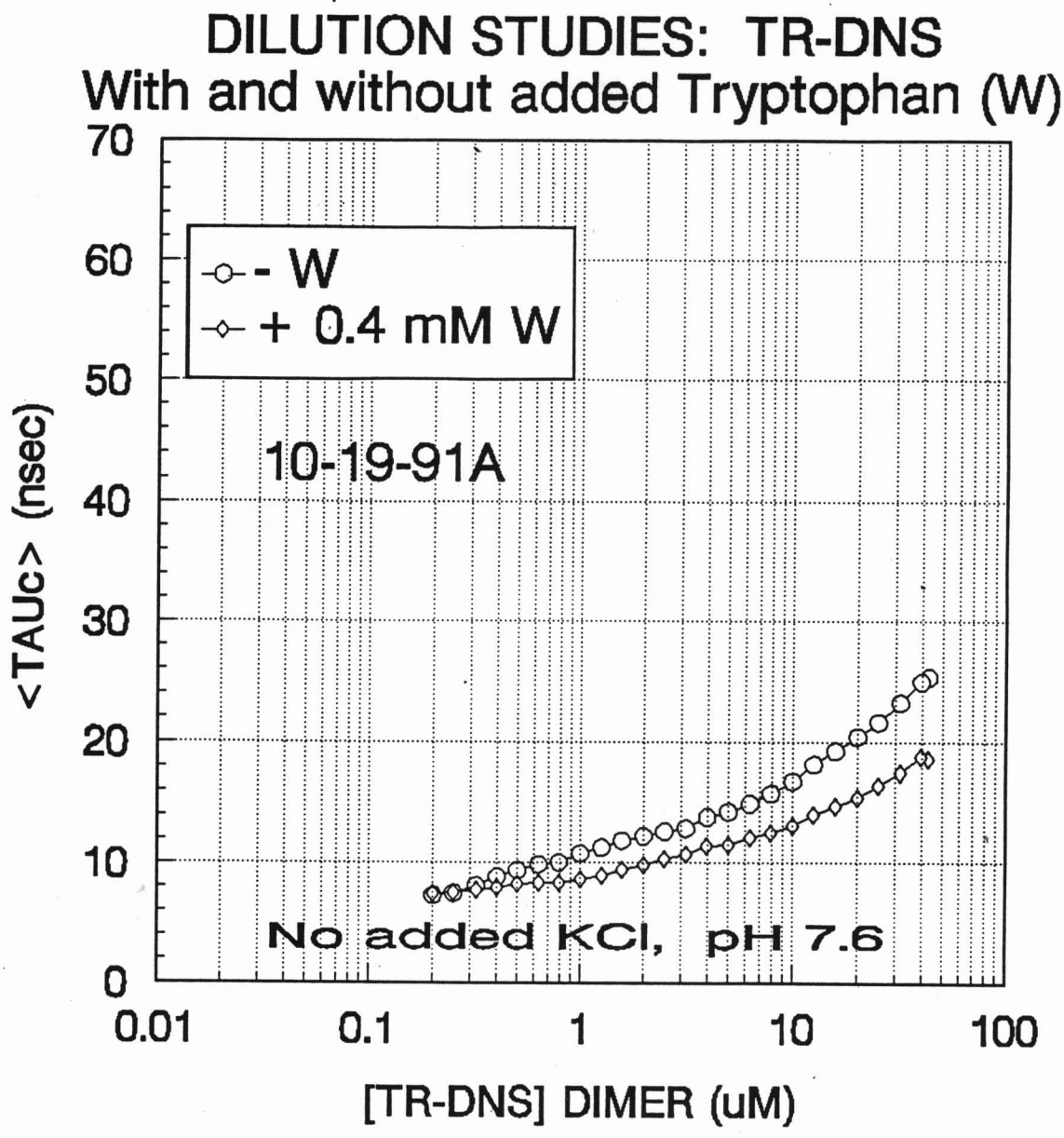
DILUTION STUDIES: TR-DNS
With and without added Tryptophan (W)
- W
+ 0.4 mM W
10-19-91A
No added KCl, pH 7.6
<TAUc> (nsec)
[TR-DNS] DIMER (uM)
0
10
20
30
40
50
60
70
0.01
0.1
1
10
100

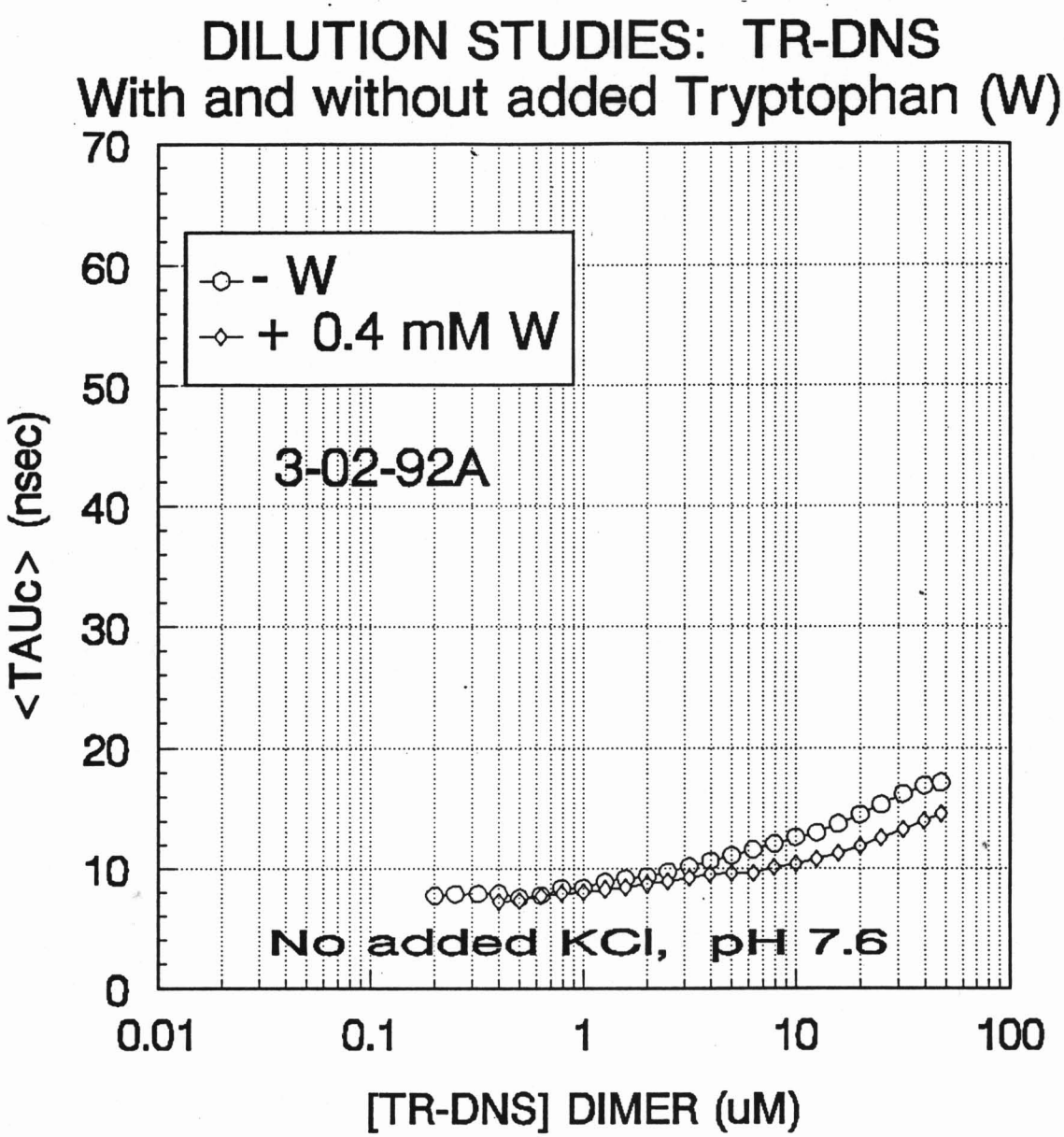
DILUTION STUDIES: TR-DNS
With and without added Tryptophan (W)
- W
+ 0.4 mM W
3-02-92A
No added KCl, pH 7.6
<TAUc> (nsec)
[TR-DNS] DIMER (uM)
0
10
20
30
40
50
60
70
0.01
0.1
1
10
100

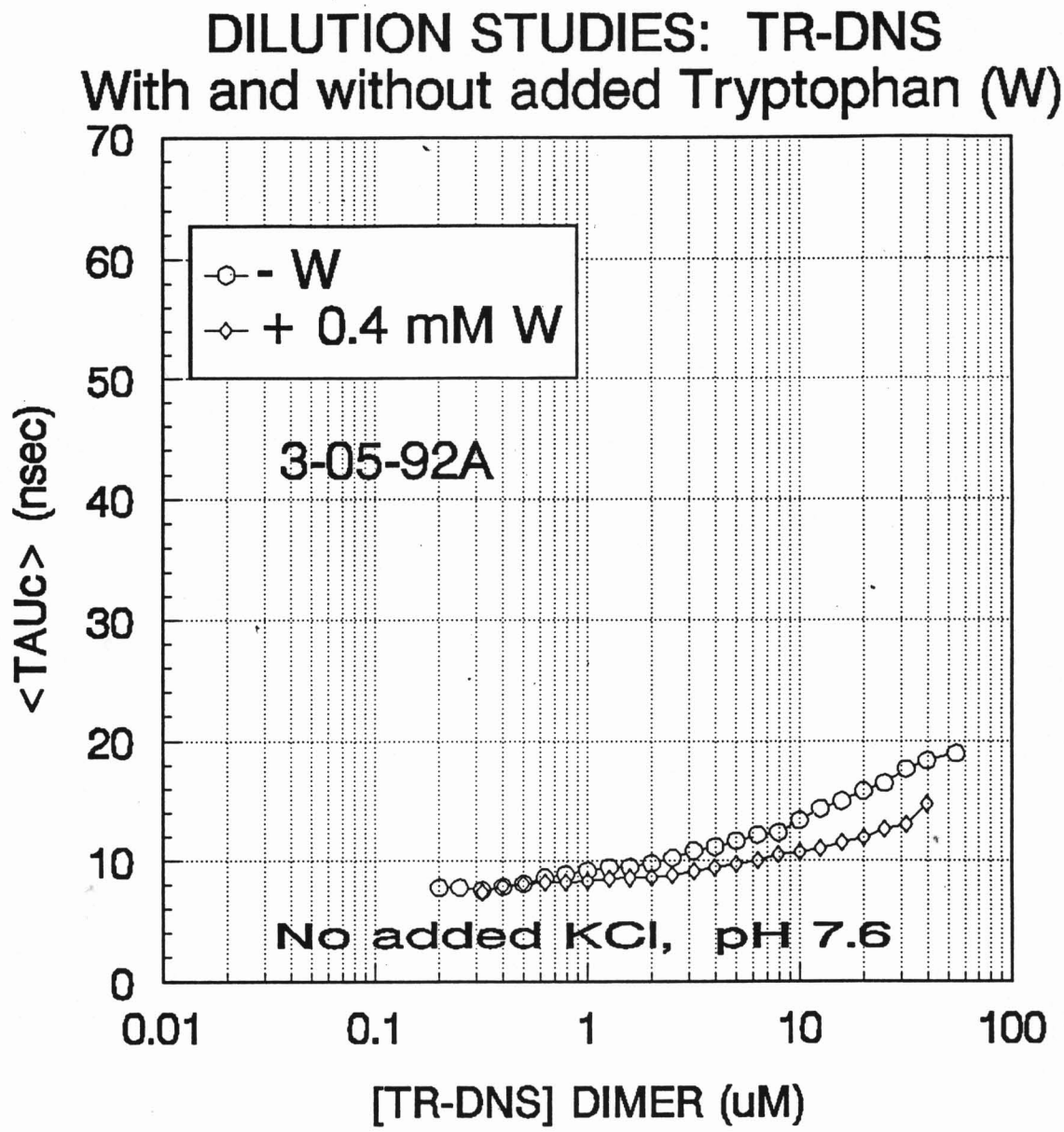
DILUTION STUDIES: TR-DNS
With and without added Tryptophan (W)
- W
+ 0.4 mM W
3-05-92A
No added KCl, pH 7.6
<TAUc> (nsec)
[TR-DNS] DIMER (uM)
0
10
20
30
40
50
60
70
0.01
0.1
1
10
100

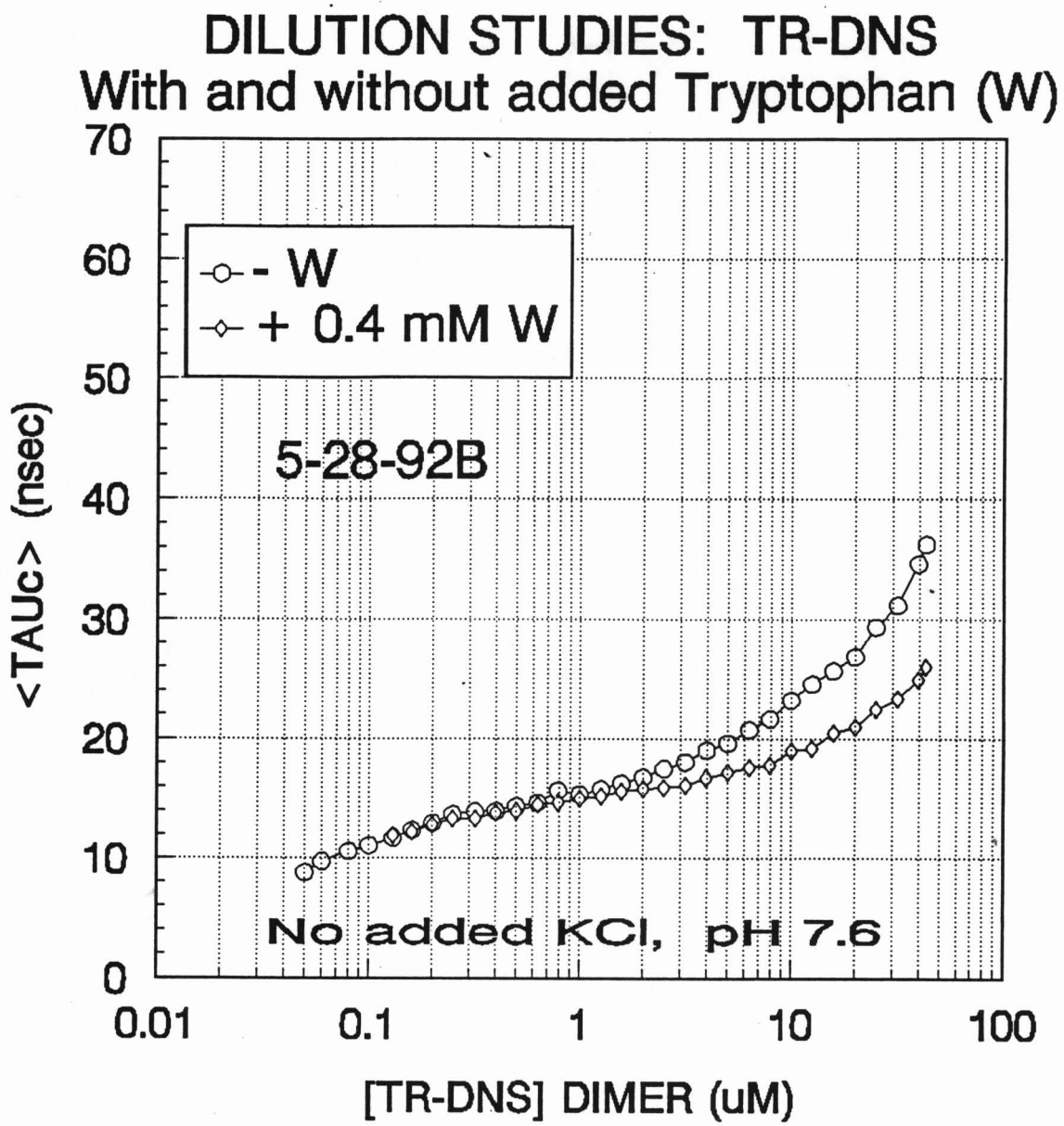
DILUTION STUDIES: TR-DNS
With and without added Tryptophan (W)
- W
+ 0.4 mM W
5-28-92B
No added KCl, pH 7.6
<TAUc> (nsec)
[TR-DNS] DIMER (uM)
0
10
20
30
40
50
60
70
0.01
0.1
1
10
100

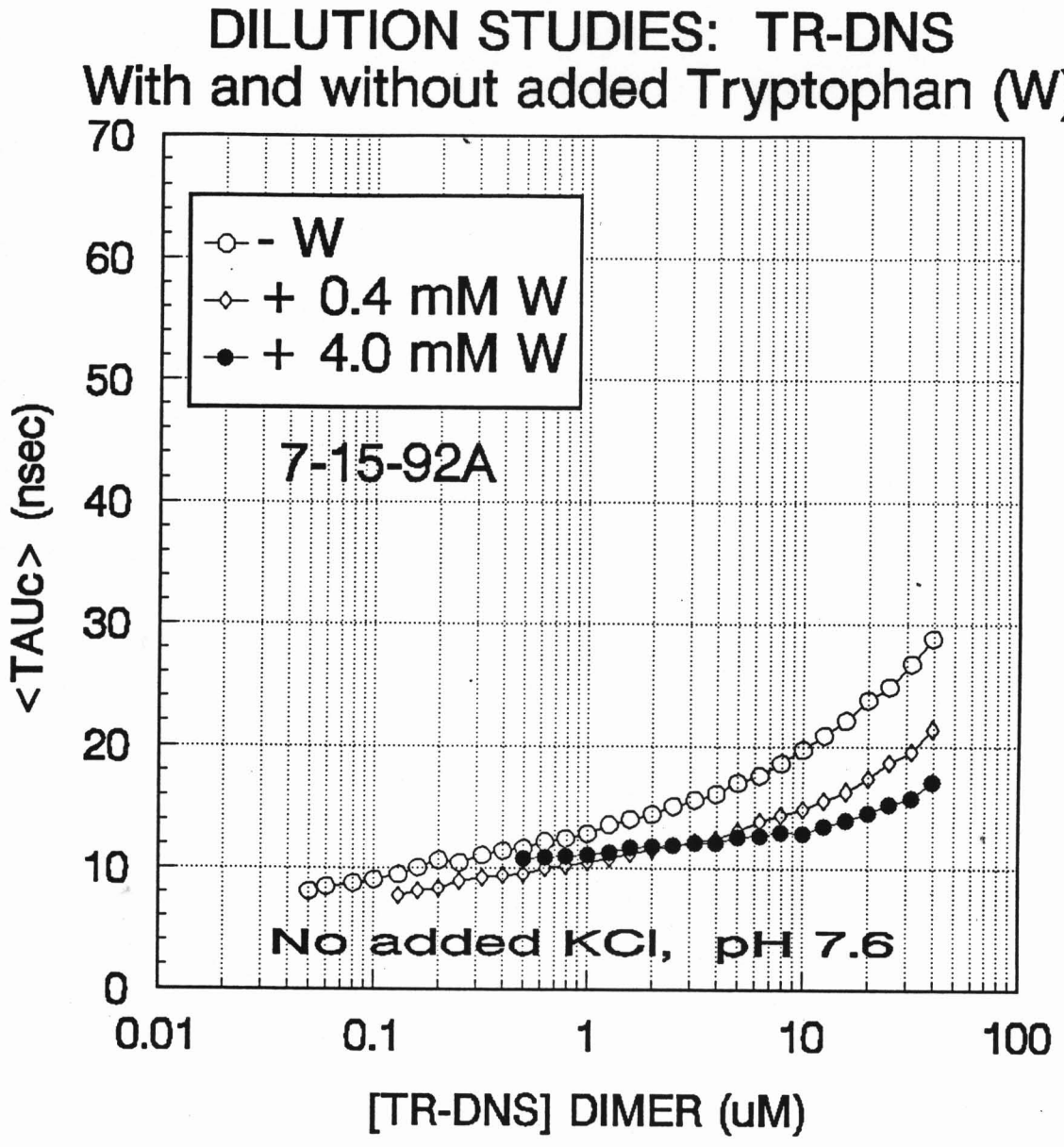
DILUTION STUDIES: TR-DNS
With and without added Tryptophan (W)
- W
+ 0.4 mM W
+ 4.0 mM W
7-15-92A
No added KCl, pH 7.6
<TAUc> (nsec)
[TR-DNS] DIMER (uM)
0
10
20
30
40
50
60
70
0.01
0.1
1
10
100

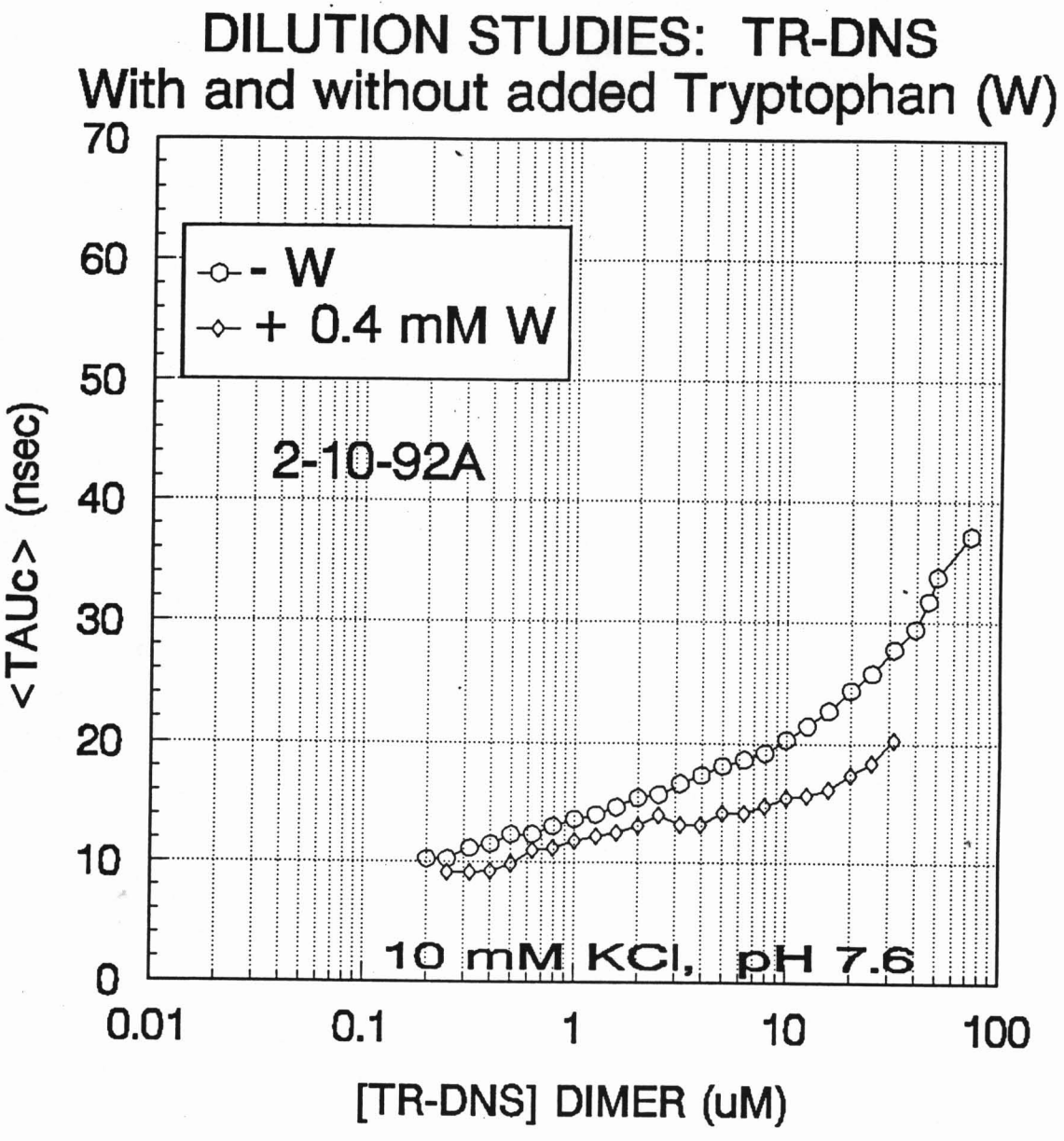
DILUTION STUDIES: TR-DNS
With and without added Tryptophan (W)
- W
+ 0.4 mM W
2-10-92A
10 mM KCl, pH 7.6
<TAUc> (nsec)
[TR-DNS] DIMER (uM)
0
10
20
30
40
50
60
70
0.01
0.1
1
10
100

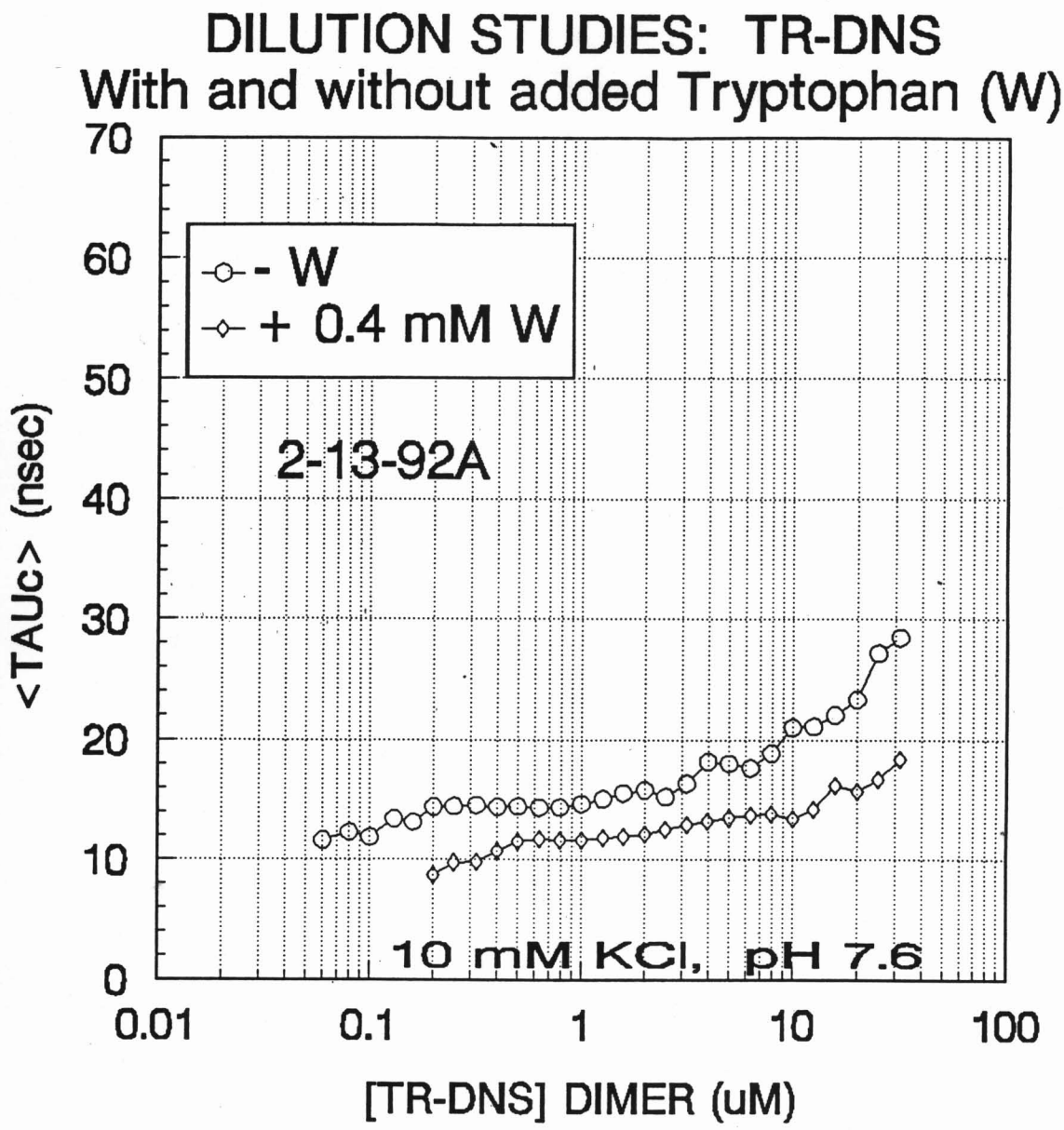
DILUTION STUDIES: TR-DNS
With and without added Tryptophan (W)
- W
+ 0.4 mM W
2-13-92A
10 mM KCl, pH 7.6
<TAUc> (nsec)
[TR-DNS] DIMER (uM)
0
10
20
30
40
50
60
70
0.01
0.1
1
10
100

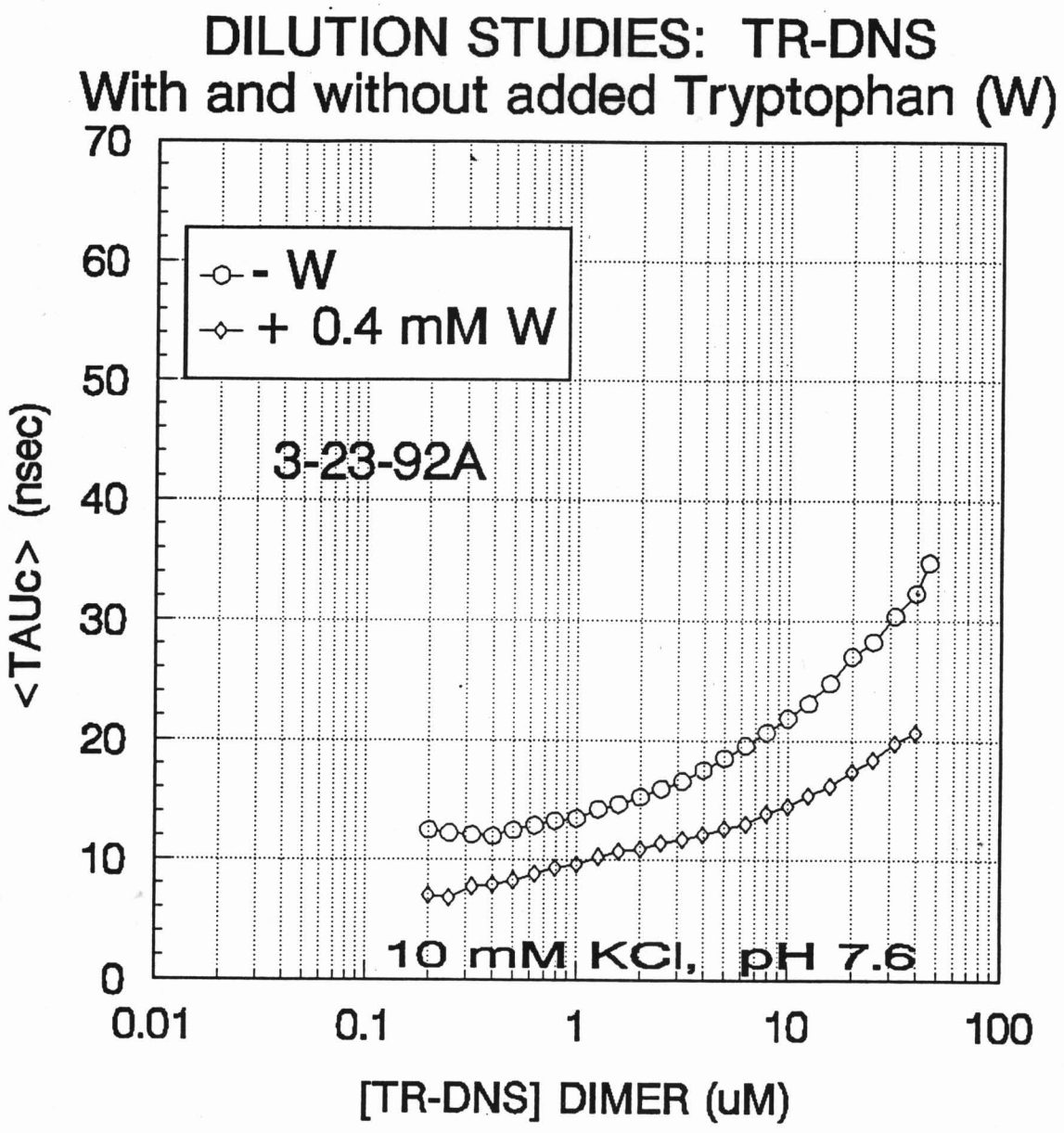
DILUTION STUDIES: TR-DNS
With and without added Tryptophan (W)
- W
+ 0.4 mM W
3-23-92A
10 mM KCl, pH 7.6
<TAUc> (nsec)
[TR-DNS] DIMER (uM)
0
10
20
30
40
50
60
70
0.01
0.1
1
10
100

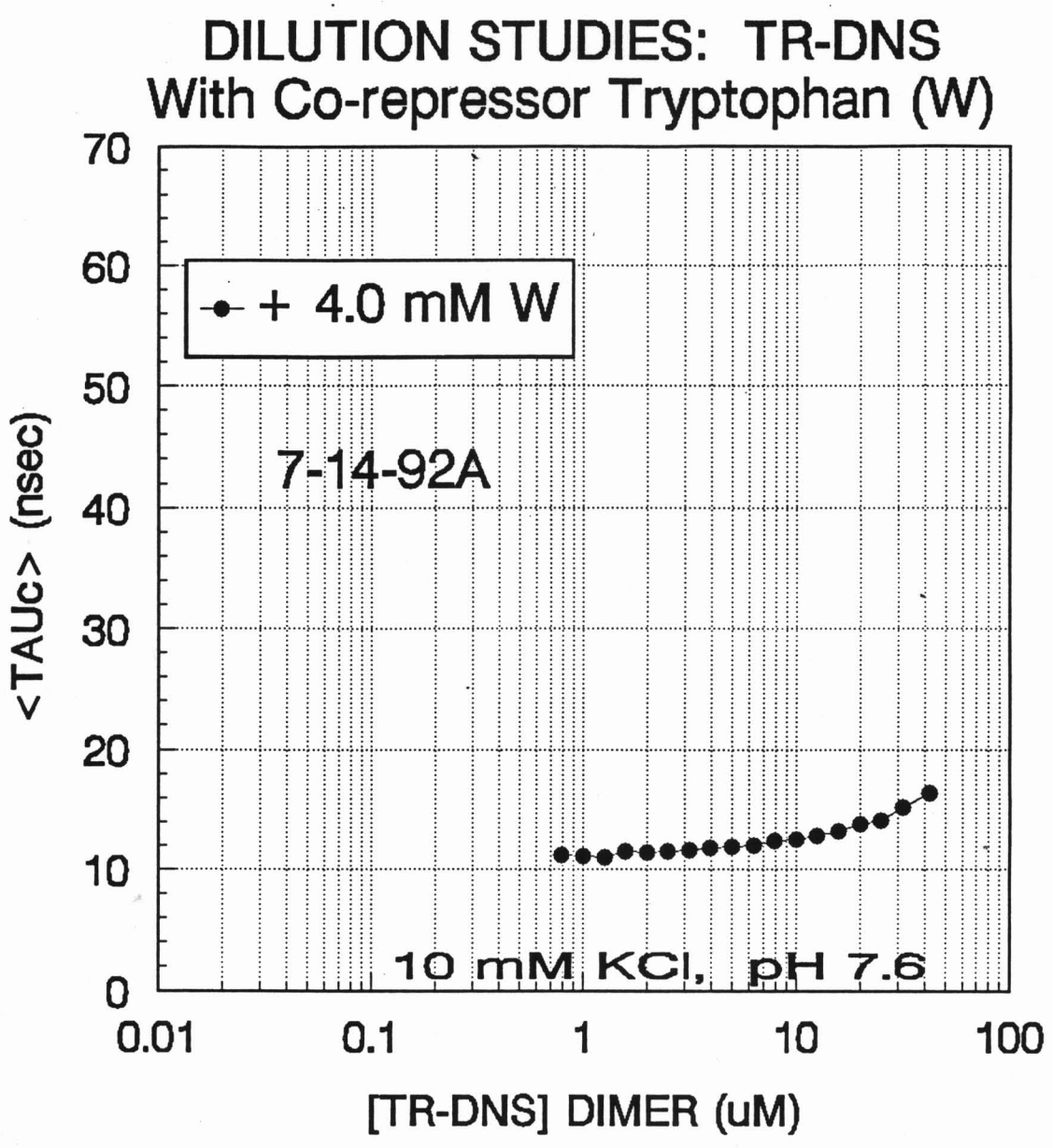
DILUTION STUDIES: TR-DNS
With Co-repressor Tryptophan (W)
+ 4.0 mM W
7-14-92A
10 mM KCl, pH 7.6
<TAUc> (nsec)
[TR-DNS] DIMER (uM)
0
10
20
30
40
50
60
70
0.01
0.1
1
10
100

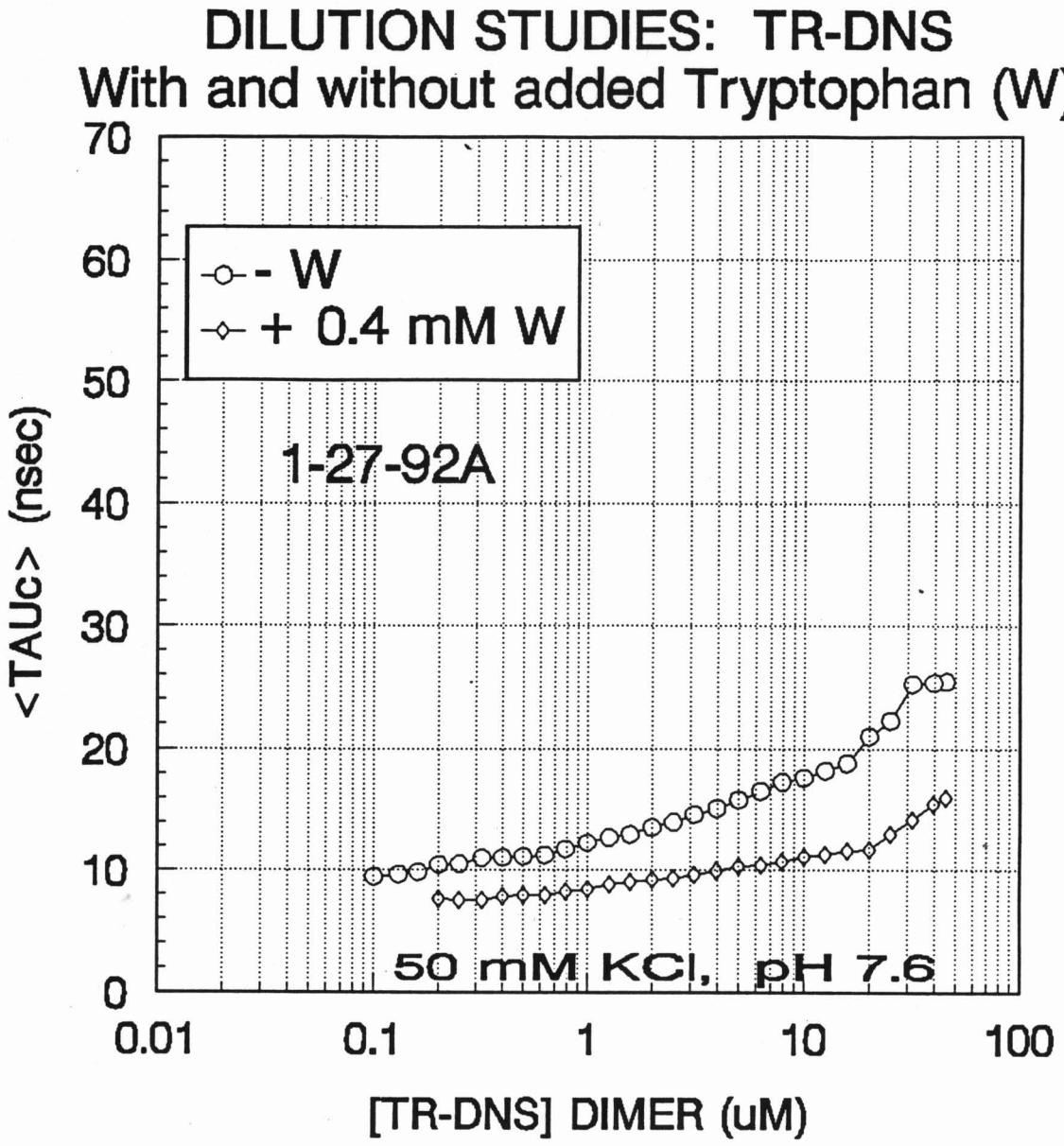
DILUTION STUDIES: TR-DNS
With and without added Tryptophan (W)
- W
+ 0.4 mM W
1-27-92A
50 mM KCl, pH 7.6
<TAUc> (nsec)
[TR-DNS] DIMER (uM)
0
10
20
30
40
50
60
70
0.01
0.1
1
10
100

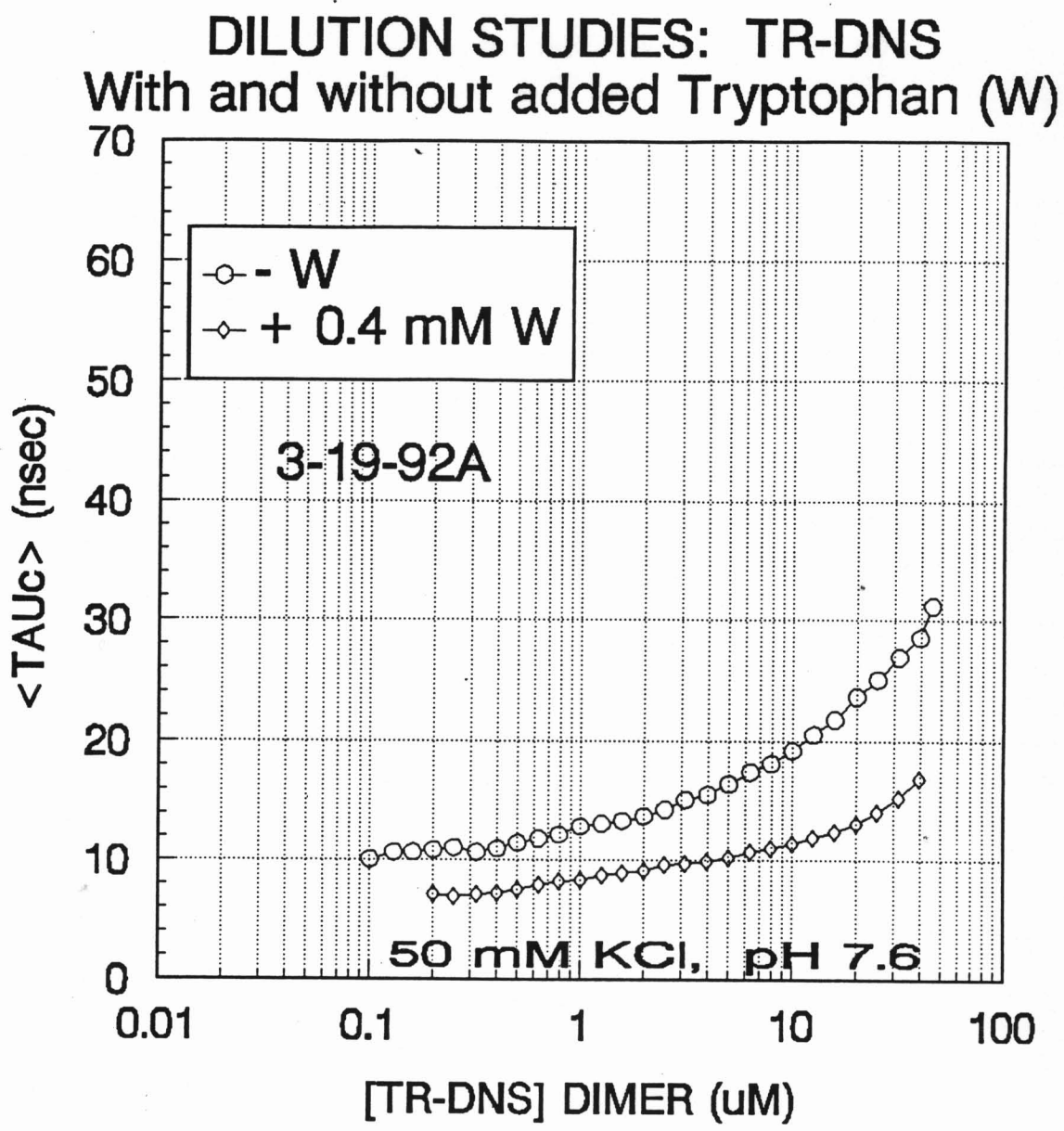
DILUTION STUDIES: TR-DNS
With and without added Tryptophan (W)
- W
+ 0.4 mM W
3-19-92A
50 mM KCl, pH 7.6
<TAUc> (nsec)
[TR-DNS] DIMER (uM)
0
10
20
30
40
50
60
70
0.01
0.1
1
10
100

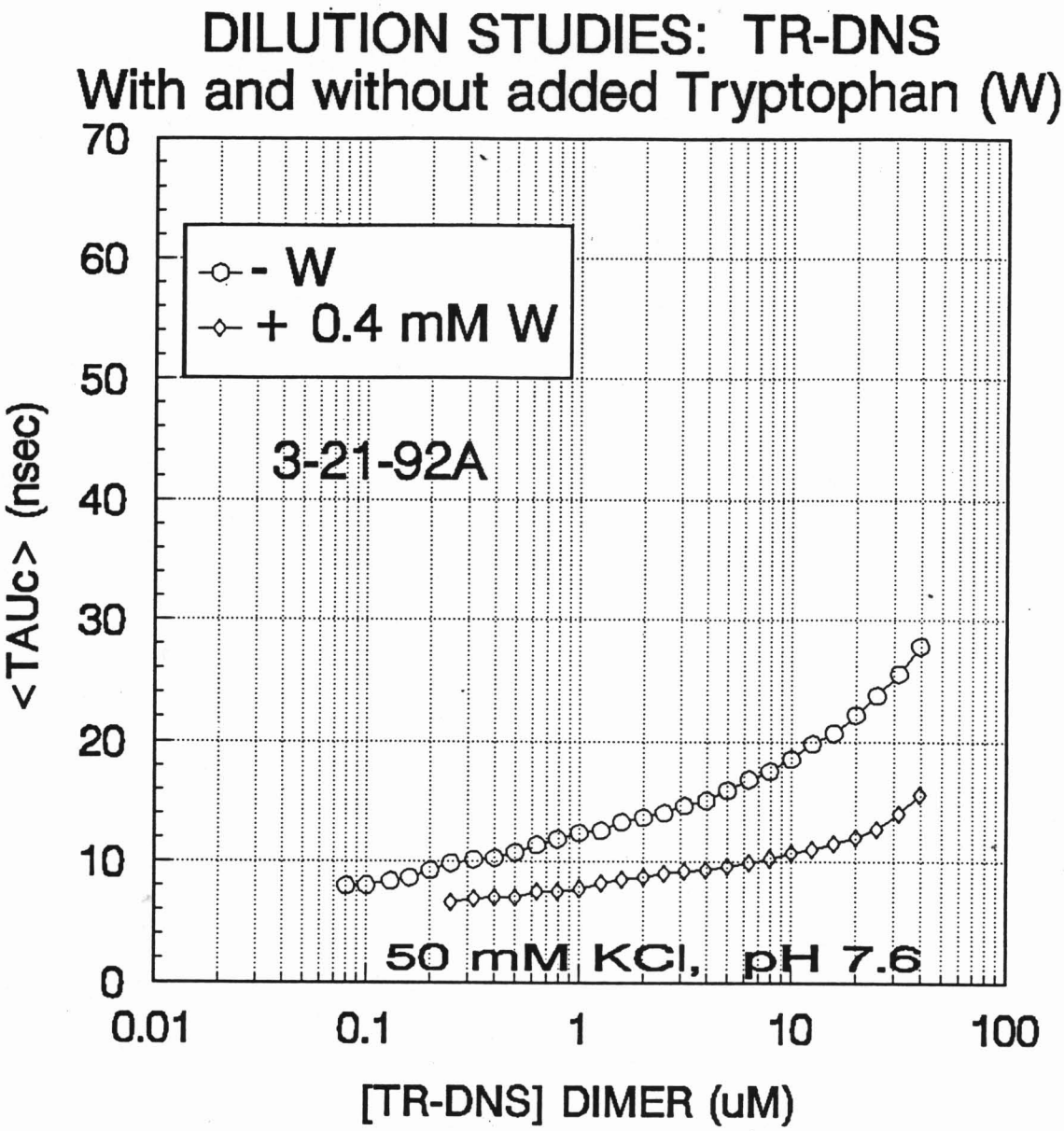
DILUTION STUDIES: TR-DNS
With and without added Tryptophan (W)
- W
+ 0.4 mM W
3-21-92A
50 mM KCl, pH 7.6
<TAUc> (nsec)
[TR-DNS] DIMER (uM)
0
10
20
30
40
50
60
70
0.01
0.1
1
10
100

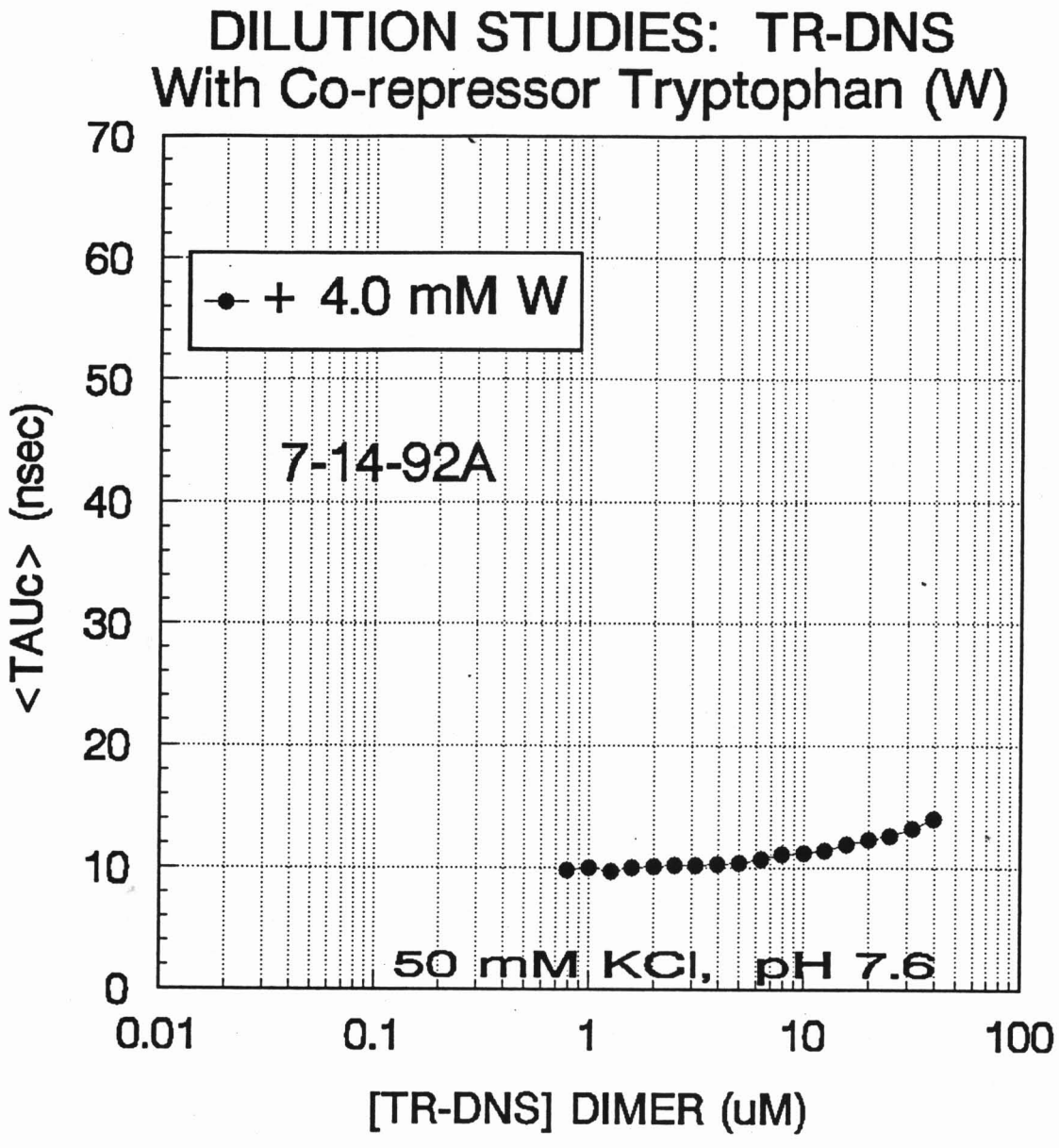
DILUTION STUDIES: TR-DNS
With Co-repressor Tryptophan (W)
+ 4.0 mM W
7-14-92A
50 mM KCl, pH 7.6
<TAUc> (nsec)
[TR-DNS] DIMER (uM)
0
10
20
30
40
50
60
70
0.01
0.1
1
10
100

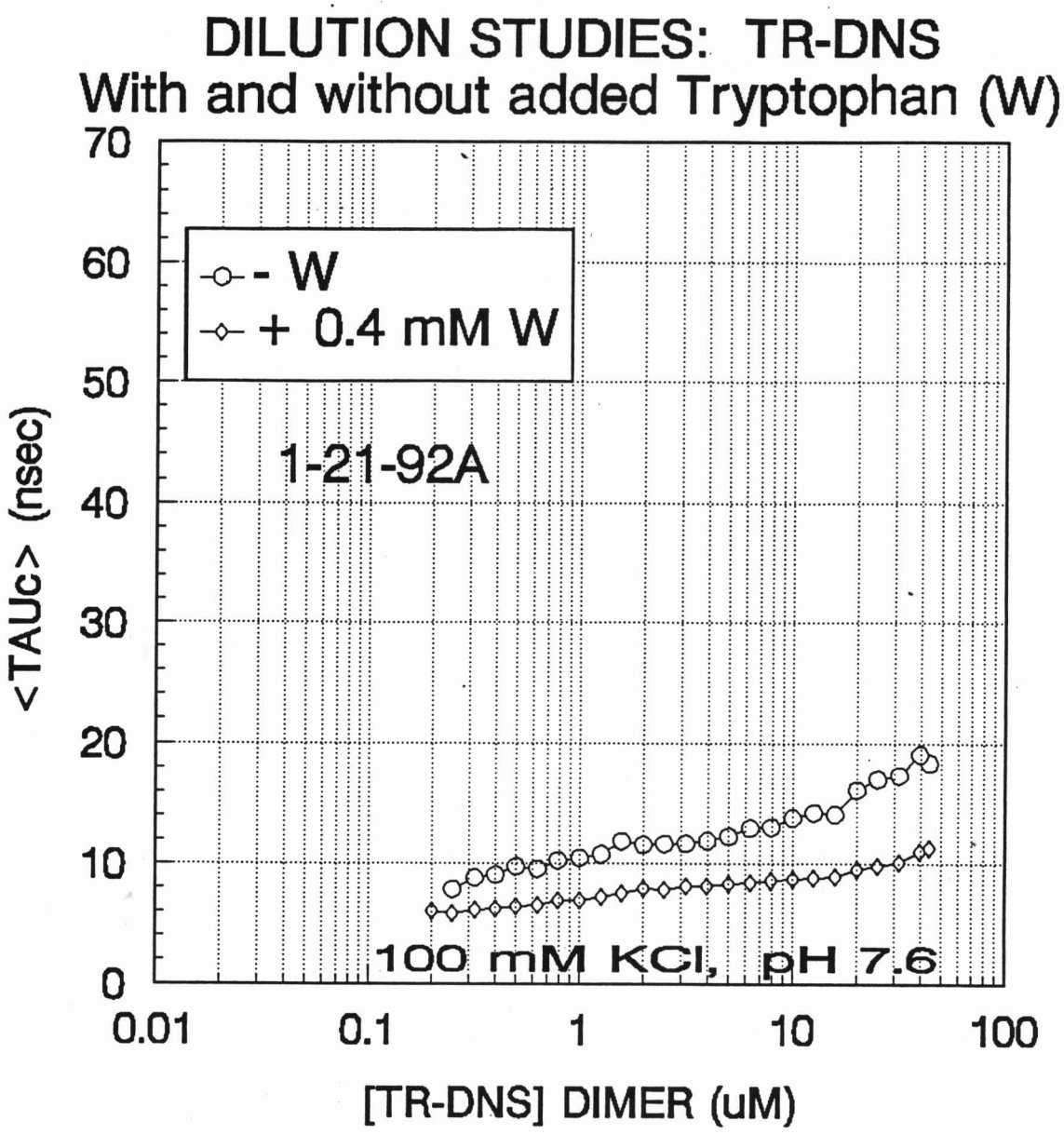
DILUTION STUDIES: TR-DNS
With and without added Tryptophan (W)
- W
+ 0.4 mM W
1-21-92A
100 mM KCl, pH 7.6
<TAUc> (nsec)
[TR-DNS] DIMER (uM)
0
10
20
30
40
50
60
70
0.01
0.1
1
10
100

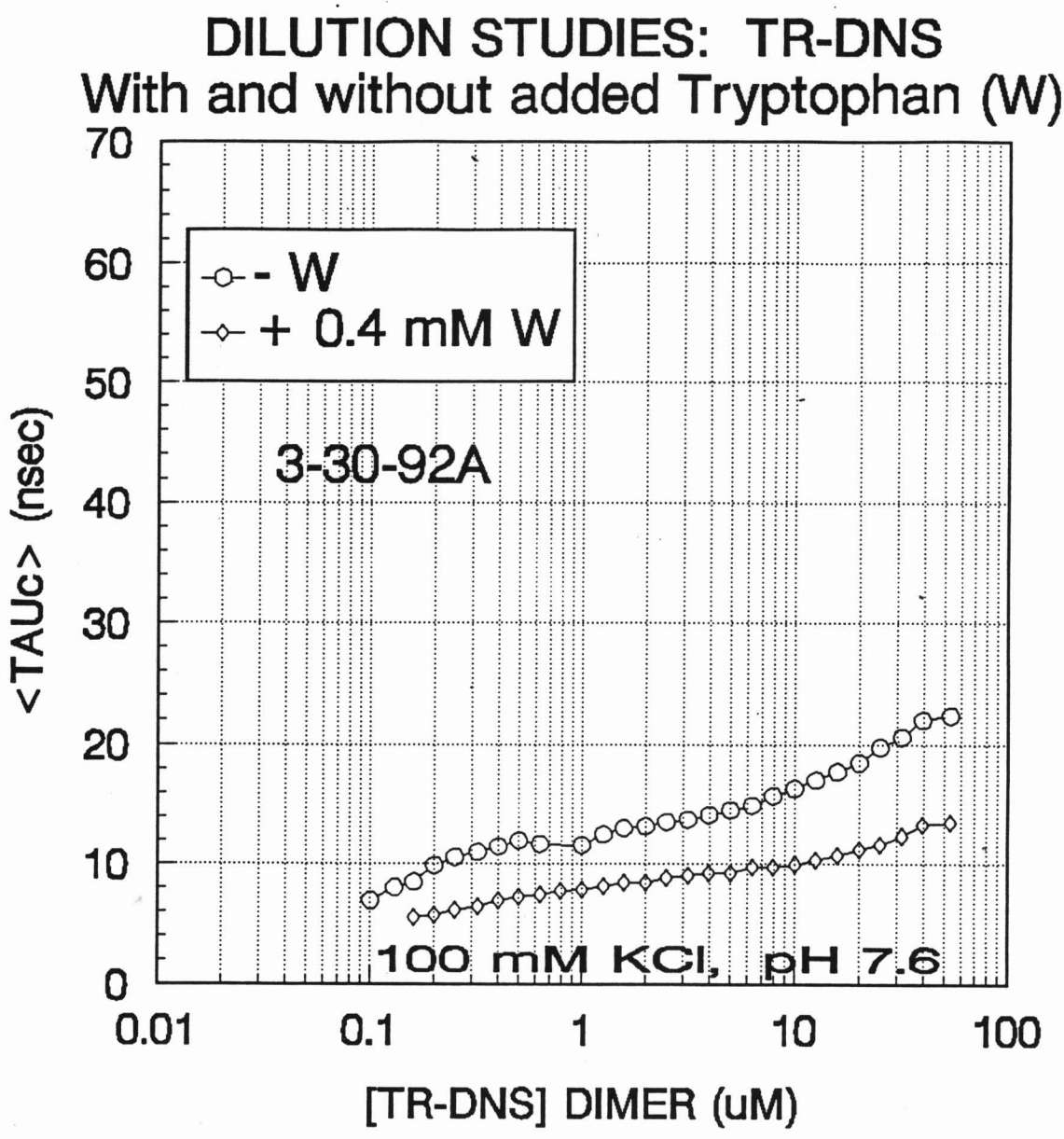
DILUTION STUDIES: TR-DNS
With and without added Tryptophan (W)
- W
+ 0.4 mM W
3-30-92A
100 mM KCl, pH 7.6
<TAUc> (nsec)
[TR-DNS] DIMER (uM)
0
10
20
30
40
50
60
70
0.01
0.1
1
10
100

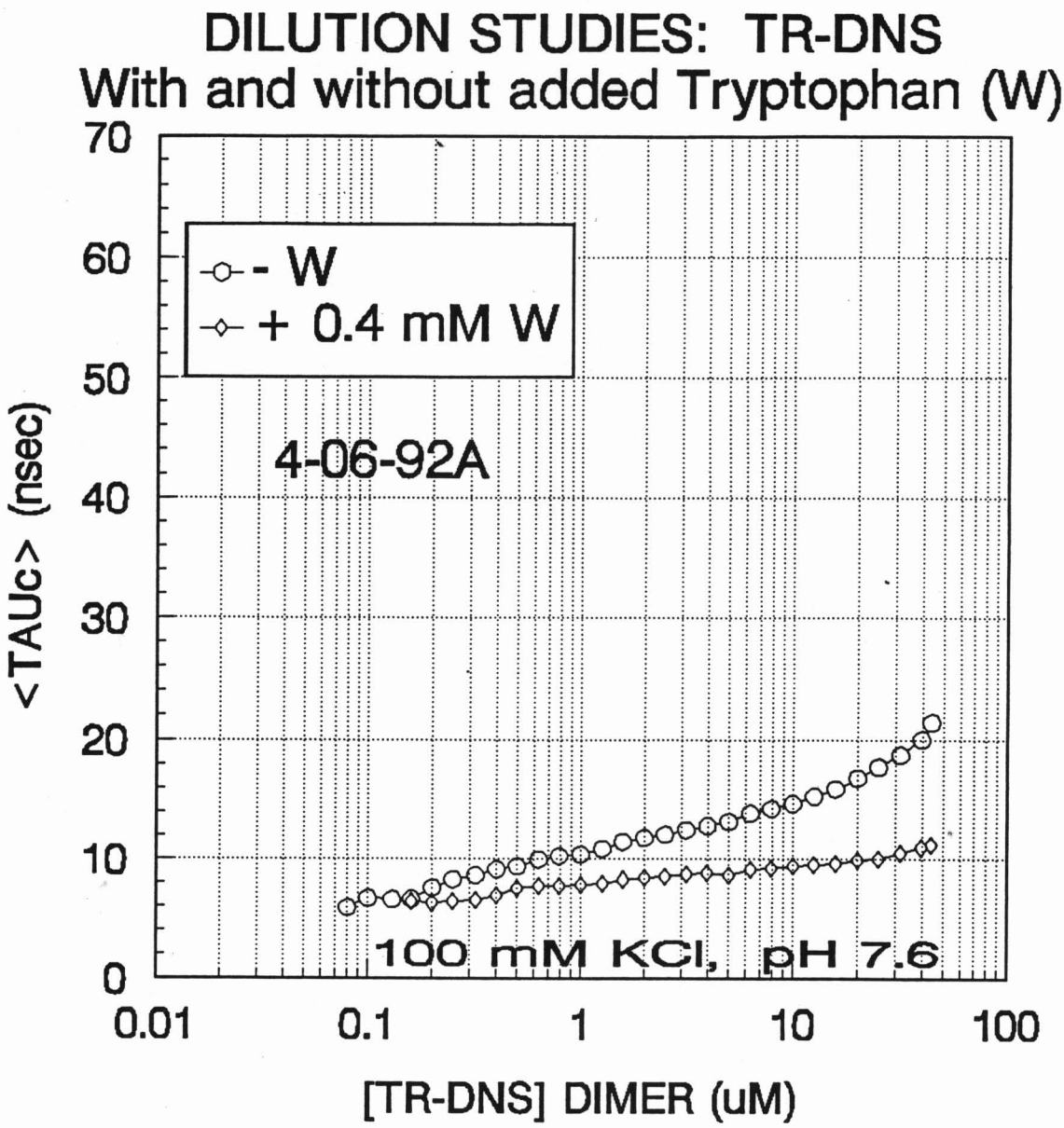
DILUTION STUDIES: TR-DNS
With and without added Tryptophan (W)
- W
+ 0.4 mM W
4-06-92A
100 mM KCl, pH 7.6
<TAUc> (nsec)
[TR-DNS] DIMER (uM)
0
10
20
30
40
50
60
70
0.01
0.1
1
10
100

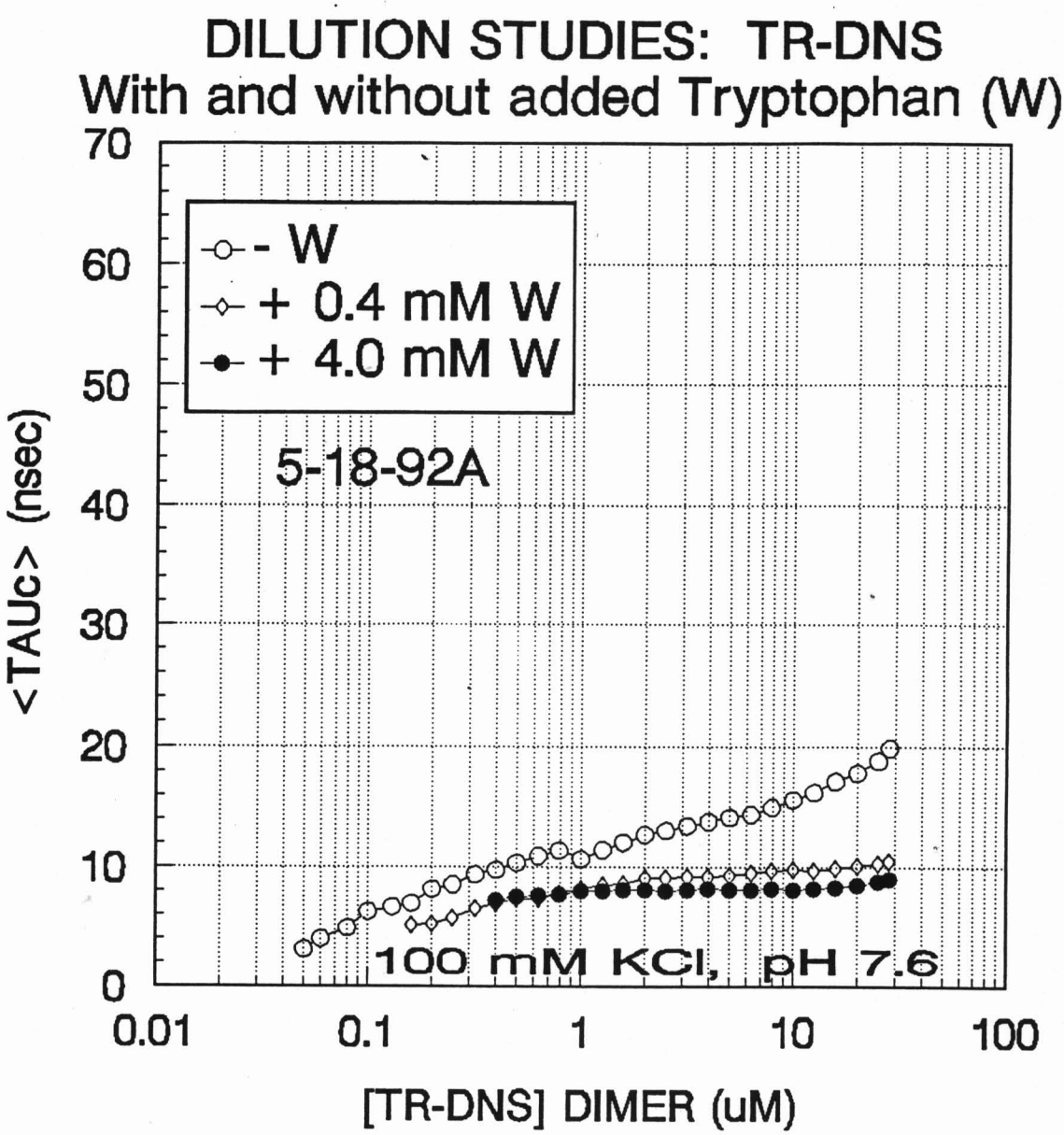
DILUTION STUDIES: TR-DNS
With and without added Tryptophan (W)
- W
+ 0.4 mM W
+ 4.0 mM W
5-18-92A
100 mM KCl, pH 7.6
<TAUc> (nsec)
[TR-DNS] DIMER (uM)
0
10
20
30
40
50
60
70
0.01
0.1
1
10
100

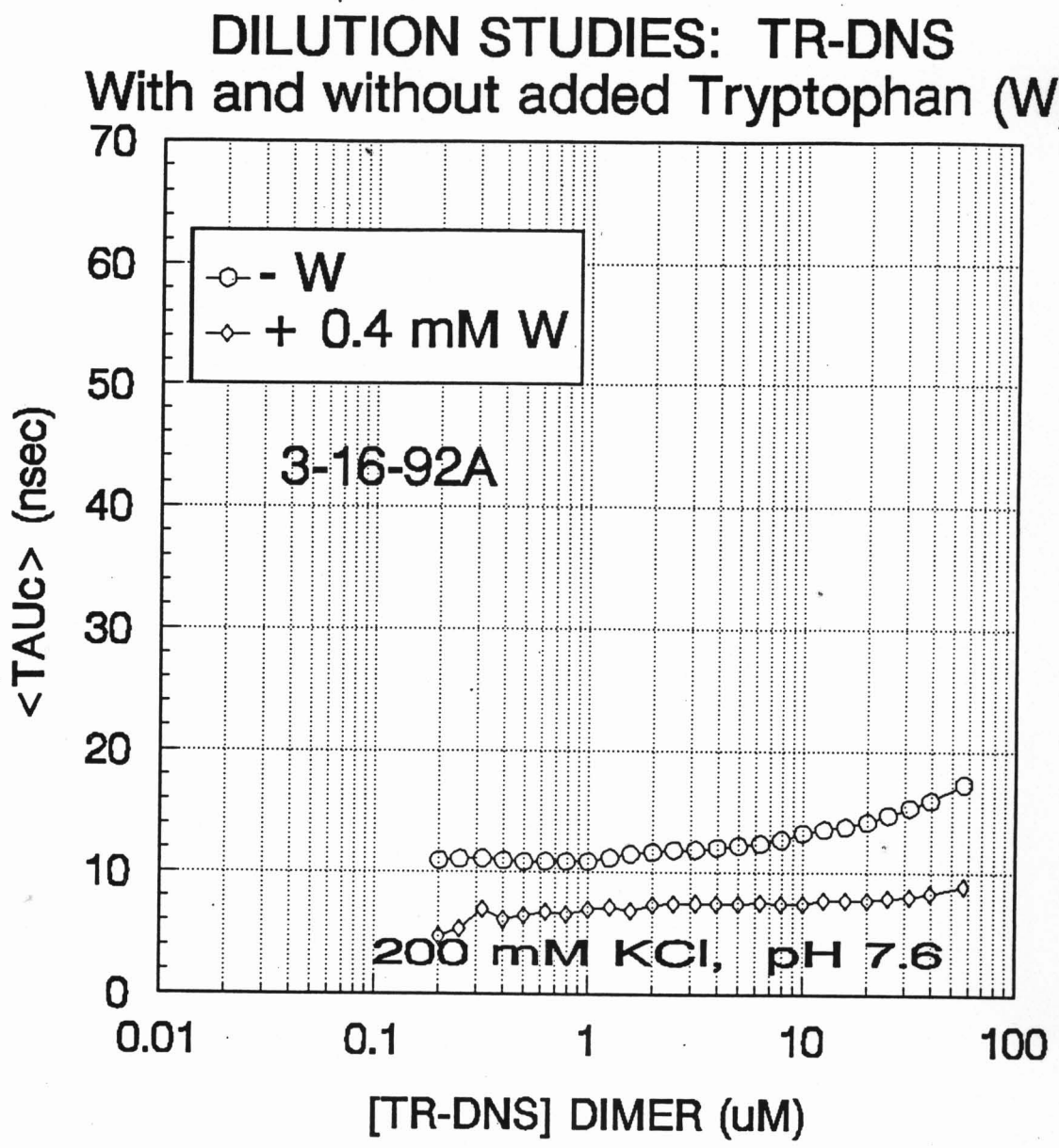
DILUTION STUDIES: TR-DNS
With and without added Tryptophan (W)
- W
+ 0.4 mM W
3-16-92A
200 mM KCl, pH 7.6
<TAUc> (nsec)
[TR-DNS] DIMER (uM)
0
10
20
30
40
50
60
70
0.01
0.1
1
10
100

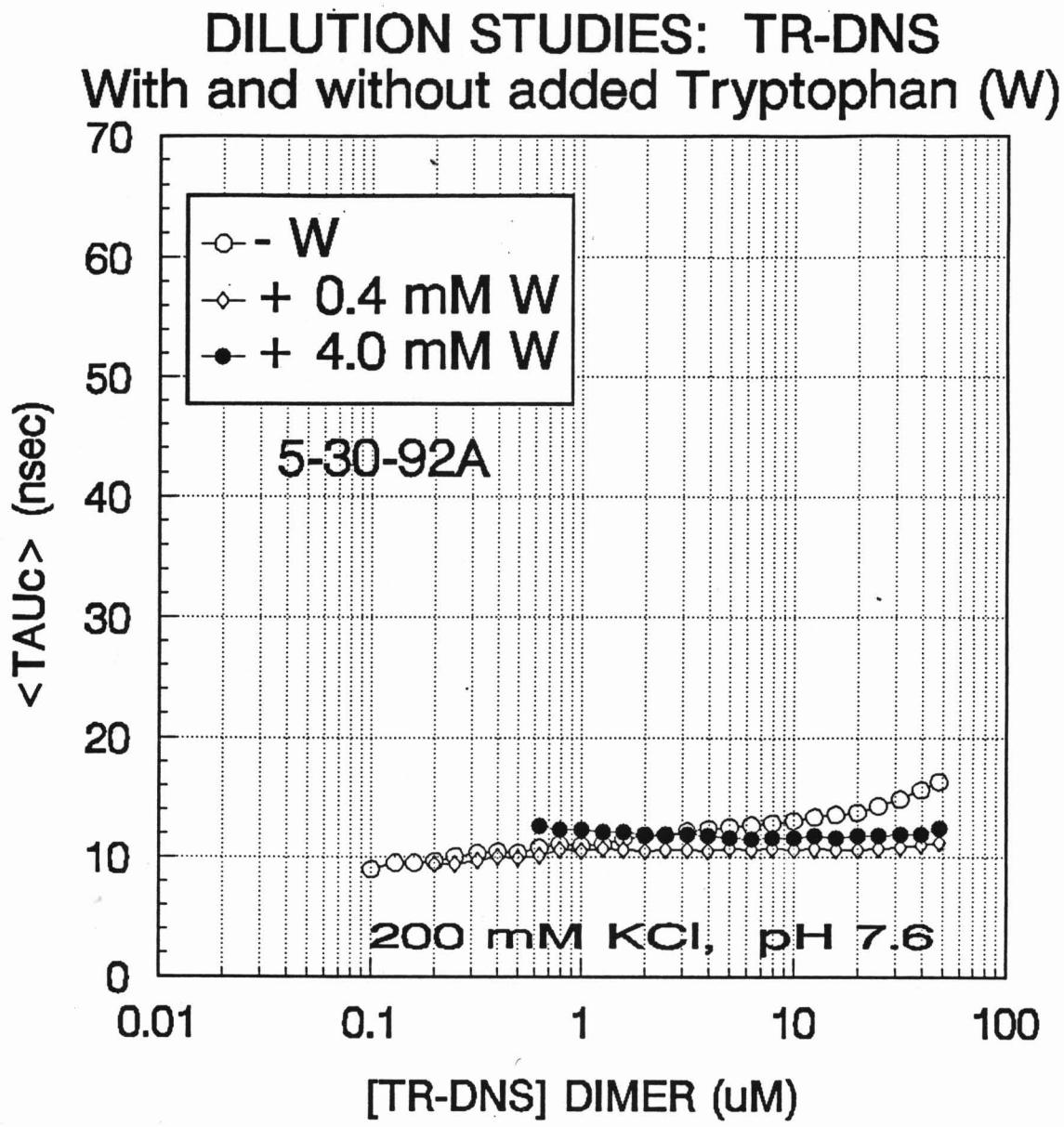
DILUTION STUDIES: TR-DNS
With and without added Tryptophan (W)
- W
+ 0.4 mM W
+ 4.0 mM W
5-30-92A
200 mM KCl, pH 7.6
<TAUc> (nsec)
[TR-DNS] DIMER (uM)
0
10
20
30
40
50
60
70
0.01
0.1
1
10
100

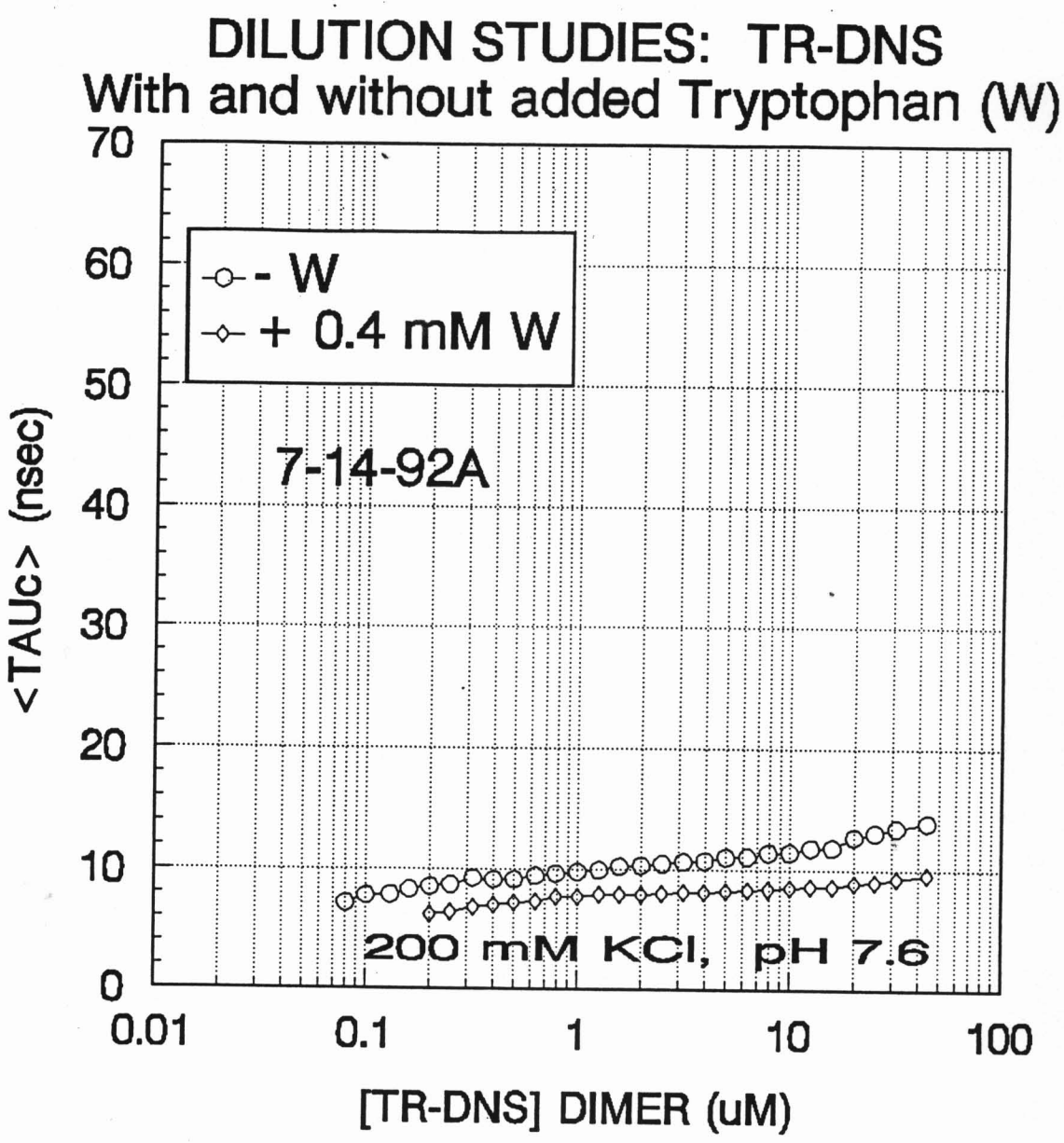
DILUTION STUDIES: TR-DNS
With and without added Tryptophan (W)
- W
+ 0.4 mM W
7-14-92A
200 mM KCl, pH 7.6
<TAUc> (nsec)
[TR-DNS] DIMER (uM)
0
10
20
30
40
50
60
70
0.01
0.1
1
10
100

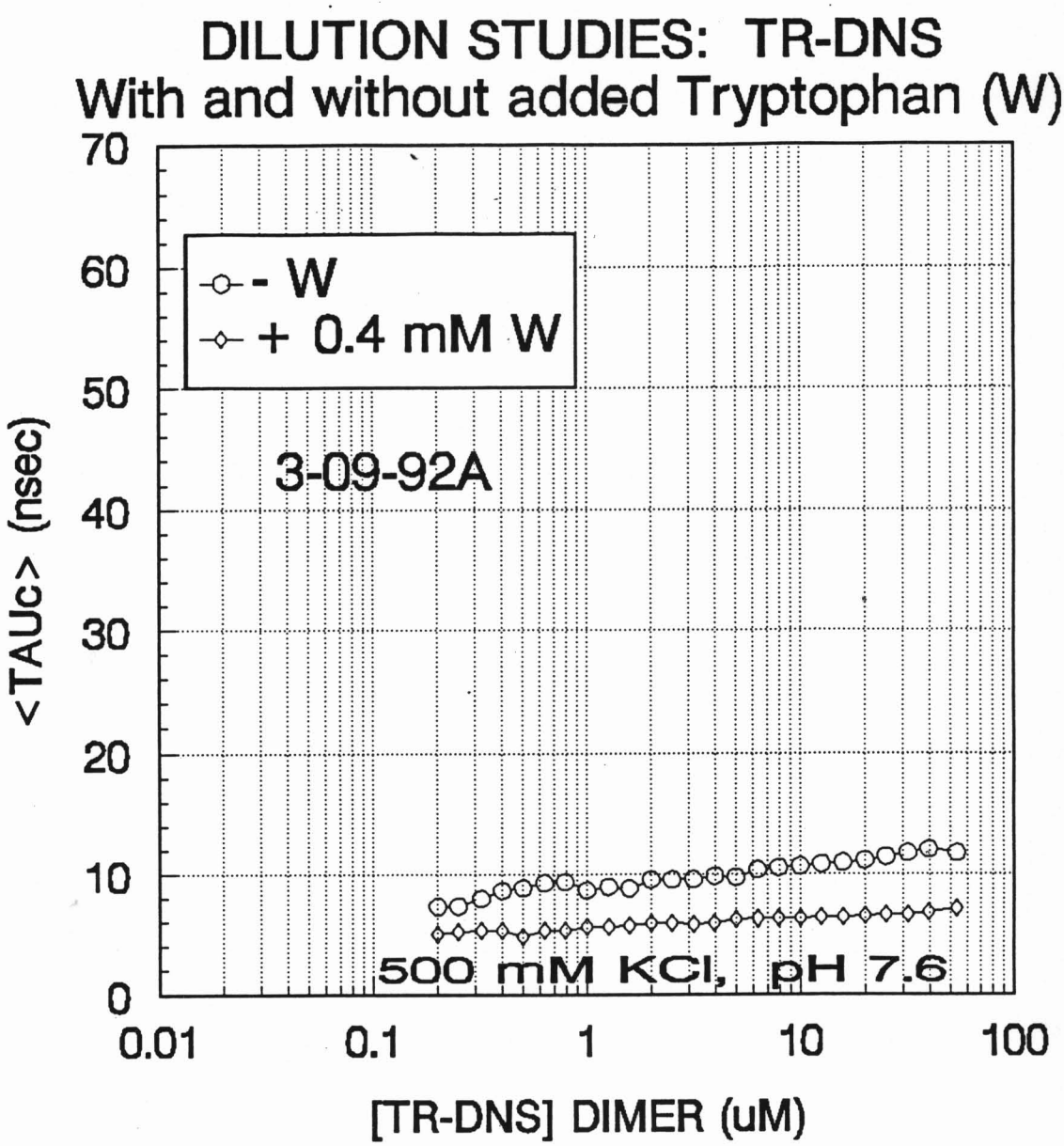
DILUTION STUDIES: TR-DNS
With and without added Tryptophan (W)
- W
+ 0.4 mM W
3-09-92A
500 mM KCl, pH 7.6
<TAUc> (nsec)
[TR-DNS] DIMER (uM)
0
10
20
30
40
50
60
70
0.01
0.1
1
10
100

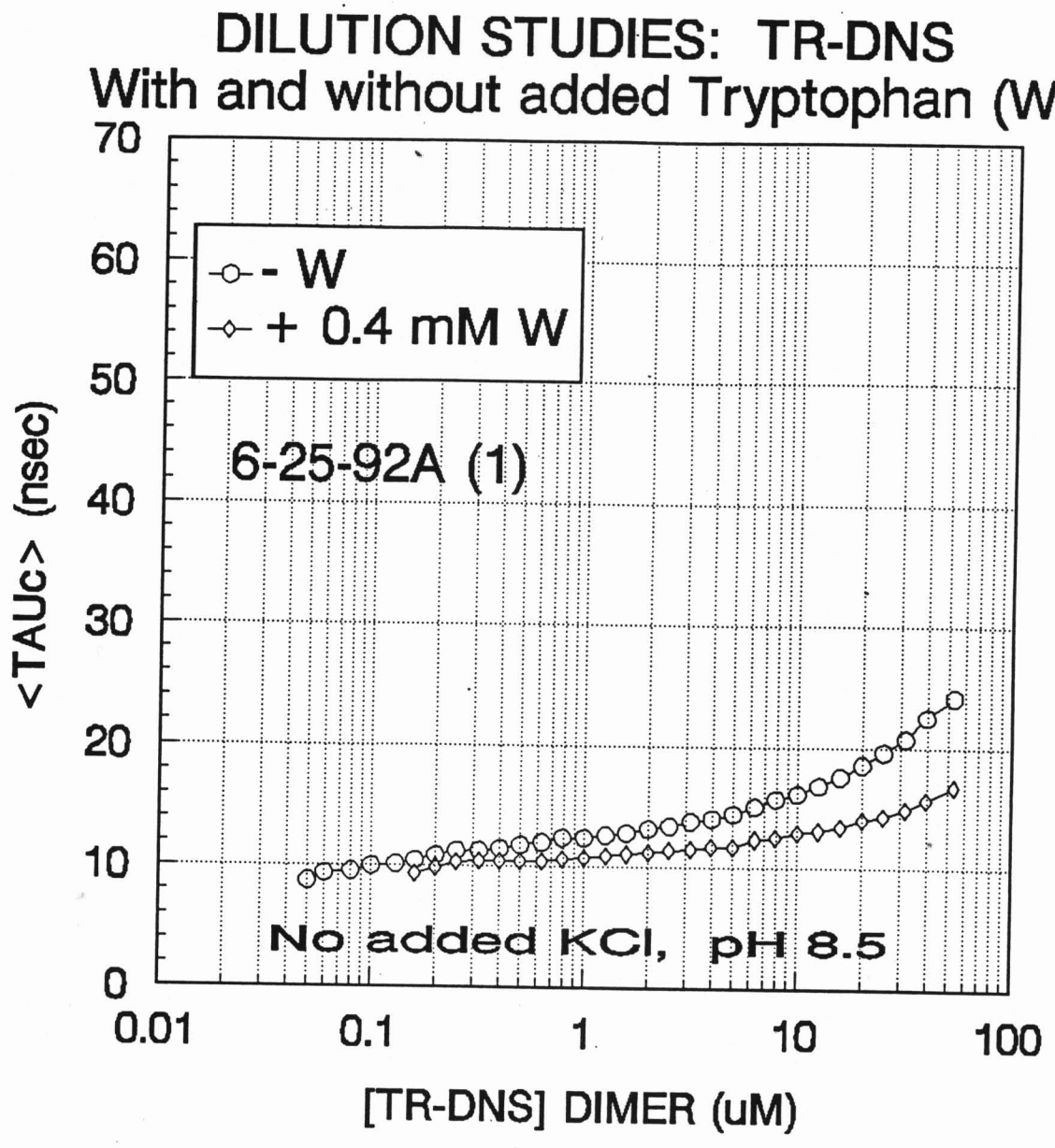
DILUTION STUDIES: TR-DNS
With and without added Tryptophan (W)
- W
+ 0.4 mM W
6-25-92A (1)
No added KCl, pH 8.5
<TAUc> (nsec)
[TR-DNS] DIMER (uM)
0
10
20
30
40
50
60
70
0.01
0.1
1
10
100

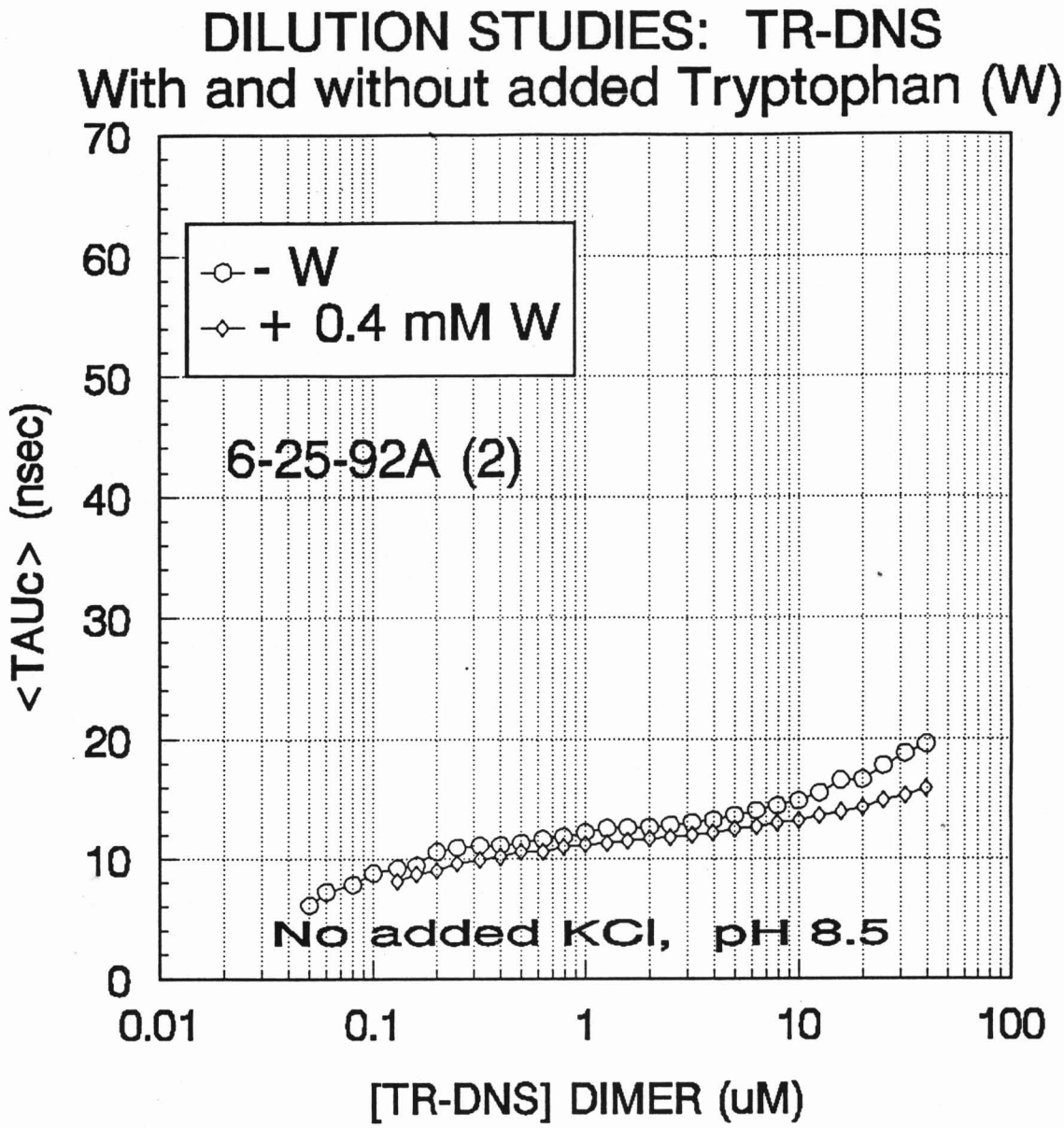
DILUTION STUDIES: TR-DNS
With and without added Tryptophan (W)
- W
+ 0.4 mM W
6-25-92A (2)
No added KCl, pH 8.5
<TAUc> (nsec)
[TR-DNS] DIMER (uM)
0
10
20
30
40
50
60
70
0.01
0.1
1
10
100

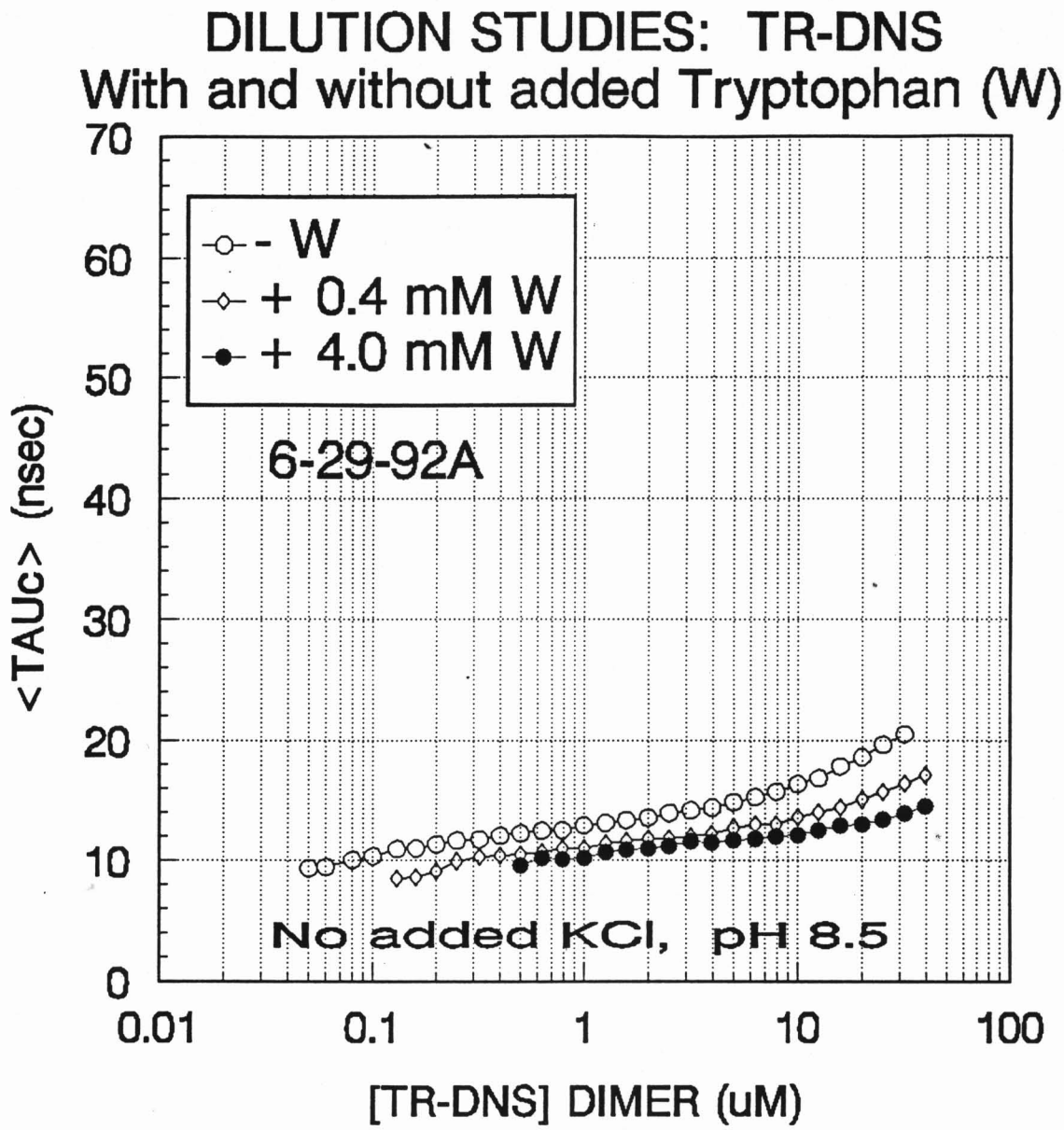
DILUTION STUDIES: TR-DNS
With and without added Tryptophan (W)
- W
+ 0.4 mM W
+ 4.0 mM W
6-29-92A
No added KCl, pH 8.5
<TAUc> (nsec)
[TR-DNS] DIMER (uM)
0
10
20
30
40
50
60
70
0.01
0.1
1
10
100

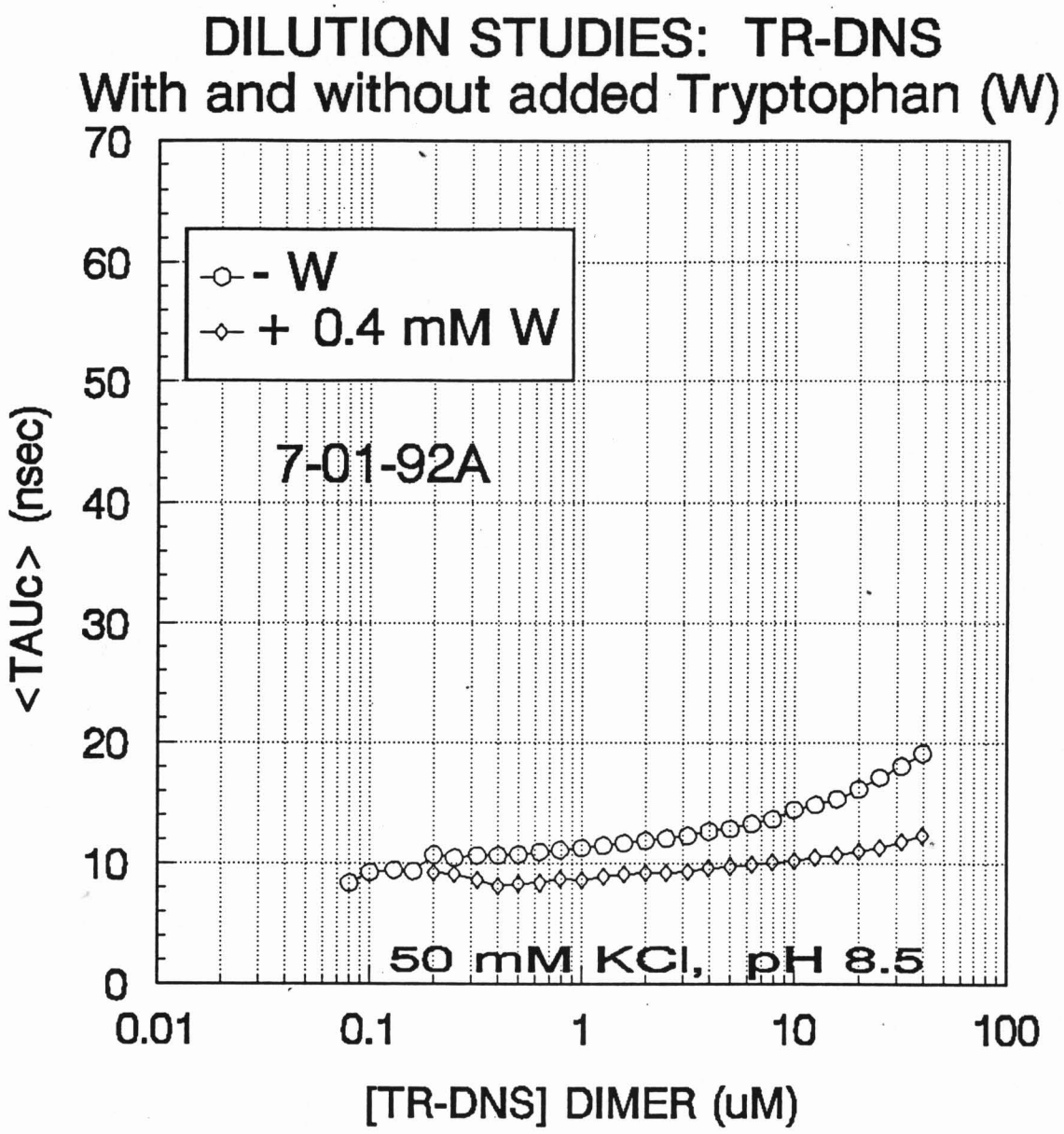
DILUTION STUDIES: TR-DNS
With and without added Tryptophan (W)
- W
+ 0.4 mM W
7-01-92A
50 mM KCl, pH 8.5
<TAUc> (nsec)
[TR-DNS] DIMER (uM)
0
10
20
30
40
50
60
70
0.01
0.1
1
10
100

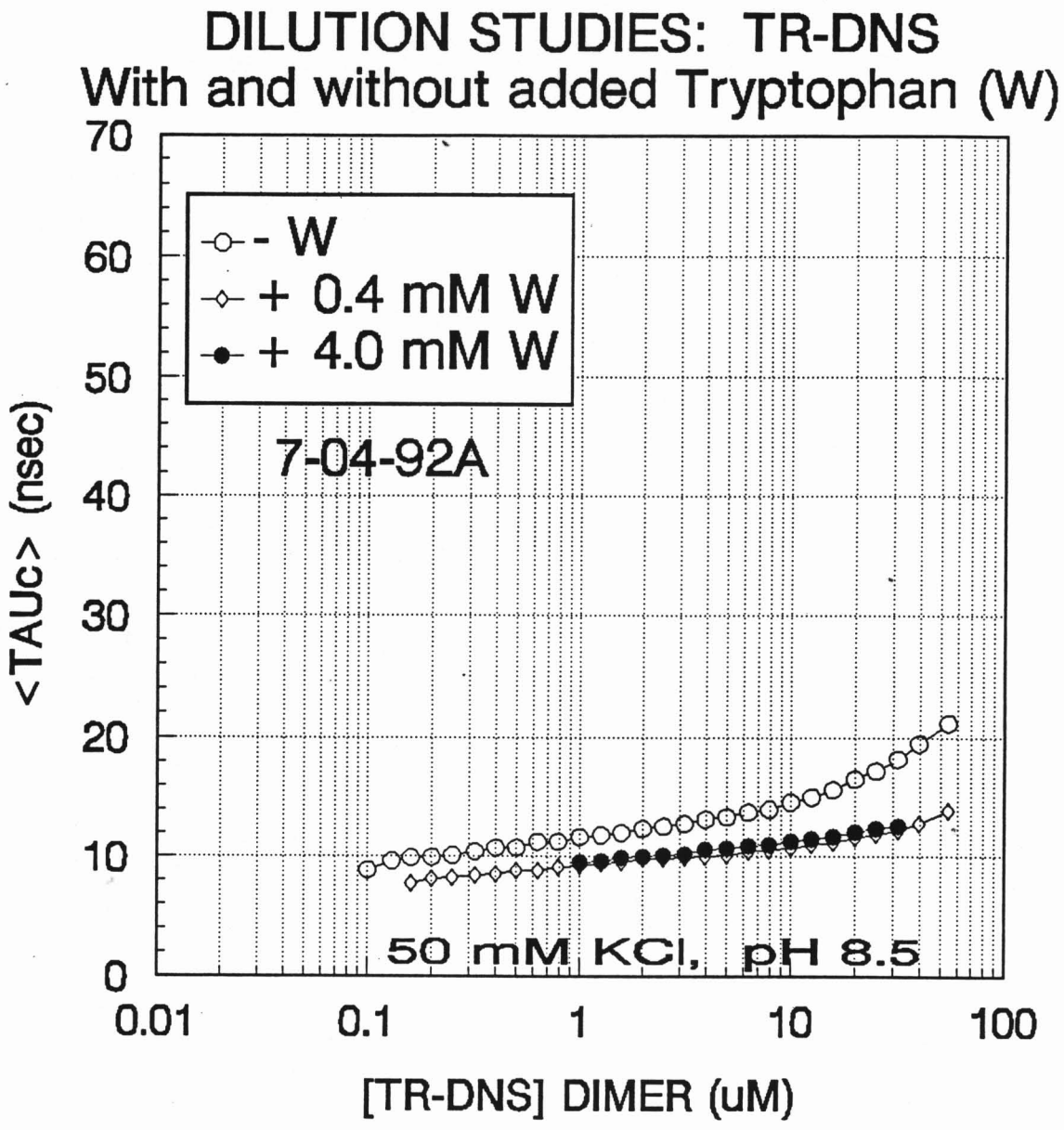
DILUTION STUDIES: TR-DNS
With and without added Tryptophan (W)
- W
+ 0.4 mM W
+ 4.0 mM W
7-04-92A
50 mM KCl, pH 8.5
<TAUc> (nsec)
[TR-DNS] DIMER (uM)
0
10
20
30
40
50
60
70
0.01
0.1
1
10
100

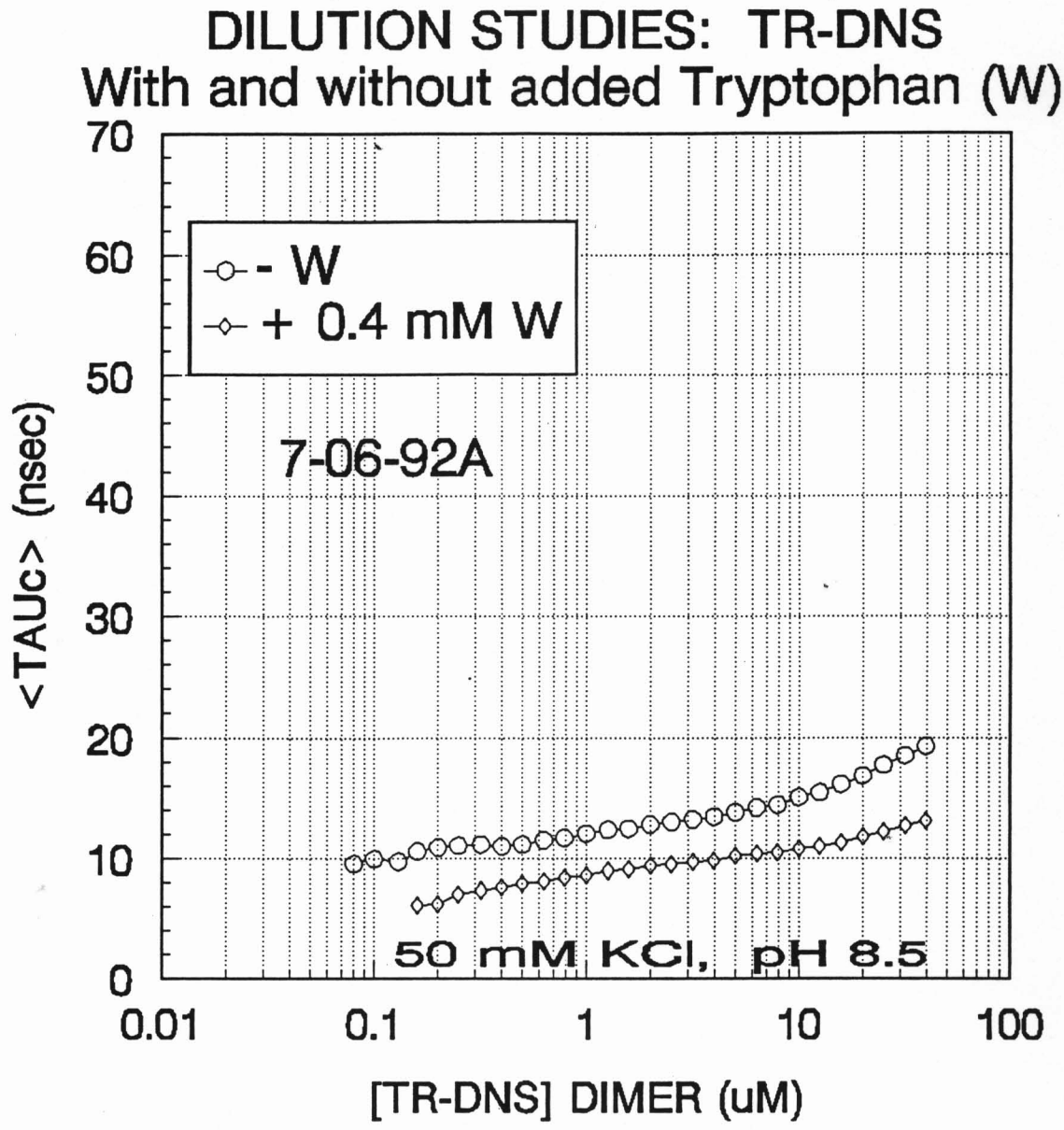
DILUTION STUDIES: TR-DNS
With and without added Tryptophan (W)
- W
+ 0.4 mM W
7-06-92A
50 mM KCl, pH 8.5
<TAUc> (nsec)
[TR-DNS] DIMER (uM)
0
10
20
30
40
50
60
70
0.01
0.1
1
10
100

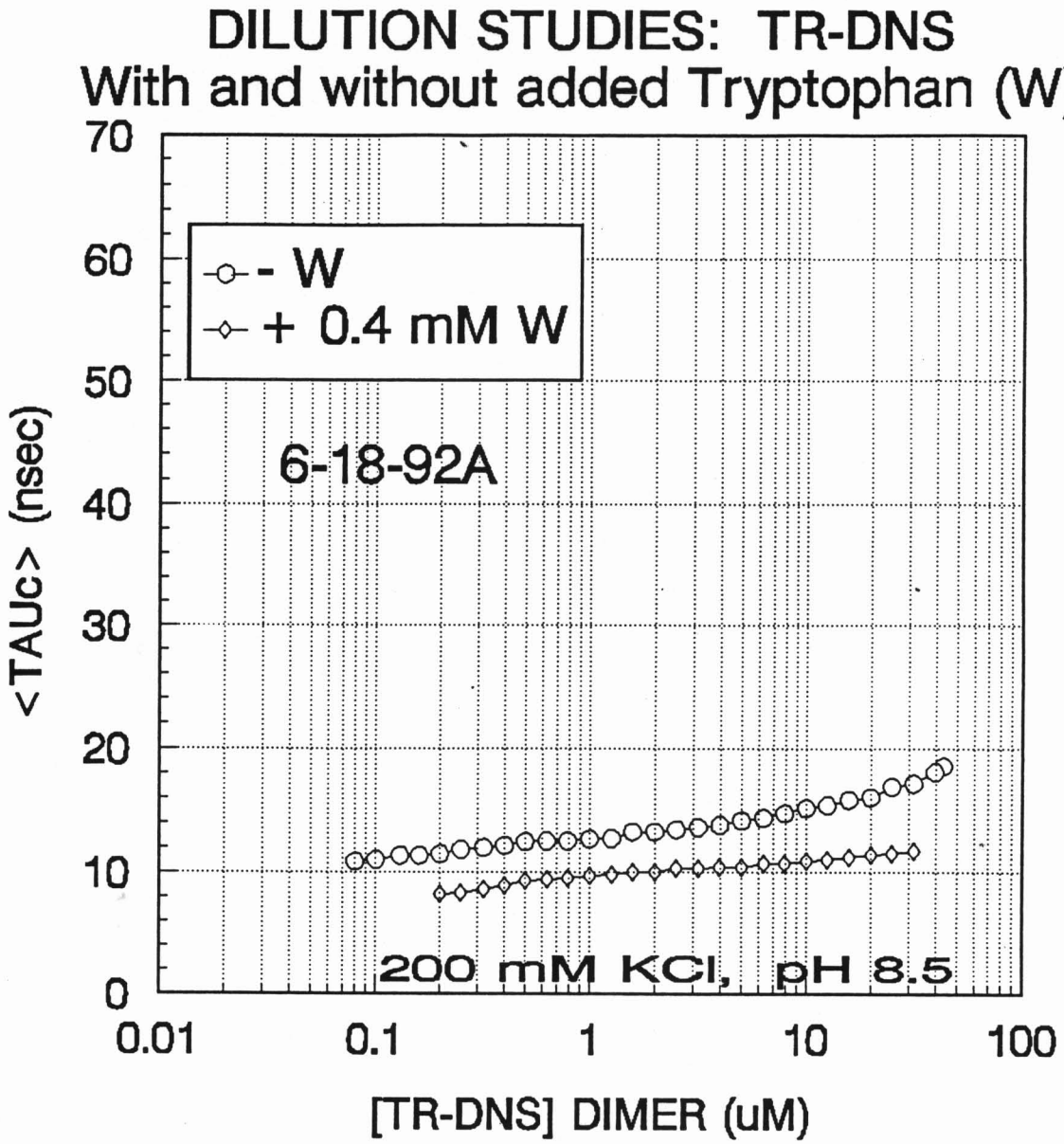
DILUTION STUDIES: TR-DNS
With and without added Tryptophan (W)
- W
+ 0.4 mM W
6-18-92A
200 mM KCl, pH 8.5
<TAUc> (nsec)
[TR-DNS] DIMER (uM)
0
10
20
30
40
50
60
70
0.01
0.1
1
10
100

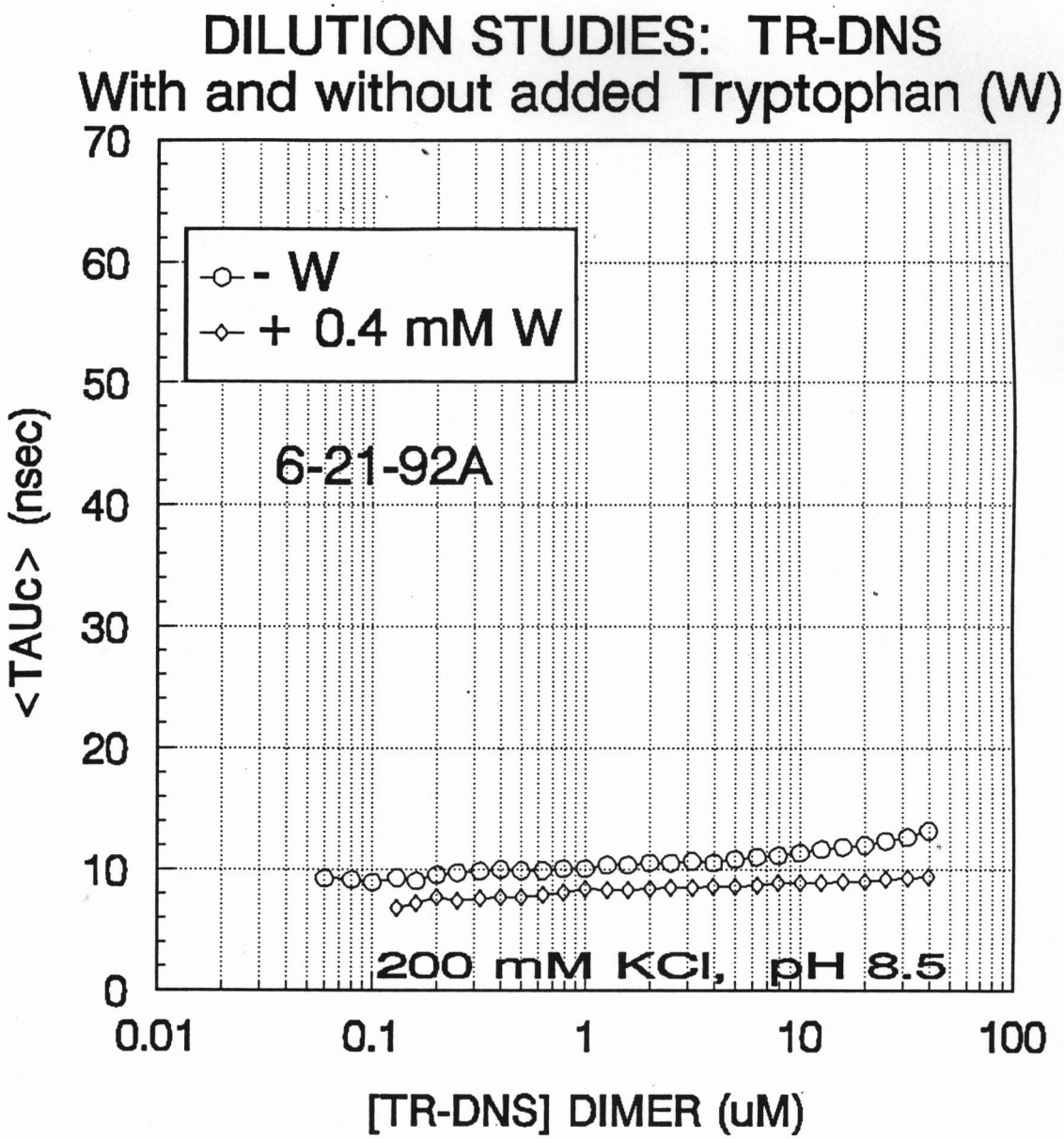
DILUTION STUDIES: TR-DNS
With and without added Tryptophan (W)
- W
+ 0.4 mM W
6-21-92A
200 mM KCl, pH 8.5
<TAUc> (nsec)
[TR-DNS] DIMER (uM)
0
10
20
30
40
50
60
70
0.01
0.1
1
10
100

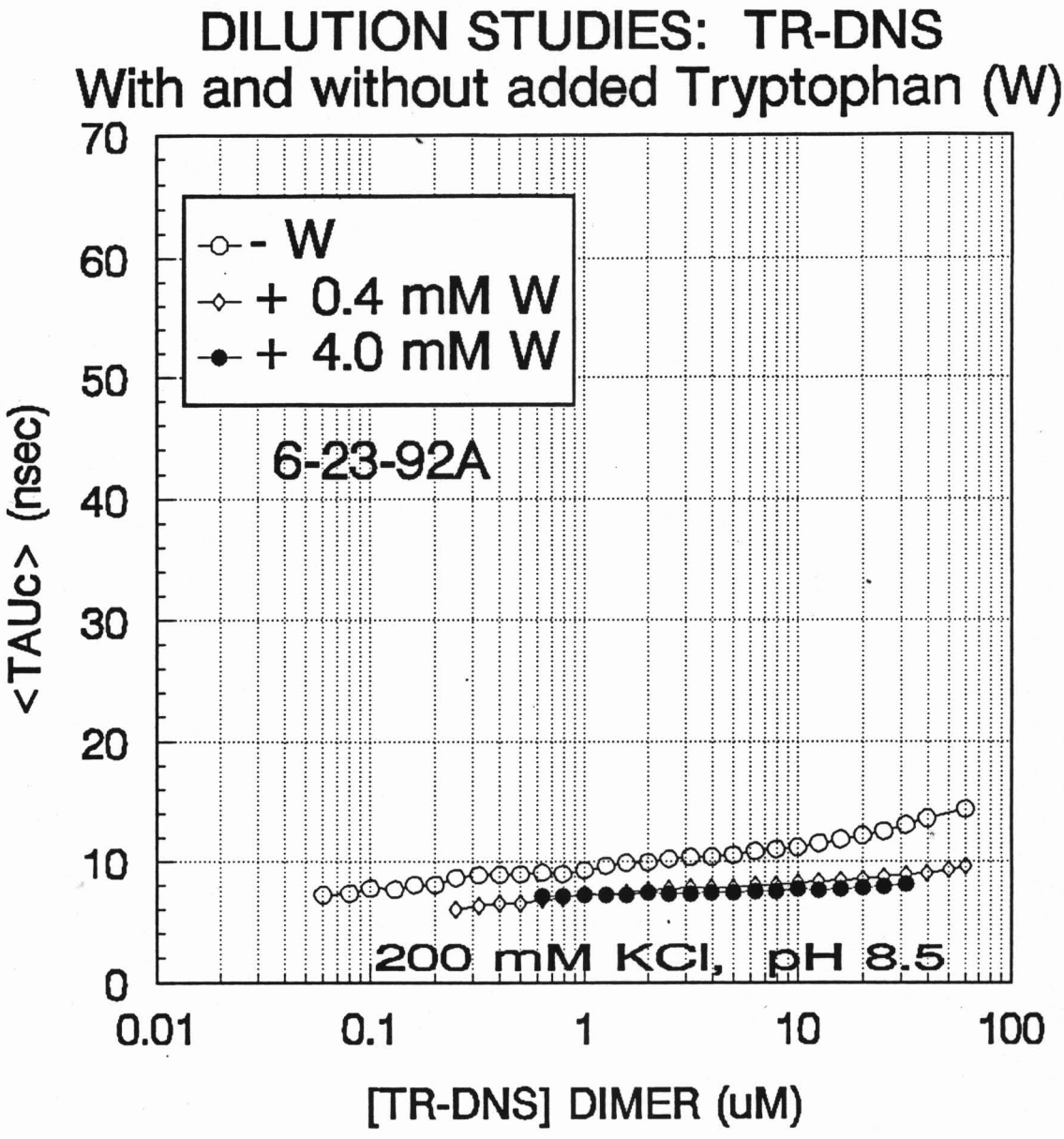
DILUTION STUDIES: TR-DNS
With and without added Tryptophan (W)
- W
+ 0.4 mM W
+ 4.0 mM W
6-23-92A
200 mM KCl, pH 8.5
<TAUc> (nsec)
[TR-DNS] DIMER (uM)
70
60
50
40
30
20
10
0
0.01
0.1
1
10
100

APPENDIX D

Individual Correlation Time Profiles which showed High Variability Among Experiments

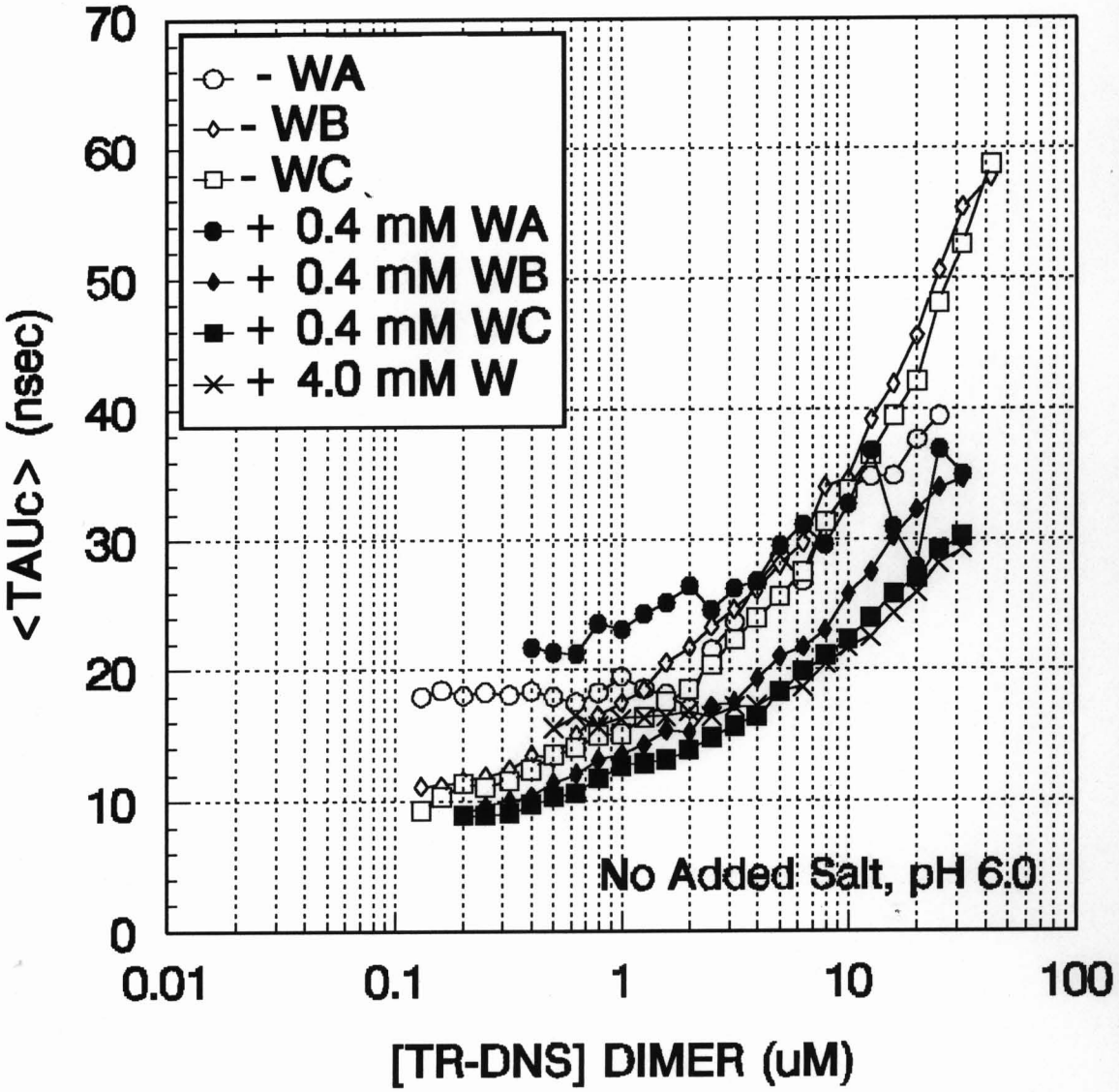

Figure D-1. Composite graph of individual ApoR and TR experimental data from studies at pH 6.0 with no added salt in the 10 mM potassium phosphate buffer. Data are shown to specifically depict the experimental variability under these solution conditions.

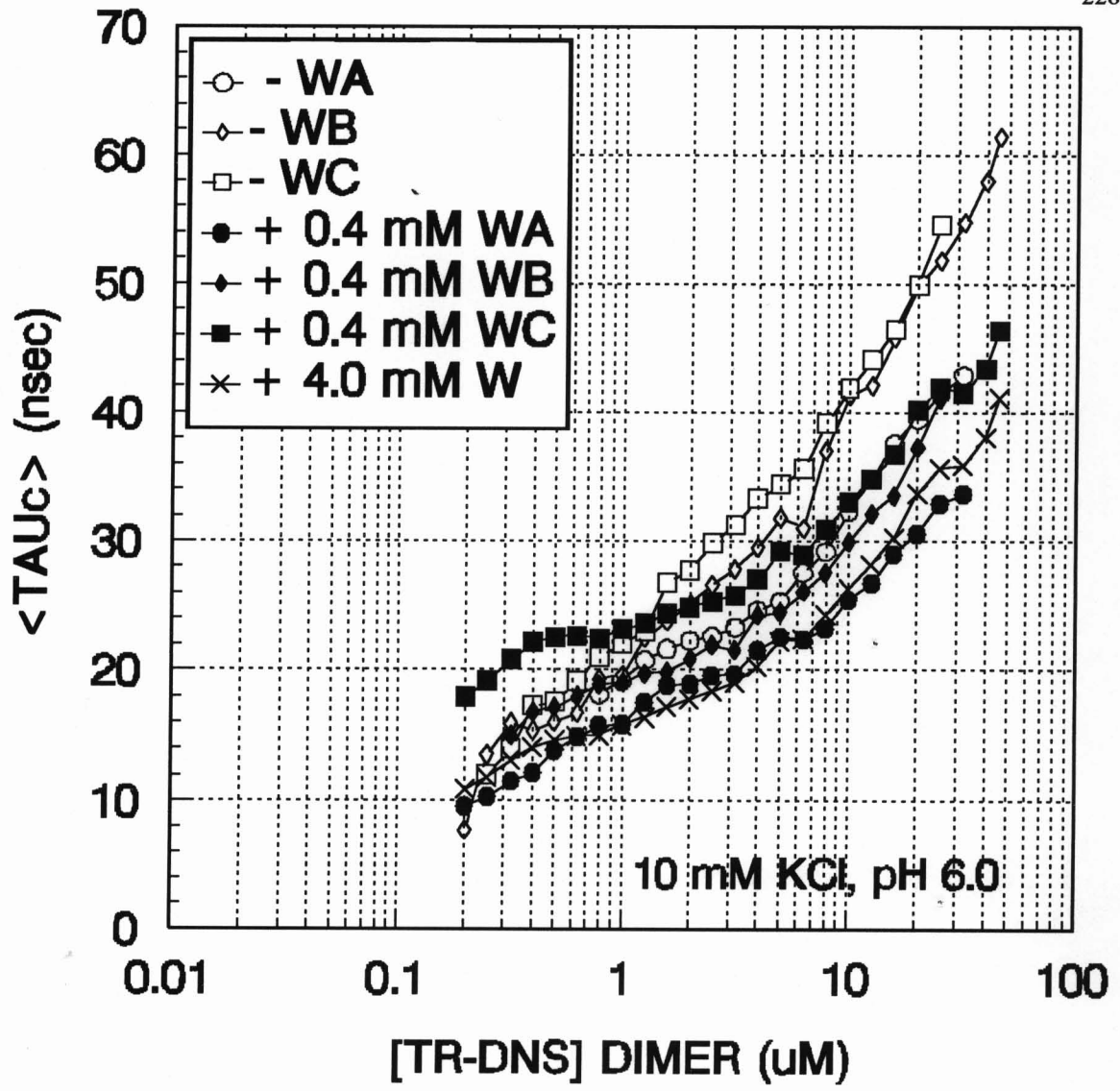

Figure D-2. Composite graph of experimental data from ApoR and TR studies done at pH 6.0 with 10 mM added KCl in the 10 mM potassium phosphate buffer. In TR studies, the corepressor concentration is 0.4 mM. Data are shown to specifically depict the experimental variability under these solution conditions.

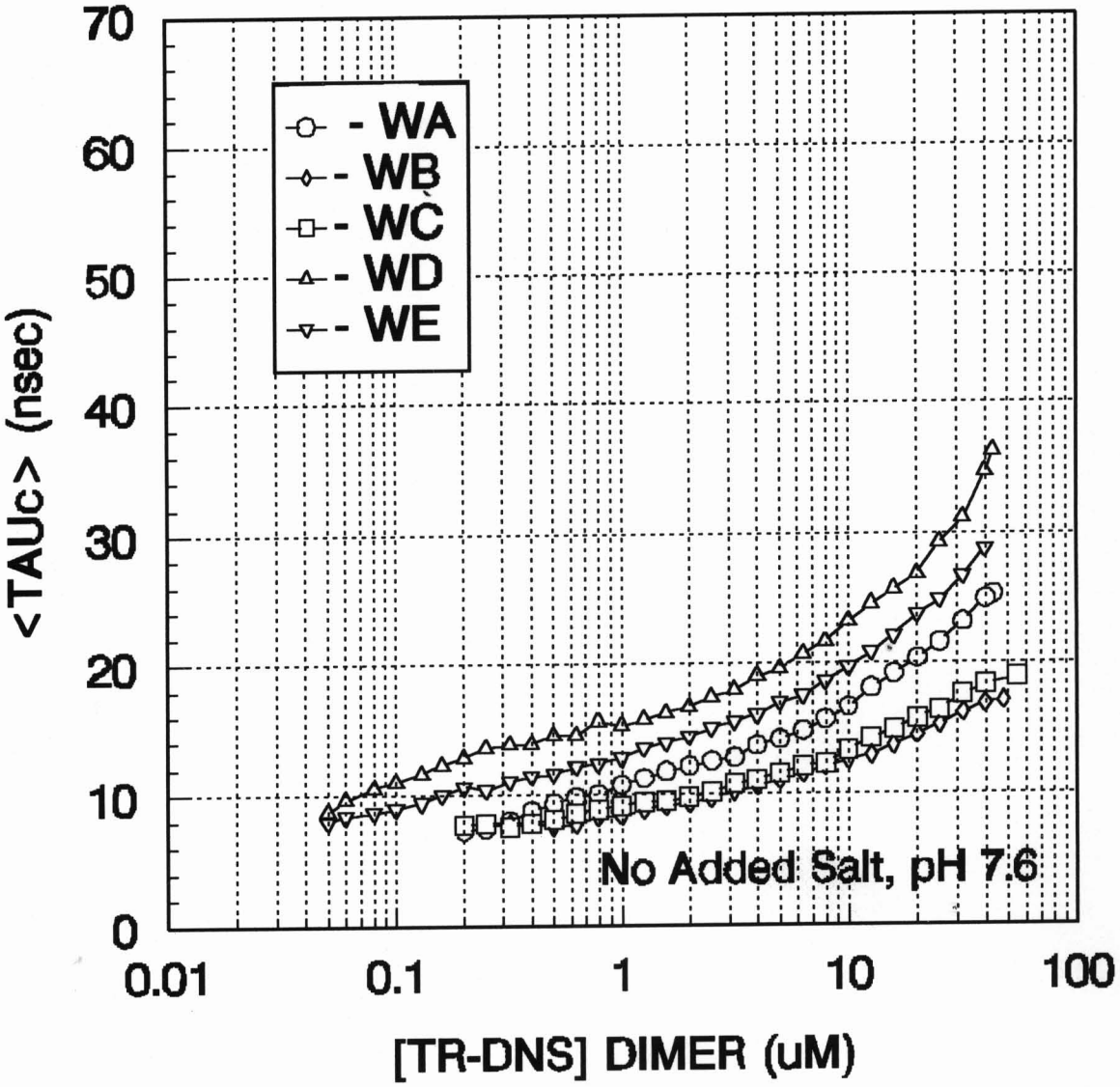

Figure D-3. Composite graph of experimental data from ApoR studies done at pH 7.6 with no mM added KCl in the 10 mM potassium phosphate buffer. Data are shown to specifically depict the experimental variability under these solution conditions.

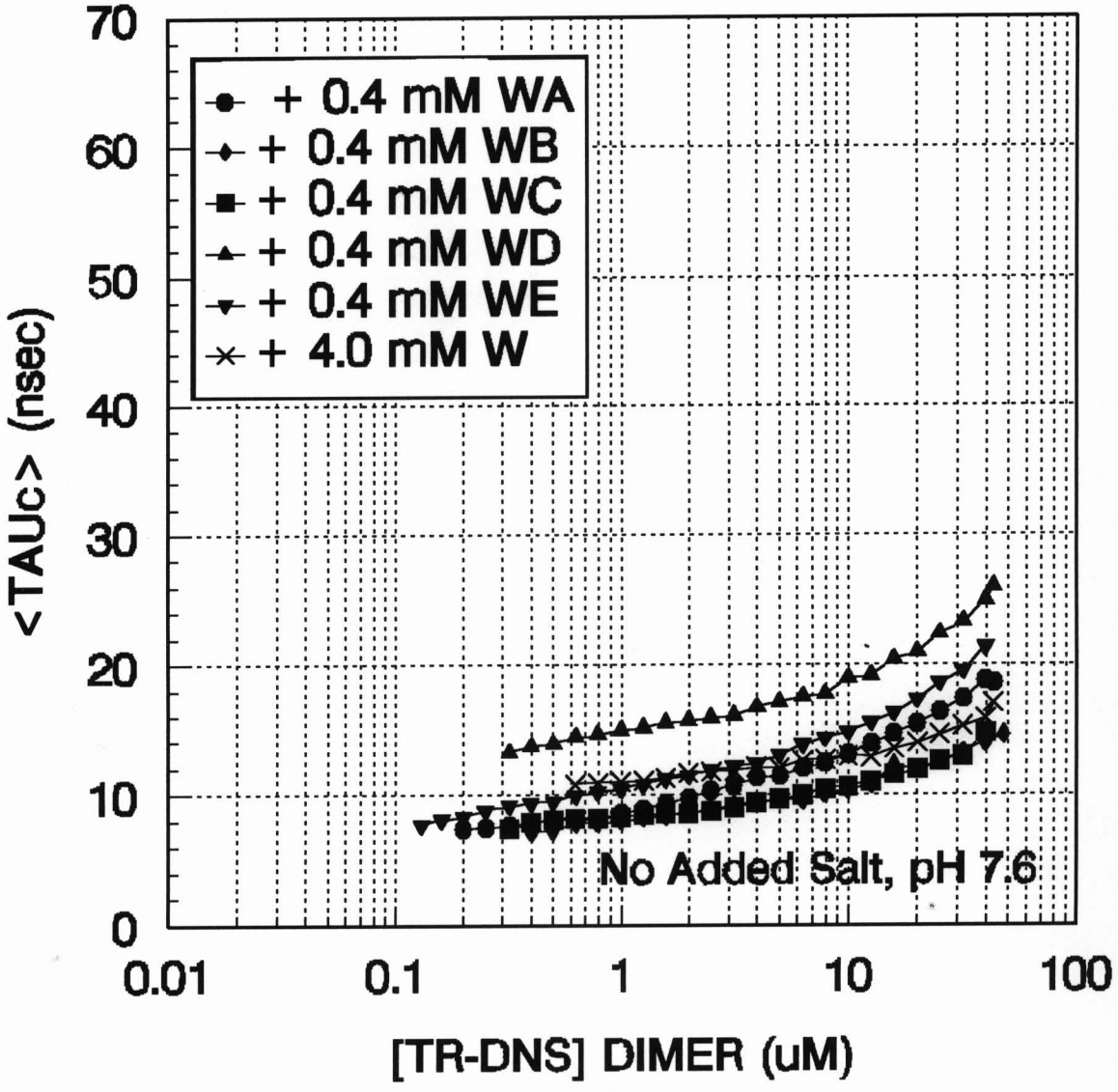

Figure D-4. Composite graph of experimental data from TR studies done at pH 7.6 with no mM added KCl in the 10 mM potassium phosphate buffer, corepressor concentration 0.4 mM. Data are shown to specifically depict the experimental variability under these solution conditions.